University of Sussex

Using mating-type switching to investigate Smc5/6 function in *Schizosaccharomyces pombe*

A thesis submitted to the University of Sussex for the degree of Doctor of Philosophy

by

Jennifer Whitwood

January 2013

Declaration

I hereby declare that this thesis has not been and will not be, submitted in whole or in part to another University for the award of any other degree

Signed:

Jennifer Whitwood

January 2013

Acknowledgements

First and foremost I would like to thank Jo Murray for giving me the opportunity to work towards this PhD as part of her laboratory at the Genome Damage and Stability Centre at the University of Sussex. I am grateful for all the help and guidance she has provided during this study. I would also like to thank my co-supervisor Eva Hoffmann for her advice and help during the project, especially during tetrad analysis and microscopy, and also to Tony Carr for all his contributions during lab meetings.

I appreciate the help of all the lab members of the Murray and Carr laboratories. In particular to Ken'ichi Mizuno for putting up with all my questions and for teaching me how to Southern blot. To Stephanie Schalbetter for always pointing me in the right direction when I was looking for strains, stocks and reagents. To Edgar Hartsuiker for teaching me how to pull tetrads and to Gokhan Akman and Louise Newnham for their help using the Delta Vision microscopes. I also want to thank all members of the Murray and Carr labs for all their help and suggestions during my PhD.

In addition to technical and experimental support I would also like to thank several members of the team at the GDSC for making the environment a wonderful place to work. To Yari Fontebasso for always lending an ear, to Ann-Sofie Schreurs for entertaining us with stories of her adventures and to members of the Jeggo and Caldecott lab for making the office a happy place to work.

Outside of University I am immensely grateful for the support of CJ Wheeler, my husband and partner, he listened during the highs and lows of my PhD and I am forever indebted to him for his company while working weekends and long nights. I would also like to thank my parents and family for the many years of support during my studies. Also a brief thank you to Sadie Doherty, my partner in dance crime, and Neil Skinner for so many campus lunches – you both helped more than you can know.

I would also like to thank the MRC for funding so that I could support myself during the PhD.

University of Sussex

Jennifer Whitwood - PhD Thesis in Biochemistry

Using mating-type switching to investigate Smc5/6 function in *Schizosaccharomyces pombe*

Summary

The essential Smc5/6 complex is structurally related to cohesin and condensin. It is required for homologous recombination (HR), rDNA stability and telomere maintenance. In *Schizosaccharomyces pombe*, two hypomorphic *smc6* mutants, *smc6-X* and *smc6-74*, have been shown to be deficient in HR-dependent processing of collapsed replication forks. Collapsed replication forks can generate single-ended DNA double strand breaks (se-DSB) which require HR to restore replication. In this study the requirements for Smc5/6 at a site-specific se-DSB at the mating-type locus and in the mating-type switching process were analysed.

In *S. pombe* mating-type switching occurs over two S phases; in the first S phase replication fork stalling at *mat1* leads to an imprint, which is converted to an se-DSB during the next S phase. This initiates the copying of the donor cassette using HR. In the absence of donors the sister chromatid is used for repair. Mating-type switching analysis showed that *smc6-74* had a defect in switching dependent on the genotype of the *smc6-74* parent.

Both *smc6* mutants had reduced viability in the absence of donors, consistent with a defect in HR repair of an se-DSB. Analysis in an inducible system (Holmes et. al., 2005) showed that in response to a se-DSB Rad52 foci appeared with wild type kinetics but the *smc6* mutants delayed entry into mitosis for approximately 2hrs, dependent on the DNA damage checkpoint kinase Chk1. In order to test whether this delay facilitated rescue by a converging replication fork a novel inducible converged fork (cf) DSB

system was developed. The cf-DSB required HR and the RecQ helicase Rqh1 for repair but did not require Mus81. The converging fork rescued *smc6-74* but not *smc6-X* showing Smc5/6 to be required for repair of both types of replication-associated DSBs.

Contents

List of figures and tables

List of abbreviations

Ade	Adenine
ARS	Autonomously replication sequence
ATM	Ataxia-telangiectasia mutated
ATP	Adenosine triphosphate
ATR	ATM – related
BIR	Break induced replication
BRCT	BRCA1 C-terminal domain
CDK	cyclin –dependent kinase
cf-DSB	converging-fork DSB
DNA	deoxyribonucleic acid
DSB	Double-strand break
DSBR	Double-strand break repair
EDTA	ethylenediaminetetraacetic acid
ELN	Extremely low nitrogen
EMM2	Edinburgh minimal medium
G1	Growth phase 1
G2	Growth phase 2
HR	Homologous recombination
Hs	*H. sapiens*
HU	Hydroxyurea
IPTG	isopropyl-β-D-thiogalactopyranoside
IR	Ionising radiation
Kb	Kilobases
Krpm	1000 x RPM
Leu	Leucine
mat	mating-type cassette
MCM	Mini-chromosome maintenence
MMS	Methylmethane sulfonate
M phase	Mitotis phase
nmt	No message in thiamine
ORC	Origin recognition complex
PCNA	Proliferating cell nuclear antigen
PRR	Post replication repair
rDNA	Ribosomal DNA
RF	Replication fork
RPA	Replication protein A
RTS1	Replication termination sequence
Sc	*S. cerevisiae*
se-DSB	single-ended double strand break
SMC	Structural maintenance of chromosomes
Sp	*S. pombe*
S phase	S phase
ssDNA	single stranded DNA

SUMO	Small ubiquitin-like modifier
Top	Topoisomerase
WT	Wild type
UV	Ultra violet
Xgal	5-bromo-4-chloro-3-indolyl-β-D-galactosidase
YE	Yeast extract
YEA	Yeast extract agar
YNBA	Yeast nitrogen base agar

Chapter 1 – Introduction

1.1 Introduction to *Schizosaccharomyces pombe*

The fission yeast *Schizosaccharomyces pombe* is a useful model organism. It has been used to extensively study cell cycle progression, DNA processing, repair and replication and has been a particularly informative for studying the checkpoints that monitor and control the DNA damage response and DNA replication pathways. It has several features that make it useful as a model organism, including short generation time and ease of genetic and molecular manipulation. In this study, mating-type switching, the method of which is specific to *S. pombe* (although other methods of switching exist in organisms such as *Saccharomyces cerevisiae* (Hicks and Fink, 1977) has been utilized to study the role of the Smc5/6 complex in ectopic recombination and single-ended double strand break repair.

1.2 The cell cycle of *S. pombe*

The cell cycle is split into four phases; Growth 1 (G1), DNA Synthesis (S phase), Growth 2 (G2) and Mitosis (M-phase). During each full cell cycle cells progress through all four phases, duplicating their DNA and dividing into two daughter cells. S phase is a crucial phase in cell cycle progression, DNA must be replicated and copied faithfully so all daughters contain a complete and correct chromosome compliment. In *S. pombe* the process of nuclear division (mitosis) and whole cell division is uncoupled (Nurse, 1990). Chromosomes segregate during mitosis (M-phase), cell then pass through a relatively short G1 phase and enter S phase, coincidently with cytokinesis (Forsburg, 2003). This uncoupling means that *S. pombe* spends 70% of its cell cycle in the G2 growth phase where cells are seen to elongate before they enter cytokinesis (Forsburg, 2003).

Progression through each phase of the cell cycle is regulated by various cyclin-dependent kinases (CDKs). In *S. pombe* cell cycle regulation is controlled by Cdc2, the functional homologue of human CDC2 (CDK1) and Cdc28 in *S. cerevisiae*. Cdc2 functions at the start of the cell cycle to initiate a new round of replication, but also acts in late G2 to initiate mitosis (Russell and Nurse, 1986, Forsburg and Nurse, 1991,

Moser and Russell, 2000). Cdc2 interacts with other cyclins to drive cell-cycle progression, in particular associating with Cig2 to initiate the start of DNA replication during S phase (Mondesert et al., 1996) and Cdc13 to initiate transition from G2 to M phase (Hagan et al., 1988).

1.3 DNA replication

1.3.1 Replication initiation

Genome replication occurs once in every cell cycle and requires the entire genome to be duplicated. In eukaryotes replication is initiated at autonomously replicating sequences (or ARS) or origins of replication throughout the genome (Chan and Tye, 1980). These are the locations for the formation of the pre-replication complex (pre-RC) during late M phase to G1 (Bell and Dutta, 2002, Newlon, 1997, Wuarin and Nurse, 1996). In most eukaryotes the pre-RC is formed of a heteromeric, six-subunit, protein complex known as the ORC (Origin Recognition Complex), Cdc6$^{S.cerevisiae}$, Cdt1 and a group of MCM helicase proteins (Mcm2-7). In *S. pombe* the pre-RC, contains the Cdc6 homologue Cdc18 and also requires Sap1, a protein initially identified as essential for mating-type switching but may also form part of a replication fork stability complex (Noguchi and Noguchi, 2007), for Cdc18 binding (figure 1-1) (Nishitani and Lygerou, 2002).

ORC directly binds to replication origins. In *S. pombe* it has been observed that Orc4 binds the AT rich portions of the ARS using AT hook motifs (Sun and Kong, 2010). Cdc18 is recruited to ORC and direct interaction with the C-terminus of Cdc18 is required for the recruitment of Cdt1 and Mcm2-7 (Nishitani et al., 2000). Cdc18 is also able to interact with the heterochromatin mediator protein Swi6 (Li et al., 2011) and may act as a positive or negative regulator of the timing of replication origin firing. It was shown *in vitro* that formation of the *S. cerevisiae* pre-RC required ATP hydrolysis for binding of the ORC complex to the replication origin and the subsequent recruitment of Cdc6 and the MCM complex (Seki and Diffley, 2000). Studies in *S. cerevisiae* and *Xenopus laevis* have also shown that an excess of MCM are bound to replication origins (Burkhart et al., 1995, Lei et al., 1996, Donovan et al., 1997, Romanowski et al., 1996, Edwards et al., 2002)
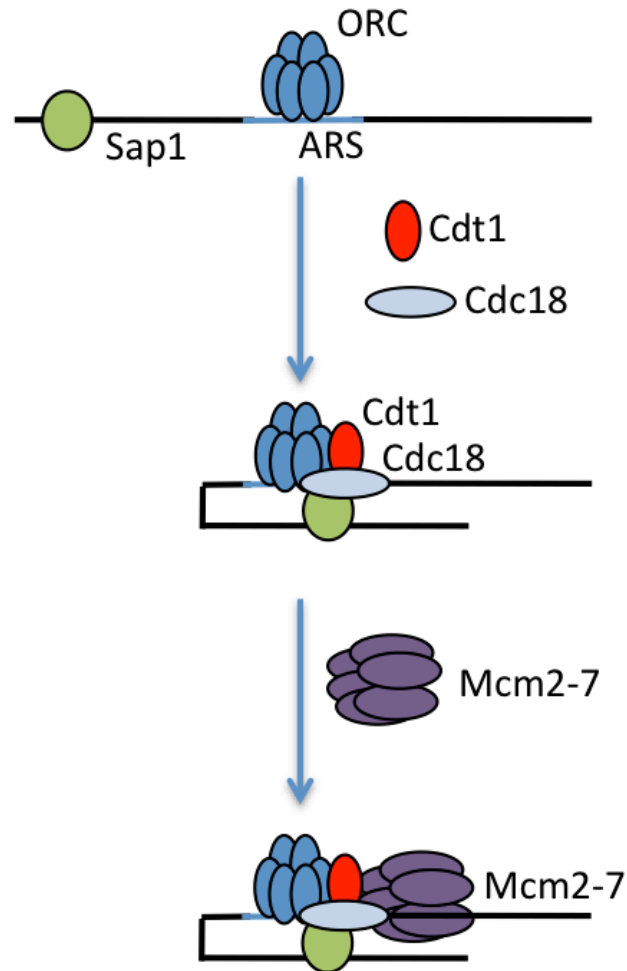
Figure 1-1 Assembly of the pre-RC in *S. pombe*

At the initiation of DNA replication Sap1 and the origin replication complex (ORC) bind to autonomously replicating sequences (ARS). Both the ORC and Sap1 are required for the binding of Cdc18 but Cdt1 can bind to ORC alone. After the recruitment of these proteins, Mcm2-7 binds to the origin of replication completing the pre-RC (adapted from Sun and Kong, 2010).

and it has been suggested that in some circumstances MCM alone could act as a pre-RC (Ibarra et al., 2008).

At the beginning of S phase the pre-RC is activated and becomes the pre-initiation complex (pre-IC). Activation occurs after an increase in activity of the S phase specific cyclin dependent kinase (CDK) Cdc28 (*S. pombe* Cdc2) and DDK (Cdc7-DBF4) (Seki and Diffley, 2000) CDK and DDK activity destabilizes Cdc18 by phosphorolyation (Jallepalli et al., 1997) however Cdt1 is also degraded at this time (Nishitani et al., 2000).This degradation is an important mechanism for the control of origin firing – the loss of Cdc18 and Cdt1 means that no more MCMs can be recruited to the origin site and prevents re-firing (Yanow et al., 2001).

An additional MCM, Mcm10, is recruited to the pre-IC and stimulates Mcm2-7 phosphorylation by Cdc7-DBF4. Mcm10 with phosphorylated Mcm2-7 recruits Cdc45 and DNA polymerase α to the origin (Homesley et al., 2000). Several proteins of the Mcm2-7 complex have been shown to have DNA helicase activity (Lee and Hurwitz, 2001) and act with Cdc45 to unwind DNA and move with the replication fork (RF) as S phase progresses (Gambus et al., 2006, Moyer et al., 2006, Pacek et al., 2006). An additional protein complex known as GINS composed of Sld5, Psf1, Psf2 and Psf3 is required for initiation and elongation of the replication fork. It is thought to form a complex, with Cdc45 and the MCMs, that opens the DNA at the origins so that DNA polymerases can be loaded ready for replication initiation (Gambus et al., 2006, Labib and Gambus, 2007). In *S. cerevisiae* additional replication elements were seen to be recruited to the pre-IC by Cdc28 and Cdc7-DBF4; Cdc28 phosphorylates Sld2 and Sld3 that they form a complex with Dpb11 (Zegerman and Diffley, 2007). This complex is required for Cdc45 loading to DNA along with DNA polymerase but does not move with the replication fork (Aves, 2009, Aparicio et al., 1997).

1.3.2 Replication progression and DNA elongation

Three polymerases are specifically required for replication; DNA polymerase α, DNA polymerase δ and DNA polymerase ε. Each polymerase performs a specific function during replication; Pol α is required for the start of DNA synthesis and can initiate

replication. It is recruited to replication origins and synthesizes RNA primers for both leading and lagging strands. Once DNA synthesis is primed Pol α is exchanged for Pol δ on the lagging strand, or Pol ε on the leading strand, for bulk DNA synthesis as these enzymes have proofreading ability (Kawasaki and Sugino, 2001).

During replication Pol δ and Pol ε associate with PCNA (Jonsson and Hubscher, 1997, Mossi and Hubscher, 1998) that links the DNA polymerase to the DNA template (Takisawa et al., 2000). It has been shown in *Xenopus* that in the absence of Pol ε, Pol δ is able to process both leading and lagging strand synthesis while Pol ε is unable to elongate when there is no Pol δ (Fukui et al., 2004). Pol ε has been shown to have a role in leading strand synthesis (Pursell et al., 2007), however its redundancy with Pol δ is not fully understood. The C-terminus of Pol ε has been shown to have a role in checkpoint control and may have a role in checking and correcting errors made by the other polymerases in *S. cerevisiae* (Kesti et al., 1999, Feng and D'Urso, 2001, Pavlov et al., 2004).

DNA polymerases are required to elongate new DNA strands by coupled leading and lagging strand synthesis until the entire genome is replicated. Leading strand synthesis is a more simple process with template DNA being read by Pol ε in a 5'-3' direction and the new complementary strain being synthesized continuously using free nucleotides. Lagging strand synthesis is more complicated and, because of its orientation and the fact that replication must progress from a 5'-3' direction, is synthesized discontinuously. Pol α primase initiates and DNA pol δ adds nucleotides to these primed sections creating small Okazaki fragments that are joined together by DNA ligase. During synthesis Replication Protein A (RPA) binds single stranded (ssDNA) that is exposed during replication (Tanaka and Nasmyth, 1998, Walter and Newport, 2000) and acts to prevent newly unwound DNA from re-annealing or forming secondary structures (figure 1-2) (RPA also plays an important role in checkpoint response and homologous recombination repair as discussed in section 1.4.2 and 1.5).

Replication forks are initiated in both directions at origins and terminate where RFs meet or where they reach the end of a linear chromosome.
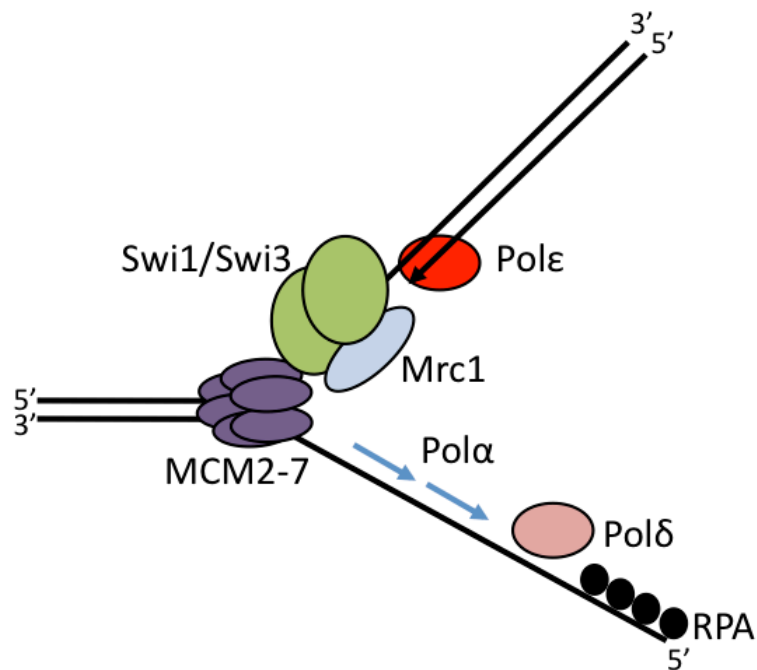
Figure 1-2 The replication fork

The MCM2-7 complex unwinds the DNA helix. RPA coats exposed single stranded DNA while DNA polymerase α primes DNA ready for extension. The fork protection complex (Swi1/Swi3) and Mrc1 bind to the fork to maintain its stability during elongation. Once priming is complete polα is exchanged for polδ/polε for bulk DNA synthesis.

When two replication forks meet they can merge through fork converging and this is a major method of un-facilitated replication termination.

1.4 Managing replication difficulties

1.4.1 Replication fork inhibition

During replication, replication forks (RF) may stall or stop, for example at protein barriers, repetitive DNA elements or DNA damage. DNA repeats can lead to secondary structures and create natural blocks for replication machinery that may inhibit replication (Mirkin et al., 2006). There are also coded regions that cause slower replication fork progression and can encourage replication fork converging at these locations. RF can be blocked at regions where there are protein/DNA interactions, for example in the *S. pombe mat1* locus replication termination sequence (RTS1) forms a barrier to replication by the binding of RTS1 factors Rtf1 and Rtf2 (Eydmann et al., 2008). Another example is the *S. cerevisiae* Fob-1 dependent rDNA barrier (Johzuka and Horiuchi, 2002). Depletion of nucleotides can also lead to replication slowing or stalling. The level of nucleotides is usually carefully regulated in the cell but can be depleted artificially using an RNR inhibitor such as hydroxyurea (HU) (Ahmet Koç, 2003). HU is commonly used in replication studies as it can induce fork stalling and activate the S phase checkpoint (as discussed in section 1.4.2). There are several types of DNA damage that can inhibit DNA replication including alkylating agents like MMS and damage from UV. When replication forks come across these types of damage a checkpoint response is triggered that stalls replication while the DNA damage is dealt with (Foiani et al., 1998).

1.4.2 The S phase checkpoint response

To ensure complete and accurate DNA replication, the S phase checkpoint is activated in response to replication perturbation (Branzei and Foiani, 2007, Paulsen and Cimprich, 2007, Tourriere and Pasero, 2007). S phase checkpoint activation requires the formation of replication forks (Stokes et al., 2002, Tercero et al., 2003) and relies on the formation of single stranded DNA (ssDNA). When a replication fork is slowed the MCM complex continues to unwind DNA in such a way that it becomes uncoupled from DNA synthesis, and can generate long stretches of ssDNA. Replication protein A

binds these long stretches of DNA and triggers the checkpoint response (You et al., 2002, Zou et al., 2003).

In *S. pombe*, as in other organisms, the checkpoint is initiated by the recruitment of sensor proteins Rad3-Rad26^{Sp} (ATR^{Hs} Mec1^{Sc} / ATRIP^{Hs} DDC2^{Sc}) to RPA coated ssDNA. Rad26 is phosphorylated by Rad3, an action that is independent of additional checkpoint proteins Rad17 and the 9-1-1 (Rad9-Rad1-Hus1) complex, showing that DNA damage sensing by Rad3 is independent of other members of the checkpoint machinery (Edwards et al., 1999, Paciotti et al., 2000). Complete activation of this checkpoint requires a further activation of two protein complexes the 9-1-1 complex and Rad17. Rad17 is an additional sensor protein that detects the ssDNA and is involved in the recruitment of the 9-1-1 complex (Majka et al., 2006, Zou et al., 2002). The 9-1-1 complex is structurally related to PCNA and Rad3 phosphorylates the C-terminus of Rad9 to initiate the recruitment of Rad4 (Dpb11^{Sc}). Rad4 is required particularly when DNA resection is limited ensuring that the checkpoint signal is strong enough to ensure a full checkpoint response (Lin et al., 2012).

The <u>m</u>ediator of the <u>r</u>eplication <u>c</u>heckpoint 1 protein (Mrc1) is thought to bind DNA and have a role in activating the replication checkpoint (Zhao and Russell, 2004). Rad3 phosphorylates Mrc1 and this signal is used to mediate a response in the checkpoint effector kinase Cds1 (Alcasabas et al., 2001, Zhao et al., 2003). This activated Cds1 is S phase specific and during S phase is activated preferentially over the DNA damage checkpoint kinase Chk1 (which is only activated when no Cds1 is present). This data inferred that Cds1 was required to maintain the RF in a stable conformation, and in its absence RF may be converted to a form that resembled DNA damage (see 1.4.5 for details).

Cds1 can coordinate further replication, inhibit DNA repair, help stabilize stalled forks and delay cell-cycle progression (Murakami and Okayama, 1995, Miyabe et al., 2009, Paparatto et al., 2009). The latter is primarily obtained through phosphorylation of Mik1 and of Wee1, proteins that determine timing of the G2/M transition (O'Connell et al., 1997).

1.4.3 Stalled and collapsed replication forks

When a replication fork is stopped in a stable configuration, that is the RF complex remains intact and associated with the DNA, it is termed a 'stalled fork'. The exact make up of a stalled fork is loosely defined, but is generally considered to be a RF that can be restarted after the block is repaired or removed. The ability to do this requires the replication fork complex to be maintained (Friedel et al., 2009). Studies in *S. cerevisiae* showed that deletion mutants of Mec1 (Rad3$^{S.\ pombe}$) and Rad53 (Cds1$^{S.\ pombe}$) were unable to complete replication after MMS treatment showing that the S phase checkpoint response is required for RF restart (Friedel et al., 2009). Furthermore a hypomorphic mutant of *mec1; mec1-100,* has a specific role in preventing the late firing of origins, however these mutants are still able to complete replication after treatment with MMS (Tercero et al., 2003) supporting the hypothesis that an active checkpoint holds the replication fork in a stable conformation and is not responsible for initiating late firing origins. Cobb and collegues (2003) showed that Mec1 and DNA helicase, Sgs1 (Rqh1^{Sp}), were required to maintain association of polymerases with the stalled replication fork, but Rad53 kinase was not required (Cobb et al., 2003), suggesting that although checkpoint function is required to prevent RF dissolution there are additional functions for Rad53 (Cds1) in checkpoint control.

Without checkpoint activation an increase in aberrant DNA structures is seen suggesting that checkpoint function is vital for accurate maintenance of a stalled replication fork (Myung et al., 2001, Myung and Kolodner, 2002). In *S. cerevisiae* mutants of Mec1 (Rad3$^{S.\ pombe}$) and Rad53 (Cds1$^{S.\ pombe}$) were hyper sensitive to DNA damage and cell cycle arrest after HU treatment (Desany et al., 1998, Lopes et al., 2001, Tercero et al., 2003) further stressing the importance in checkpoint response in stability of DNA replication. The ability of Rad53$^{S.\ cerevisiae}$/Cds1$^{S.\ pombe}$ to stabilize replication forks was shown in *S. cerevisiae* using 2-D gels to study replication intermediates. A reduction in the amount of the arc, corresponding to Y shaped replication intermediates, suggested that replication was stopped or slowed in the presence of Rad53. This coupled with an increase of unusual DNA structures suggested that cells were not able to complete repair and accumulated aberrant recombination

products (Lopes et al., 2001). Similar data have been observed in an *S. pombe* strain defective in Cds1 (Noguchi et al., 2003, Noguchi et al., 2004, Froget et al., 2008, Ampatzidou et al., 2006). Noguchi et al. (2003, 2004) showed RF progression at the rDNA required the replication fork issegrega protein Swi1 in addition to Cds1, similarly to *S. cerevisiae*. Swi1 and Mrc1 have been shown to function in stabilizing replication forks (figure 1-2) and were shown to be defective in resuming DNA replication after and HU block and release. However it was also noted that the phenotype differs from Rad53 mutants as aberrant DNA structures were not seen on 2-D gels (Tourriere et al., 2005).

When maintenance of the checkpoint is lost, the replisome becomes dissociated from the stalled fork and the fork collapses, accumulating aberrant structures and joint molecules. The recombination machinery is required to restore the fork (Cox, 2002, Lambert et al., 2005). This process of restart is somewhat different to that in prokaryotes where RecA-dependent replication fork restart is largely dependent on the formation of a fork reversal intermediate known as the chicken foot structure. This structure is equivalent to a Holliday junction and can be resolved by branch migration or by cleavage at the HJ site (Seigneur et al., 1998, Courcelle et al., 2003).

1.4.4 DNA damage checkpoint and collapsed replication forks

When replication cannot be restarted and the replication machinery is disassociated during fork collapse the DNA damage checkpoint that usually controls G2/M transition can become activated. The exact nature of this process is not known but it is thought that structures such as DNA lesions, breaks associated with replication forks and cleaved regressed replication forks can trigger an additional checkpoint response (Cimprich and Cortez, 2008, Shiotani and Zou, 2011). Activation of the DNA damage checkpoint leads to the recruitment of several proteins that have a role in S phase checkpoint response, suggesting that there is some crossover between pathways (O'Connell et al., 2000).

In humans ATM (Tel1[Sp,Sc]), is the main sensor protein of DSBs and serves as the primary mediator for DNA damage checkpoint response. ATM exists as a heterodimer,

however upon exposure to DNA damage the isseg breaks apart and the resulting monomers auto-phosphorylate due to the conformational change (Bakkenist and Kastan, 2003). Proteins that accumulate at the site of a DNA break such as the MRX complex, Mre11-Rad50-Xrs2^{Sc} (or Rad32-Rad50-Nbs1^{Sp}) are essential for the recruitment of ATM to the break site (Paull and Lee, 2005). However some of this pathway is redundant in yeast and Rad3^{Sp} or Mec1^{Sc} (ATR^{Hs}) are the main sensors for both the S phase and DNA damage checkpoint responses as DSBs are rapidly converted to ssDNA that activates ATR^{Hs}/Rad3^{Sp}. Deletion of tel1Δ (ATM^{Hs}) in *S. pombe* or *S. cerevisiae* has little effect on checkpoint activation (O'Connell et al., 2000).

In *S. pombe*, during the DNA damage response the checkpoint protein Chk1 (rather than Cds1) is activated by phosphorylation by Rad3, mediated by Crb2. Crb2 has two BRCT domains that bind phosphorylated or methylated histones formed in response to DNA damage (Kilkenny et al., 2008). Rad3 mediates Chk1 interaction with Crb2 after DNA damage and activation of the Chk1 kinase directly leads to mitotic delay.

1.4.5 Cell cycle arrest and recovery

Both DNA damage and S phase checkpoint activation lead to delay of cell cycle progression. The DNA damage response checkpoint kinase Chk1 and the S phase checkpoint mediator Cds1 phosphorylate Cdc25 to inhibit its activity (Furnari et al., 1999, Zeng and Piwnica-Worms, 1999). Chk1 and Cds1 have also been shown phosphorylate Wee1, increasing its activity (Boddy et al., 1998, O'Connell et al., 1997). Both events reinforce inactivation of Cdc2 through maintained phosphorylation on the tyrosine15 (Y15) and cause cell cycle delay (O'Connell et al., 1997).

When DNA damage occurs, whether at a damaged replication fork or a DNA break, DNA resection leads to the generation of ssDNA (Byun et al., 2005). This ssDNA coupled with the disturbance of replication forks enzymatic activity are through to lead to the recruitment of checkpoint proteins. (Recolin et al., 2012) After DNA repair, or the cause of replication stress has been removed the checkpoint signal is lost as there is no longer any ssDNA. It has been shown that the phosphotase Dis2 is involved in the timing of release of the checkpoint block (Calonge and O'Connell, 2008, den Elzen and

O'Connell, 2004, Harrison and Haber, 2006).

In humans HR is not always the most reliable method of repair for DSBs, the choice between repair pathways is dictated by the level of 5' resection. The production of ssDNA is inhibited by Rif1 and mediated by 53BP1, the prevention of resection reduces the amount of ssDNA preventing HR and checkpoint activation, instead promoting repair by the more regularly used repair method NHEJ (Zimmermann et al., 2013).

1.5 Homologous Recombination

Eukaryotic cells have multiple pathways for the repair of DNA damage, examples include: nucleotide excision repair (NER), non-homologous end joining (NHEJ) and homologous recombination (HR). DNA damage from external agents such as IR can lead to DSBs, which in yeasts are primarily repaired via HR (Raji and Hartsuiker, 2006). Encountering a DNA lesion can lead to RF stalling or collapse (Raji and Hartsuiker, 2006). Mus81 can cleave stalled replication forks generating double strand breaks that must be repaired to start replication (Hanada et al., 2007) (see section 1.8). HR is also required for replication restart at collapsed replication forks (Humpal et al., 2009, Lambert et al., 2005).

At a DNA DSB break free ends are found that must be processed before repair can take place. The MRN complex, composed of Rad32^{Sp} (Mre11^{Sc})-Rad50-Nbs1 binds the ends of the DNA break with the help of protein Ctp1 (Limbo et al., 2007). It is proposed that MRN holds the ends of the break together while waiting to recruit repair machinery (as defined in *S. cerevisiae* (de Jager et al., 2001, Lobachev et al., 2004). For HR to occur 3' ssDNA ends of DNA must be available for a homology search and these are exposed by resection of the 5'-3' strand by Exo1 and Sgs1 helicases. (figure 1-3 (A-B)).

Exo1 is required for strand resection and plays an important role in repair of a collapsed fork (figure 1-3 (C)). However while resection occurs in G2 cells that have been exposed to DNA damage Rad53 prevents Exo1 resection at stable stalled replication forks preserving their structure and priming them for restart without the
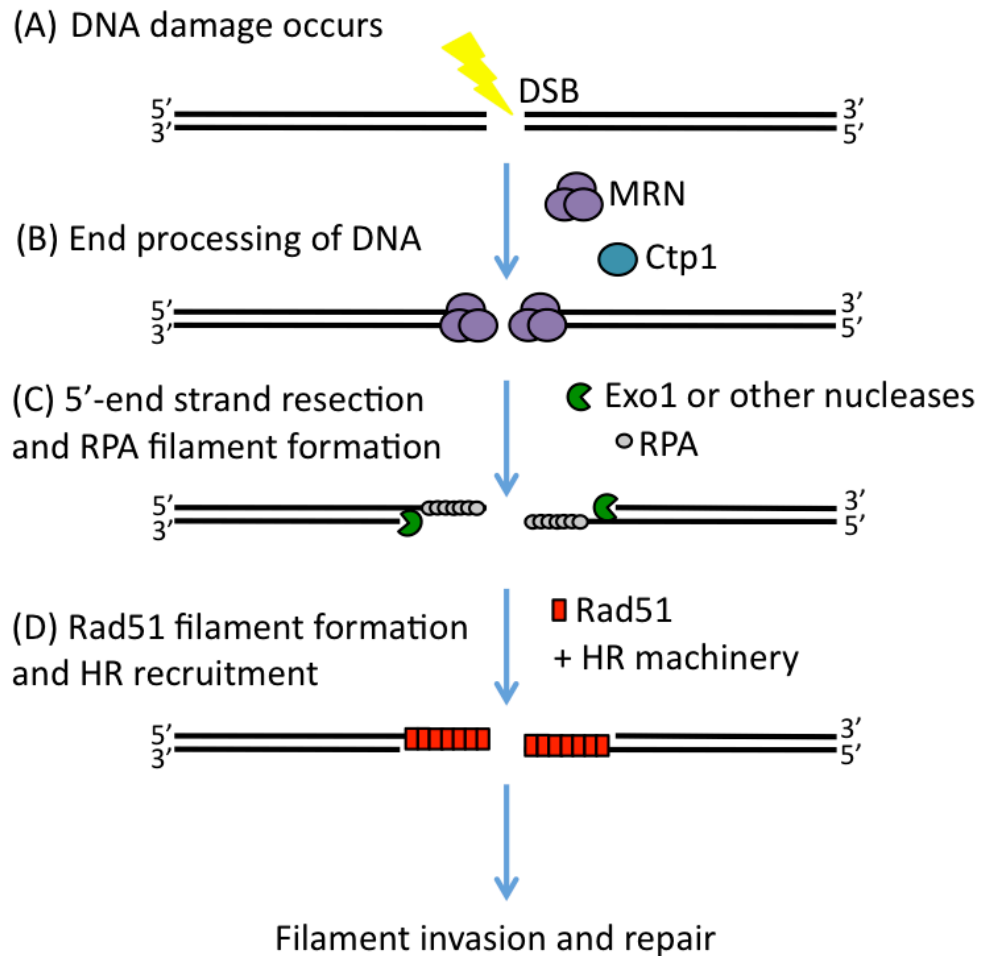
Figure 1-3 Initiation of homologous recombination
(A) Double strand breaks are formed as a result of DNA damage. (B) MRN is recruited to DSBs in the early with the help of Ctp1 to hold the DNA ends together before resection. (C) 3' DNA is usually resected by Exo1 but can be also resected by other proteins. Once ssDNA is exposed it is coated by RPA. (D). RPA-coated single-strand DNA is replaced by Rad51-filament and HR machinery is recruited so that the filament can invade homologous DNA forming a D-loop.

need for HR (Segurado and Diffley, 2008, Cotta-Ramusino et al., 2005). In *S. cerevisiae, rad53Δ* mutants were seen to have a lower level of aberrant DNA structures after the deletion of Exo1 and *exo1Δ* cells were able to restore viability in *rad53Δ* mutants in MMS. However, this was not the case in cells treated with HU, where replication intermediates were reduced, but viability was not restored. These data suggested that there was an Exo1 independent role for RF stabilization in cells blocked with HU, but when cells were exposed to DNA damaging reagents Exo1 was required for repair of the collapsed fork.

The free 3' ends become coated with RPA. This loading of RPA can function in the activation of checkpoint response and by inference cell cycle delay while DNA repair takes place. The recombination mediator protein Rad52 promotes binding of Rad51 to the RPA coated DNA displacing the RPA and creating a Rad51 filament by wrapping around the ssDNA (figure 1-3 (C-D) (Song and Sung, 2000, Sung, 1997b, Sung, 1997a). This filament protects the ssDNA and its formation is also promoted by the Rad55-57 heterodimer and Rad54. Rad55-57 and 54 are required during the search for homology and strand exchange (Heyer et al., 2006). Once a homologous region is found the free 3' end of DNA invades the new template forming a D-loop where DNA is copied along the template and a new strand is synthesized.

Resolution of the HR event is thought to be via the double-strand break repair model (DSBR). This model suggests that after D-loop formation and copying the DNA creates at least one double Holliday junction (HJ) that can be resolved by crossovers or non-crossovers events depending on the orientation of cleavage by a resolvase. In *S. pombe* the Mus81-Eme1 heterodimer is able to cleave HJs and can form gene conversion events containing a crossover (Osman et al., 2003). HJs can also be recovered by dissolution by Rqh1-Top3 (as discussed in section 1.7), and this leads to a non-crossover product (Doe et al., 2000) (Figure 1-4 (A)).

HR in *S. pombe* is also dependent on checkpoint protein Cdc2 (section 1.2). Cdc2 mutants are unable to form Rad51 filaments early in the recombination process, but

Figure 1-4 – HR at a double strand breaks and at a replication associated se-DSB

(A) HJ resolution: at DSBs resection allows for 3' strand invasion and second end capture forming double HJs. DSBR can resolve double HJs with or without crossovers depending on how the HJs are resolved (black dashed arrows). (B) HJ dissolution: HJ branch migrates and the strands are decatenated to restore the DNA. This action is dependent on Rqh1/Top3 (green dashed arrows). (C) In BIR only one Rad51 filament invades homologous DNA. DNA is extended until SRS2 helicase (purple arrow) is requires to resolve the D-loop. (D) Restoration of replication forks at a se-DSB: Strand resection allows for 3' invasion and D-loop nicking by Mus81 (yellow dashed arrow) allows the fork to be restored by gap filling (Roseaulin et al., 2008).

Two End

DSB

5'-3' Resection

Strand Invasion

D-loop Extension

HJ Processing

Resolution (non-crossover)

Resolution (crossover)

Dissolution (non-crossover)

DSBR

(A)

(B)

One End

DSB at a Replication Fork

5'-3' Resection

Strand Invasion

D-loop nicking

Gap Filling

Fork re-establishment

BIR

se-DSB repair at a replication fork

(C)

(D)
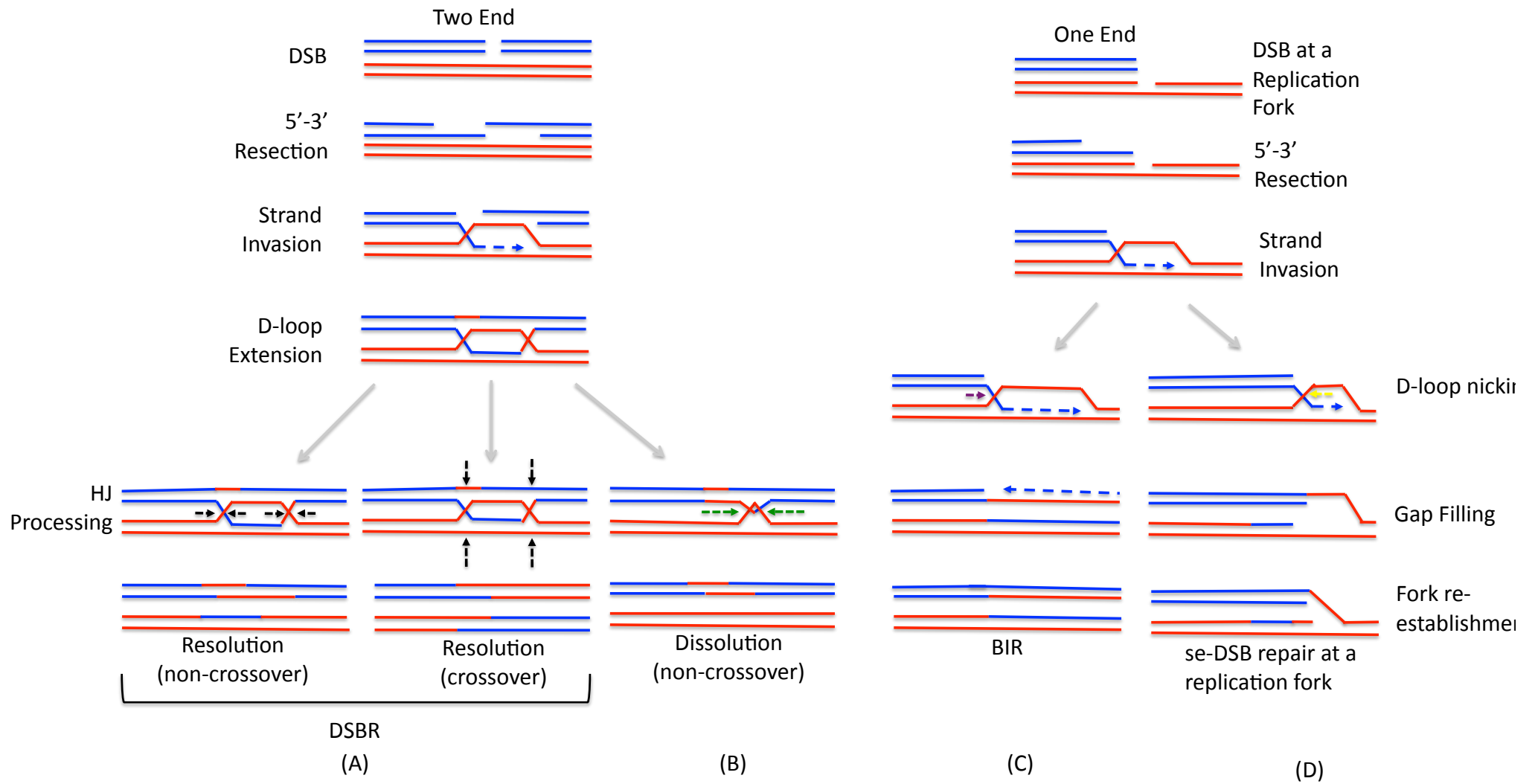
are also unable to resolve the recombination intermediates due to an improper regulation of Top3. Crb2, another protein that functions in checkpoint activation, mediates this function of Cdc2 in HR. The fact that checkpoint proteins have important roles in HR further emphasizes the importance of thorough regulation of HR in order to minimise the effects of DNA damage (Caspari et al., 2002).

1.6 Repair by break induced replication

Break-induced replication (BIR) is a type of recombination associated replication repair. It is related to the PriA-dependent error-free replication restart seen in prokaryotic organisms (Gabbai and Marians, 2010). BIR is a one sided repair event where only one 3' end is available to invade a homologous region and no double HJ is formed during repair (figure 1-4 (C)). BIR has been primarily analysed in *S. cerevisiae* using non-homologous chromosomes where only one region at the break site has homology leading to a repair event limited to one 3' invasion. Site-specific endonucleases such as HO have been used to investigate this situation and BIR was seen to copy DNA from the non-homologous chromosome downstream from the break site . One hypothesis to explain this phenomena is that the free 3' end from only 1 ssDNA-Rad51 filament invades the sister to form a one-sided D-loop structure. The strand is extended by DNA polymerase and cleaved in a manner dependent on *SRS2^{Sc}* forming a replication fork, that can be used to complete repair (Lydeard et al., 2010). This model requires SRS2 helicase for resolution of the D-loop in *S. cerevisiae* and Rqh1 is required to move the filament back to the original strand. This repair method may by issegre by cells in order to help to prevent DNA rearrangements by limiting crossing over (Ira et al., 2003, Llorente et al., 2008).

1.7 RecQ helicases in replication fork reset

S. pombe Rqh1 is part of the RecQ helicase family and is homologous to Sgs1[S. cerevisiae] and BLM/WRN[humans] (Murray et al., 1997, Stewart et al., 1997). Mutants of these proteins lead to hyper recombination events (Watt et al., 1996). In *S. cerevisiae* Sgs1 is recruited to origins of replication and associates with the replication fork

(Cobb et al., 2003). It is also requires for full checkpoint activation during S phase (Willis and Rhind, 2009) and an interaction has been observed between the FHA region of Rad53 and Sgs1 (Bjergbaek et al., 2005). Both Sgs1 and Mec1 were required for DNA polymerase α and ε to remain associated with stalled replication forks (Cobb et al., 2005). It is thus proposed to have a role in preventing stalled fork collapse.

RecQ helicases have a role in HJ resolution. In *S. pombe* Rqh1 was required for viability after UV damage in G2 and *rqh1Δ* was defective in HR repair at a stage after Rad52 focus formation (Laursen et al., 2003). In *S. cerevisiae* over expression of Sgs1 has been shown to suppress the formation of crossovers (Ira et al., 2003) when paired with Top3. BLM and Sgs1 have been shown to act together with Top3 to dissolve HJs without the formation of crossing over (Ahmad and Stewart, 2005) and its proper function is related to checkpoint activation dependent on Crb2 (Caspari et al., 2002) (figure 1-4 (B)).

These studies support the idea that in order to preserve DNA integrity RecQ helicases and Top3 have multiple functions at stalled and collapsed replication forks to ensure that resetting and repair do not result in crossing over. In *S. pombe rqh1Δ* mutants that were blocked in replication by HU were able to complete DNA synthesis on release but were found to have improper chromosome segregation (Stewart et al., 1997). This aberrant segregation is consistent with the hypothesis that Rqh1 and Top3 are required to prevent recombination events at collapsed replication forks. Sgs1 prevents recombination at stalled forks in *S. cerevisiae* rDNA, regions of DNA that stall frequently (Versini et al., 2003). As in *sgs1Δ* after exposure to MMS, unresolved recombination intermediates accumulate indicative of a defect in HJ resolution (Liberi et al., 2005).

1.8 Mus81

1.8.1 Overview of Mus81

Mus81 was first identified in *S. pombe* by its interaction with the checkpoint kinase Cds1 (Boddy et al., 2000, Interthal and Heyer, 2000). It forms a complex with Eme1 which has shown to have endonuclease activity, in particular in response to replication

stress (Chang et al., 2008). Studies suggested that Mus81 functions as a HJ resolvase and genetic data support a role in resolving nicked HJ *in vivo* (Gaskell et al., 2007). Mus81 was found to act on several different RF like Y structures and D-loops formed during 3' invasion (Whitby et al., 2003). A role in the resolution of D-loops at 3' invading DNA ends at a arrested replication fork may suggest a role for Mus81 in the specialize form of repair BIR (break induced replication) as described earlier. It was though that Mus81 plays a key role in resolving DNA structures that occur before HJ formation, a role that may compete with that of RecQ/Top3 discussed earlier (section 1.7). *mus81Δ rqh1Δ* double mutants show synthetic lethality that can be rescued by the removal of recombination factors (such as Rad51), indicative of overlapping roles in the resolution of recombination (Doe et al., 2002, Fabre et al., 2002).

Based on this, it could be proposed that both Rqh1-Top3 and Mus81-Eme1 are able to process structures that result from the repair of collapsed replication forks, but the one used is dependent on that nature of the stall and the type of damage. Rqh1-Top3 would function to maintain arrested forks and ensure restart without crossovers. Mus81-Eme1 could function to restore replication at broken forks where recombination events were required (figure 1-4 (D)). This hypothesis is supported by the observation that the deletion of *rqh1*, where most repair must be performed by Mus81, shows an increase in recombination mutants.

1.8.2 Mus81 activity at a se-DSB

A study into the role of Mus81 at the *S. pombe mat* locus utilized mating-type switching as a way of studying arrested replication forks . Mus81 was shown not to be required for mating-type switching process as Swi9 and Swi10 are responsible for cleaving the joint molecules formed during switching instead. However, it was required for the repair of *mat1* when the *mat2* and *mat3* donors were not present. The results of this analysis showed that Mus81 was required for the repair of a single-ended double strand break that is formed as the result of a replication fork encountering a 'DNA lesion', in this case a modified 'imprint' in DNA. Joint molecule intermediates were seen to accumulate, consistent with a requirement for Mus81 activity to reset the fork during HR-dependent restart. This is discussed in further detail in chapter 4

and 5.

1.9 Mating-type switching

1.9.1 Overview of mating-type switching

The process of mating-type switching occurs naturally as part of vegetative growth in *S. pombe* cells (Leupold, 1970). It occurs during S phase and over two cell cycles (Arcangioli and de Lahondès, 2000). Recently, better understanding of mating-type switching has led to new tools for utilising this system to study other aspects of the DNA repair machinery (these are discussed in the introduction to Chapter 4).

The mating system in *S. pombe* was initially characterised in the 1950s and patterns of sexual reproduction, meiosis and sporulation were investigated by U. Leupold. Early observations showed that *S. pombe* grows vegetatively as a haploid with two mating-types (Leupold, 1970). Heterothallic (mixed parent) *S. pombe* cells express one of two mating-types, *h+* (plus P) and *h-* (minus M), and during times of nutritional stress (particularly nitrogen starvation (Egel, 1971) these cells can conjugate forming a diploid zygote. Diploids are a relatively transient stage of the *S. pombe* sexual cycle and rapidly undergo meiosis to produce four haploid spores. These tetrads contain two of each mating-type and contribute to the diversity of the *S. pombe* cell culture.

In addition to h^+ and h^- there is a third mating-type, h^{90} (that is considered to be the 'original yeast' as it is found naturally in the environment), that is demonstrated to have homothallic properties in that mating, meiosis and sporulation can occur within a colony originating from a single cell. The original characterisation showed that in h^{90} strains 90% of cells from a single colony would form spores when under nutritional stress (Egel, 1977). Furthermore it has been shown that h^{90} is capable of mating with heterothallic *h+* and *h-* strains producing a 2:2 segregation of h^{90} to h^+/h^- spores.

Diploid cells enter meiosis spontaneously, and sporulation is only possible if the mating-type alleles are both h^+ and *h-* to ensure correct 2:2 segregation (Egel and Eie, 1987). Sporulating cells form a starch-rich ascus around the spores that is stained dark black or grey upon exposure to iodine. It was observed that h^{90} colonies would stain

darkly most of the time but occasionally a non-sporulating colony would be observed (a rate of approximately 1/300) (Bresch et al., 1968). Isolation of these non-sporulating colonies formed the basis for the first studies on genes involved in meiosis and sporulation.

The first observations regarding the mating-type (or *mat*) region were by Leupold who examined crossing over in the mating-type region and proposed the presence of two genes that confer a mating-type that could spontaneously rearrange to produce heterothallic h^+ and h^- strains. The hypothesis that homothallism was caused by frequent mutation from *h+* to *h-* and vice versa was first stipulated by (Gutz and Doe, 1975), who tested several strains from different geographical origins for hetero and homothallism. All *S. pombe* strains tested were found to behave in a manner similar to the previously characterised strains. Further re-arrangements in the "mat locus" were investigated and discussed in (Gutz and Doe, 1973, Meade and Gutz, 1976) with additional characterisation of h^{+N}, h^{-S} (stable), h^{-U} (unstable), among others (table 1-1), demonstrating that different alleles in the *mat* locus could potentially re-arrange to other mating-types providing further evidence for a multi-loci mating-type switching system.

As an organism that preferentially grows in the haploid state it can be assumed that a mating-type switching system would be evolutionary beneficial to *S. pombe* as it would ensure that a population would remain sexually mixed during vegetative growth, thus allowing mating and sporulation when subjected to nutrition and other stresses. The switching process itself was studied in detail by following a homothallic *h90* strain during successive generations of mitosis and meiosis on sporulation media. It was discovered that only one in four daughter cells in two successive generations switched mating-type (Miyata and Miyata, 1981).

1.9.2 The *mat* locus

The current model of a three gene system that switched by transposition was first hypothesised and confirmed by (Egel and Gutz, 1981), (Beach et al., 1982, Beach, 1983).

Strain	Imprinting	Donors	Switching	Description
h^{90}	Yes	Yes	Yes	Original unmodified *S. pombe* switching strain
h^{+N}	No	Yes	No	Complete donors with duplication of *mat2* and *mat3* between the *mat1* cassette
h^{-S}	Yes	No	No	Intact *mat1* fused *mat2:3*
h^{-U}	No	Yes	No	Complete donors with duplication of *mat2* and *mat3* between *mat1* cassette. Has a tendency to revert to h^{90} of h^{+N}
h^{-L}	No	No	No	Fused *mat1:3* and episomal *mat2:1*

Table 1-1 –Some common rearrangements of the *S. pombe mat* locus
Name and structure of *mat* locus rearrangements and the strains ability to imprint and switch are shown. Whether there are intact donors is also shown in the table.

Southern blot analysis of h^{90}, h^+ and h^- genomic DNA hybridised with the plasmid pMT$_{3.2}$ that carried *mat*-P (h^+) activity (Beach, 1983) showed that the *mat* locus consisted of three similar loci that were named *mat1*, *mat2-P* and *mat3-M*. Electron microscopy and hybridisation showed that all three loci showed homology to each other, but hybridisation of the *mat* regions to each other formed heteroduplex DNA between *mat2-P* and *mat3-M* and additionally between *mat1-P* with *mat3-M* and *mat1-M* with *mat2-P.* The flanking regions of these genes would form about 60bp of homologous DNA either side of all three *mat* genes. These regions were termed H1 and H2 (Beach, 1983), all three *mat* genes are flanked directly by these two homology boxes with an additional H3 homology box present next to H2 in *mat2* and *mat3*. The "H" regions have close homology and are able to help facilitate homologous recombination between *mat1* and *mat2* or *mat3* during the switching process (Arcangioli and de Lahondès, 2000) (figure 1-5 (A)). The H regions are essential for accurate switching as the homology of the H1 boxes allow for 3' invasion once the se-DSB is made (see section 1.9.5). The copying of the new *mat* cassette during mating-type switching leads to the formation of heteroduplex DNA and upon the arrival of the new strand at the H2 homology box the newly synthesised strand can anneal to the H2 box of the original *mat1* cassette. This annealing can then be resolved by the HR machinery and nucleases Swi9 and Swi10. It is also thought that the H3 box is also required to terminate copying of the new strand most likely through the formation of a stem loop structure leading to the annealing of the new strand at H2 (Schmidt et al., 1989, Egel et al., 1984b).

In addition to *mat1*, *mat2* and *mat3* a further component of switching competence was also mapped to the *matI* locus close to *mat1*. The *smt*, or switching of mating-type, element was found to be essential for switching, an *smt* mutant named *smt0* has a 263bp deletion region upstream of *mat1* H1 but the rest of the *mat* locus remains intact.

The *mat* locus is situated on the right arm of chromosome II (Egel, 1980) and stretches over 30Kb. The locus also consists of two spacer regions between the *mat* genes; the L-region between *mat1* and *mat2* and the K region between *mat2* and *mat3*.

Figure 1-5 *S. pombe* mating-type switching

(A) The *S. pombe mat* locus. *mat1* (white box) is flanked by regions of homology H1,2 and 3 (pink boxes) and has *mat2* and *mat3* silenced donor regions downstream. (B) During the first S phase and imprint is made on the lagging strand. (C) The imprint is converted to a se-DSB during the second S phase. (D) Swi2/5 helps to initiate strand invasion of the correct downstream donor at the H1 homology box. (E) Swi9/10 resolve recombination intermediates between *mat1* and the donor. (F) The lagging strain re initiates. (G) Switching is finished, one sister is switched, one is imprinted (adapted from Roseaulin et. al., 2008)

(A)

Active
mat1

Silent
2P   *3M*

RTS1

H3

H2   H1

Imprint
Site

smt0

L Region

K Region

Centromere

Telomere

(B)

1st S phase

RTS1

mat1

Imprint

(C)

2nd S phase

RTS1

mat1

se-DSB

(D)

Donor
cassette

mat2 or mat3

RTS1

mat1

Swi2/5

(E)

Swi9/10
dependent
cleavage

mat2 or mat3

RTS1

mat1

(F)

RTS1

mat1

(G)

Switched *mat1*
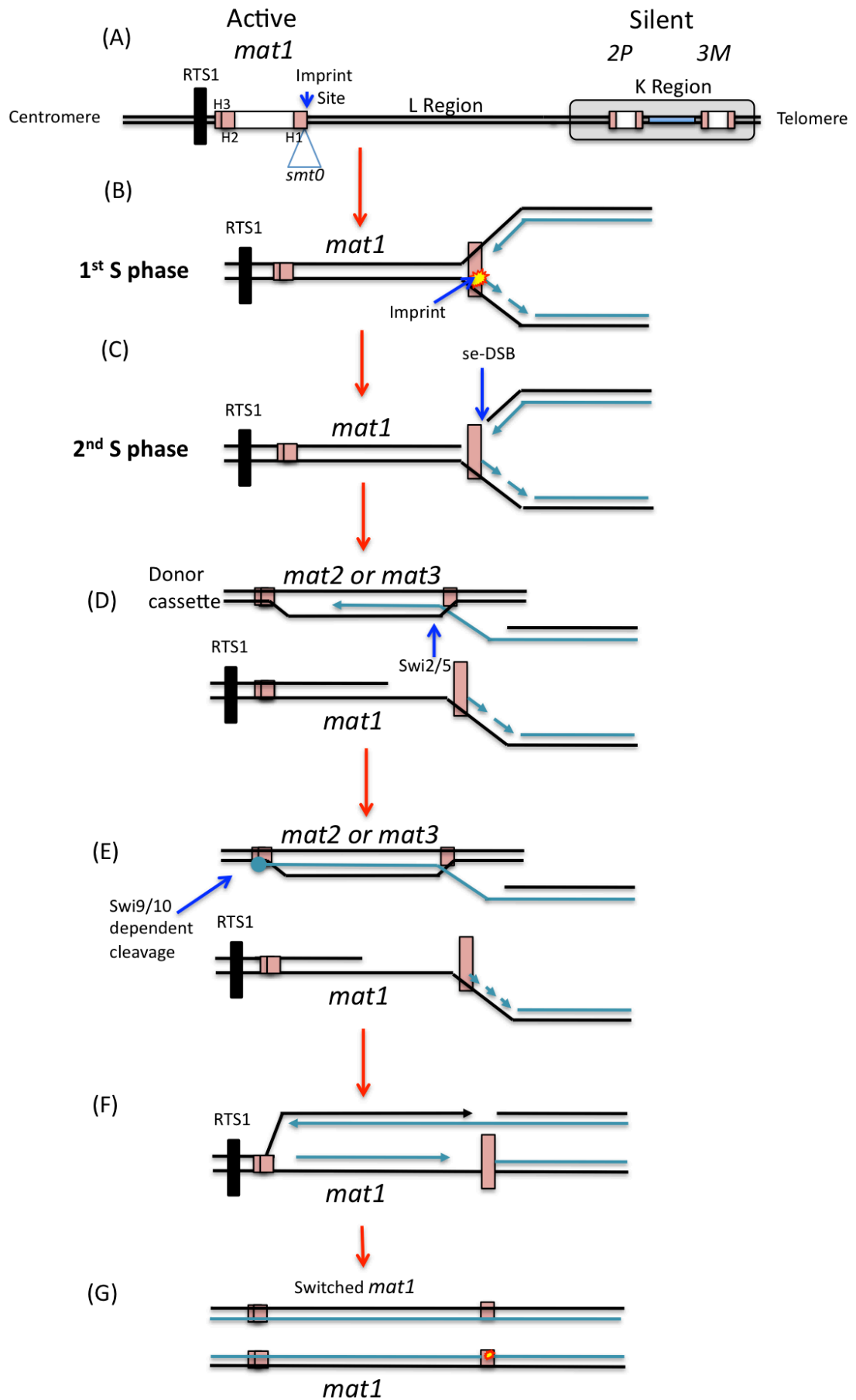
mat1

Both the 17Kb L region and *mat1* are transcriptionally active with *mat1* expressing the mating-type pheromones (Kelly et al., 1988). Pheromones are diffusible proteins produced at the *mat1* locus and induce mating-specific changes in cells of the opposite mating-type that are required for successful mating and sporulation (Nielsen and Davey, 1995). The 11Kb K-region contains centromeric repeats and is flanked on either side by inverted repeats that are thought to be involved in silencing of the *mat2,3* region (Singh and Klar, 2002). This region has a highly regulated heterochromatic structure (Grewal and Klar, 1997) where not only are levels of transcription reduced but levels of recombination are repressed in a Swi6 dependent manner, this has led to the region being known as a cold spot (Klar and Bonaduce, 1991).

1.9.3 Switching mutants

Switching mutants were initially defined as stains where the numbers of switching colonies produced from a cross with a homothallic strain were reduced (Meade and Gutz, 1976, Egel and Gutz, 1981). Genetic analysis of the mutants assigned them to linkage groups and classes based on their levels of recombination and the type of mottled and iodine-negative staining (Egel et al., 1984a). Southern blot analysis of *Hin*dIII digested DNA with a *mat1-M* probe revealed fragments that corresponded to a double strand break (DSB) being made in the *mat1* region designated <u>S</u>witching of <u>M</u>ating-<u>T</u>ype (or *smt*). The ten switching-defective mutants were named *swi1* to *swi10* and were split into three classes: class Ia was unable to make the break at the *smt* site (*swi1*, *swi3*, and *swi7*), class Ib made the break but could not select an appropriate donor for the repair of the break (*swi6*, *swi2* and *swi5*) and class II was defective in the termination of the switch (*swi4*, *swi8*, *swi9*, *swi10*) (Gutz and Schmidt, 1985). (The details of these different mutants is discussed throughout sections 1.8.4 and 1.8.5)

This analysis of these non-switching strains by Southern blotting revealed the nature of the *mat* locus in stabilised non-switching strains and provided information about the structure of the *mat* locus.

Gene	Class of switching mutant	Defect			Function
		Imprinting	Switching	Resolution	
swi1	Ia	-			Fork protection complex
swi2	Ib		-		Homology search and donor recognition
swi3	Ia	-			Fork protection complex
swi4	II			-	Mismatch repair
swi5	Ib		-		Homology search and donor recognition
swi6	Ib		-		Heterochromatin association protein
swi7	Ia	-			DNA polymerase α
swi8	II			-	Mismatch repair
swi9	II			-	Excision repair
swi10	II			-	Excision repair

Table 1-2 – *S. pombe* switching mutants

Names of the switching genes in *S. pombe* are included in the table along with the defined class of each mutant. The part of the switching process each gene is defective in and the known function of each gene is also shown.

1.9.4 Switching Initiation and Imprinting

Mating-type switching occurs during S phase and over two mitotic divisions (Arcangioli and de Lahondès, 2000). A replication fork passing through the expressed *mat* locus, *mat1*, is stalled at the polar <u>mat1</u> <u>p</u>ause <u>s</u>ite (MPS1) during the first division (Dalgaard and Klar, 2000, Dalgaard and Klar, 2001b) to allow the introduction of an imprint in the DNA. Homologous recombination is utilised during the second S phase to repair the single-ended double-strand break (se-DSB) caused by replication of the 'imprint (Kaykov et al., 2004).

The programmed fork stalling and introduction of the modified 'imprint' in the lagging strand is dependent on replication passing through *mat1* from the telomeric side. Most replication occurs in this direction due to efficient firing of an origin in the L region. Replication from the other direction is prevented by the replication termination site (RTS1) on the centromeric site of *mat1* (Dalgaard and Klar, 2001a). The DNA is copied until the replication fork reaches MPS1 (Dalgaard and Klar, 1999), adjacent to H1 homology box where replication is stalled stably dependent on Swi1 and Swi3, components of the fork protection complex (Noguchi et al., 2004). 2-D gel analysis of replication intermediates confirmed the role of Swi1 and Swi3 in imprinting as fork stalling at MPS1 was abolished in their absence (Dalgaard and Klar, 2000). Single stranded Southern analysis showed that as replication is stalled distal to MPS1 an 'imprint' is made to the lagging strand (Dalgaard and Klar, 1999, Dalgaard and Klar, 2001b) of the replication fork. Class Ib mutant *swi7* (polα) has been implicated in the generation of the imprint and analysis showed that the mutation altered the catalytic subunit of DNA polymerase-α implicating Pol α as the polymerase that introduces the imprint to newly replicated DNA (Singh and Klar, 1993) (figure 1-5 (B)).

The precise nature of the imprint is still a cause for debate. Initial evidence that the imprint was a double-strand break was dismissed as an artefact of DNA preparation techniques as it was no longer detected after DNA was prepared in agarose plugs using a more gentle technique (Arcangioli, 1998). More recent evidence has suggested that the imprint is either a two-ribonucleotide insertion (as characterised by a ligation-

mediated PCR) (Vengrova and Dalgaard, 2006) or a strand-specific modified nick with a 3'OH and 5'OH termini (Kaykov and Arcangioli, 2004).

The imprint is maintained throughout the cell cycle until the next S phase. Swi1 and Swi3 have been implicated in this preservation and the prevention of checkpoint activation and DNA repair mechanisms during the first round of replication (Noguchi et al., 2003). Once replication is completed the sister chromatid with the imprint is segregated into one daughter while the unimprinted sister chromatid is segregated into the other daughter cell.

1.9.5 Second division

In the next cell cycle the imprint is on the strand replicated by the nascent leading strand and is the catalyst for the second half of the switching process. The replication fork encountering the imprint causes replication arrest, the leading strand becomes disassociated from the lagging strand, resulting in a one sided blunt-end DNA break (figure 1-5 I) (Kaykov et al., 2004). This single-ended DSB is a substrate for the DNA repair machinery and is processed so that the resulting free 3' end can be used in the search for homology in order to repair the stalled fork. Repair occurs by utilising the homologous sequence at the H1 in *mat2* or *mat3* as a substrate for HR.

The search for homology in neighbouring DNA regions is a process that is critical to mating-type switching. The inability to find the correct donor is characteristic of type Ib mutants like *swi6*, *swi2* and *swi5*. All three proteins are involved in regulating the heterochromatic structure of the donor region. Swi6 (HP1 homologue) is required for heterochromatin formation at the centromeric repeats in the K-region and the donors and helps prevent recombination in the *mat2-mat3* donor region (Klar and Bonaduce, 1991, Nakayama et al., 2000). Swi2 and Swi5 form a recombination mediator complex that is paramount in determining donor choice (Akamatsu et al., 2003).

The exact mechanism dictating donor choice is not yet determined but the distribution of the Swi2/5 complex over the silenced region is important in switching. This differs in *h+* and *h-* cells as in an *h-* cell the Swi2/5 complex binds across the whole of the

chromatin region. This facilitates the free 3' end of the *mat1* locus preferentially finding homology in the closer *mat2P* locus (Jia et al., 2004). The distribution differs in an *h+* cell as the Swi2/5 complex is only present on the silent *mat3M* locus, causing a greater binding affinity for the *mat3M* locus so that the 3' tail can invade the chromatin more easily than at the unbound *mat2P* locus , even though *mat2P* is in closer proximity to the DSB at *mat1*. This ensures that the cell will always switch from an *h+* cell to an *h-* cell and vice versa.

The 3' end of the DSB at *mat1* invades the region of homology in the H1 boxes of the *mat3M* or *mat2P*, and the DNA in the donor cassette is replicated to the H2/H3 boxes (figure 1-5 (D)). The H3 box has a sequence that has evolved to form a series of stem loops. This secondary structure is cleaved in a Swi9/10 and Rad16 dependent manner (Carr et al., 1994) (figure 1-5 (E)) forming a free 3' end that invades the homologous H2 region at *mat1*, completing the ectopic recombination event.

At *mat1* the original template strand is degraded and the leading strand copied from the *mat* donor. Replication on the lagging strand resumes creating a new imprint (figure 1-5 (F-G)).

1.10 Introduction to SMCs
1.10.1 Introduction and prokaryotic SMCs
The Structural Maintenance of Chromosomes (SMC) family of proteins is an important group of structurally related proteins that are conserved throughout eukaryotes and prokaryotes. In eukaryotic organisms there are at least 6 SMC proteins that have specific roles in chromosome dynamics and organisation. They are essential proteins that were identified using genetic viability screens in yeast (Strunnikov et al., 1993). In bacteria there are similar SMC proteins but these are typically reduced number or non-SMC functional homologues (Hirano, 2005). The bacteria *E. coli* does not have a direct homologue with high sequence homology, but has a issegrega-like chromosome maintenance complex called MukBEF (Niki et al., 1991, Yamazoe et al., 1999). MukB has little sequence homology to yeast and mammalian SMCs but has similar structural domains, a globular C and N terminal, coiled coil domains and a hinge region.

Additionally similar to the eukaryotic SMCs additional co-factors are required for a functional complex, these are MukE and MukF (Fennell-Fezzie et al., 2005). Temperature Sensitive (TS) Muk mutants have been shown to shown to lead to cells lacking chromosomes and deficiency in chromosome segregation (Yamazoe et al., 1999) a phenotype similar to the direct SMC homologues seen in *Bacillus subtillis* (Graumann, 2000). A recent study showed that issegr of MukB were bound at the globular domain by MukF. Furthermore it was shown that ATP hydrolysis broke the connection at MukF opening the structure. This study provided insight into the structural mechanism of bacterial issegrega and suggested that several MukBEF molecules may form rings around the DNA. Hydrolysis of MukF may open the ring and allow the accumulation of other factors and conformational changes to the DNA (Woo et al., 2009).

In *S. pombe*, *S. cerevisiae* and humans, there are 6 SMC proteins that are structurally similar, they function in heterodimeric pairs: Smc1/3 (cohesin) (Michaelis et al., 1997), Smc2/4 (issegrega) (Stray et al., 2005) and Smc5/6 reviewed in (Murray and Carr, 2008). Structural analysis suggests that all SMCs are similar in structure with two long coiled coil regions with a hinge region in the middle and globular amino and carboxyl groups at the terminal regions (Melby et al., 1998). The core SMC proteins interact with other proteins to form functional complexes.

1.10.2 Cohesin

Smc1 and Smc3 are the structural core of the cohesin complex, which contains two additional proteins Scc1 and Scc3 (figure 1-6 (A)) (Gruber et al., 2003). Smc1/3 have been shown to have a role in holding chromatids together during meiosis via sister-chromatid cohesion, identified in screens that showed improper chromosome segregation. In yeast cohesin is well characterised. It is loaded onto the chromosomes during S phase but is removed to allow sister chromatid separation at the metaphase anaphase transition (Uhlmann and Nasmyth, 1998). This is slightly different to higher organisms where most cohesin is removed at prophase leaving small amounts at the centromeres that are removed at the metaphase to anaphase transition (Waizenegger et al., 2000).

Figure 1-6 – Structural Maintenance of Chromosomes (SMC) Complexes
Diagram of the three SMC complexes found in yeast. (A) Cohesin's SMC elements are Smc1 and Smc3. The globular head of the complex is bridged by two non-SMC elements sister chromatid cohesion protein 1 (Scc1) and Scc3. (B) Condensin's ring structure is formed of Smc2 and Smc4 and the globular head domains are bound by Cnd1, Cnd2 and Cnd3 (also known as CAP-D2, CAP-G and CAP-H) (C) The Smc5/6 complex and its associated non-SMC elements. Nse1,3-5 are thought to interact with the ATP hydrolysis head region. Nse2 is associated with Smc5. Rad60 has been loosely associated with the complex. Hypomorphic mutants *smc6-X* (mapped to the hinge region) and *smc6-74* (close to the ATP hydroloysis domain) approximate locations are marked with arrows (adapted from Murray and Carr, 2008).

Cohesin

Hinge

Smc1   Smc3

Scc1

Scc3

(A)

Condensin

Hinge

Smc2   Smc4

H

D   G

(B)

Smc5/6

Hinge   *smc6-X* (A151T)

Smc5   Smc6

Nse2

Nse5   Nse6

Nse1   Nse4   *smc6-74* (R706C)

Nse3

Rad60
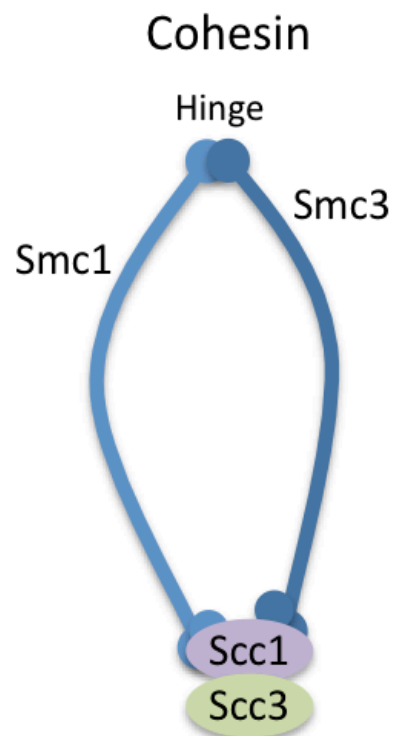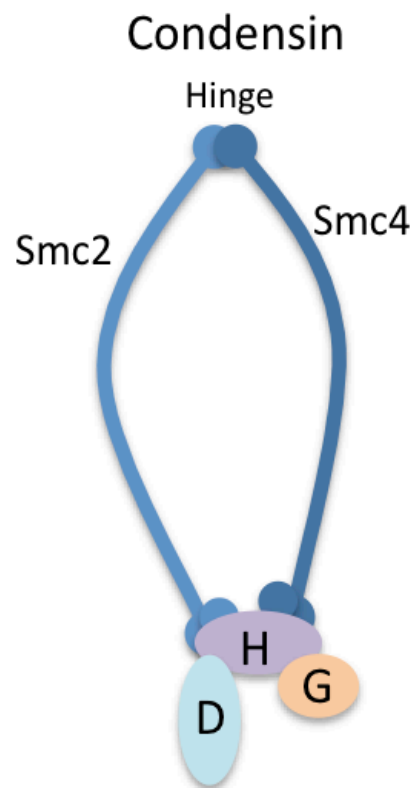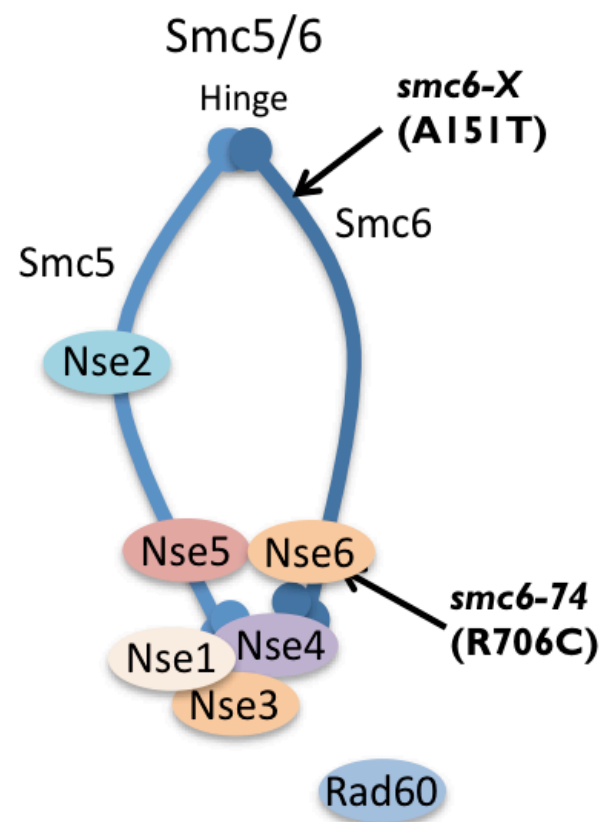
(C)

In both cohesin removal is mediated by separase dependent cleavage of Scc1 (Uhlmann et al., 1999). During Meiosis I cohesin remains along the arms of the chromosomes allowing homologues to separate but keeping the sister chromatids together (Klein et al., 1999). This remaining cohesin is cleaved during Meiosis II by separase dependent cleavage of REC8 (a meiotic specific variant of SCC1) (Buonomo et al., 2000). The correct association of cohesin during mitosis and meiosis is vital to cell viability as cells that do not maintain cohesion correctly fail to segregate chromosomes faithfully, conversely, in strains that cannot cleave cohesin with separase the chromosomes cannot segregate properly, leading to catastrophic mitoses (Hauf et al., 2001).

1.10.3 Condensin

Condensin, or the Smc2/4 complex, contains three other non-SMC proteins Cnd1, Cnd2 and Cnd3 (also known as CAP-D2, CAP-G and CAP-H) and forms a five protein complex (figure 1-6 (B)). The issegrega complex was discovered by purifying *Xenopus laevis* mitotic chromosomes (Hirano et al., 1997). Condensin is required to condensed chromosomes at mitosis. In *S. pombe* mutants of *cut3* and *cut14* (later confirmed to be Smc2 and Smc4) were observed to have a cut phenotype where the dividing septum 'cuts' through improperly segregated DNA (Saka et al., 1994). Condensin has been shown to bind DNA, dependent on its ATPase domain and to induce positicve supercoiling in the presence of type II topoisomerases (Kimura et al., 1999). It has been suggested that overall cohesin functions by stabilising loops of positively supercoiled DNA (Kimura et al., 1999).

1.11 Smc5/6

1.11.1 Smc5/6 Structure

At present the role of Smc5/6 is structurally but not yet functionally defined. Studies have shown that Smc5/6 is required for repair of DNA damage caused by UV-C and γ irradiation and that the complex is involved in homologous recombination (as reviewed by Murray and Carr 2008) with particular relevance to the repair of stalled or collapsed replication forks (Ampatzidou et al., 2006, Irmisch et al., 2009).

The Smc5/6 complex is made of the core proteins, Smc5 and Smc6, which interact with six <u>n</u>on-<u>S</u>mc <u>e</u>lements, or Nses (figure 1-6 I). Smc5 and Smc6 are more diverged in sequence than Smc1-4 but have conserved structural similarities to the other Smc proteins. Smc5 and Smc6 consist of two coiled-coil regions linked by a hinge region that has been shown to be essential for the to the interaction between the two proteins (Sergeant et al., 2005).

Smc5 and Smc6 are bridged by the Nse protein; Nse4. Nse4 has structural motifs that indicate a winged-helix and helix-turn-helix structure and is a member of the kleisin family. Other proteins in this family are Scc and Cap-H proteins found in cohesin and issegrega further supporting the relatedness of the SMC complexes as a whole (Palecek et al., 2006). Nse1 has a RING finger domain and the human NSMCE1 has been demonstrated to have ubiuitin E3 ligase activity when in complex with Nse3 (Pebernard et al., 2008a), which contains a MAGE (typeII melanoma antigen)-domain (Pebernard et al., 2004). Nse2 (NSMCE2 in humans) is different to other Nse elements as it does not interact with the globular head region but instead binds to the coiled-coil domain of Smc5 (McDonald et al., 2003). Nse2 has been shown to have a RING domain that is associated with E3 SUMO ligase activity and is required for the complex's function in DNA damage repair (Andrews et al., 2005). Nse5 and Nse6 are not highly conserved, while essential in budding yeast, they are not essential in *S. pombe* and deletion mutants have a slow growth and DNA repair defective phenotype (Pebernard et al., 2006). Nse5 has no known conserved domains and Nse6 has HEAT domain repeats.

In *S. pombe* another protein, Rad60 has been shown to loosely or transiently associated with the Smc5/6 complex (Morishita et al., 2002, Morikawa et al., 2004). Rad60 has been shown to be required for repairing DNA damage in S phase and is synthetically lethal with the hypomorphic mutant *smc6-X* (figure 1-3).

1.11.2 Smc5/6 localisation

In several model organisms it has been shown that Smc5/6 is associated with chromatin (Tsuyama et al., 2006, Taylor et al., 2001, Pebernard et al., 2008a,

Pebernard et al., 2008b). ChIP analysis was used to investigate the localisation of Smc5/6 along the whole genome in *S. pombe* and *S. cerevisiae* (Pebernard et al., 2008b, Lindroos et al., 2006). The pattern was similar to that of cohesin but unlike cohesin which is chromatin associated from S phase until its removal at anaphase, in budding yeast Smc5/6 is mainly seen at the G2/M transition. In fission yeast Smc5/6 was seen to be loaded genome wide during S phase, and in budding yeast it was seen to be enriched in intergenic sites. Smc5/6 was found at the centromeric regions and rDNA in both yeasts (Torres-Rosell et al., 2005b).

The rDNA region is difficult to replicate and it was hypothesised that Smc5/6 has a role in ensuring the correct replication of this region (discussed in section 1.10.4) (reviewed in Murray and Carr 2008). This hypothesis is supported by the observation that HU treatment of cells increases the association of Smc5/6 with rDNA in *S. pombe* (Pebernard et al., 2008b). However the same outcome is not observed in *S. cerevisiae*, in fact, there is an observed reduction in Smc5/6 enrichment after treatment with HU (Lindroos et al., 2006). In both types of yeast Smc5/6 has been seen to localise to telomeres (as above and (Torres-Rosell et al., 2005a).

1.11.3 Smc5/6 and DNA repair

Smc6 was originally identified as Rad18 in fission yeast as it was originally characterized as a radiation sensitive mutant (Nasim and Smith, 1975). Deletion mutants of Smc6 are lethal making direct genetic studies difficult and the use of hypomorphic mutants essential. In *S. pombe* mutants of Smc6 has been shown to be sensitive to DNA damaging agents (e.g. UV and IR) (Verkade et al., 1999). Two hypomorphic mutants *smc6-74 74* (Verkade et al., 1999) and *smc6-X* (Nasim and Smith, 1975) have been extensively characterized. They are sensitive to a range of DNA damaging agents, epistatic to HR defective mutants e.g. *rhp51* and proficient in checkpoint activation. However, it was observed that the delay was not sufficient to complete repair of the damage (Verkade et al., 1999).

In human cells site specific induced break sites were used to investigate the role of Smc5/6 in DSB repair response. It was shown that Smc5/6 did not localize at DSB sites

that would not be able to repair by HR, i.e. in G1 when no sister chromatid is available. The HR specificity of Smc5/6 was further confirmed when RNAi was used to knock down Smc5/6 activity during all stages of the cell cycle and repair activity was decreased in G2/M phase but not in G1 suggesting the Smc5/6 has little role in DSB repair at G1 (Potts et al., 2006). Accumulation at DSB sites was shown to be MRE11 dependent in budding yeast however the precise nature of its recruitment is unknown in other organisms (Lindroos et al., 2006).

One hypothesis for Smc5/6 role in DSB repair is in holding chromosomes together while a repair event can take place. This proximity of chromatids during repair has been shown as a role for Smc5/6 in budding yeast (Strom and Sjogren, 2007) however this has not directly been shown in other organisms. In humans Smc5/6 was shown to be required for the localization of Cohesin at induced double strand breaks but recently this was reported to be due to off target effects of the siRNA. In relation to this it has been shown that Nse2 targets two components of the cohesin complex for sumoylation however the function of these events is not known. (Potts et al., 2006, Wu et al., 2012).

1.11.4 Smc5/6 function at rDNA

Smc5/6 was shown to issegre at rDNA and this increases upon replication stress. Smc5/6 complex mutants have improper segregation of the rDNA and loss of HR does not restore the segregation defects (Torres-Rosell et al., 2005b, Torres-Rosell et al., 2007) This was unexpected as it suggests that the mis-segreation defects are not due to a defect in HR and 2-D gel analysis of replication intermediates in the rDNA showed that mutants did show incomplete replication before the initiation of metaphase. Full replication was restored by removing the polar replication barrier Fob, confirming that incomplete replication was the origin of the phenotype. It is important to note that this situation is distinct from other segregation defects in Smc5/6 as no collapsed RF are seen indicating that replication is more likely slowed in Smc5/6 mutants or that these strains are unable to fully merge converged replication forks that meet in the rDNA region (Torres-Rosell et al., 2005b).

1.11.5 Analysis of Smc5/6 in *S. pombe*

Two hypomorphic mutants *smc6-74* and *smc6-X* (Nasim and Smith, 1975, Lehmann et al., 1995) have been extensively characterized in *S. pombe*. These mutants are viable at all temperatures (*smc6-X was* originally reported to be TS (Lehmann et al., 1995) but this was dependent on the media used and the mutant is not TS under the conditions used in this thesis) but are sensitive to a range of DNA damaging agents, such as UV and IR, and epistatic to HR defective mutants e.g. *rhp51* (Verkade et al., 2001).

The two mutations are located at different regions of Smc6, *smc6-X* (R706C) is located in the hinge, close to the second region of coiled-coils and *smc6-74* (A151T) is in an issegre finger close to the ATP binding domain in the N-terminal globular head (Lammens et al., 2004). Further analysis of *smc6-X* and *smc6-74* revealed a separation of function. It was shown that the DNA damage sensitivity of *smc6-74*, but not *smc6-X*, was rescued by the over expression of Brc1, a gene that has been shown to be required for correct mitotic segregation but is not required for DNA repair of checkpoint activation (Verkade et al., 1999). Brc1 has homology to Rtt107/Esc4 that functions in S phase DNA repair in *S. cerevisiae* (Rouse, 2004) and is a 6-BRCT domain protein. Interestingly Brc1 rescues *smc6-74* not only in S phase but also in G2 but it has not been shown to interact directly with *smc6-74.* Supression of the repair defect in *smc6-74* by Brc1 over-expression requires the process of post-replication repair, or PRR, a process that allows continued replication by bypassing lesions and allowing replication to continue (Lee et al., 2007). It could be that the over-expression of Brc1 encourages more PRR and therefore more replication bypass of lesions or errors that form as a result of Smc5/6 malfunction. Deletion mutants of Apn2, the AP endonuclease involved in base excision repair was shown to be synthetically lethal with *smc6-74* and *smc6-X* (Lee et al., 2007) it has been suggested that its role as a 3'-5' exonuclease (Unk et al., 2001) may be playing a role in the viability of Smc6 mutants by degrading blocked 3' ends at collapsed replication forks. The *S. pombe* exonuclease Mus81-Eme1 has been shown to function as a nuclease on 3' flap DNA and *smc6-74 mus81Δ* double mutants are not as well rescued by Brc1 as *smc6-74* single mutants.

1.11.6 The role of Smc5/6 at stalled and collapsed forks

In *S. pombe smc6-X* and *smc6-74* was analysed in response to hydroxyurea (HU) Both mutants were sensitive to HU but *smc6-74* was consistently less sensitive than *smc6-X*. Further investigation utilised double and triple mutants of the S phase checkpoint *cds1. Cds1* null mutants in HU treatment fail to stabilise the stalled replication forks leading to a disassociation of the replication fork machinery and fork 'collapse' (Lindsay et al., 1998). 2-D gel analysis was used to visualise replication intermediates in the rDNA in single and double mutants. In both *smc6* mutants replication forks were stably maintained in the presence of the checkpoint but were not proficient at repairing collapsed forks (*cds1* null background) and accumulated replication and recombination intermediates (Ampatzidou et al., 2006).

HR-defective mutants are sensitive to HU and this has been hypothesised to be due to a requirement for HR to repair any stalled forks that become unstable and collapse. In wild type cells Rad52 (Rad52 is encoded by *rad22* in *S. pombe* but in this thesis Rad52 is used to be consistent with the nomenclature in other organisms) foci appear after release from HU stalling, consistent with a temporal separation of replication and resection for HR repair (Meister et al., 2005). *Smc6* mutants are epistatic to HR mutants in response to HU and a similar number (1-2) of Rad52 foci has been seen in both *smc6-X* and *smc6-74* on release from HU. In *cds1* double mutants both *smc6-X* and *smc6-74* accumulate Rad22 foci similarly to WT showing that Smc5/6 is not required for recruitment of Rad52 to collapsed replication forks. *Cds1* null cells in HU are arrested by the DNA damage checkpoint and do not enter mitosis. In contrast, the *smc6* single mutants, while activating the G2 DNA damage checkpoint and delaying entry into mitosis like wild type cells, undergo mitotic catastrophe as the chromosomes fail to segregate. This mitotic catastrophe is suppressed in HR mutant backgrounds. This supports the hypothesis that that Smc5/6 has a 'late' role in HR after the recruitment of Rad52 to collapsed forks which results in incomplete repair and the accumulation of recombination-dependent intermediates (Ampatzidou et al., 2006). Such intermediates are blind to the DNA damage checkpoint, presumably because there is no ssDNA to signal, and thus cells enter mitosis with catastrophic results. This has been termed a checkpoint maintenance defect (Verkade et al., 1999).

ChIP (Chromatin Immino-Precipitation) analysis was used to detect RPA and Rad52 association at stable stalled forks in *smc6* mutants (Irmisch et al., 2009). *Smc6-74,* but not *smc6-X,* was found to have a reduction in RPA association after replication stalling in HU. Replication stalling generates ssDNA, which recruits RPA, leading to checkpoint activation and fork stabilisation (Forsburg, 2008). RPA coated ssDNA is also a substrate for Rad52 and Rad52 association was also reduced in *smc6-74*. Additional analysis using rDNA marker loss as a measure of HR, showed that *smc6-X* had increased marker loss indicative of increased illegitimate recombination. *Smc6-74* had decreased marker loss, consistent with the decrease in Rad52 chromatin association leading to a decrease in HR (Irmisch et al., 2009). This suggests that the Smc5/6 complex has a role in the stabilisation of stalled replication forks, which maintains the topology of the fork and allows recruitment of Rad52. This was termed the 'early role' in HR.

Overall 'early' role and 'late' roles in HR can be defined for Smc5/6 (figure1-7). *Smc6-74* is defective in the early role of loading RPA and recruiting Rad52 at stalled replication forks and both *smc6-X* and *smc6-74* are deficient in the 'late' role in homologous recombination resolution at collapsed replication forks. Both of these roles have not only been defined in the rDNA but also genome wide consistent Smc5/6 having a genome wide role in replication fork stability and repair (Irmisch et al., 2009).

1.12 Project Aims

1.12.1 A role for Smc5/6 in mating-type switching?

The Smc5/6 complex has been shown to have a role in the process of collapsed and stalled replication forks and has a role in the repair of DSBs by HR and maintaining checkpoint response. Mating-type switching is a process that requires the repair of a site-specific collapsed replication fork during the second S phase after the RF encounters the imprint (Kaykov et al., 2004, Arcangioli, 1998). The repair of this replication-coupled break is dependent on the recombination machinery and uses the downstream donors as a template. The role of Smc5/6 during mating-type switching has not been investigated but it seems likely that if Smc6 mutants are defective in the

Early Role
Stalled replication fork
(stable)

Late Role
Collapsed fork

S phase check
point Cds1

Replication Complex
dissociates

smc6-74
Fork less flexible

**Smc5/6
keeps
stalled fork
primed for
restart**

Strand invasion,
dependent on HR

**Smc5/6 required
for HJ resolution
and fork
resetting**

smc6-X
Fork less flexible.
Increased potential
for fork collapse

Both *smc6-74* and
smc6-X are defective

Replication restart

Figure 1-7 – Summary of early and late roles of Smc5/6
Early role: Cds1 is required to keep stalled forks in a stable conformation and Smc5/6 keeps the fork primed ready for restart. This restart relies on Rad52 loading and *smc6-74* is defective in this role. *smc6-X* is less stable and may collapse, but it is not defective in Rad52 loading. Late role: Rad52 loads to collapsed replication forks independently of Smc5/6 and both *smc6* mutants are unable to restore collapsed forks at the point of HJ resolution (adapted from Irmisch et al., 2009).

repair of collapsed replication forks then some defect may be seen in the ability to switch mating-type. Furthermore the separation of function seen in *smc6-X* and *smc6-74* may result in a separation of function phenotype in this system.

By crossing the h^{90} *mat* locus into *smc6-X* and *smc6-74* it would be possible to detect synthetic lethality or a switching defect by monitoring the outcome of crosses via tetrad analysis. Interestingly in this system if switching defects are seen it may be possible to draw conclusions about the role of Smc5/6 in the based on potential switching defects. It is possible that due to the defect of *smc6-74* in Rad52 and RPA accumulation at stalled replication forks that *smc6-74* may show a defect similar to that of type-Ia switching mutants and not imprint as it cannot hold the replication fork in a stable conformation. Furthermore the late role in resolving HR structures may mean that a different type of switching defect could be seen. Details of this analysis are in chapter 3.

1.12.2 Does Smc5/6 have a role in se-DSB repair?

An adapted version of the mating-type switching is the site-specific se-DSB system and which was used to investigate Mus81 and its essential role in processing se-DSBs (Roseaulin et al., 2008). A se-DSB is formed when the RF collides with the imprint during S phase. The formation of this break was visualised in Roseaulin et al. 2008 using Southern analysis after synchronisation in an inducible break system. In the inducible system cells were prevented from switching by inducing transcription through the imprint with a strong promoter. Cells cultures could be grown to a suitable concentration and then switching was induced simultaneously in all cells when the promoter was turned off allowing the analysis of many cells at once during the same stages of the switching process. Analysis showed a fragile site corresponding to the *mat1* break with the correct formation kinetics expected for a break that was specific to the mating-type switching pattern. This se-DSB is similar in structure the one formed during mating-type switching but the method of repair is different. Mating-type switching is dependent on recombination mediators like Rad52 (Roseaulin et al., 2008), however it has specific mediator proteins, Swi5 can replace Rhp57 (Haruta et al., 2008), that mediate copying from the ectopic donors. When the donors are deleted

the se-DSB is repaired using the intact *mat1* region as a template for repair. In the se-DSB system *rad50Δ exoIΔ* double mutants were synthetically lethal suggesting that ExoI could substitute for the MRX complex (Roseaulin et al., 2008) but this eventuality would not be expected to generate the amounts of ssDNA required to generate a full checkpoint response.

There are several possible roles for Smc5/6 in se-DSB repair. The 'early' role, defective in *smc6-74*, of holding the stalled fork in the correct conformation to facilitate RPA loading to ssDNA, may or may not be required. The 'late' role for Smc5/6 in resolution of HR and DNA damage checkpoint maintenance would be expected to be important in this type of repair as the repair of a se-DNA break is dependent on HR and Rad52 for repair. This system would show whether the Smc5/6 is defective in se-DSB repair and further analysis using an inducible version of this system would help to elucidate the role. See chapter 4 onwards.

1.12.3 An inducible converged fork system

By removing the replication termination site RTS1 at *mat1* the se-DSB converted by a converging replication fork to a two-ended DSB. The checkpoint and DNA repair response may be different in a converging fork (cf)-DSB. For example the recruitment of recombination factors to the site may be different, the checkpoint response may be altered due to an alteration of the amount of ssDNA or the further triggering of the DNA damage checkpoint. In particular Mus81 is proposed to be responsible for cutting nicked HJs and Y strictures similar to RFs (Doe et al., 2002, Fabre et al., 2002, Gaillard et al., 2003) and has been shown to be essential for se-DSB repair. In contrast, Rqh1-Top3 has been shown to be required at two-ended DSBs (Goodwin et al., 1999, Ahmad and Stewart, 2005, Laursen et al., 2003). Previous studies suggested that Mus81 and Rqh1-Top3 compete for substrates during repair of RFs and this system may separate the type of structures they repair.

This system is an interesting extension for the study of Smc5/6. The type of lesion at a cf-DSB is likely to be similar to DSBs formed during γ-irradiation. Smc5/6 mutants are unable to repair this type of lesions (Verkade et al., 1999). Most inducible DSB systems

use enzymes to create breaks, like the HO endonuclease responsible for *S. cerevisiae* mating-type switching (Kostriken and Heffron, 1984). However, in these systems in S and G2 both sister chromatids are cut, and repeatedly. In contrast a site-specific cf-DSB provides the opportunity to study repair events at a DSB in a single sister chromatid.

Chapter 2 – Materials and Methods

2.1 *S. pombe* techniques

2.1.1 *S. pombe* growth and selection media

<u>Yeast Extract (YE)</u>

5g/l yeast extract (Bacto), 30g/l glucose, 200mg/l adenine and 100mg/l of issegreg, uracil, leucine and argenine

<u>Yeast Extract Agar (YEA)</u>

As YES with the addition of 30g/l agar

<u>Yeast Nitrogen Base Agar (YNBA)</u>

1.9 g/l YNB (Formedium), 5g/l ammonium sulphate, 20g/l glucose and 30 g/l agar. Amino acid supplements were added to a final 1 x stock concentration.

<u>Extremely Low Nitrogen (ELN)</u>

27.3g/l EMM (Formedium), 50 mg/l ammonium chloride, 200mg/l adenine and 100mg/l of issegreg, uracil, leucine and argenine

<u>Amino Acid stock solutions</u>

100 x stock solution – 7.5 g/l of adenine, issegreg, leucine and argenine

50 x stock solution – 3.5 g/l of Uracil

<u>Edinburugh minimal medium (EMM2)</u>

50ml/l 20x EMM2 salts, 25 ml/l Nh_4Cl, 25 ml/l 0.4 M Na_2HPO_4, 1ml/l 1000x vitamin stock and 100µl/l 10000 x trace elements. Amino acid supplements were added to a final 1 x stock concentration.

<u>Stock solutions for EMM2</u>

20 x EMM2 salts – 61.2 g/l potassium hydrogen phthalate, 20 g/l KCL, 21.4 g/l $MgCl_2.6H_2O$, 200mg/l Na_2SO_4 and 250 mg/l $CaCl_2.2H_2O$

1000 x Vitamins – 1 g/l pantotenic acid, 10 g/l nicotinic acid, 10 g/l inositol and 10 mg/l biotin

10000 x Trace elements – 5 g/l H_3BO_3, 4g/l $MnSO_4$, 4g/l $ZnSO_4.7H_2O$, 2 g/l $FeCl_3.6H_2O$, 1.5 g/l Na_2MoO_4, 1 g/l KI, 400 mg/l $CuSO_4.5H_2O$, 10 g/l citric acid

Concentrations of additional media supplements:

Phloxin B – 5 mg/l

Thiamine – 3 µM

HU – as stated in text, usually 5mM

2.1.2 Growing *S. pombe*

S. pombe cells were cultured in YE or on YEA and incubated at 30°C unless otherwise stated. Where auxotrophic markers were used cells were grown on YNBA supplemented with appropriate amino acids at 75 mg/l for issegreg, leucine, issegre, uracil and adenine. For liquid cultures one loop of cells was inoculated and grown over night in 10ml of yeast extract (YE) medium as a pre-culture, then an appropriate number of cells was inoculated into a larger culture. The concentration of cell cultures was counted using a haemocytometer and logarithmic cells were harvested at a cell concentration of 5 $x10^6$ cells/ml. For plating assays, cells were either patched or streaked onto agar plates and fresh patches were used in all experiments. When using the inducible mating-type switching system cells were cultured in EMM2 media or grown on YNBA plates without thiamine.

2.1.3 Crossing

Cells for crossing were grown over night on YEA agar and a fresh loop of *h+* and *h-* were patched together on ELN agar the following day. Crossed strains were grown at 30°C for 2-3 days and checked for the formation of spore asci under a light microscope. Spores from successful crosses were separated by tetrad dissection or by using random spore analysis.

For crosses involving the h^{90} switching strain measures were taken during crossing to ensure that the h^{90} parent strain did not cross to itself. Parents in an h^{90} cross

contained complementing adenine auxotrophic markers *ade6-m216* and *ade6-m210* (Szankasi et al 1988) that form functional Ade6 in a diploid. H^{90} parents were patch crossed on ELN for close to 12 hours and cells from the cross were streaked to YNBA - adenine and grown to single colonies (approximately 3 days). The ade+ diploids were then sporulated on ELN for a further 2 days, or until asci formed.

2.1.4 Random spore analysis

Cells crossed on ELN were checked after 2-3 days under the microscope for the formation of asci. For random spore analysis a loop of cells was inoculated into a 200-fold dilution of helicase (Helix Pomatia Juice) in sterile H_2O and the cell mixture was incubated at room temperature for at least 6 hours. After incubation the cell suspension was spun for 5 minutes at 13 krpm and the pellet was re-suspended in 1ml of H_2O. The number of spores per ml was calculated using a haemocytometer and diluted to $1x10^4$ cells/ml so that an appropriate number of spores could be plated on YEA. Plates were incubated at 30°C for 3 days, or until colonies had formed, and colonies were replica plated. When using the inducible system spores were plated on YNBA agar fully supplemented with all amino acids but lacking in thiamine in order to prevent undesirable induction.

2.1.5 Tetrad dissection

Crossed strains were sporulated by patching onto ELN agar for 2-3 days or until asci formed. A small amount (less than 1 loop) of cells was taken from the patch containing the asci and mixed with 20 μl of dH_2O. The cell suspension was spread onto one side of an agar plate forming a 'pool' of cells that was accessible using the micromanipulator. Plates were incubated for 1-3 hours at 30°C to break down the ascus so that spores can be manipulated. Dissections were carried out using a Singer Instrument MSM System micromanipulator. Four spores from the same asci were dissected and placed in adjacent columns. Once an entire plate of spores was dissected (around 18 tetrads) they were incubated at 30°C until the spores were able to germinate and form colonies.

2.1.7 Replica-plating

Colonies formed after tetrad or random spore analysis were replica plated to check the segregation of alleles. Replica colonies were pressed onto a Whatman filter disk using a replica-plating block and transferred to different types of selection media. Selection plates were grown for 1-3 days, depending on the type of media, at 30°C so that the segregation of alleles could be determined.

2.1.8 Checking UV-C response

Checking a strain's response to DNA damage by UV-C was used to determine whether cells were *smc6-X* or *smc6-74*. Freshly replica plated cells on plates were supplemented with 5mg/ml of phloxin B were exposed to 100J/m2 of UV-C using a UV Stratalinker 2400 and survival checked after over night incubation at 30°C.

2.1.9 Checking for sporulation and mating-type switching

Sporulation analysis was used to check the mating-type of new strains. Cells were crossed to fixed mating-type WT strains (J331 *h-* and J334 *h+*) and checked for sporulation to determine mating-type of the new strains. Plates were placed over solid iodine crystals until a colour change was observed. Iodine vapours cause spore asci to discolour and colonies containing spores turn grey while those that could not sporulate turn yellow upon iodine exposure. The ability of cells to mate and sporulate was also used as an indication of mating-type switching in h^{90} strains. Cells were replica plated or patched to ELN agar for 3 days at 30°C and the resulting colonies were exposed to iodine vapours to check for sporulation.

2.1.10 Creating *S. pombe* stocks

For long term storage of *S. pombe* strains cells were patched over. 1 loop of the fresh patch was re-suspended in a YE/glycerol mix (50% YE, 50% of 60% glycerol) and stored in a screw top cryo-tube at -80°C.

2.2 *S. pombe* analytical techniques

2.2.1 Spot test survival analysis

Strains were freshly patched overnight and harvested the following day in logarithmic phase. Cells were counted using a haemocytometer and diluted to 10^7 cells/ml with sterile water. 10-fold serial dilutions were made to create four cell suspensions at the following concentrations: 10^7, 10^6, 10^5 and 10^4 cells/ml. 3μl of each dilution was spotted onto plates containing selective agents or exposed to UV-C.

2.2.3 Microcolony viability analysis

Microcolony viability analysis was a technique used to determine the viability of different mutants in response to induction of the se-DSB and cf-DSB. One loop of logarithmic cells was inoculated into 1ml of sterile dH$_2$O and counted using a haemocytometer. The cell suspension was serially diluted to a concentration of 1×10^4 and 20 μl was spotted onto YNBA plates supplemented with amino acids and with or without 3μM thiamine. Before spots dried the plate was tipped so that the cell suspension spread evenly in a line across the plate and then left at room temperature (RT) to dry. Plates were then grown for 16 hours (or 24 hours in the case of *rhp51Δ*) at 30°C. After incubation microcolonies were viewed under a light microscope and the number of cells per microcolony were counted. Microcolonies were categorised as either viable (21 or 31+ cells) dead (1 cell) or slow growing, (2-20/30 cells). In this analysis *rhp51Δ* was slower growing than other strains so it was grown for longer and the higher values of the categories were used.

2.2.4 Cell length analysis

Cells were plated in the same manner as for microcolony analysis (section 2.2.3) however plates were incubated for 24 hours (or 36 hours for *rhp51Δ*) at 30°C. The resulting microcolonies were imaged using a USB camera with a microscope adapter. The resulting images were proportionally printed and the length of at least 35 cells was measured by hand and the magnification was determined using the average diameter of *S. pombe* cells (Das et al., 2007). The average cell length was calculated for each strain in conditions with or without thiamine.

2.2.5 Pedigree analysis

Logarithmic phase cells were patched to a pool on YNBA plates that were supplemented with amino acids with or without 3 µM thiamine. This was performed similarly to the plate setup for tetrad analysis. The Singer MCM Micromanipulator system was used to separate individual cells into spaces so that a single cells could be followed through successive divisions. Plates were incubated at 30°C but were checked every 2 hours to check whether cells had divided. If the cells had divided the two daughters were separated following a specific pattern so that the each cell's parent, sister and daughters could be traced. Images of the resulting pedigree were taken using the USB microscope camera. Based on the pattern of separation it was possible to deduce the pedigree of the cells that had been separated. These pedigrees were drawn for each individual starting cell and the viability of sisters and parent/daughters in each generation was calculated (as outlined in section 5.6). The ratio of viable: inviable sisters/daughter cells was determined and an average viability was calculated based on the data for at least 10 pedigrees per strain.

2.2.6 Cell survival after exposure to IR

A loop of logarithmically growing cells was inoculated in 1ml of growth medium, counted with a haemocytometer, diluted to a concentration of 1×10^4 cells/ml and aliquoted into several tubes of cells. Cells were irradiated with indicated range of doses of IR (γ-irradiation) and equal numbers of cells were plated on duplicate plates. Cells were incubated for 3-4 days at 30°C until colonies formed. The number of colonies per plate was counted using a colony counter.

2.2.7 Mitotic progression after exposure to IR

Suspensions of logarithmic phase cells were exposed to 450 GY γ-irradiation in EMM2 media supplemented with amino acids. The suspension was then incubated for a further 300 minutes at 30°C and cell samples were harvested every 20 minutes after irradiation. Cell samples were fixed (section 2.3.3) and visualised using the Core Delta Vision microscope and the number of cells past mitosis was scored for each sample.

2.3 Microscopy preparation and analysis

2.3.1 Cell synchronisation by lactose gradient

Nine lactose fractions were made by mixing the following concentrations of 30% and 7% lactose in 15 ml falcon tubes:

Final % of lactose	Volume of 30% lactose (ml)	Volume of 7% lactose (ml)	Fraction no.
30	10	0	1
28	8.75	1.25	2
24	7.5	2.5	3
21	6.25	3.75	4
18.5	5	5	5
16	3.75	6.25	6
13	2.5	7.5	7
10	1.25	8.75	8
7	0	10	9

Individual gradients were made by applying 1.5 ml of 30%, 28%, 24%... etc. of lactose to a 15ml falcon tube using a cut tip. A 200 ml culture at a concentration of 5×10^6 cells/ml was concentrated by centrifugation for 3 minutes at 3000 rpm. 1.5 ml of the resulting concentrated cells was applied to the gradient using a cut tip. Gradients loaded with cells were spun at 1 krpm for 8 minutes at RT (room temperature). Between 100-200 μl of G2 phase cells were harvested from the gradient and checked under the microscope. Synchronous cells were re-suspended in an appropriate volume of EMM2 ready for further experimentation.

2.3.2 Induction of the se-DSB system and harvesting synchronised *S. pombe* cells for septation index analysis

Cells were grown in 200 ml of EMM2 media to the concentration of 5×10^6 cells/ml. Depending on the experimental procedure cultures were induced (activating the se-DSB) by adding 30 mM thiamine to a final concentration of 3 μM either after synchronisation by lactose gradient, or 180 minutes prior to synchronisation.

Synchronised cell fractions were re-suspended in 10 ml of EMM2 containing 3 μM thiamine and incubated at 30°C while shaking. Cell samples were taken every 20 minutes after synchronisation, pelleted for 1 minute at 13 krpm and fixed by re-suspending in 250 μl of methanol ready for septation analysis.

2.3.3 Fixed Cell Microscopy

Pelleted cells were fixed by the addition of 250 μl of methanol. For fixed cell microscopy, cells were spun at 3 krpm for 1 minute and 10 μl of concentrated cells was spread on a microscope slide. Slides were left to dry and 5 μl of DAPI (4'6-diamidino-2-phenylindole)/calcofluor staining solution (DAPI 1 mg/ml calcofluor 2 mg/ml in dH$_2$O) was used to stain the cell septum and nuclear DNA. A cover slip was placed over the slide and ready for imaging using the Leitz Diaplan microscope set to the DAPI filter. Cell samples were observed under the microscope and the number of cells with a septum (appearing as a bright white line in the middle of the cells) or with separated nuclei were counted. Approximately 100 cells in total were counted and the percentage of cells with mitotic nuclei or formed septum were expressed as a percentage of the total cells counted (septation index).

For fixed cell imaging using the Core Delta Vision microscope slides were prepared as in the protocol above, however cover slips were sealed using clear nail varnish. In images taken with the Delta Vision microscope cell length of was measured using softWoRx or Omero software.

2.3.4 Live cell imaging

Cultures for live cell imaging were grown to 1-5x10^6 cells/ml. Cultures were induced by the addition of thiamine to the concentration of 3 μM and incubated while shaking for 180 minutes (the approximate time taken for G2 cells to have made the imprint and progressed through cytokinesis). After incubation cells are synchronised in G2 by lactose gradient (section 2.3.1) and re-suspended in 1 ml of EMM2 media containing thiamine. The number of cells in the suspension was counted using a haemocytometer to determine the cell/ml concentration (typically between 1x10^7-1x10^8) and the suspension was kept at RT while imaging chambers were prepared.

Two cultures were analysed at once using a 4 well imaging chamber (LabTech). A thin layer (~ 20 μl) of 0.1% concanavalin A (con-A) was applied to the base of the chambers and left to dry for 15 minutes. 100 μl of cell suspension (approximately 5×10^7 cells) was applied to the top of the con-A and left to settle for a further 10 minutes. Excess cell suspension was removed leaving cells deposited on the base of the chamber. 1 ml of fresh EMM2 media containing thiamine was carefully added to the chambers. Lactose gradient and chamber preparation take approximately 80-90 minutes leaving approximately 30 minutes for microscope set up before imaging is begun.

Live cell imaging was performed using an Applied Precision pDV microscope. Cell chambers were incubated at 30°C for the duration of the time course and Rad52::GFP foci were visualised using the FITC filter. Time courses were set up to record only the FITC channel to minimise photo bleaching (Z-sectioning was also not used) as the background fluorescence was enough to determine the outline of the cells and the moment of cytokinesis. Images were taken every 5 minutes for 6 hours beginning close to 300 minutes after induction. Images were analysed using Omero and softWoRx

2.4 PCR

PCR is a method used to amplify specific regions of DNA using short oligonucleotide primers (Mullis and Faloona, 1987). It was used in several aspects of this study but the method was modified slightly to suit the purpose. A list of primers used in this study is found in appendix B.

2.4.1 Yeast colony PCR

PCR using yeast colonies is a quick and easy method of gene amplification as no DNA extraction step is required. This technique was used for several purposes for example; a quick method for identifying the mating-type of colonies after crossing or for the initial step in creating a DNA probe for southern analysis.

The day before PCR cells from the colony of interest were streaked onto a YEA plate and incubated at 30°C overnight. A small loop of cells was mixed with 5 μl of dH$_2$O and heated to 95°C for 10 minutes. The PCR reaction mixture contained the 5 μl of cell mix,

2.5 µl 10 x Taq polymerase buffer, 2.5 µl of 2mM dNTPs 0.05 µl of 100 pM forward and reverse primer, 2.5 µl 25 mM $MgCl_2$, 0.125 µl of Taq polymerase. The final volume was adjusted to a total of 25 µl with dH_2O.

The reaction mixture was heated to 95°C for initial denaturing step of 3 minutes. 32 cycles of the following programme were then executed; 95°C for 30 seconds, 58°C for 30 seconds and 72°C for 1 minute. Followed by an additional 10 minutes of final extension at 72°C and then holding at 4°C until required.

2.4.2 PCR for sequencing

PCR was used to amplify specific regions of DNA sequencing. Before PCR DNA was extracted from cell cultures as outlined in section 2.7.1 but DNA was re-suspended in 1xTE after the first ethanol wash. Because of the large volume of DNA required for sequencing (~2µg) several duplicate reactions were set up for each sample to be sequenced. Approximately 10 ng of template DNA was used per reaction and the PCR programme was carried out in a manner similar to above (section 2.4.1).

2.4.3 Creating DNA hybridisation probes using PCR

For Southern analysis the region of DNA that was required was amplified using PCR. The reaction was carried out as in yeast colony PCR (section 2.4.1) and the fragments were extracted using Quiagen DNA extraction kits and the fragment was cloned into a plasmid see section 2.6.2.

For creation of the probe fragment PCR was used to amplify the region from the purified plasmid. 10-15ng of purified plasmid was used as the DNA template for the reaction and the reaction mixture was as follows: 10-15ng of purified plasmid DNA, 5 µl 10 x Taq polymerase buffer, 5 µl of 2mM dNTPs 0.1 µl of 100 pM forward and reverse primer, 5 µl 25 mM $MgCl_2$, 0.2 µl of Taq polymerase. The final volume was adjusted to a total of 50 µl with dH_2O. The reaction was carried out as outlined in section 2.4.2 and the resulting PCR products were gel extracted (section 2.5.2) re-suspended in 1xTE and stored at -20°C until required for hybridisation.

2.5 Electrophoresis and sequencing

2.5.1 DNA electrophoresis

DNA products from PCR or restriction digest reactions were run on a 0.8% agarose gel for 30-90 min at 50-100V depending on the type of separation required. The agarose gel was made using 0.5x TBE and gels were run using the same buffer containing 10μl of ethidium bromide (5 x TBE stock 54g tris base 27.5g boric acid, 20ml 0.5M EDTA (pH 8) in 1l H_2O).

2.5.2 DNA electrophoresis for extraction

PCR products were run on a 0.8% low melting point (LMP) gel in 0.5xTBE buffer for 80 minutes at 50 volts. Gels were stained with 10 μl of ethidium bromide. PCR product was extracted from LMP agarose gel using a Qiagen gel extraction kit.

2.5.3 Sequencing

Purified PCR product was extracted from LMP agarose gel using a Qiagen gel extraction kit and DNA was re-suspended in 1xTE at a concentration of 20-50 ng/μl.

DNA was sent for sequencing at GATC Biotech according their instructions with appropriate primers.

2.6 Bacterial techniques

2.6.1 Media

Luria-Bertami (LB)

1 g/l Bacto tryptone, 5 g/l Bacto yeast extract, 5 g/l NaCl, 1 g/l glucose (pH 5.6)

LA

As LB with 12.5 g/l Difco agar

2.6.2 DNA ligation

Purified PCR products (preparation as described in section 2.4.3 and 2.5.2) were cloned into the TA vector pCR2.1 (Invitrogen) carrying ampicillin resistance and a lac selection marker. Ligation reactions were set up as following 1μl PCR product, 1μl TA vector, 1 μl

10x TA buffer, 6.5 ul dH$_2$O and 0.5 ul of T4 DNA ligase. The reaction mixture was incubated over night at 18°C and an extra 0.5 µl T4 ligase was added the next morning.

2.6.3 *E. coli* transformation

Competent DH5α cells were thawed on ice. 50µl of competent cells were aliquoted into two tubes, one was mixed with ligated DNA and one was a –DNA negative control. Both tubes were incubated on ice for 20 minutes then heat shocked at 42°C for 60 seconds. Heat shocked cells were incubated on ice for 2 minutes and 100ul of sterile LB media was added and cells were revovered at 37°C for 30 minutes. After which cells were plated on LA plates that were supplemented with 50 µg/ml of ampicillin and 40µg/ml Xgal and 0.1mM IPTG and grown over night at 37°C. Plates with colonies were stored at 4°C to aid development of the blue/white selection.

2.6.4 Plasmid purification

Colonies from the transformation containing the correct selection markers were grown overnight in LB media +50 µg/ml of ampicillin. Plasmid DNA was purified using miniprep and maxiprep kits and following the instructions that were supplied by Qiagen. After plasmid extraction the presence of the probe region was checked by restriction digest and amplified for Southern analysis by PCR (section 2.6.5 and 2.4.3).

2.6.5 Restriction digest of plasmid DNA

Purified plasmid DNA was checked for correct integration by restriction digestion. The TA plasmid was checked by digesting with *Eco*RI as follows: 2 µl of plasmid DNA, 2 µl, 10 x restriction enzyme buffer (as supplied by NEB), 1 µl *Eco*RI and 15 µl dH$_2$O. Reaction mixture was incubated at 37°C for 1 hour and fragments were separated on a 0.8% agarose gel.

2.7 Southern Analysis

2.7.1 Extraction of genomic DNA for Southern analysis

1 loop of recently patched cells was grown in 10ml of liquid culture overnight to late log phase. Cells were washed at 3krpm for 5 minutes, washed with sterile H$_2$0 and re-suspended in 1 ml of CSE (1.2M Sorbitol, 20mM citrate/phosphate pH 5.6, 40mM EDTA

adjusted to pH5/6 with 1M NaOH) and 1mg/ml of Lyticase (Sigma-Aldrich). The cell suspension was incubated at 37°C for 10-20 minutes and cells were checked for the presence of spheroplasts under a microscope (5μl cells and 2μl 2% SDS mixed on a slide). Spheroplasts were spun for 5 minutes and re-suspended in 450μl of 5xTE (50mM TrisHCl, 5mM EDTA) followed by 50μl of 10% SDS and incubated at room temperature for 5 minutes. After incubation 150μl of 5M Kac was added and tubes were placed on ice for 10 minutes. Samples were spun for 10 min and 1 volume of propan-2-ol was added to the supernatant. The suspension was spun for 10 minutes, and washed with 70% ethanol, then re-suspended in 250μl of 5xTE and 5μl 10mg/ml RNAseA and incubated at 37°C for 20 minutes. 2μl 10% SDS was added with 10μl of 10mg/ml ProteinaseK and incubated at 37°C for overnight. DNA was precipitated twice with 1 volume of phenol/chloroform:isoamyl alcohol, spun at 13 krpm at room temperature for 5 minutes and the supernatant was ethanol precipitated with 1/10 volume 3M NaAc and 3.5x volume of 100% ethanol or propan-2-ol. The resulting pellet was washed with 70% ethanol and re-suspended in 30-50μl of 1x TE (10mM TrisHCl pH7.5, 1mM EDTA).

2.7.2 Restriction digest of genomic DNA

Southern analysis was used to check the conformation of the *mat* locus or to detect levels of imprinting. Enzymes used were; *Hind*III, *Pvu*II and *Xho*I. Typically between 200-500μg of DNA was digested with 100 units of enzyme in a total reaction volume of 150μl of 1x reaction buffer (as supplied New England BioLabs). Digests were incubated over night at 37°C and ethanol precipitated, re-suspended in 10 μl 1xTE, and run on an agarose gel.

2.7.3 Electrophoresis for Southern analysis

Digested genomic DNA was separated on a 1% agarose gel made with 0.5x TBE (Tris-Boric Acid-EDTA) without ethidium bromide and run for 21 hours at 50 Volts.

2.7.4 Transferral of DNA to hybridisation membrane

The gel was washed at room temperature while shaking in depurination solution (0.25M HCl) for 20 minutes, followed by 20 minutes in denaturing solution (1.5M NaCl;

0.5M NaOH) and finally neutralising buffer (1M Tris pH8; 1.5M NaCl) for 20 minutes. DNA was transferred to 'GeneScreen' neutral membrane (PerkinElmer) by capillary force technique in 10xSSC buffer (1.5M NaCl; 0.15M sodium citrate pH7) for 4-16 hours.

After blotting, the membrane was washed in 2xSSC for 5 minutess then dried and DNA was cross-linked to the membrane using a UV Stratolinker 2400 at 1200 Jm^2, once on each side. The cross-linked membrane was stored in filter paper at 4°C until required.

2.7.5 Preparing the membrane for hybridisation

Membranes were washed for 5 minutes to rehydrate in H_2O and then warmed to 65°C in pre-hybridisation solution (6xSSC; 1xDeinhardt; 1% sarcosyl; 0.1% BSA) for up to 20 hours.

2.7.6 Labelling the DNA probe and hybridization

50ng of purified probe DNA (see section 2.4.3) was made up to 45µl with dH_2O and prepared for radio-labelling by denaturing at 100°C for 3 minutes and rapidly cooling on ice for 3 minutes. DNA was labelled using Ready-to-go DNA labelling beads (GE Healthcare) and 5µl dCTP 5' α^{32}P-triphosphate (PerkinElmer) and incubated at 37°C for 15 minutes. The probe was purified using a MicroSpin G-50 column (GE Healthcare) twice and added to a preheated (to 65°C) hybridisation buffer (6xSSC; 1xDeinhardt; 1% sarcosyl; 200µl/20ml salmon sperm DNA). The pre-hybridisation solution was removed from the membrane and replaced with the hybridisation buffer which was incubated at 65°C overnight while rotating.

2.7.7 Post-hybridization washes

After hybridisation the membrane was washed with wash buffer I (2xSSC; 1% SDS) that was warmed to 65°C for 15 minutes in the hybridisation oven. The buffer was removed replaced with fresh warmed buffer I and washed for a further 15 minutes. The membrane was then washed twice at room temperature with wash buffer II (0.1xSSC; 0.1% SDS) that had been warmed to 42°C for 15 minutes each. The membrane signal

was checked using a Geiger counter then dried, wrapped in saran wrap and placed in a phosphor screen cassette over night.

2.7.8 Detection and quantification of signal

Phosphor screens were scanned using a Storm 840 scanner. The bands on the resulting image were quantified using ImageJ software.

If re-probing was required the membrane was washed with boiling probe removal buffer (0.05xSSC, 0.01 EDTA pH8, 0.1% SDS) for 15 minutes. Fresh boiling buffer was added for a second 15 minute wash and then a final wash of 0.01xSSC . The membrane was checked using a Geiger counter and if sufficiently clean was immediately pre-hybridised, if not the boiling washes were repeated.

2.8 Statistical Tests

For tetrad analysis the G-test was used to determine if the frequencies of the different tetrad classes were random or significant. Expected values would be evenly distributed across all classes and the G-test could detect a significant deviation from this expectation.

Where specific values for expectations were determined by normalising the data in comparison to WT data chi-squared was used to determine whether expected data significantly deviated from the WT results.

Chapter 3 – Using the *mat* locus to investigate the function of Smc6 in mating-type switching

3.1.1 Introduction

Smc5/6 has 'early' and 'late' roles in homologous recombination (section 1.10.5) that were defined during the investigation of two hypomorphic mutants. *Smc6-74* is defective in the early role of loading RPA and recruiting Rad22 at stalled replication forks and both *smc6-X* and *smc6-74* are deficient in the 'late' role in the resolution of homologous recombination at collapsed replication forks. Both of these roles have not only been defined in the rDNA but also at genome wide sites suggesting that Smc5/6 has a genome wide role (Irmisch et al., 2009).

In addition it had been observed that when *smc6-X* and *smc6-74* were crossed to a homothallic switching h^{90} strain the mutants behaved differently indicating a further separation of function. A *smc6-X* h^{90} strain grew normally after crossing and was proficient in switching. However *smc6-74* h^{90} cells were initially smaller and slower growing and larger non-switching colonies accumulate as the isolates were grown. When these colonies were analysed it was found that the *mat* locus had been rearranged (A. Irmisch, personal communication) suggesting that *smc6-74* had a switching defect and that the early role was required for switching. This additional separation of function indicated that the analysis of mating-type switching in *smc6* mutants was likely to be informative.

Mating-type switching offers an ideal environment to study the role of Smc6 in replication fork stability, homologous recombination (HR) and the separation of function mutants, *smc6-X* and *smc6-74*. The process itself occurs naturally as part of vegetative growth in *S. pombe* cells (Leupold, 1970) during S phase and over two mitotic divisions (Arcangioli and de Lahondès, 2000).

A replication fork passing through the expressed *mat* locus, *mat1*, is stalled at the MPS1 pause site during the first division (Dalgaard and Klar, 2000, Dalgaard and Klar, 2001b) to allow for the introduction of an imprint in the DNA (figure 1-6 (A-B)).

Homologous recombination is utilised during the second replication to repair the se-DSB caused by replication of the 'imprint' (Kaykov et al., 2004). The programmed fork stalling and introduction of the modified 'imprint' in the lagging strand means there is no need to stall replication forks artificially with agents such a hydroxyurea (HU). Furthermore, as switching is a specifically programmed DNA replication-based event all of the controls for the initiation, processing and resolution of the process are present in the cell in its natural state. However even more useful to the analysis is that there is a specific DNA locus dedicated to the process, meaning replication barriers like RTS1 are already present in the DNA and that stalling and recombination are completed at site-specific, strand-specific locations allowing detection of the processing events. Finally, better understanding of mating-type switching has led to new tools for utilising this system to study other aspects of the DNA repair.

An important study used mating-type switching to explore the role of Mus81 in recombination repair of a single-ended double strand break (se-DSB) and introduced several strains with variations of the *mat* locus conformation as tools for the analysis of proteins that function in HR (Roseaulin et al., 2008). Repair of the se-DSB by mating-type switching (ectopic recombination) and repair by homologous recombination using the sister chromatid were analysed in two separate systems. In the presence of the donors (*mat2* and *mat3*), downstream of the imprint site, the se-DSB generated by the replication fork running into the imprint at *mat1* is repaired ectopically (from non-sister DNA) using either *mat2* or *mat3* as template by an HR-dependent method that results in the switching of the DNA at *mat1*. In the absence of donors repair of the imprint occurs using DNA from the duplicated sister chromatid sequence resulting in a non-switching repair event. These systems were used to detect elements of the HR machinery that were specific to either sister chromatid or ectopic DNA repair methods (Roseaulin et al. 2008) and in this analysis were adapted to look at the role of Smc6 in se-DSB repair and mating-type switching.

3.1.2 A mating-type switching system to study Smc6

During the analysis strains to be studied, *smc6-X, smc6-74* and others were crossed to the tester strains containing the alternative *mat* loci (the origins of these strains are

outlined in appendix A). The first strain used in analysis is the standard homothallic switching h^{90} strain. H^{90} is naturally occurring in *S. pombe* and it has an unaltered *mat* locus; this strain is used to determine the gene of interest's role in mating-type switching. After analysis of homothallic switching strains several heterothallic strains were used to further investigate the role of Smc6 in recombination repair. The first heterothallic tester strains to be used in this study is *smt0,* referred to in future as *smt0^{no imprint}*, no imprinting control. This strain has a 263bp deletion corresponding to the DSB region proximal to the *mat* H1 box leading to no imprint formation in the cells and therefore no need for repair (Styrkarsdottir et al., 1993). The next strain, *mat2.3D (*referred to in future as *mat2.3D^{no donors}*), contains a deletion of the entire *mat2, mat3* donor region including the *K-region* and is marked with a LEU2 insertion. This strain is used to investigate homologous recombination repair of a se-DSB, using the sister chromatid, as, in the absence of donors, the se-DSB can only be repaired by HR using the sister chromatid at *mat1* as a template (Kaykov et. al. 2004a). As a further negative control, a strain with the deletion at the *smt0^{no imprint}* region and a deletion of *mat2.3D::*LEU2^{no donors} was used to determine the effect of the donor deletion on a strain that does not imprint (table 3-1 and figure 3-1).

By using a mating-type switching system it is possible to investigate the role of Smc5/6 during recombination events between *mat1* and the donor regions during mating-type switching (chapter 3.3.2 – 3.3.5) and *mat1* and its sister chromatid in single-ended double strand break (se-DSB) repair (chapter 4.3.1 – 4.3.2.).

smc6-X, *smc6-74* and several recombination mutants with defined h^+ or h^- *mat* loci configurations were crossed to the various tester strains of the opposite mating-type and maintained as diploids utilising the *ade6-M210/ade6-M216* complementing alleles (see section 2.3.1). This allowed the introduction of the new *mat* locus conformation into the strain of interest.

	Genotype of Interest	h^{90}, h^{+}, h^{-}	imprint	donors	Strain Number
Testers	h^{90}	h^{90}	✓	✓	PB46
	h^{90}	h^{90}	✓	✓	PB47
	$mat2.3D^{no\ donors}$	$h^{-mat2,3D}$	✓	✗	PB70
	$smt0,mat2.3D^{no\ imprint,\ no\ donors}$	$h^{-smt0,mat2,3D}$	✗	✗	JZ108
	$smt0^{no\ imprint}$	h^{-smt0}	✗	✓	J1507
Base	WT	h^{-S}	✓	✗	J331
	WT	h^{+N}	✗	✓	J334
	smc6-74	h^{-S}	✓	✗	J1938
	smc6-74	h^{+N}	✗	✓	J1939
	smc6-X	h^{-L}	✓	✗	J1941
	smc6-X	h^{+N}	✗	✓	J1943
	rad22-67	h^{+N}	✗	✓	JW226D

Table 3-1 –Strains used in this chapter
Base strains, tester strains and their genotype are shown in this table. The mating type at the mat locus is also shown along with whether strains are able to imprint or have donors. The strain number as outlines in Appendix A is shown for reference.

Figure 3-1 - *mat* locus conformation of tester strains

Diagrams showing the conformation of the *mat* locus in tester strains used throughout this study. Cassettes *mat1*, *mat2* and *mat3* are shown as boxes, h^- is blue and h^+ is pink, and flanked by white boxes indicating H1, H2 and H3 homology boxes. L and K regions are labelled and K-region heterochromatic repeats are shown as a black box. In strains that do not imprint the *smt0* deletion is marked with a triangle. Whether each strain is imprinting proficient or contains donors is marked with a ✓ or ✗. Cassette conformation was confirmed by Southern analysis (figure 3-2).

The diploids were then sporulated on extremely low nitrogen (ELN) media and tetrads of haploid spores separated using a micromanipulator. Spores were grown to colonies on rich yeast extract (YEA) media and replica plated onto various selective media plates. Using this method it was possible to determine the genotype of the spores isolated from the cross based on the segregation of the alleles seen during replica plating on selective media.

smt0 was identified by crossing to *h+* (as it would be the only expected *h-* outcome in a cross) or colony PCR to detect the deletion. The *mat2.3D$^{no\ donors}$* conformation is marked with *S. cerevisiae* LEU2 gene, and strains grew on leucine deficient media. *Smc6* mutants were not marked directly, but were detected on the basis of UV sensitivity by subjecting plates containing phloxin B to 100 J/m^2 of UV light and looking for dark pink colonies. *rad22-67* was detected using rich solid YEA media containing 5mM hydroxyurea (HU) (figure 3.4).

After plating to several types of media it was possible to determine whether switching mutants were viable or inviable in various *mat* locus backgrounds by determining whether colonies grow after sporulation. Spores from at least 100 tetrads were counted and the number of viable colonies were expressed as a percentage of the total number of colonies analysed.

3.1.3 Checking the conformation of the *mat* locus in strains to be analysed

Many lab strains of *S. pombe* have stabilised *mat* loci that do not switch. While it is not expected that the starting *mat* locus conformation of the strains to be investigated would affect analysis it was important to ensure that the *mat* locus of these strains was as expected. In addition to checking the mat locus of the strains to be tested it was also important to check the conformation of the tester strains (outlined in table 3-1) provided by the Arcangioli lab (see appendix A).

To confirm the orientation of the *mat* locus of the tester strains used in this investigation DNA was isolated from *smc6+* (henceforth known as WT) tester strains using a standard *S.pombe* genomic DNA preparation (section 2.7.1) techniques. The

isolated genomic DNA was digested with *Hind*III restriction enzyme and subjected to Southern blot analysis. A purified PCR product specific to both *h+* and *h-* was used as a specific probe to determine the size and number of fragments in the whole of the *mat* locus (see section 2.4.3). This PCR product contained the H1 homology box and as such was able to anneal to the whole of the *mat* locus as the H1 box is found at the start of each *mat* cassette (figure 1-6).

In *Hind*III digested DNA an unaltered h^{90} strain shows 3 bands when probed with a *mat* specific probe; *mat1*, *mat2* and *mat3* producing bands of three different sizes, 10.4Kb, 6.6Kb and 4.2Kb respectively (Beach and Klar, 1984). In DNA isolated from a log phase culture additional bands at 5.4 and 5 Kb also appear (Beach and Klar, 1984), these correspond to a broken fragile site, the result of imprinting at *mat1*. $Smt0^{no\ imprint}$ strains have a 268bp deletion at *mat1* that is detectable as a slight reduction in size of the *mat1* band but no changes to the bands corresponding to *mat2* or *mat3* and no bands corresponding to imprinting. $Mat2.3D^{no\ donors}$ has no alteration at *mat1* but a deletion of the donor region so that the 6.6 and 4.2 Kb bands are absent. In this strain imprinting still occurs as there is a band at 5.4Kb. Finally the $smt0\ mat2.3D^{no\ imprint,no\ donors}$ strain has the reduced size at *mat1* corresponding to the deletion at *smt0*, no *mat2* and *mat3* bands corresponding to the *mat2.3D* region and no 5.4kb imprinting band. All tester strains analysed showed the correct and expected *mat* locus conformation (figure 3-2).

H^{90} is one of the natural states of the *S. pombe mat* locus, however because of the strains ability to switch mating-type and spontaneously cross to itself when grown on low nutrient media h^{90} was not a suitable strain for use in many labs. In typical lab analyses stabilised versions of the *S. pombe mat* locus are used. The two conformations commonly seen arise as spontaneous rearrangements in h^{90} and these form the standard laboratory strains, h^{-S} and h^{+N} (Leupold, 1970). The remaining lab strains are found as either h^{90} or variations on the stabilised non-switching conformation such h^{-L}, h^{-S}, h^{+L} (Beach and Klar, 1984). The conformation of the *mat* locus would not be expected to play a significant role in the viability.
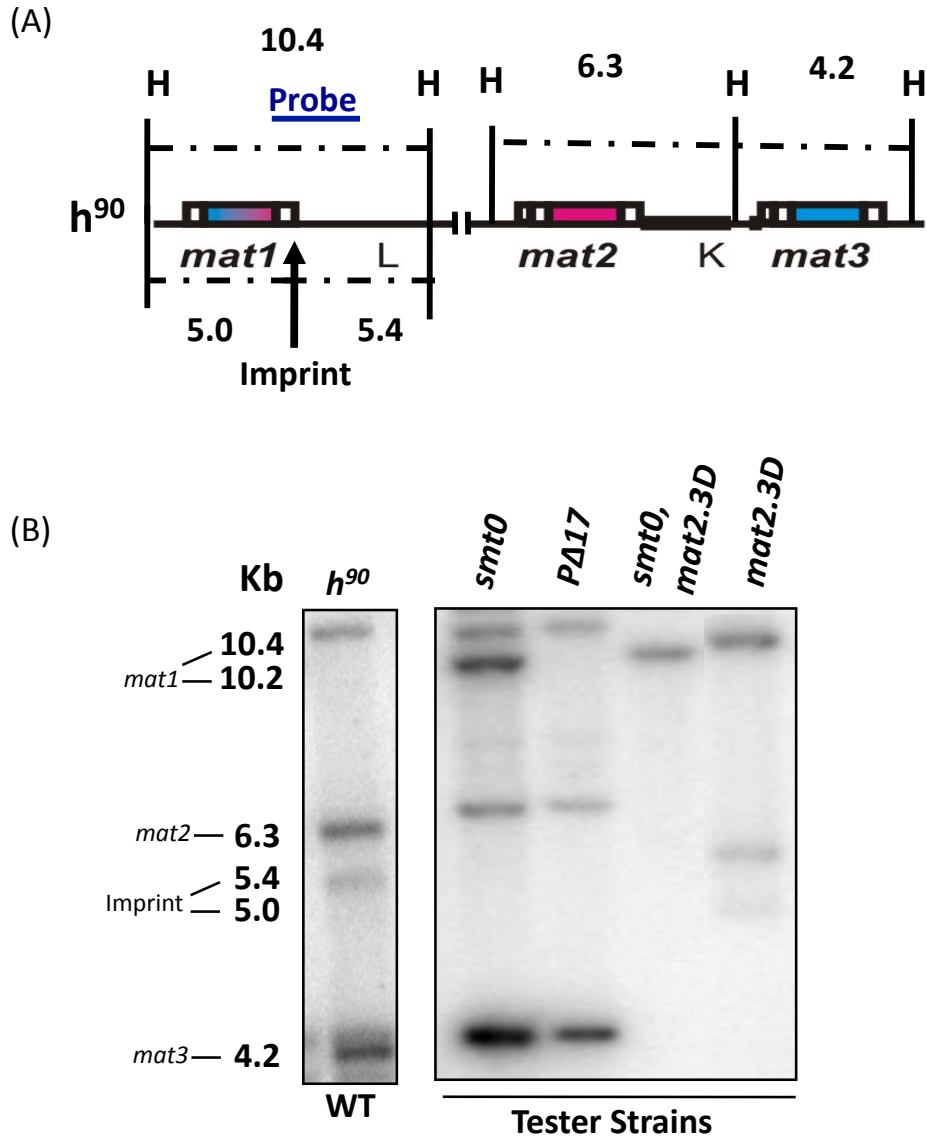
Figure 3-2 – Southern analysis of tester strains

(A) Schematic of the h^{90} mat locus showing all three donors and the locations of HindIII (H) sites. All fragment sizes are labelled in Kb and the probe region is marked with a blue line. The imprinting location is marked with an arrow. (B) Genomic DNA harvested from WT h^{90} and tester strains smt0[no imprint], smt0.mat2.3D[no imprint, no donors] and mat2.3D[no donors] (PΔ17 is a non-switching strain with donors that was not used further in this analysis) was digested with HindIII enzyme and run on a 1% gel. DNA was hybridised to a mat1+/- homology box specific probe (see section 2.4.3 and 2.7 for more information).

However, some conformations, like h^{-L}, maintain part of the *mat* locus episomally and, since this reduces stability and the episomal region contains essential genes, viability is reduced (Beach and Klar, 1984). Because of this the *mat* locus conformation must be taken into account when conducting the analysis and it was important to check the conformation of the *mat* locus for each of the strains analysed.

All strains used in this assay, WT, *smc6-74*, *smc6-X*, and *rad22-67* in both *h+* and *h-* strains, were analysed by *Hind*III digest and Southern blotting to determine the conformation of the *mat* locus. All lab *h+* strains were seen to be in the common stabilised form of *h+* known as *h+N* (figure 3-3) In this strain there is a duplication of the donor and K-region that is fused to the natural *mat1* locus- this fusion is known as *mat3:1* and disrupts imprinting and eliminates switching into the active *mat1* locus. The duplicated and fused *mat* locus lead to an alteration in the number of bands seen on the Southern blot, the four bands correspond to the duplicated *mat2*, *mat3:1* and the original *mat2* and *mat3* regions at 8.2, 6.7, 6.3 and 4.2 Kb respectively. It is important to note that no imprinting is seen in this strain.

In the majority of cases in this study *h-* lab strains were shown to be h^{-S}. This is the common *h-* conformation and is thought to arise spontaneously when a switching h^{90} does not terminate switch correctly and deletes the K-region, forming a fusion between *mat2* and *mat3* known as *mat2.3* (Beach and Klar, 1984). Because *mat1* is not disrupted in this strain imprinting still occurs, but the fused *mat2:3* donor region leads to a switching event that does not change mating-type. In this case the normal sized *mat1* and imprinting bands appear as expected in the h^{90} position of 10.4 and 5.4 Kb but the deletion at the donor regions mean that the *mat2:3* fusion band appears at 5.9 Kb and some imprinting can be seen at 5.4 and 5.0 Kb (depending on the mating-type specificity of the probe used) (figure 3-3).

Lab strains of WT and *smc6-74* was shown to have the standard lab strain conformation of h^{-S} and h^{+N}. However, *smc6-X* was found to have the h^{+N} arrangement in the *h+* isolates, but in *h-* the rearrangements were not the expected h^{-S}
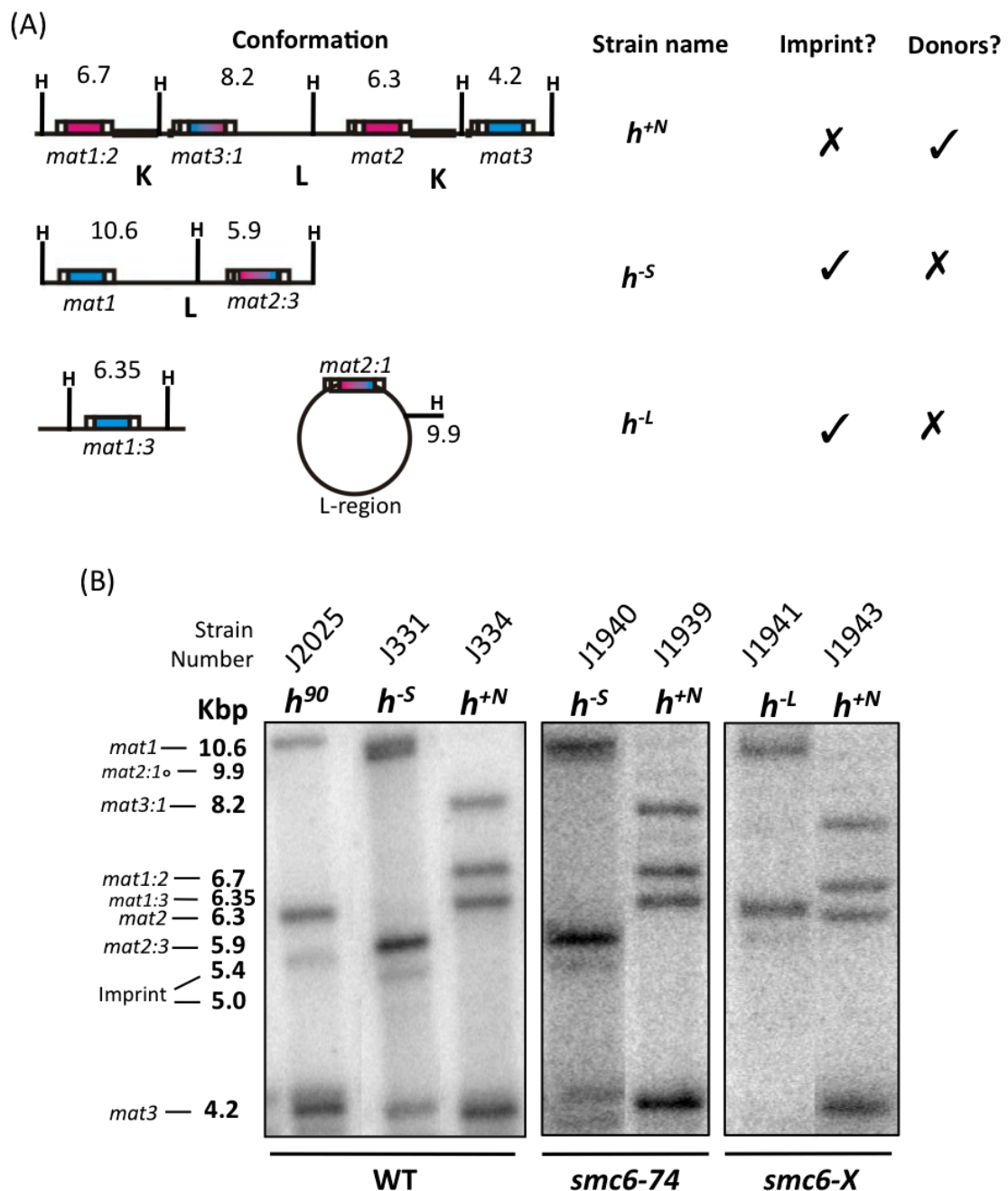
Figure 3-3 – Southern analysis to determine the conformation of the *mat* locus of base strains used in this study

(A) Graphical representation of the *mat* locus in base strains used in this study including *Hind*III sizes and locations (H) (see figure 3-1 for details of colour coding). (B) Genomic DNA harvested from *WT h⁹⁰, h⁻ˢ, h⁺ᴺ, smc6-74 h⁻ˢ, h⁺ᴺ and smc6-X h⁺ᴺ and h⁻ᴸ* used in this study was digested with *Hind*III enzyme and run on a 1% gel. DNA was hybridised to a *mat1+/-* H1 homology box specific probe. The *h⁻ᴸ* episomal fragment is labelled *mat2:1°*. Further details of corresponding strain numbers are found in the strain list (see appendix A).

This separate and distinct *h-* rearrangement has a Southern blot profile that is consistent with a published h^{-L} *mat* locus in which fusion of *mat1* and *mat3* leads to the loss of the L-region. The *mat1:3* fusion runs at 6.35 KB and the essential L-region is carried episomally and this runs at 9.9 kb (labelled mat2:1◦ on figure 3-3). H^{-L} is less stable than other *mat* locus arrangements due to the occasional loss of the episome during mitosis.

For consistency an attempt was made to cross defined h^{+N} *smc6-X* strains to WT h^{-S} strains in order to isolate *smc6-X* with an h^{-S} *mat* locus. However no *smc6-X* h^{-S} strains were isolated and Southern analysis confirmed that of the ten *h-* strains selected for further analysis all were h^{-L}. Since no h^{-L} strains were present in the parents of the cross it seemed likely that the *smc6-X* strains inheriting the h^{-S} *mat* locus were spontaneously rearranging to the h^{-L} conformation. It is likely that this is the result of *smc6-X* being unable to accurately repair the *mat* locus after imprinting that occurs in h^{-S} but this was not confirmed. HR mutants such as *rhp51Δ* are inviable as h^{-S} due to the inability to repair the se-DSB during switching and therefore the h^{-L} rearrangement seen in *smc6-X* is consistent with its published HR defect.

In order to check if the conformation of the *mat* locus could have any effect on the viability of strains after crossing in *smc6-X* an h^{+N} and a h^{-L} *smc6-X* were crossed to a WT strain of each defined mating-type. Equal numbers of spores were plated on solid media and the number of colony forming units (CFU) were counted. The percentage of CFU was reduced in both *smc6-X h+* and *h-* parents, compared to WT crosses where equal numbers of spores germinated. It was observed that in the strain where h^{+N} *smc6-X* was crossed to a WT h^{-S} the number of spores able to form colonies was reduced to 26%, approximately half that in the same cross using a *h+ smc6-X* strain. This is consistent with the observation that *smc6-X* has a generally sick phenotype and in particular that the h^{-L} phenotype arises from the instability of *smc6-X* in the h^{-S} conformation.

3.2 Crossing to the negative control s*mt0^{no imprint}* determines whether strains are able to cross and sporulate efficiently

WT, controls and the *smc6* mutants, *smc6-74* and *smc6-X*, were crossed to *WT smt0^{no imprint}* and the viability of the resulting spores were calculated using tetrad analysis. The *smt0^{no imprint}* tester is most similar to *h^{90}* and contains a normal *mat2*, *mat3*, L and K-region but the 263 bp deletion at *mat1*, which prevents imprinting (Styrkarsdottir et al., 1993). These are therefore control crosses that test the ability of the strains to undergo meiosis, indicating whether any reduction in viability is due to a meiotic defect, and used to estimate the general viability of strains after crossing.

Smt0^{no imprint} is an *h-* strain so analysis was conducted by crossing *h+* strains of *smc6+*, *smc6-X* and *smc6-74* to *h- smt0*. After crossing and replica plating to check the segregation of alleles, tetrads were checked and where colonies had grown the spores were considered viable and where no spore had germinated they were considered inviable. Tetrads were then grouped into categories based on the ratio of viable:inviable cells − 4:0, 3:1, 2:2, 1:3 and 0:4. The *total viability* percentage was calculated as: (total viable spores/total spores analysed)*100 and individual classes (viable:inviable) expressed as a percentage of the total tetrads.

After crossing to *smt0^{no imprint}* WT spores had a total viability of 90% and 82% of tetrads analysed were in the 4:0 class, with 4 viable tetrads (table 3-1). It would be expected that in a completely unperturbed cross all of the tetrads should be class 4:0, however this is rarely the case as spores sometimes die in WT strains. To correct this, statistical data was normalised and compared to the data seen in the WT cross, the five categories from each cross were compared to the data observed in the WT cross and subjected to the G-test (see section 2.8) to detect the differences in distribution across the population.

Smc6-74 did not show a meiotic defect when crossed to the *smt0^{no imprint}* strain and spores showed an overall viability of 88% and not significantly different to WT with a P value of 0.68 (see figure 3-4 for tetrad images). *Smc6-X* was found to have a small

reduction of viability with 81% of spores being viable. Statistical analysis showed that this was a significant reduction in viability when compared to WT with a P value of $3x10^{-6}$. The majority of *smc6-X* tetrads were split between class 4:0 and 3:1 at 57% and 27% of total tetrads respectively. This larger number of tetrads in the 3:1 class is what most likely contributed to the significance in the viability decrease, especially when considering that WT and *smc6-74* had 5% and 6% of total tetrads in the 3:1 class respectively. At present the precise nature of this viability defect is not clear but as Smc5/6 is required for meiotic recombination (Wehrkamp-Richter et al., 2012) it is likely that *smc6-X* has a meiosis defect that is reflected in the reduction of viability. However, meiotic defects typically show an increase in the 2:2 and 0:4 class that would be seen in a lethal heterozygous or homozygous cross. It is possible that a more complex interaction is taking place that has not yet fully been characterised. This data corresponds to the fact that *smc6-X* is less stable in the *h-* form but as the h^{+N} strain was crossed *smt0*$^{no\ imprint}$ the reduction in viability cannot be explained by this alone. Analysis by crossing h^{90} to these strains was continued despite the lower than expected viability in *smc6-X* as more than one mating-type could be crossed as part of analysis and data could be normalised to account for the higher number if 3:1 tetrads.

As a further control a switching mutant in *rad22*, *rad22-67*, (Ostermann et al., 1993) was used in this analysis. *Rad22-67* has a switching defect where the strain cannot process the ectopic recombination event between *mat1* and the donors. It is also proficient in normal HR repair and does not show UV sensitivity. However, it does show a slight sensitivity to HU but its phenotype is not as severe as *smc6-X* or *smc6-74* (figure 3-5). In crosses to *smt0* this mutant also shows a significant deviation from the WT strains viability, not for the overall percentage at 89%, but due to the increased number of tetrads, 27%, that fall into the 3:1 class $P=6x10^{-5}$.

As with *smc6-X* the overall viability of this strain after crossing was high and it was mainly that the number of tetrads showing a 3:1 ratio of alive to dead cells increased. As with *smc6-X* there did not seem to be a direct correlation between the mutant phenotype and cell death as only 9% of the dead spores carried the mutation.

Parents	Viable;Dead Spores					Total	% Viable	% of Inviable cells with mutation
	4;0	3;1	2;2	1;3	0;4			
WT *h+* x *smt0*	123	8	9	3	7	150	90	n/a
% of Total	*82*	*5*	*6*	*2*	*5*			
smc6-74 h+ x *smt0*	76	6	9	4	3	98	88	19
% of Total	*78*	*6*	*9*	*4*	*3*			
smc6-X h+ x *smt0*	68	32	7	8	5	120	81	40
% of Total	*57*	*27*	*6*	*7*	*4*			
rad22-67 h+ x *smt0*	53	19	6	0	1	79	89	9
% of Total	*67*	*24*	*8*	*0*	*1*			

Table 3-2 – Summary of tetrad data after crossing to $smt0^{no\ imprint}$
Base strains were crossed to the $smt0^{no\ imprint}$ tester strain and analysed by tetrad dissection (see methods). The number of tetrads with 4, 3, 2, 1 or 0 viable colonies was counted and the percentage of total colonies was calculated. When possible, the phenotype of inviable cells was determined and the percentage of inviable cells containing the mutation of interest was determined.

Figure 3-4 – Distribution of *smt0^(no imprint)* tetrads across viability categories
Strains were crossed to the *smt0^(no imprint)* tester strain and the resulting tetrads were plated on YEA agar and grown for 3 days at 30°C. Tetrads were categorised based on the numbers of viable tetrads (section 3.2). (A) Examples of tetrads seen from each cross. *smc6-74* and *smc6-X* were detected using UV at 100J/m² and plating on YEA agar supplemented with 5μg/ml phloxin B. *rad22-67* was detected using 5mM HU on YEA plates supplemented with phloxin B. Right hand panels show genotypes of spores *smt0* open circles, *smc6* or *rad22-67* mutant triangle. (B) The percentages of tetrads in each viability category (viable:dead).

(A) Tetrads analysis after crossing to *smt0^no imprint^*
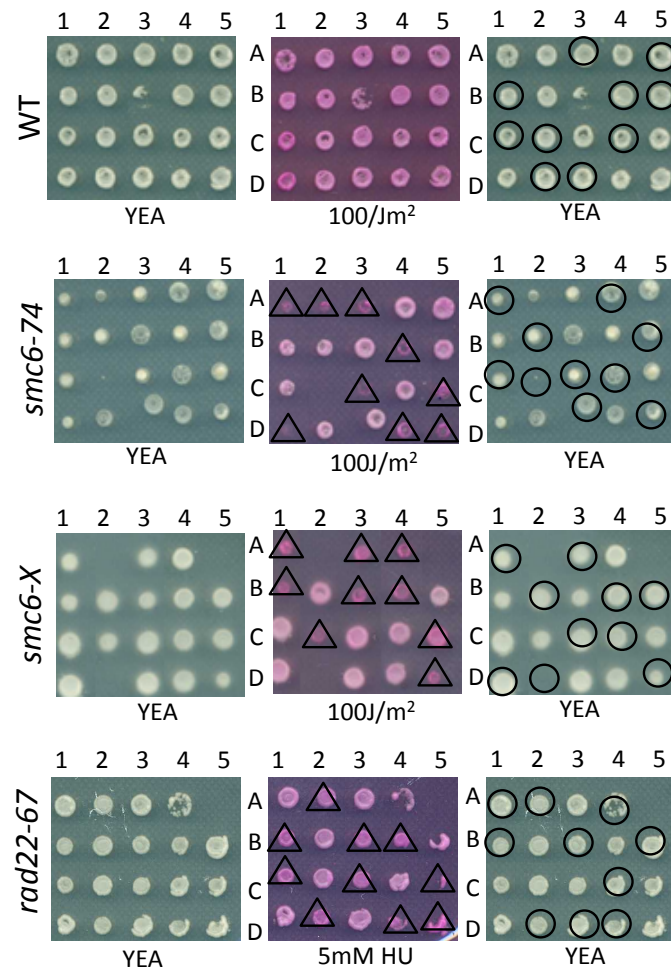
(B)
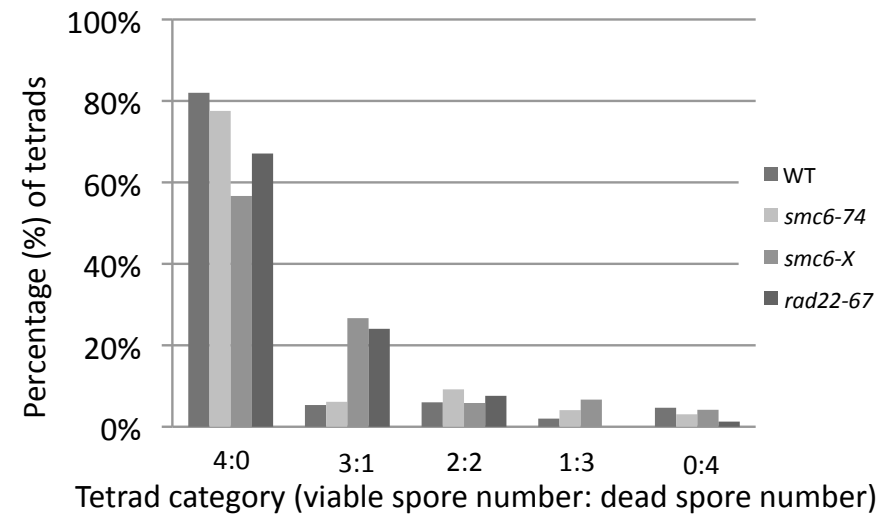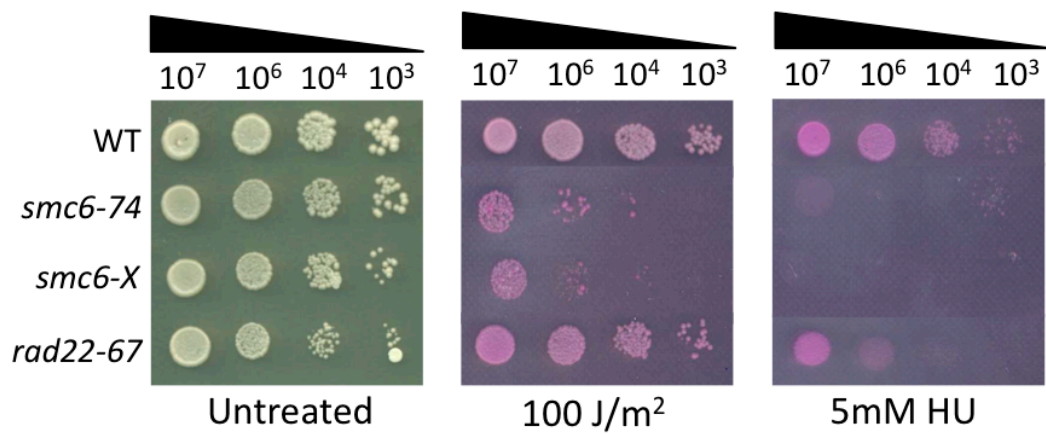
Figure 3-5 – Spot test analysis of base strains

10 fold serial dilutions of 1×10^7 cells/ml were spotted onto YEA plates and exposed to 100J/m^2 UV or spotted onto YEA media supplemented with 5mM HU and 5µg/ml of Phloxin B. Plates were then grown for 3 days at 30°C.

This coupled with the fact that the overall viability was so high suggested that there was no severe meiotic defect in *rad22-67Δ* or *smc6-X*.

3.3.1 Viability of mutant strains after crossing to homothallic switching strain *h⁹⁰ switching*

To analyse switching proficiency in *smc6* mutants the viability of strains containing the *h⁹⁰ switching mat* locus conformation were checked. As a negative control switching was also analysed in *rad22-67*, defective in mating-type switching, but not defective in HR due to an additional 6.5 kb insertion that complements the mutation (Ostermann et al., 1993), was also analysed. Where possible, over 100 tetrads were checked to attempt to obtain reliable segregation into classes. However it is still possible that even with 100 tetrads analysed there may be some anomalous results skewing the data.

To ensure out-crossing of *h⁹⁰ switching* complementing *ade6-210* and *ade6-216* alleles were used, as in a diploid containing both alleles a functional *ade6* gene product is produced and the colonies are white in the absence of adenine, whereas cells only expressing one allele are red and dead (Szankasi et al., 1988). In all *h⁹⁰ switching* crosses freshly crossed diploids were held on agar without adenine before sporulation to ensure that diploids were the result of a two parent cross.

When *rad22-67* and *smc6-74* were crossed to *h⁹⁰ switching* there was not a significant reduction in viability overall (P values are included in table 3-2). As *h⁹⁰ switching* can mate with both *h+* and *h-* the crosses were also analysed by mating-type of the parental strains. In crosses from *h-* parents *smc6-X* had an overall viability of 75% and *smc6-74* had a viability of 84%, which was not a significant decrease in viability when compared to the WT viability of 80% (table 3-2 and figure 3-6). Thus, all strains had a reduction in viability in an *h-* x *h⁹⁰ switching* cross but the reason for this is not yet fully understood.

Parents	Viable;Dead Spores					Total	% Viable
	4;0	3;1	2;2	1;3	0;4		
WT $h+$ x h^{90}	19	2	3	0	0	24	92
% of Total	79	8	13	0	0		
WT $h-$ x h^{90}	13	4	1	1	2	21	80
% of Total	62	19	5	5	10		
smc6-74 $h+$ x h^{90}	25	7	5	3	0	40	84
% of Total	63	18	13	8	0		
smc6-74 $h-$ x h^{90}	49	22	11	3	0	85	84
% of Total	58	26	13	4	0		
smc6-X $h+$ x h^{90}	28	14	5	2	5	54	77
% of Total	52	26	9	4	9		
smc6-X $h-$ x h^{90}	22	15	16	2	1	56	75
% of Total	39	27	29	4	2		
rad22-67 $h+$ x h^{90}	11	4	2	0	0	17	87
% of Total	65	24	12	0	0		

Table 3-3 – Summary of tetrad data after crossing to h^{90}

Base strains were crossed to the h^{90} tester strain and analysed by tetrad dissection (see methods). The number of tetrads with 4, 3, 2, 1 or 0 viable colonies was counted and the percentage of total colonies was calculated.

Viability of tetrads analysis after crossing *to h^{90}*

Legend:
- WT h+
- WT h-
- *smc6-74 h+*
- *smc6-74 h-*
- *smc6-X h+*
- *smc6-X h-*
- *rad22-67 h+*

Y-axis: Percentage (%) of tetrads

X-axis: Tetrad category (viable spore number: dead spore number)
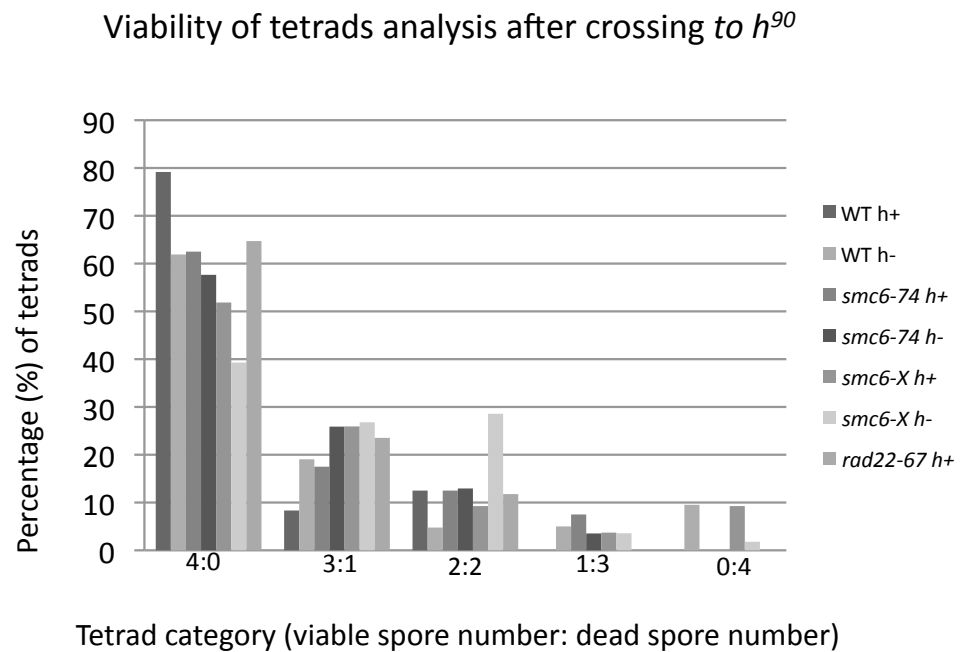
Figure 3-6 – Distribution of *h^{90}* tetrads across viability categories
The percentages of tetrads in each viability category (viable:dead) were determined based on the number of viable spores. The results were plotted graphically (see table 3-3 for further details and numerical data).

For *smc6-X* there was a significant reduction in viability in *h+* x *h$^{90\ switching}$* crosses (77%, a reduction of 15% when compared to the *smc6+* viability level of 92% (P=0.04)), comparable to the reduction in viability seen in *smc6-X smt0$^{no\ imprint}$* crosses. *Rad22-67 h+* did not show a significant reduction in viability after crossing to *h$^{90\ switching}$*.

3.3.2 Switching Analysis

To analyse the proficiency of switching diploids were sporulated on ELN medium and segregation analysis was performed on dissected tetrads. The tetrad type (parental di-type (PD), tetrad-type (TT) or non-parental ditype (NPD)) (figure 3-7) was determined by replica plating to follow the segregation of alleles.

In a parental di-type *smc6-X* or *smc6-74* co-segregated with the original mating-type (*h+* or *h-*), in a tetrad-type one mutant *smc6* allele segregated with the switching allele, and in a non-parental di-type both of the mutant *smc6* alleles will have segregated with the ability to switch. Thus, the number of spore colonies that are expected to switch after the cross can be estimated using the following equation

Number expected to switch = N(Tetra type) + 2N(Non-parental di-type)

This 'expected switching' number was used as the basis of the switching analysis and as the expected observation during statistical analysis..

Switching analysis of the negative control *rad22-67*, was used as a base line for a mutant displaying a switching defect (only an *h+ rad22-67* was available as recombination mutants tend to stabilise in *h+* conformation (Ostermann et al., 1993)). Out of 17 tetrads analysed a total of 20 individual spores were expected to switch, but only 4 were actually stably switching (20%) and able to form colonies (figure 3-8, table 3-3 and figure 3-9). The other 16 were found to be stably non-switching, suggesting a re-arrangement of the *mat* locus (Ostermann et al., 1993). It is important to note that the viability was not significantly reduced in this strain and the inability to switch did not cause cell death. Overall *rad22-67* showed a switching defect with 80% of spores stably non-switching.
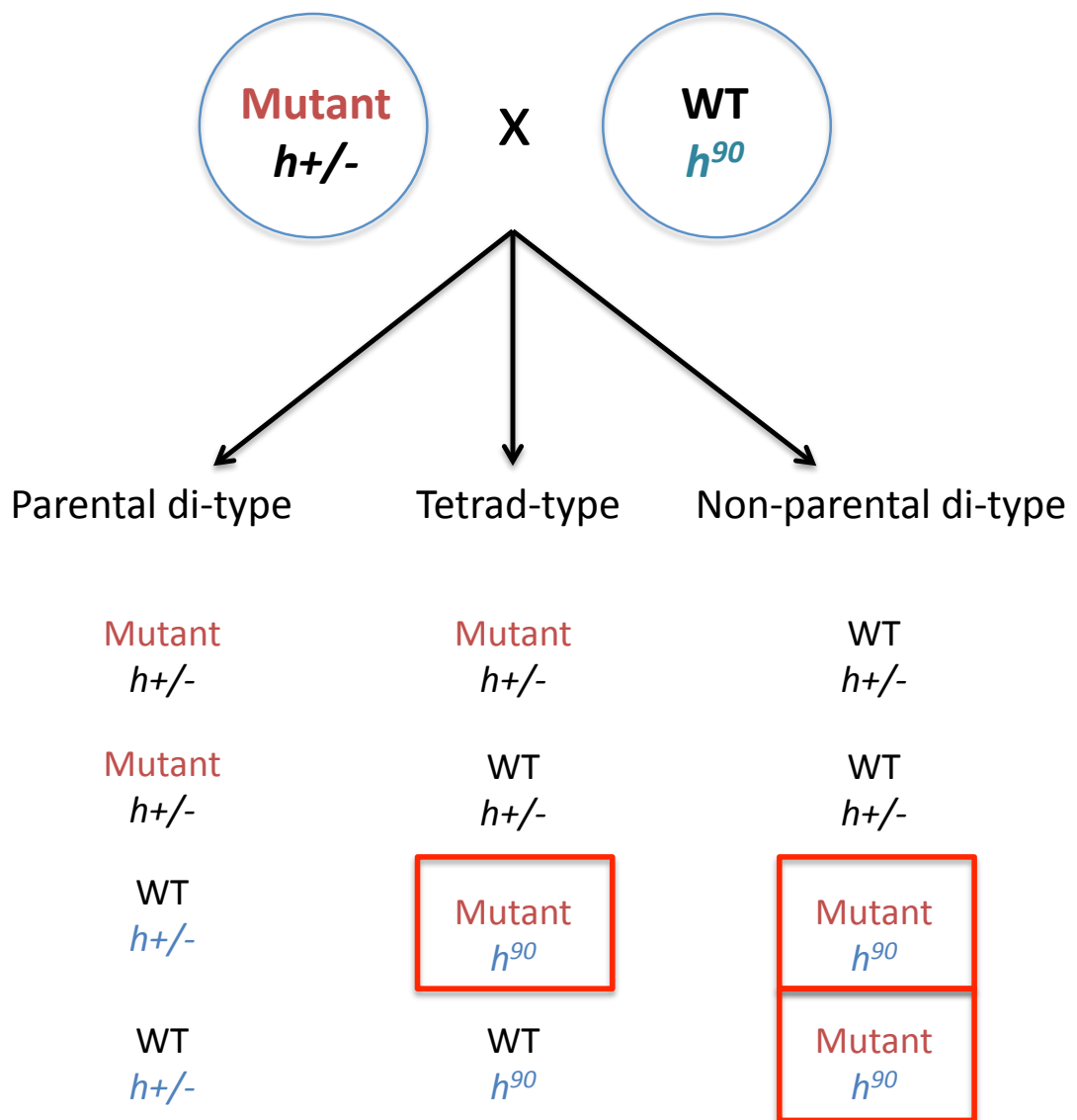
Figure 3-7 – Schematic of expected switching results after crossing a mutant strain to h^{90}

Switching analysis relies on determining the type of tetrads formed during the cross. The type of tetrad produced is a random event based on unlinked gene segregation during meiosis. Thus there should be an equal chance of obtaining any of the three tetrad types. By analysing tetrads the expected number of *smc6/rad22* mutants that are able to switch can be determined allowing any reduction in switching to be quantified. Spores of interest are boxed in red as these are the mutant strains that have inherited the h^{90} allele and are expected to switch.

In contrast in WT positive control strains 93.8% of colonies expected to switch were able to switch, the remaining 6.2% were dead.

3.3.3 Switching analysis of *smc6* mutant strains

In *smc6-X* the combined percentage of switching representing both *h+* and *h-* parental strains was determined and an overall switching defect was not detected as 86% of colonies were seen to switch as expected. When *h+* and *h-* crosses were analysed separately, it was found that in crosses when an *h+ smc6-X* was crossed to an h^{90} ^{switching} 87.3% of spores that were expected to switch were found to be stably switching and the remaining 12.7% were dead. When *h- smc6-X* was crossed to an $h^{90\ switching}$ strain a similar level of switching occurred with 85.1% switching and the remaining 14.9% dead. The dead spores in this analysis are likely the result of the slight growth defect as indicated by the cross to *smt0* $^{no\ imprint}$ (figure 3-4) rather than indicative of a switching defect (figure 3-8, 3-9 and table 3-3).

Overall, *smc6-74* was found to have a slight reduction in switching as 77.7% spores were able to switch. However, when parent strains were separated into h^{-S} and h^{+N} there was a specific reduction in switching in crosses from h^{-S} parents. *Smc6-74* h^{+N} cells crossed to $h^{90\ switching}$ yielded a similar level of switchable spores as WT strains (92.3% of spores stably switching and 7.7% dead). In contrast, *smc6-74* h^{-S} strains crossed to $h^{90\ switching}$ were found to have 70% of expected switching spores to be switching. Of those not switching 8.5% of spores were dead and 21% were stably non-switching. Thus, *smc6-74* has a switching defect but only when *h- smc6-74* cells are crossed to $h^{90\ switching}$ (figure 3-8, 3-9 and table 3-3). The defect is less severe than *rad22-67*, which has a severe switching defect and only 20% of cells are still stably switching. It is also unusual as HR mutants that cannot switch typically rearrange to an h^{+N} as h^{-S} mutants switch silently from h- to h- and so continue to require recombination for repair of the imprint (figure 3-3 shows imprinting in h^{-S}). These data assume that WT strains isolated from this cross are proficient at switching, a reasonable assumption based on $h^{90\ switching}$ x WT cross data.
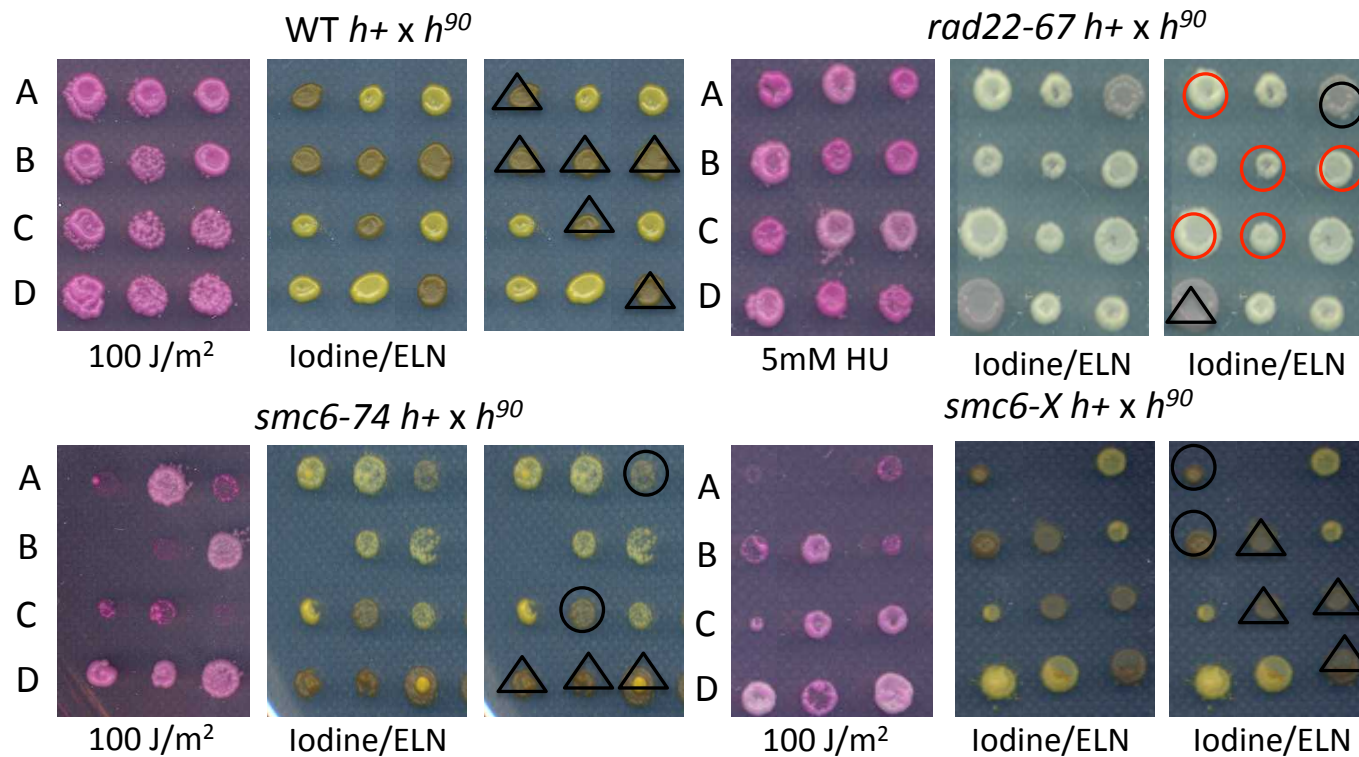
Figure 3-8 Tetrad analysis of h^{90} crosses

WT, *rad22-67*, *smc6-74* and *smc6-X* were crossed to h^{90}, sporulated on ELN agar and the resulting spores were separated by tetrad dissection. After growing tetrads for 3 days colonies were replicated to YEA media supplemented with Phloxin B and exposed to 10J/m^2 UV to detect *smc6* mutants and *rad22-67* was detected using YEA plates supplemented with 5mM HU. To check switching ability, colonies were grown on ELN for 3 days and exposed to iodine vapours so that switching colonies turned grey. Right hand panels show distribution of switching alleles, triangle is WT switching, black circle is mutant switching and red circle is non-switching mutant.

Parents	Mating Type of Parent	Tetrad Type			Total	Number expected to Switch	% Switching	% Stable non-switching	% Dead
		Parental Ditype	Tetratype	Non-Parental Di-type					
WT x h^{90}	+	-	-	-	24	48	93.8%	0%	6.3%
WT x h^{90}	-	-	-	-	21	42	81.0%	0%	19.0%
smc6-74 x h^{90}	+	8	21	9	38	39	92.3%	0%	7.7%
smc6-74 x h^{90}	-	19	44	19	82	82	70.7%	20%	8.5%
smc6-X x h^{90}	+	6	29	13	48	55	87.3%	0%	12.7%
smc6-X x h^{90}	-	9	37	5	51	47	85.1%	0%	14.9%
rad22-67 x h^{90}	+	3	8	6	17	20	20.0%	80%	0.0%

Table 3-4 – Summary of switching analysis data after crossing to h^{90}

Tetrads from several crosses were split into tetrad-type based on the phenotype of the spores obtained from the cross. . The total number colonies expected to be switching was compared to the observed phenotype of the cells.
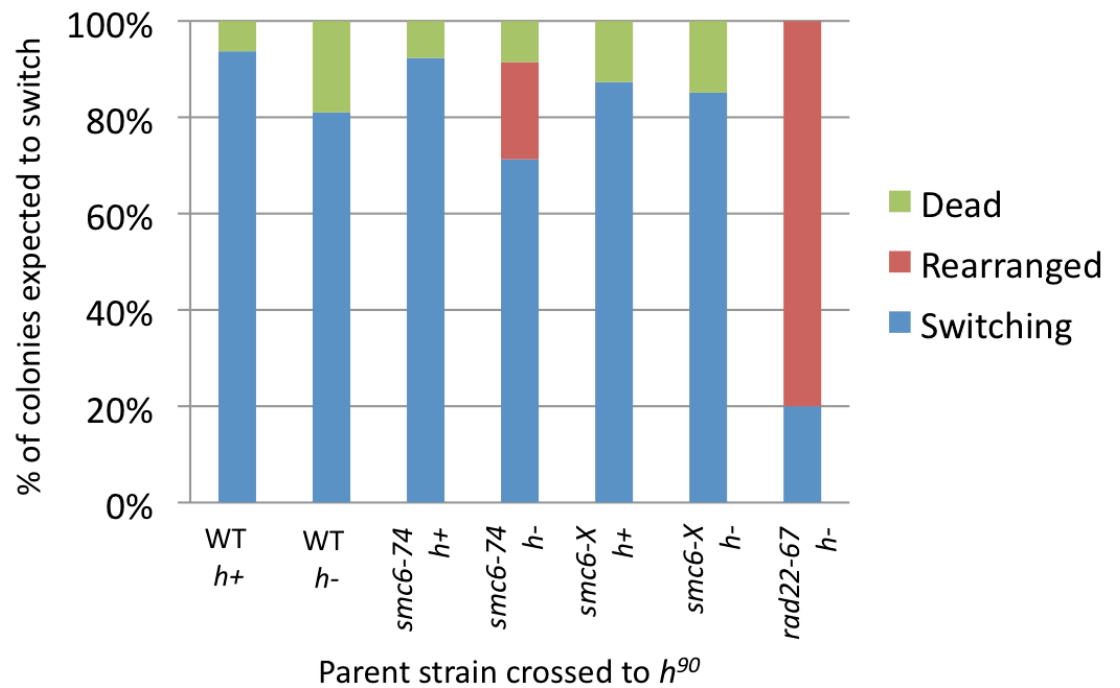
Figure 3-9 – Percentage of mutant strains that are switching, rearranged or dead after crossing to h^{90}

The expected phenotype for each tetrad was calculated based on the alleles observed in tetrads (see figure 3-9). Using this expected phenotype it was possible to determine the number of *smc6-74*, *smc6-X* and *rad22-67* colonies that were expected to switch. The percentage of strains that were actually switching, rearranged into a stable non-switching form (rearranged) or dead were calculated and plotted so that rearranging strains can be clearly seen (for numerical data see table 3-4)

Stable non-switching *smc6-74* strains were analysed by Southern blotting to determine whether the inability to switch was due to a rearrangement of the *mat* locus into a non-switching conformation (as in *rad22-67* (Ostermann et al., 1993)), or to the generation of a switching suppressor where the $h^{90\ switching}$ *mat* locus remained intact. Genomic DNA was digested with *HindIII* enzyme, which generates well characterised fragment sizes for *mat1* (10.6Kb), *mat2* (6.4Kb) and *mat3* (4.2Kb) ((Beach and Klar, 1984), see section 3.1.3). All ten non-switching isolates tested showed rearrangements of the *mat* locus. Seven to the h^{-S} conformation and three had rearrangements similar to the h^{+N} conformation but with extra bands (figure 3-10). The h^{+N} was not a conformation in either of the parent strains in this cross and was therefore an unexpected outcome of the cross. It has been suggested by Beach and Klar, 1984, that h^{+N} arises during a P to M switch, which fails to resolve normally and copy synthesis of the *mat3-M* cassette continues into the K region. Resolution at the next possible site, the H2 region of *mat2-P*, results in the formation of h^{+N}. Further rounds of copy synthesis would generate additional bands, as been observed in class II switching mutants that fail to resolve the ectoptic recombination event (Fleck et al., 1992). H^{-S} could also result from faulty initiation or resolution of switching (Beach and Klar, 1984).

3.3.4 Different conformations of the parental *mat* locus alter the effects of switching in *smc6-74* mutants

These data suggest that the *mat* locus conformation of the parent strain that is crossed to the $h^{90\ switching}$ strain is an important factor in determining whether *smc6-74* strains are able to switch. This is novel mating-type switching defect. The data suggest that the h^{-S} parent is key to the defect in *smc6-74*. There are two key alterations to the h^{-S} conformation: the first is that *mat1* is *h-*, the second that the donor region is rearranged and missing all of the centromeric repeats of the K-region. If the mating-type of the parent strain is important it would be predicted that the direction of the switch causes the defect. In an *h-* x $h^{90\ switching}$ cross the initial switch in switching spores after sporulation would be from *h+* to *h-* as $h^{90\ switching}$ can only mate or sporulate when in the opposite conformation to the stable h^{-S}.
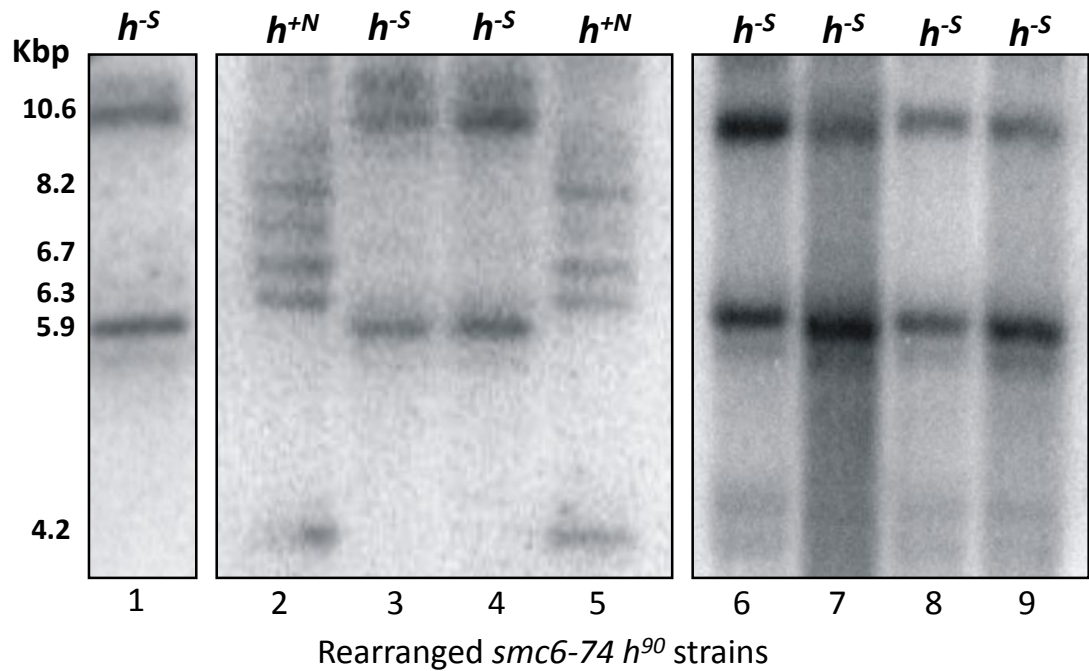
Figure 3-10 – Southern analysis of rearranged *smc6-74 h⁹⁰* strains
Cells from stably non-switching rearranged *smc6-74* colonies were harvested. Genomic DNA from 9 strains from three batches of tetrad analysis were digested with *Hind*III and subjected to Southern analysis (as described in section 2.7). Based on the banding pattern of the Southern blot it was possible to determine the type of rearrangement in each isolate.

If this is the defect it would be expected that all strains that are *h-* at *mat1* would cause the defect in switching.

To investigate whether the switching defect was a result of the direction of the switch itself or another aspect of the conformation of the *mat* locus new *smc-74* strains were derived from the original tester strains, containing issegreg arrangements of the *mat* locus. *Smc6-74 h- smt0 $^{no\ imprint}$* and *smc6-74 h- smt0 $^{no\ imprint}$ mat2.3D $^{no\ donors}$* were used to investigate the switching defect by crossing to *h$^{90\ switching}$*. Both *smc6-74 h- smt0 $^{no\ imprint}$* and *smc6-74 h- smt0 $^{no\ imprint}$ mat2.3D $^{no\ donors}$* strains have the *h-* phenotype so if the conformation of *mat1* in the parent strain is important to conferring switching ability in *smc6-74* these strains should also demonstrate a switching defect.

In *smc6-7 h- smt0 $^{no\ imprint}$* x *h$^{90\ switching}$* 94% of expected switching cells were proficient at switching and the remaining 6.5% were dead (similar to WT). This suggests that the conformation of *mat1* alone is not sufficient to cause the switching defect (table 3-4 and figure 3-11). In contrast, *smc6-74 h- smt0 $^{no\ imprint}$ mat2.3D $^{no\ donors}$* crosses did show a switching defect, as of the 41 mutant cells expected to switch 58.8% were switching, 5% were stably non-switching and 41.5% were dead. This unusually high proportion of dead cells suggests that the defect in switching is more severe than that seen in *smc6-74 h^{-S}* x *$^{h90\ switching}$* crosses. In control crosses WT *h-* and *smc6-X h- mat2.3D^{nodonors}* strains showed efficient switching with over 90% of the strains successfully able to switch, indicating that the defect was dependent on *smc6-74.*

At present it is not clear which aspect of the *smc6-74 h^{-S}* and *smc6-74 h- smt0 $^{no\ imprint}$ mat2.3D $^{no\ donors}$* is causing the defects in switching, however the lack of a K-region is a common feature to both strains (figure 3-1 and 3-3 (A)). In the *h^{-S}* strain there is a fusion between *mat2P* and *mat3M* that results in a single donor cassette and loss of the intervening K region, and in *smc6-74 h- smt0 $^{no\ imprint}$,mat2.3D $^{no\ donors}$* the K-region and both donors are completely lost.

Parents	Mating Type of Parent	Tetrad Type			Total	Number expected to Switch	% Switching	% Stable rearranged	% Dead
		Parental Ditype	Tetratype	Non-Parental Di-type					
smc6-74 x h⁹⁰	+	8	21	9	38	39	**92.3%**	**0%**	**7.7%**
smc6-74 x h⁹⁰	-	19	44	19	82	82	**70.7%**	**20%**	**8.5%**
smc6-74 smt0 x h⁹⁰	+	5	34	14	53	62	**93.5%**	**0%**	**6.5%**
smc6-74 smt0 mat2.3D x h⁹⁰	-	4	23	9	36	41	**58.5%**	**5%**	**41.5%**
smc6-74 h-mat2.3D x h⁹⁰	-	4	10	4	18	18	**94.1%**	**0%**	**5.9%**
smc6-74 h+ mat2.3D x h⁹⁰	+	8	13	2	23	17	**61.1%**	**0%**	**38.9%**
smc6-74 h⁹⁰ x h⁹⁰	*h⁹⁰*	4	13	2	19	17	**94.1%**	**0%**	**5.9%**

Table 3-5 – Switching analysis data after crossing several defined *smc6-74* strains to *h⁹⁰*

Several new isolates of *smc6-74* were created by crossing to the various tester strains used in this study. Switching analysis was repeated and the percentages of switching, rearranged and dead colonies were calculated.
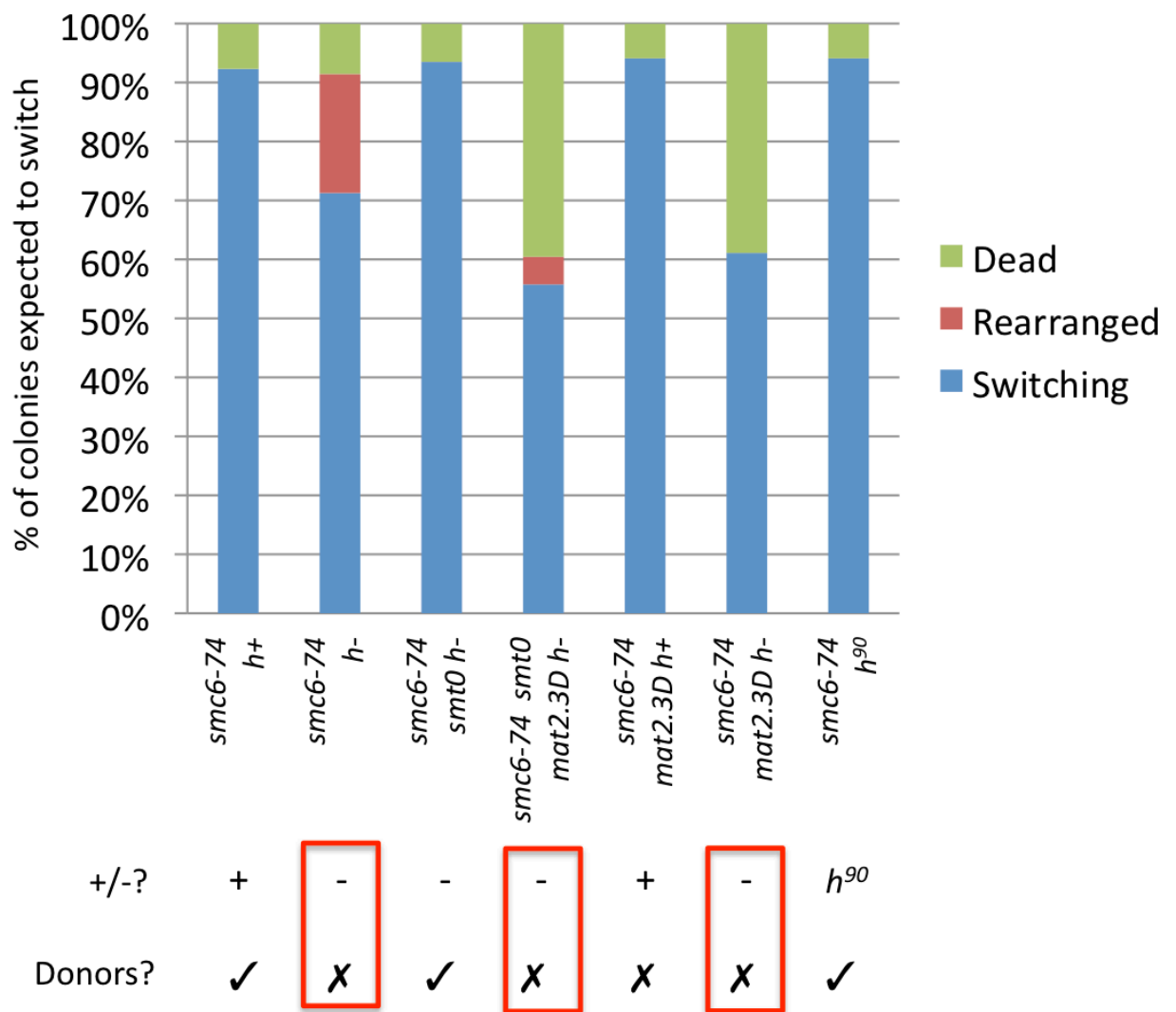
Figure 3-11 – Switching analysis of *smc6-74* strains with defined *mat* locus backgrounds

Switching analysis was conducted as previously described and the resulting percentages of switching, rearranged and dead colonies was calculated. In addition the mating type of the parent strain (+/-) and the presence of donors was determined and those strains displaying a switching defect, either by cell death or rearrangements, were indicated (red box).

This common feature could be the cause of the reduction in switching, and is consistent with the defect being more severe in *smc6-74 h- smt0 $^{no\ imprint}$ mat2.3D $^{no\ donors}$* where the entire donor region is removed.

To investigate whether the reduction of switching was dependent on the absence of the K-region two further strains, *smc6-74 h- mat2.3D $^{no\ donors}$* and *smc6-74 h+ mat2.3D $^{no\ donors}$* were compared. When *smc6-74 h-,mat2.3D $^{no\ donors}$* was crossed to *h$^{90\ switching}$*, of the switching spores produced 61.1% were viable. The remaining switching spores were classed as dead and never formed colonies. In contrast, when the *smc6-74 h+ mat2.3D $^{no\ donors}$* parent was crossed to *h$^{90\ switching}$* 94.1% of spores were able to switch, the remaining 5.9% of cells were dead and no re-arranged strains were detected. This result was unexpected and suggests that both the absence of donors and the mating-type contribute to the switching defect. –These data show that a switching defect, that is reduced switching either due to inviability of switchable cells or to *mat* locus rearrangements, only occurred when *smc6-74* parent strains lacked the donor regions, had an *mat1 h-* conformation and that imprinting and se-DSB formation occurred at *mat1*.

Since the potential switching strains must inherit the *h$^{90\ switching}$* conformation, the problem must be occurring in the *smc6-74/*WT *h-$^{imprint+}$mat2.3D$^{no\ donor}$/ h$^{90\ switching}$* heterozygous diploid. *H$^{90\ switching}$* strains have been previously shown to switch in the diploid state (Egel and Eie, 1987) and it is therefore possible that in *smc6-74* heterozygous diploids rearrangements occur which are detected after sporulation.

3.3.5 Switching *smc6-74* isolates remain switchable

Since the recombination event leading to rearrangements at the *mat* locus during switching could be occurring in the diploid, the tetrad data was separated into categories depending on how long strains were held as a diploid, as strains held as a diploid for longer would have more of an opportunity to rearrange. Strains were typically held as a diploid for 3 days until colonies formed on –adenine plates and were then patched on ELN media for sporulation. For strains held as a diploid single adenine

colonies were re-streaked onto selective plates   instead of sporulation media and grown to colonies a second time (–adenine plates for 6 days total) before sporulating.

When *smc6-74* mutants were held as a diploid the number of rearranged stable unswitchable spores was reduced. 11% (12/ 106 tetrads analysed) were found to be rearranged after 6 days compared to 31% unswitchable and 65% switching proficient after 3 days. This result suggested that something was occurring in diploids held for longer that prevented rearrangements from occurring either in the diploid or after sporulation. It is unclear why the initial switches lead to rearrangements but if the first few switches are successful then the strain stabilises in the $h^{90\ switching}$ form and the longer the strain is held as a diploid the more chance that the strain will be switching proficient. It was interesting to note that previously isolated $h^{90\ switching}$ *smc6-74* strains were very stable and did not show any reduction in viability when compared to wild type and *smc6-74* in *h-, h+, smt0* $^{no\ imprint}$ and *smt0* $^{no\ imprint}$*,mat2.3D* $^{no\ donors}$ strains (figure 3-12).

It is possible that only the initial switches in the diploid are likely to cause rearrangements and these are diluted out of the population as the colony grows. Alternatively, the stabilisation of the smc6-74 $h^{90\ switching}$ could be due to the accumulation of a suppressor of the mutant phenotype. To investigate this a previously isolated *smc6-74* $h^{90\ switching}$ strain was crossed to WT $h^{90\ switching}$ in order to determine whether the previously stabilised strain was destabilised by re-crossing. Of the tetrads analysed 94% (16/17) of spores expected to switch were seen to switch, all of the non-switching spores were dead and no rearrangements were seen. This result could support the hypothesis that an accumulated suppressor in the diploid *smc6-74*.

$H^{90\ switching}$ is allowing the strain to stabilise in a switching conformation before meiosis. It is also possible that since the switching defect depends on *smc6-74* being in the *h-* conformation with a deletion in the donor region and both parents in the cross are h^{90} ^{switching} the rearrangements do not occur. Crossing *smc6-74* $h^{90\ switching}$ to wt h^{-S} would help to support or refute the suppressor hypothesis.
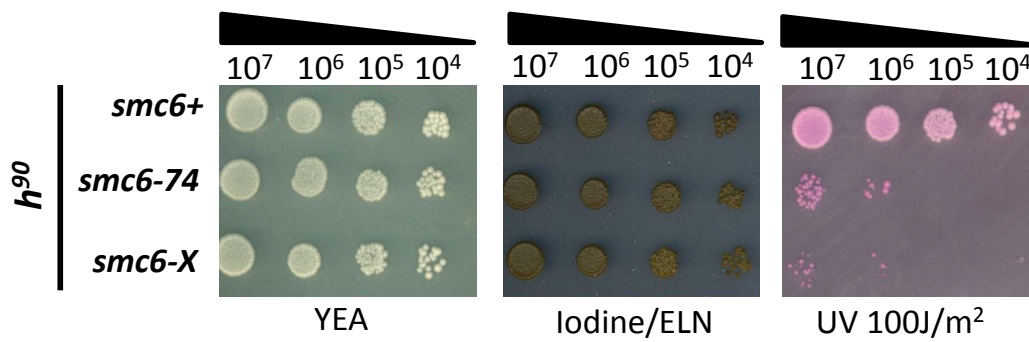
Figure 3-12 – Spot test analysis of switching *smc6* mutant isolates
10 fold serial dilutions of $1x10^7$cells/ml were spotted onto YEA plates and exposed to 100J/m^2 UV to detect *smc6* mutants and spotted onto ELN media and exposed to iodine vapors to detect switching.

3.4 Summary

Analysis of *smc6* using mating-type switching proved more complicated than initially expected. The analysis confirmed that *smc6-X* has more severe slow growth phenotype than *smc6-74* suggesting that *smc6-X* is more defective in Smc5/6 function. The investigation of *smc6-X* and *smc6-74* in switching further confirms the separation of function seen in these two alleles; *smc6-74* was defective in mating-type switching whereas *smc6-X* was not. This could imply that the early role of *smc6-74* (as described in section 1.10.5) is required for mating-type switching, or alternatively, that there is an additional role for Smc5/6 in mating-type switching that is defective in *smc6-74*.

The switching defect in *smc6-74* was less severe than that seen in the HR mutant *rad22-67*. Both led to the rearrangements in the *mat* locus but in *smc6-74* these rearrangements were dependent on the conformation of the mat locus in the *smc6-74* parent. The importance of the mating-type of the *smc6-74* parent adds an extra layer of complexity and suggests that interactions in the diploid stage of the cross are required for the defect. Since the diploid is heterozygous for *smc6-74*, a phenotype manifesting in the diploid suggests that the *smc6-74* mutation is dominant.

Data from this study suggest that there are three requirements in the parent strain for a defect in mating-type switching in *smc6-74*: lack of the donor K region, *mat1* must be in the *h-* conformation, competent to initiate switching (imprint and se-DSB) and held as a diploid for a short time. At present the distinction between the deletion of the K – region leaving a single donor cassette and complete deletion of the donor region has not fully been investigated. However, there seems to be a correlation between the more of the donor region that is deleted the more lethal the phenotype. In *h-* parent strains where the entire donor region was deleted up to 40% of the spores expected to carry the $h^{90 \ switching}$ locus were inviable and in contrast the h^{-S} parent strain where a single donor cassette remains (the donor genes of *mat2* and *mat3* are still present in a fused form of *mat2:3*) 8.5% of the spores carrying the $h^{90 \ switching}$ were dead and a further 20% were seen to be rearranged.

The influence of the parental mating-type conformation and the requirement for the donors region for switching proficiency in *smc6-74* is consistent with an epigenetic effect. Since the lack of donors and K-region contribute to the loss of switching it could be linked to the heterochromatic nature of this region. The K region contains centromeric repeats which are silenced, dependent on Swi6 (HP1 homologue) (Klar and Bonaduce, 1991). This helps to ensure the correct template is used during switching through the binding of specialist recombination mediators, Swi5/Swi2, which direct recombination during switching and there is some evidence that in mating-type switching the recombination event must be driven away from the sister to use the donor region downstream (Akamatsu et al., 2003, Haruta et al., 2008). It is possible that without the K region there is an incorrect distribution of Swi factors and this reduces the ability to switch efficiently.

Interestingly the direction of the first switch after spore germination is also important in the generation of rearrangements. In crosses using *smc6-74 h-* the first switch at the $h^{90\ switching}$ locus in the diploid would be from the *h+* conformation to *h-*. Similarly, after sporulation as the diploid can only enter meiosis when two opposite mating-types are present, the first switch is from *h+* to *h-*. This suggests that the switch from *h+* to *h-* utilising the donor *mat3-M* is likely to be important in generating the rearrangements. This could also be related to the conformation of the heterochromatic donor region as the direction of the switch depends on the distribution of Swi5/Swi2 over the two donor cassettes (see introduction 1.8.5).

Chapter 4 – Using the mat locus single-ended double-strand break (se-DSB) repair

4.1 Introduction

Single-ended double-strand break repair (abbreviated to se-DSB) sometimes known as polar breaks, have been detected as meiotic intermediates (Hunter and Kleckner, 2001) however, this study focuses on replication associated se-DSBs. A se-DSB can be formed when a replication fork hits a DNA lesion, such as a single strand nick, causing replication fork collapse. Unlike replication forks stably stalled due to depleted nucleotides (as caused by HU) HR is required for fork resetting when forks collapse (replisome dissociated) or break (se-DSB) (Saleh-Gohari et al., 2005, Lambert et al., 2005).

The Arcangioli lab developed the *mat* locus as a tool to study se-DSB repair and showed that HR and the structure-specific nuclease Mus81 were essential for se-DSB repair (Roseaulin et al, 2008). This study utilised the same system to analyse se-DSB repair in *smc6-X* and *smc6-74.* The strain used to determine the effects of an se-DSB on strain viability was the *mat1h- mat2.3D^{no donor}*, where the *mat2* and *mat3* donors as well as the intervening K-region is replaced with the *S. cerevisiae LEU2* gene (Klar and Miglio, 1986). During mating-type switching pausing of the replication fork in the first S phase leads to the formation of an imprint at *mat1* (section 3.1.3) and this is converted to a se-DSB when the replication fork reaches the imprint in the second S phase (Roseaulin et al., 2008). In the absence of the donor region mating-type switching cannot be completed and the se-DSB must be repaired using the sister chromatid (figure 4-1).

H+ strains of interest, *smc6-X*, *smc6-74*, WT and *rad22-67*, were crossed to an *h- mat2.3D^{no donor}* strain and the resulting spores were dissected using a micromanipulator. Colonies were grown on YEA media and replica plated to selective media in order to track alleles. The *LEU2* marker in *mat2.3D^{no donor}* was followed using leucine negative media. Because the *mat2.3D^{no donor}* allele comes from one parent two
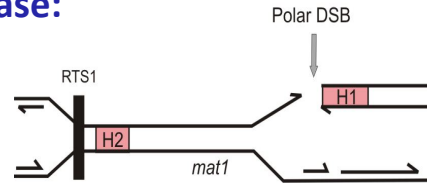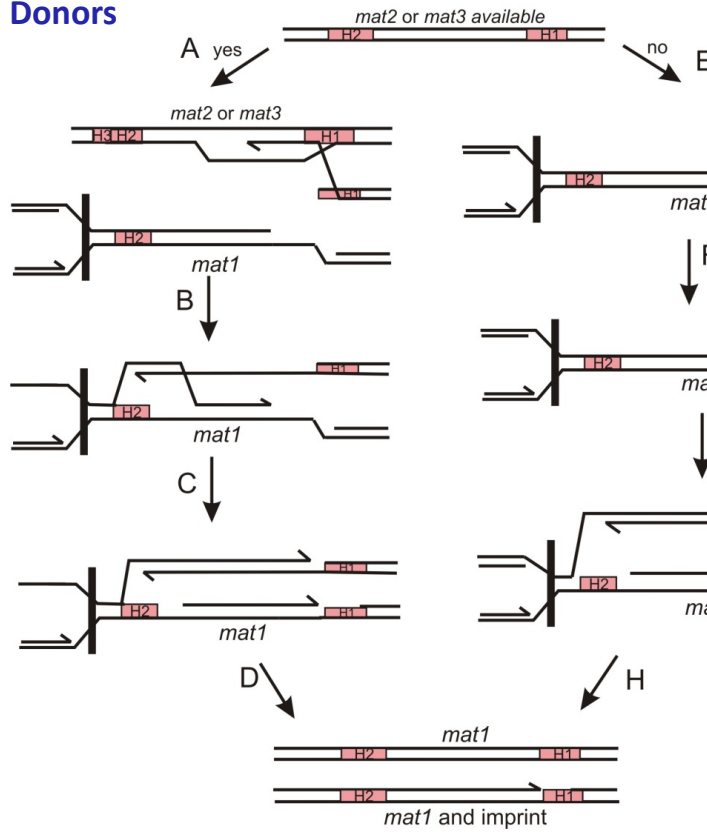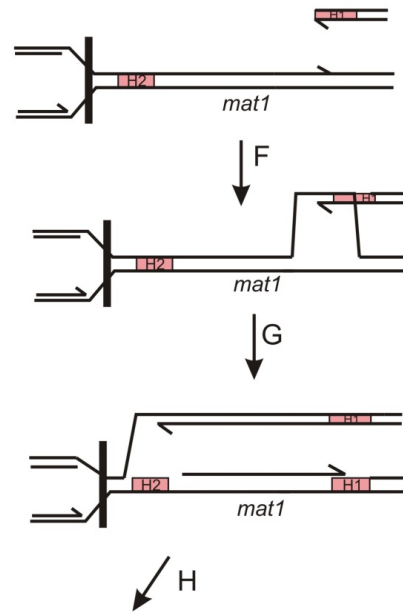
Figure 4-1 – Model for the recombination/replication coupled repair of a polar break with donors (A-D) and without donors (E-G) (Adapted from Roseaulin et. al. 2008)

spores out of the four tetrads will be LEU2+ and therefore be repairing the se-DSB. In addition as one parent is WT and one carries the *smc6* mutant phenotype two of the progeny will carry this gene. Using this information strains carrying the *smc6* mutation and the *mat2.3D^{no donor}* allele were determined so that the viability of mutant strains that repair the se-DSB can be detected and observed.

For this analysis inviable cells were split into 4 categories **+D$^+$** (WT (*smc6+, rhp51+, rad22+*) +donors), **+D$^-$** *(*WT −donors), **MD$^+$** (*smc6, rhp51* or *rad22* mutant +donors) and **MD$^-$** (*smc6* or rad22 mutant −donors). The phenotype of the living cells enables the genotype to be deduced in the dead cells as long as at least two cells are surviving (although 2 living cells may not be enough in every case). The percentages of inviable cells in each phenotype group were calculated and compared to the expected percentages, assuming 25% in each category, and significance determined by *chi^2* analysis (see section 2.8).

4.2 Crossing to negative control, *smt0^{no imprint}mat2.3D^{no donor}*, does not show a reduction in viability in any mutant background

A negative control for this analysis was the strain *smt0^{no imprint}mat2.3D^{no donor}* strain (figure 4-2). This strain has the same *no donor* deletion as outlined above with the addition of the deletion at *smt0* that prevents imprinting (Styrkarsdottir et al., 1993). This strain can be used to determine if deletion of the donors has any affect on viability when the cells are not imprinting.

When WT was crossed to the switching negative strain *h- smt0^{no imprint}mat2.3D^{no donor}* the viability was 94%. *Smc6-74* showed an overall viability of 86% and while this may appear to be a slight decrease when compared to WT when the data was separated into classes (as outlined in section 3.2) the reduction was not significantly different (P= 0.0645). *smc6-X* had an overall viability of 89%, P = 0.1 not significant after segregation into classes (figure 4-3).

	Conformation	Strain name	Imprint?	Donors?
Tester Strain	mat1 L mat2:3d:LEU2	h- mat2,3d::LEU2	✓	✗
	mat1 L mat2:3d:LEU2	h- smt0 mat2,3d::LEU2	✗	✗

Figure 4-2 - Tester strain *mat* locus conformation

Schematic diagram showing the conformation of the *mat* locus in *mat2.3D$^{no\ donor}$* and *smt0,mat2.3D$^{no\ imprint,\ no\ donors}$*. *mat1* and its homology boxes are labelled blue and white respectively and past the L-region is the LEU2 gene that marks the *mat2.3* deletion. Whether each strain is imprinting proficient or contains donors is marked with a ✓ or ✗. (Southern analysis of these strains can be seen in figure 3-2).

Figure 4-3 –Tetrad viability analysis of *smt0,mat2.3D*[no imprint, no donor] tetrads Strains were crossed to the *smt0* tester strain and the resulting tetrads were categorised based on the numbers of viable tetrads. (A) Examples of tetrads seen from each cross. *smc6-74* and *smc6-X* were detected using UV at 100J/m² UV on YEA plates supplemented on 5μg/ml PhloxinB. *rad22-67* was detected using 5mM HU on PhloxinB plates. The right hand panel shows segregation of alleles circle is *smt0 mat2.3D*[no imprint,no donors] triangle is *smc6/rad22-67* mutants (B) The percentages of tetrads in each viability category (viable:dead) were determined based on the number of viable spores.

(A) Tetrads analysis after crossing to *smt0,mat2.3D*[no imprint, no donors]

(B)

Tetrad category (viable spore number: dead spore number)
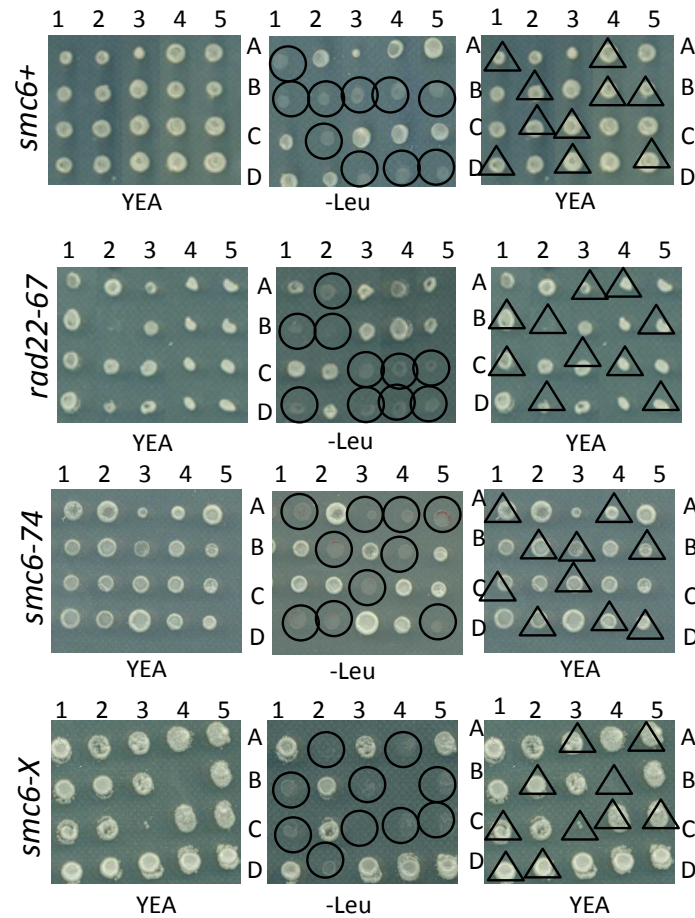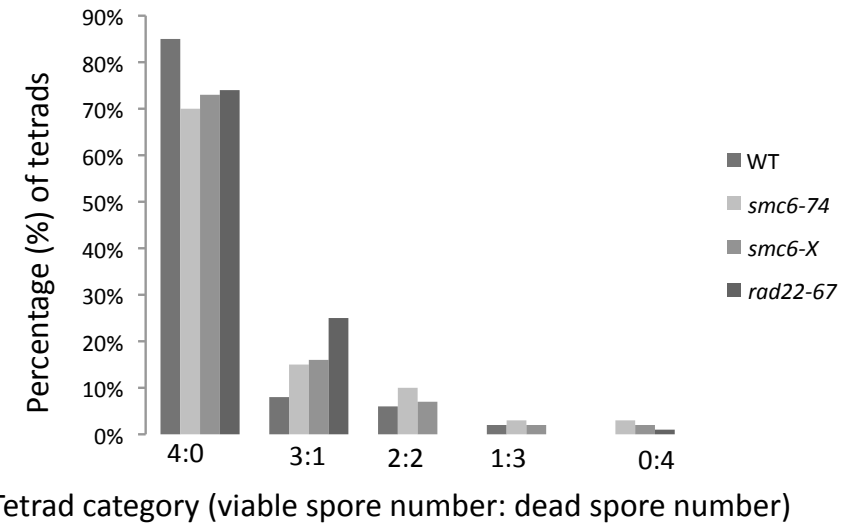
4.3.1 se-DSB analysis using *mat2.3D*^{no donor}

se-DSB repair was investigated after crossing to the *h- mat2.3D*^{no donor} strain. For WT 121 tetrads were analysed and of those 93% of spores were viable (table 4-1) showing that WT cells can efficiently repair the se-DSB. Of the cells that were not viable the percentage of inviable spores with or without the donors cassette was calculated (by following LEU2). It could be expected that in an unbiased situation 50% of inviable cells would have the deleted donors and 50% would have the donors present. It was found that 56% of inviable cells had the donors and 44% of inviable cells had the donors deleted. These values were close to the expected values, and as the number of inviable cells was so low, it seemed unlikely that the deletion of the donors was having a significant affect on viability in WT cells. Examples of tetrads can be seen in figure 4-4.

Se-DSB repair was also investigated in *rhp51Δ,* which encodes Rad51. Mutants in *rhp51* are deficient in HR and very sensitive to to ionising radiation (IR), which causes DSBs (Muris et al., 1997). Consistent with the Roseaulin study (2008), in this mutant only 75% of spores were viable and the majority of dead cells, 73%, had a genotype corresponding to category 4 MD- (table 4-1) showing, as would be predicted, that Rad51 is required for repair of the se-DSB.

Rad52, encoded by *rad2*2, is required for all HR and consistently, Roseaulin et al (2008) found *rad22-d* to be defective in se-DSB repair. We therefore analysed the *rad22-67* strain as this was reported to have a switching-specific defect but not to be sensitive to IR (Ostermann et al., 1993). Thus, it would not be expected to be defective in se-DSB repair. 67 tetrads were analysed and of these 91% of cells were viable suggesting that, as predicted, *rad22-67* is not defective in processing se-DSBs. Of the inviable cells 35% fell into category 4, MD- (*rad22-67* no donors). As there are four categories it would be expected that the percentage of cells in each category would be 25% so the increase to 43% looks striking. However it is important to remember that this is the percentage of inviable cells and is only 23 of the total number of cells analysed (n=256). When this is compared to the 15% of total cells that are viable with the *rad22-67* no donors genotype it can be concluded that *rad22-67* does not show a large reduction in

Parents	Viable;Dead Spores					Number of tetrads	Number of inviable cells	% ++D	% LEU+ +-D	%M+D	% LEU+ M-D
	4;0	3;1	2;2	1;3	0;4						
WT h+ x mat2.3D	121	23	1	1	3	146	40	56	44	0	0
% of Total	83	16	1	1	2						
smc6-74 h+ x mat2.3D	59	24	2	6	13	91	102	10	10	17	63
% of Total	65	26	2	1	14						
smc6-X h+ x mat2.3D	83	56	12	2	12	153	134	18	18	23	41
% of Total	54	37	8	1	8						
rad22-67 h+ x mat2.3D	47	11	6	0	0	64	23	21	27	17	35
% of Total	73	17	9	0	0						
rad51Δ h+ x mat2.3D	2	7	2	2	0	13	17	0	0	27	73
% of Total	15	54	15	15	0						

Table 4-1 – Summary of tetrad data after crossing to mat2.3D [no donors]
Strains were crossed to the *mat2.3D*[no donors] tester strain and analysed by tetrad dissection. The number of tetrads with 4, 3, 2, 1 or 0 viable colonies was counted and the percentage of total colonies was calculated. Based on the category distribution the total number of inviable cells was determined and the phenotype of each inviable cell was determined (for this part of analysis only class 4;0, 3;1 and 2;2 were used as phenotypes of inviable cells cannot be calculated in class 3;1 and 0;4). The percentage of inviable colonies with each phenotype (++D, +-D, M+D, M-D see section 4.1 for details) was then calculated.
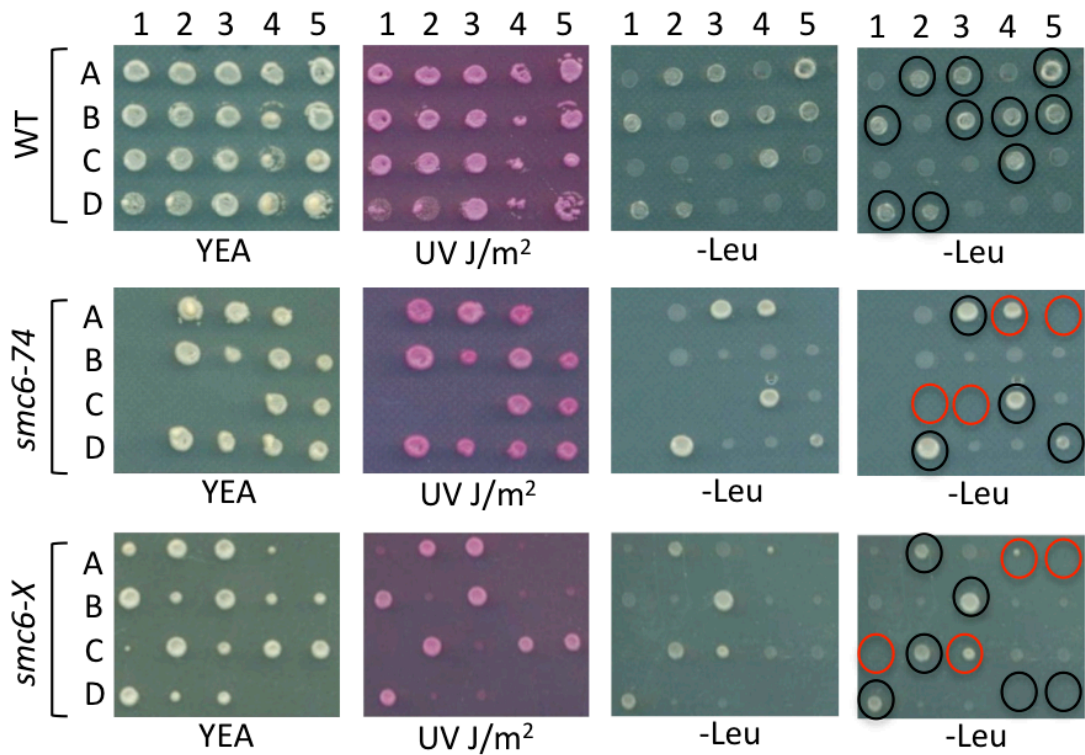
Figure 4-4 – Tetrad viability analysis of *mat2.3D*[no donor] crosses

Strains were crossed to the *mat2.3D*[no donor] tester strain and the resulting spores were plated on YEA and grown for 3 days. Tetrads were replica plated to selective media to detect interesting alleles. *smc6-74* and *smc6-X* were detected using UV at 100J/m² and plating on YEA supplemented with 5µg/ml phloxin B. The *mat2.3D*[no donor] deletion is marked with LEU2+ and was detected using supplemented YNBA minimal agar without leucine. Growing colonies on –Leu agar had deleted donors. The right hand panel shows the segregation of alleles black circle is WT with *mat2.3D*, red circle is *smc6* mutant with *mat2.3D*.

viability in the presence of an se-DSB. Thus, the *rad22-67* mutant is a separation of function allele that, unlike *rad22-d*, does not have a defect in se-DSB repair.

4.3.2 *smc6-74* and *smc6-X* mutants were defective in se-DSB repair

During se-DSB analysis both *smc6-X* and *smc6-74* displayed a similar phenotype. Both strains showed a reduction in viability; *smc6-74* had a viability of 76% and *smc6-X* had a viability of 79%. In *smc6-74* 63% of inviable cells were *smc6-74* mutants lacking in donors (MD-) and in *smc6-X* 41% of inviable cells are *smc6-X* and without donors (MD-) (table 4-1 figure 4-5). In both cases the distribution of dead cells was compared to the expected values if distribution was random, that is 25% for each category, and tested using chi-squared statistical analysis. There was a significant difference in the distribution when compared to the expected values from random distribution, $P=9.9 \times 10^{-20}$ for *smc6-74* and $P=8.52 \times 10^{-5}$ for *smc6-X*. Thus, the reduced viability and the skewed distribution suggest that both mutants have a defect in se-DSB repair.

Tetrad analysis is useful as a quantitative measure of viability however there are limitations to this analysis as strains must pass through meiosis and grow on challenging selective media. Spot tests were used to assess whether loss of viability was due to passing through meiosis. Viable colonies formed as a result of crossing mutants to *mat2.3D*$^{no\ donors}$ were isolated and grown on YEA media. Both *smc6-X* and *smc6-74* had a reduction in viability when compared to WT (figure 4-6)

4.4 Surviving *smc6-X* and *smc6-74 mat2.3D*$^{no\ donor}$ isolates maintain the conformation of the *mat* locus and imprint

Spontaneous rearrangements can occur at the *mat* locus and so the conformation of the *mat* locus in viable *smc6-X* and *smc6-74 mat2.3D*$^{no\ donor}$ isolates was checked by PCR and sequencing to determine if there had been a spontaneous deletion at *mat1* that prevented imprinting. PCR analysis of the *mat1* region showed that DNA from the stabilised *mat2.3D*$^{no\ donor}$ strains was the expected size, 1.009 kb (figure 4-7) and no rearrangements were seen on sequencing.
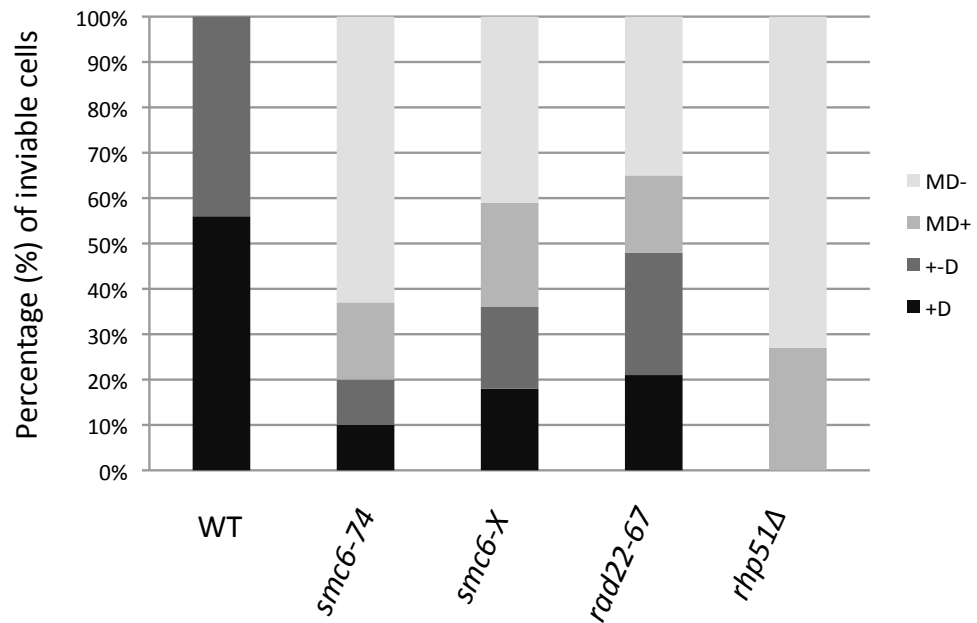
Figure 4-5 – Phenotypes of inviable cells after crossing to *mat2.3D^no donor*
Strains were crossed and sporulated on ELN agar. After tetrad dissection and replica plating colonies were grown on various media to determine the phenotype of any inviable cells (see figure 4-4 for examples of tetrads). Inviable cells were split into 3 categories; +D (WT +donors), +-D (WT – donors), MD+ (*smc6* or *rad22/51* mutant + donors) and MD- (*smc6* or *rad22/51* mutant –donors). The percentage of inviable cells in each category is plotted graphically.
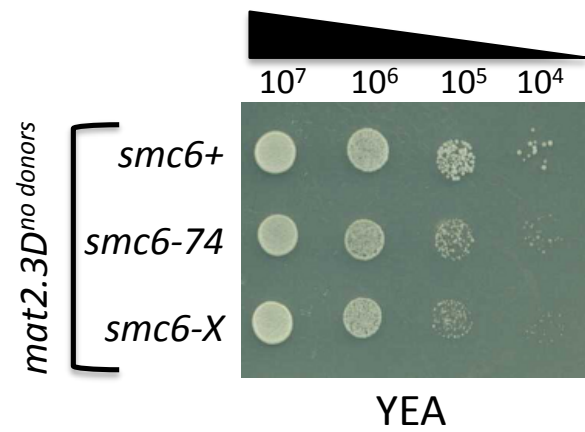
Figure 4-6 – Spot test analysis of *mat2.3D^no donor* isolates
10 fold serial dilutions of $1x10^7$ cells/ml were spotted onto YEA and grown for 3 days to check for any changes in viability in *mat2.3D^no donor* isolates.

(A)

Primer *smt0_F*

1kb

mat1   H1

Primer *smt_0R*

(B)

Marker No DNA No Primers   *smc6+*   *smc6-74*   *smc6-X*

1 Kb →

1 2 3 4   1 2 3 4   1 2 3 4

(C)
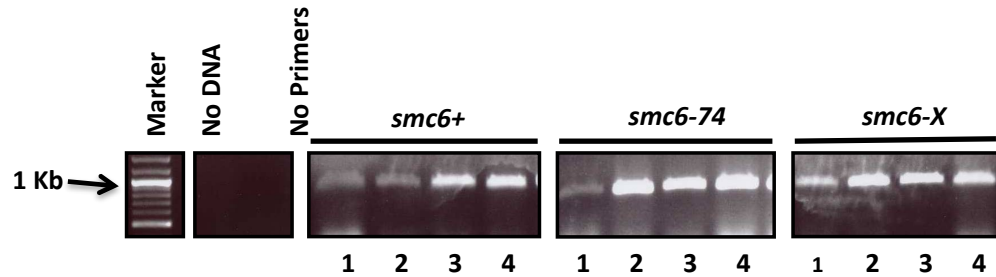
```
        1         10        20        30        40        50        60        70        80        90        100       110       120       130
        |---------+---------+---------+---------+---------+---------+---------+---------+---------+---------+---------+---------+---------|
smc6+1  GAAAAGGGGATTAAAAGAATGCTCTATGGT-GAGGAAGTGGAACGTAAGATATTAAAGGAATAGGGATGTGAATGTAAAGAGTGGGTAGATGCATTTGGGATGAGGTTTAATATATGTTTATAAAGGAAA
smc6-741    AATAGGGATTATAAGA-TGCTCTATGGT-GAGGAAGTGGAACGTAAGATATTAAAGGAATAGGGATGTGAATGTAAAGAGTGGGTAGATGCATTTGGGATGAGGTTTAATATATGTTTATAAAGGAAA
smc6-X1     ATAAGGGATTTAAAGATGCTCTATGGTTGAGGAAGTGGAACGTAAGATATTAAAGGAATAGGGATGTGAATGTAAAGAGTGGGTAGATGCATTTGGGATGAGGTTTAATATATGTTTATAAAGGAAA
Consensus ...RaaaGGGATTaaARgaaTGCTCTATGGT.GAGGAAGTGGAACGTAAGATATTAAAGGAATAGGGATGTGAATGTAAAGAGTGGGTAGATGCATTTGGGATGAGGTTTAATATATGTTTATAAAGGAAA

        131       140       150       160       170       180       190       200       210       220       230       240       250       260
        |---------+---------+---------+---------+---------+---------+---------+---------+---------+---------+---------+---------+---------|
smc6+1  ATGGCTAATGGATATGAAGTATTGGTGTAAGGAGTTCAAGATGTATGGGGAGAAAGAGGATGGTTGATGGGGTGGTTGAGCGAGGAAAGTGTTGAAGTATAGTGTGTATGGTAGGAATGAGTAATGAGAT
smc6-741 ATGGCTAATGGATATGAAGTATTGGTGTAAGGAGTTCAAGATGTATGGGGAGAAAGAGGATGGTTGATGGAGTGGTGGAGCGAGGAAAGTGTTGAAGTATAGTGTGTATGGTAGGAATGAGTAATGAGAT
smc6-X1  ATGGCTAATGGATATGAAGTATTGGTGTAAGGAGTTCAAGATGTATGGGGAGAAAGAGGATGGTTGATGGAGTGGTTGAGCGAGGAAAGTGTTGAAGTATAGTGTGTATGGTAGGAATGAGTAATGAGAT
Consensus ATGGCTAATGGATATGAAGTATTGGTGTAAGGAGTTCAAGATGTATGGGGAGAAAGAGGATGGTTGATGGaGTGGTcGAGCGAGGAAAGTGTTGAAGTATAGTGTGTATGGTAGGAATGAGTAATGAGAT

        261       270       280       290       300       310       320       330       340       350       360       370       380       390
        |---------+---------+---------+---------+---------+---------+---------+---------+---------+---------+---------+---------+---------|
smc6+1  GTAGTGAAAGTATAATATTAGTGAGTATATTATGTAGGGAGTGCGTAGCGTAGCGAAGCAAATATCTCGTTAGAGGGGAAGGGGAAGGTAGAAGGGCGCACACAAAAAGGGAAAATTGGAGGGGAGAATGA
smc6-741 GTAGTGAAAGTATAATATTAGTGAGTATATTATGTAGGGAGTGCGTAGCGTAGCGAAGCAAATATCTCGTTAGAGGGGAAGGGGAAGGTAGAAGGGCGCACACAAAAAGGGAAAATTGGAGGGGAGAATGA
smc6-X1  GTAGTGAAAGTATAATATTAGTGAGTATATTATGTAGGGAGTGCGTAGCGTAGCGAAGCAAATATCTCGTTAGAGGGGAAGGGGAAGGTAGAAGGGCGCACACAAAAAGGGAAAATTGGAGGGGAGAATGA
Consensus GTAGTGAAAGTATAATATTAGTGAGTATATTATGTAGGGAGTGCGTAGCGTAGCGAAGCAAATATCTCGTTAGAGGGGAAGGGGAAGGTAGAAGGGCGCACACAAAAAGGGAAAATTGGAGGGGAGAATGA

        391       400       410       420       430       440       450       460       470       480       490       500       510       520
        |---------+---------+---------+---------+---------+---------+---------+---------+---------+---------+---------+---------+---------|
smc6+1  ATGACACGAACAGCATAATTGGAAACATGGAAACGAACGAGAGAAAACAAAGGAGAAAGACTATACATTTATATTACAAAAAAATTATTGAAAATAAATAAAAACGAATAAAAAAAAACAGCATATTTCGA
smc6-741 ATGACACGAACAGCATAATTGGAAACATGGAAACGAACGAGAGAAAACAAAGGAGAAAGACTATACATTTATATTACAAAAAAATTATTGAAAATAAATAAAAACGAATAAAAAAAAACAGCATATTTCGA
smc6-X1  ATGACACGAACAGCATAATTGGAAACATGGAAACGAACGAGAGAAAACAAAGGAGAAAGACTATACATTTATATTACAAAAAAATTATTGAAAATAAATAAAAACGAATAAAAAAAAACAGCATATTTCGA
Consensus ATGACACGAACAGCATAATTGGAAACATGGAAACGAACGAGAGAAAACAAAGGAGAAAGACTATACATTTATATTACAAAAAAATTATTGAAAATAAATAAAAACGAATAAAAAAAAACAGCATATTTCGA

        521       530       540       550       560       570       580       590       600       610       620       630       640       650
        |---------+---------+---------+---------+---------+---------+---------+---------+---------+---------+---------+---------+---------|
smc6+1  TAGAATCAGGGCAGTAAAATCCATGTTATTACTTTATGTAAGGAGATTTTAGGAAGCATCACCCTCTAAAACAGTATGGCATTACAGTGCTTAGAACTACGTTATGTTAGCATAACAGATATAAATCGCAA
smc6-741 TAGAATCAGGGCAGTAAAATCCATGTTATTACTTTATGTAAGGAGATTTTAGGAAGCATCACCCTCTAAAACAGTATGGCATTACAGTGCTTAGAACTACGTTATGTTAGCATAACAGATATAAATCGCAA
smc6-X1  TAGAATCAGGGCAGTAAAATCCATGTTATTACTTTATGTAAGGAGATTTTAGGAAGCATCACCCTCTAAAACAGTATGGCATTACAGTGCTTAGAACTACGTTATGTTAGCATAACAGATATAAATCGCAA
Consensus TAGAATCAGGGCAGTAAAATCCATGTATTACTTTATGTAAGGAGATTTTAGGAAGCATCACCCTCTAAAACAGTATGGCATTACAGTGCTTAGAACTACGTTATGTTAGCATAACAGATATAAATCGCAA
```

Approximate *smt0* imprint location

Figure 4-7 – DNA sequencing showed that *mat2.3D^{no donor}* isolates had no spontaneous mutations in *mat1*
(A) Schematic of *mat1* and the location of primers either side of the H1 homology box. (B) Cells from mutant *mat2.3D* colonies were grown and subject to colony PCR to check if there were any spontaneous mutations that lead to increased viability. (C) DNA sequencing of the 1 kb PCR product was performed showing the H1 imprinting site (black box) and the sequence either side.

Southern blot analysis was used to detect imprinting. An *h-* specific 1 kb probe, overlapping the region approximately 650 bp upstream and 350 bp downstream of the imprint site at *mat1,* was synthesised using PCR. DNA was isolated using the standard genomic DNA preparation method (outlined in methods 2.7.1) and digested with *Hin*dIII. After imprinting the site is fragile and breaks during the DNA isolation process giving rise to two fragments of 5kb (upstream of *mat1*) and 5.4kb (downstream of *mat1*) in addition to the 10.4kb full length band (figure 4-8). Four isolates of WT, *smc6-74* and *smc6-X* were analysed and in all isolates both bands corresponding to imprinting were detected confirming that imprinting and, by deduction, se-DSB repair occurs in all isolates. (Analysis that demonstrates the conversion of the imprint into a se-DSB is shown in Rosealin et al (2008) Sup. Figure 3).

4.5 Summary

This analysis using the *mat2.3D* $^{no\ donor}$ strain has provided an interesting insight into the role of Smc6 in response to a se-DSB. The viability of both *smc6-X* and *smc6-74* was reduced when the strains are required to repair such a break. This defect is not as severe as that seen in recombination mutant *rhp51Δ* or that reported for *mus81Δ*, (Roseaulin et al, 2008) suggesting that Smc6 does not play such a crucial role in se-DSB repair as Rad51 or Mus81. However, the other mutants analysed were null mutants, and, as Smc6 is an essential protein, the strains used in this analysis were hypomorphic mutants with residual function. It is possible that Smc6 is involved in regulating repair either directly by recruiting factors or indirectly by modifying DNA structure to allow access by other proteins such as HR mediators or Mus81.

Previous studies in the lab using *smc6-X* and *smc6-74* mutants have shown a separation of function, in particular in the response to DNA damage and replication fork stalling. This analysis has highlighted a common defect in se-DSB repair, which is characterised in more detail in the following

(A)

H   10.4 Kb   H

mat1
mat2.3D^(no donors)

5.0 Kb   Imprint 5.4 Kb
Probe

(B)

Kb
10.4
5.4
5.0
Isolate 1 2 3 4   1 2 3 4   1 2 3 4
WT   *smc6-74*   *smc6-X*
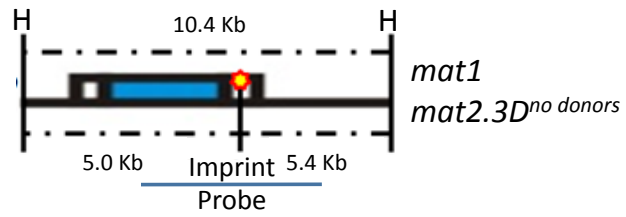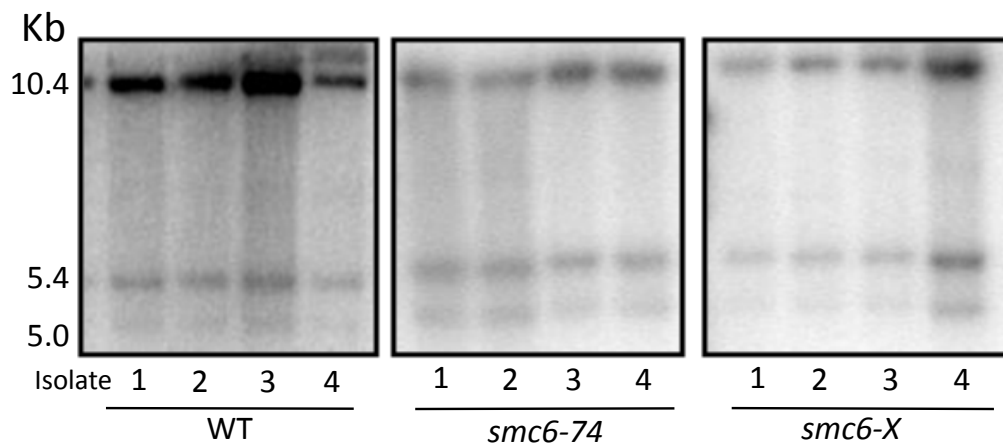
Figure 4-8 – Southern analysis of *mat2.3D^(no donor)* isolates
(A) Map of *mat2.3D^(no donor) mat1* (blue box) flanked by the homology boxes (white) and showing *HindIII* digest sites (H). During genomic DNA preparation the imprint site is broken resulting in two fragments, 5.0 Kb and 5.4 Kb, and the 1 Kb *mat1 h-* specific probe covers this entire break region. (B) Southern analysis was performed on genomic DNA. The non-imprinting whole *mat1* fragment runs at 10.4 Kb and the broken imprinting strains have additional bands that run at 5.4 and 5.0 Kb.

Chapter 5 – Using an inducible mating-type switching system to investigate the role of Smc6 in single-ended double-strand break repair

5.1 An inducible single-ended double strand break repair system

The Arcangioli lab initially developed an inducible mating-type switching system, to study the h^{90} switching strain (Holmes et al., 2005). In a second study the inducible mating-type switching system was introduced into the *mat1M mat2.3D$^{no\ donor}$* background creating an inducible single-ended DSB (se-DSB) system (Roseaulin et. al. 2008).

In the inducible system imprinting at *mat1* is prevented by transcription through the imprinted region, which inhibits further mating-type switching. Transcription interferes with imprinting as after the imprint is introduced during S phase it is repaired during transcription (Holmes et al, 2006). The inducible promoter *nmt1* (no message in thiamine) was used to regulate transcription enabling reversible inhibition of imprinting. Thiamine is an essential co-factor and is produced in the cell when it is not present in the medium. In media lacking thiamine (-T) the *nmt1* promoter is induced but it is repressed in the presence of thiamine (+T) (Schweingruber et al., 1992). The strong inducible promoter *nmt1*, based on plasmid pFA6a-kanMX6-P3nmt1, and marked with *KanMX6* was inserted 256 base pairs downstream (telomeric proximal) of the H1 homology box at *mat1*. This created an inducible h^{90} switching strain (Holmes et. al. 2006) that where switching is induced when the *nmt1* promoter is repressed upon the addition of thiamine to the growth media (+T). Thus, strains can be prepared and grown in media lacking in thiamine to prevent mating-type switching, then, when switching is required thiamine is introduced to the growth medium, repressing transcription and repair of the imprint. Upon the addition of thiamine it has been shown that imprinting is detectable as soon as 30 minutes after induction (Holmes et al, 2006; Roseaulin et al, 2008).

The *nmt1* promoter was also introduced into the *mat2.3*^{No Donor} strain to create an inducible single-ended DSB system (Roseaulin et al. 2008). The benefit of this system is that large cultures of cells can be grown and induced simultaneously. Strains can also be grown and stored in conditions that would not induce one-ended break repair minimising the selection for suppressors. Most importantly the use of synchronous cultures enables many repair events to be monitored simultaneously, so that, even if repair leads to cell death events, can be analysed by microscopy, PCR and Southern analysis. Another advantage is that crossing is not required for each analysis and this not only saves time, but also ensures that all cell backgrounds are the same and any possible interference of the parental *mat* locus conformation (as seen with the *smc6-74* switching defect) would be eliminated. This inducible system was used to investigate the repair defects in *smc6* mutants. (Figure 5-1 and 2-2).

5.2 Analysis of mutant strains containing the single-ended break system

A series of mutants that carried the inducible se-DSB repair system was created. Strains for investigation were positive (wild type WT, *rqh1Δ*) controls that had previously been shown to not be defective in this system (Roseaulin et al., 2008) and negative controls (*rhp51Δ*, *rhp57Δ*, *mus81Δ* (Roseaulin et al, 2008)). The two *smc6* mutants, *smc6-X* and *smc6-74* (see appendix A for further strain information).

Spot tests were used to identify differences in ability to process a se-DSB as mutants that experienced difficulty processing the break should grow slower or have more dead cells per colony than those that were proficient in repair. Different series of freshly patched strains were plated on fully supplemented media +T (se-DSB induced) or −T (se-DSB repressed). To highlight the difference between dead cells and slow growing cells media was supplemented with PhloxinB which is actively excluded from cells but accumulates in dead cells turning them a bright pink colour.

The WT strain showed little difference between colonies grown on agar with +T (DSB on) or −T (DSB off) with circular colonies growing in the first three dilutions of $1x10^7$, $1x10^6$ and $1x10^5$ cell ml^{-1} and similar sized colonies growing at the $1x10^4$ dilution and all colonies were very pale pink (figure 5-3 line 1).

(A) *mat1M,nmt1::KANMX6, mat2.3D^{no donors}*

-Thiamine

mat1P   *nmt1::kanMX6*

nmt1   *LEU2*   *mat2.3D::LEU2*

256bp

(B)

Imprint

+Thiamine

mat1P   *nmt1::kanMX6*

nmt1   *LEU2*   *mat2.3D::LEU2*
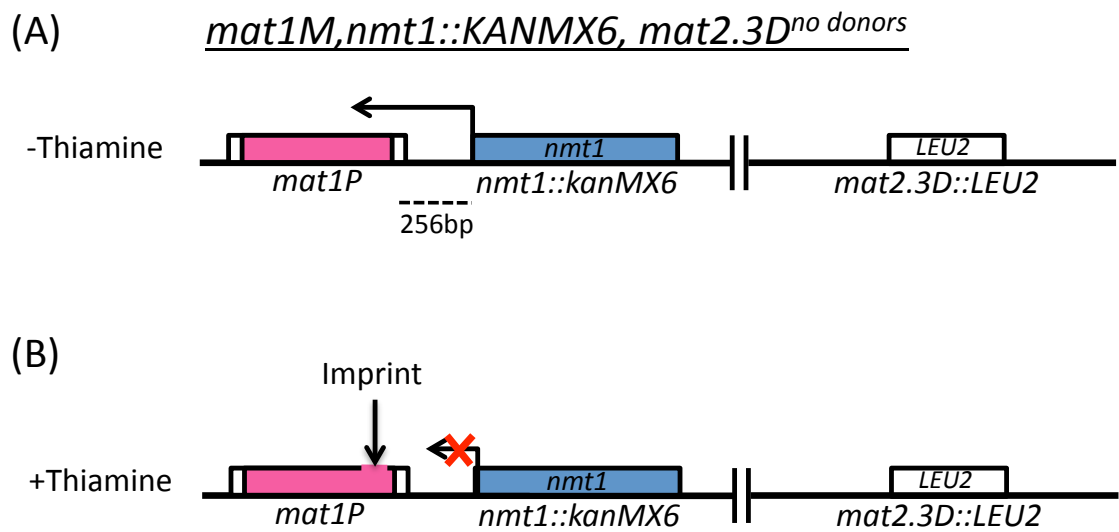
Figure 5-1- Inducible *mat* locus conformation

To create the inducible one-ended break repair strain the *mat1M,mat2.3D^{no donor}* the nmt1 promoter was introduced to create a thiamine dependent inducible system. (A) The nmt1::kanMX6 plasmid was inserted at a neutral point 256bp downstream of the H1 homology box and in the absence of thiamine transcription prevents the imprint being formed. (B) Upon the addition of thiamine the promoter is turned off and imprinting is maintained at *mat1* leading to a se-DSB repair event.
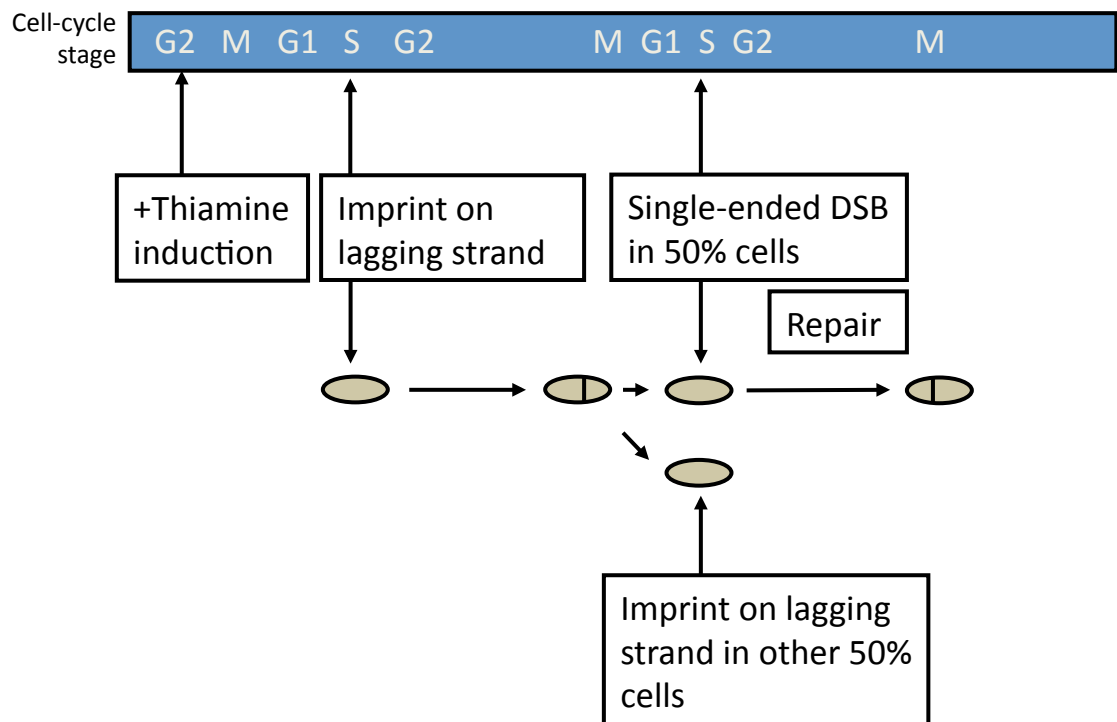
Figure 5-2- Timing of the single-ended DSB break after induction with thiamine

After the addition of thiamine to a mostly G2 asynchronous cell culture, cells must progress through the next S-phase for imprinting to take place in the cells. Once the imprint is made it is maintained throughout the cell cycle and after mitosis it is converted to a single-ended DSB in 50% of the cells. The remaining 50% of cells imprint while the break is repaired.
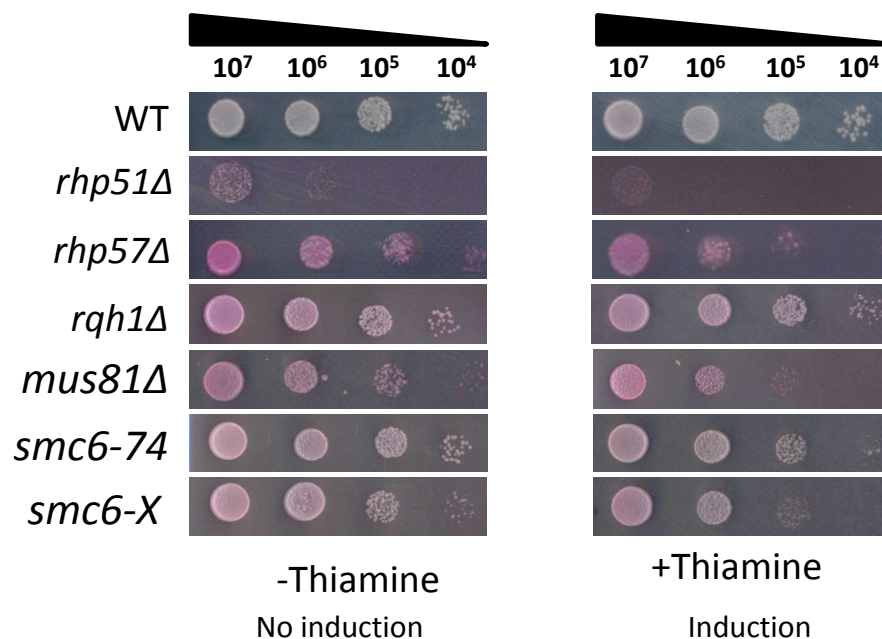
Figure 5-3- Analysis of strains in response to single-ended DSB repair

Spot test analysis was used to investigate several mutant's response to se-DSB repair. 10-fold serial dilutions of 1×10^7 cells/ml were spotted on to media +/- thiamine, cells were grown for 3 days at 30°C. Strains used are WT, recombination mutants *rhp51Δ* and *rhp57Δ*, HJ resolvase *rqh1Δ*, se-DSB specific mutant *mus81Δ* and *smc6* mutants *smc6-74* and *smc6-X*.

Recombination mutants have severe growth defects. Consistently *rhp51Δ* appeared to be very sick, even on −T plates. *Rhp57Δ* was more viable, however in both strains colonies were dark pink in colour indicative of a high number of dead cells. A further loss of viability seen when the DSB was induced (+T) showed that they were deficient in se-DSB repair. *Rhp51Δ* has a severe growth defect growth in the 1×10^7 and 1×10^6 dilutions and growth was reduced 10 fold as not colonies were seen at 1×10^6 cells ml^{-1} on plates +T. *rhp57Δ* was able to grow at a dilution of 1×10^4 −T and 1×10^5 +T. This is consistent with there being two recombination mediator complexes in *S. pombe*: Rhp55/Rhp57 and Swi5/Sfr1 *(Akamatsu et al., 2003)* (figure 5-3 line 2 and 3).

Mus81Δ also has a growth defect (Haber and Heyer, 2001) and was very slow growing with or without thiamine. Colonies grew on the −T$^{no\ DSB}$ plate up to the concentration of 1×10^5, however on the +T^{DSB} plate *mus81Δ* colonies only grew to the 1×10^6 dilution showing that the defect in se-DSB repair reduces the viability of colonies by an approximate factor of 10. This is consistent with data seen in both recombination controls (figure 5-3 line 5).

Spot test analysis confirmed that *smc6-X* and *smc6-74* have a defect in se-DSB repair as there was a slight reduction in viability when the se-DSB was induced (+T). This change in viability was difficult to quantify as it appeared to be small and was similar to that seen in typical se-DSB repair mutant *mus81Δ* and less severe than recombination mutants (figure 5-3 lines 6 and 7).

Generally the loss of viability in all strains was not large suggesting that there may be a more affective way to conduct this analysis.

5.3 Development of a microcolony assay as a tool for investigating inducible se-DSB repair

As the defects in *smc6-X*, *smc6-74* and *mus81Δ* were first seen using tetrad analysis, where colonies are grown from a single spore after crossing, it became apparent that it was worth observing the growth of early generations after se-DSB induction as they became microcolonies. Cells from mutants with se-DSB repair defects die more

frequently or are slower to progress through the cell cycle after DSB induction than the non-imprinting cells within the population. This would be represented in the overall cell number in a microcolony and it could be expected that se-DSB repair defective microcolonies would have a different morphology to those where cells were growing 'normally'.

To test the practicality of the microcolony assay several strains were analysed (see 5.1.2). Cells were plated at low dilution $+T^{DSB}$ or $-T^{no\ DSB}$ and grown for 24-36 hours before analysis of microcolonies. After approximately 6-10 mitoses microcolonies were observed under a light microscope and numbers of cells per microcolony were counted. Microcolonies were divided into three categories; a single cell was considered dead, colonies with less than 20 cells were considered slower growing and those with 20 cells or more were categorised as viable.

In this analysis it is important to not only consider each category of cells individually. For example the dead single cells represent the plating efficiency and the general viability of each strain. The nature of the inducible se-DSB system means that repair is not required in the earliest divisions and any cells that die before the four cell stage are unlikely to be dying because of an se-DSB specific deficiency. Conversely, any microcolonies that are growing well must be repairing the polar break in a number of cells in the population at any given time. Slow growing microcolonies are likely to be those that are unable to repair the se-DSB. In this case it could by hypothesised that cells that fail to repair the se-DSB will die and those cells that have not imprinted can keep growing producing colonies that are slightly smaller than the expected size (figure 5-4). Thus the percentage of viable microcolonies is the simplest readout of proficiency of se-DSB repair but it is also important to examine slow growing colonies to gain a fuller picture of the strains response to a one-ended break.

As expected the WT strain was able to efficiently repair the se-DSB break formed at *mat1*. This is consistent with data from the tetrad analysis where 93% of crosses produced successfully growing colonies (see chapter 4.3.1). In WT 88% of colonies growing on agar $-T^{no\ DSB}$ were viable (greater than 20 cells) and 92% of colonies grown

(A) Viable cell pedigree

Generation – Cell Number

F0 - 1

F1 - 2

F2 - 4

F3 - 8

F4 - 16

F5 - 32
F6 - 64

(B) Slow cell pedigree

Generation – Cell Number

F0 - 1

F1 - 2

F2 - 4   ○ Viable

F3 - 7   ● Imprinting

                ● One-end break/Dead
F4 - 11

F5 - 16

F6 - 22

(C) Inviable cell pedigree

Generation – Cell Number

F0 - 1   ● Dead
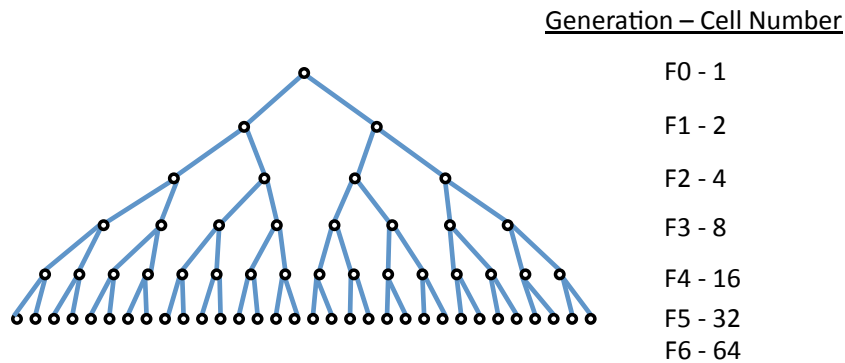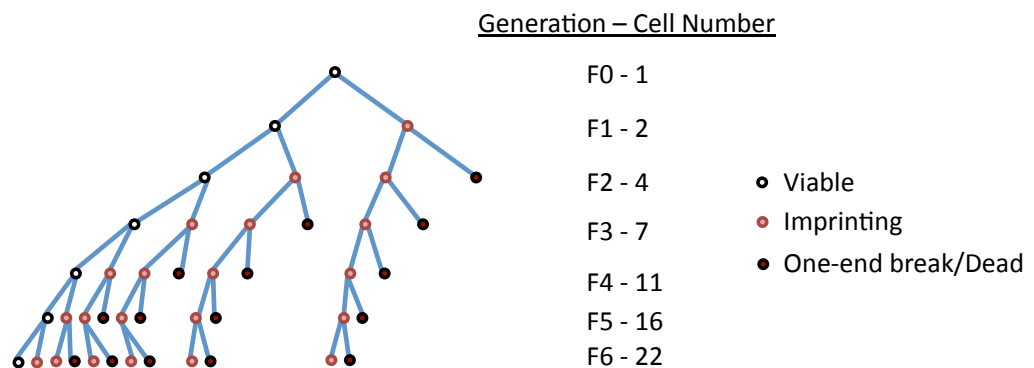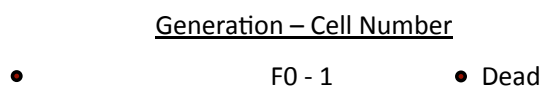
Figure 5-4- Theoretical pedigrees predict the number of cells seen in a microcolony after 6 generations (~24 hours)

(A) In cells where se-DSB repair does not affect viability or speed of cell cycle progression it would be expected that after 6 generations at 4 hours per generation a microcolony of 64 cells would be seen. Colonies containing more than 20 cells were considered viable in microcolony analysis. (B) A schematic pedigree showing colony development if all cells that failed to repair the one-ended break were inviable. Microcolonies that showed a reduction in cell number after 24 hours were classified as slow growing. (C) Cells that did not grow past the single cell stage were considered inviable and most likely were an artefact of plating efficiency.

on media $+T^{DSB}$ were viable (5-1 and figure 5-5). In both media with and without thiamine there is little change in the number of dead cells. There was a decrease in the numbers of slow growing colonies from 7% on $-T^{no\ DSB}$ agar to 2% on $+T^{DSB}$ agar. This may reflect thiamine induction or be an artefact of the numbers investigated in this analysis.

Recombination mutants show a defect in se-DSB repair in the microcolony assay. *Rhp51Δ* proved difficult to analyse as the slow growth phenotype of the strain meant that the colonies needed to be grown for approximately 48 hours before they were suitable for analysis. On $-T^{no\ DSB}$ media *rhp51Δ* mutants had a viability of 49% (table 5-1 lines 3 and 4 and figure 5-5) consistent with its sick phenotype. On media $+T^{DSB}$ the percentage of viable colonies reduced further to 22% (p=0.0002). Showing that the defect in repairing the se-DSB reduces the viability by a further 50%. The number of colonies categorised as slow on media almost doubled from 29% to 47% after DSB induction, showing that a defect in se-DSB repair increases the number of slower growing colonies.

The less sick *rhp57Δ* mutant displayed a similar phenotype to *rhp51Δ*, with a decrease in viability from 56% to 32% (p=0.03) upon induction on a thiamine positive media (table 5-1 and figure 5-5). As with *rhp51Δ* there was an increase in the percentage of slower growing colonies from 14% to 32% after se-DSB induction. The milder phenotype of *rhp57Δ* has been shown in several previous studies (Tsutsui et al., 2000) and while *rhp57Δ* was not reported to be defective in se-DSB repair after tetrad analysis (Roseaulin et al, 2008) it is possible that this analysis is a more sensitive analysis than tetrad analysis.

Consistent with the findings of Roseaulin et al (2008) that mus81Δ is defective in se-DSB repair the microcolony analysis showed a reduction in viability when growing on agar $+T^{DSB}$ from 52% to 32% (table 5-1 and figure 5-5) (p=0.0001). There is an increase in the number of slower growing colonies from 16% to 33%. This data shows that the microcolony analysis provides a good readout of se-DSB repair defects based on the reduction in viability and increase in amounts of slower growing colonies.

	Thiamine	Total Cell	Number of viable colonies	% Viable	Number of slow colonies	% Slow	Number of dead cells	% Dead	P value
smc6+	-	308	270	88	21	7	17	6	
	+	323	297	92	6	2	20	6	0.07
rhp51Δ	-	182	89	49	52	29	38	23	
	+	104	23	22	49	47	28	31	0.0001
rhp57Δ	-	63	35	56	9	14	19	30	
	+	106	34	32	34	32	38	36	0.03
rqh1Δ	-	104	90	89	6	6	5	5	
	+	99	89	90	4	4	6	6	0.91
mus81Δ	-	395	205	52	63	16	127	32	
	+	229	74	32	76	33	79	35	0.0001
smc6-74	-	243	197	81	22	9	24	10	
	+	354	223	63	70	20	61	17	0.0001
smc6-X	-	294	210	71	43	15	41	14	
	+	345	202	59	84	24	32	17	0.007

Table 5-1– Microcolony viability data
Strains were grown for 16-24 hours on media +T and –T at 30°C. The number of cells per microcolony was calculated and microcolonies were categorised as viable (>20/30 cells), slow (2-20/30 cells) and dead (1 cell) (20 cells was used for 16 hour analysis, 30 cells was used for 24 hour analysis). P values were calculated using the Z-ratio for difference in proportion between +T and –T.
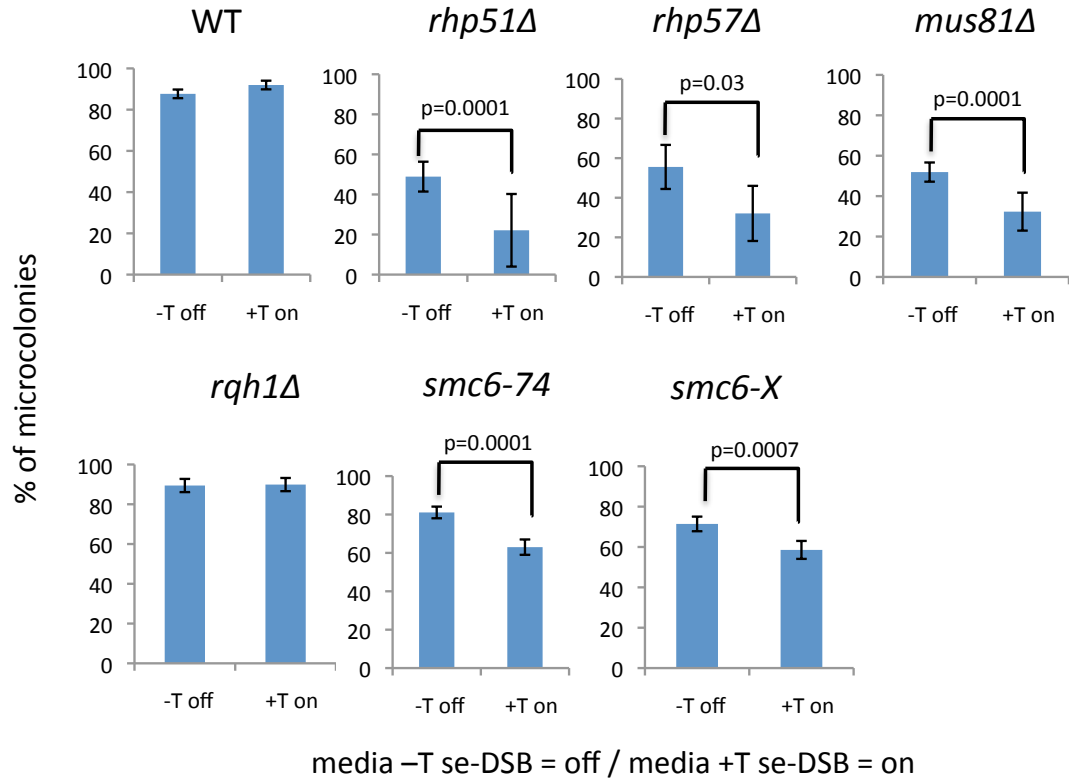
Figure 5-5- Microcolony analysis of strains grown on agar with or without thiamine

Strains were incubated for 16-24hrs depending on doubling times before analysing the number of cells per microcolony. Recombination mutants and *mus81Δ* have growth defects and a plating efficiency of approx. 70% (approx. 30% single dead cells in the microcolony assay in off conditions). Viability was assessed by the number of colonies with more than 10 cells as expect 16-32 cells after 5 generations (see figure 5-2). The loss of viability on induction of the break is deduced from the difference in viability between off and on.

The RecQ helicase mutant *rqh1Δ* was not defective in se-DSB repair by tetrad analysis (Roseaulin et al, 2008). The mutant *rqh1Δ* was used as a negative control for this analysis and was not found to be defective in se-DSB repair. On media +T and –T the percentage of viable colonies was 90% and 89% respectively and there was little change in viability seen upon the induction of the se-DSB (table 5-1 and figure 5-5). This is an expected result as Rqh1 is not usually involved in the repair of se-DSB and is used for the resolution and issegregat of double HJs.

Both *smc6-X* and *smc6-74* mutants were defective in se-DSB repair in the tetrad analysis (Chapter 4). Microcolony analysis showed *smc6-X* to have a slightly lower plating efficiency on media –T$^{no\ DSB}$. Both *smc6-X* and *smc6-74* showed a reduction in viability when plated on media +T^{DSB}. The viability of *smc6-74* dropped from 81% to 63% (p=0.0002) when growing on plates containing thiamine and the slightly sicker *smc6-X* strain also showed a reduction in viability from 71% to 59% (p=0.0002). In both strains there was a comparable increase in the number of slower growing colonies suggesting that the decrease in viability is due to a specific defect in se-DSB repair (table 5-1 and figure 5-5).

5.4 Cell length analysis

In response to DNA damage checkpoint-proficient cells delay the cell cycle and in *S. pombe* this is seen as an increase in cell length. Consistently Roseaulin et al (2008) showed that *mus81Δ* displayed an elongated phenotype on se-DSB induction. It was hypothesised that strains defective in se-DSB repair would be unable to repair the DSB and so elongate before dying without entry into mitosis. This leads to a population of elongated cells that do not divide any further. Such a population can be easily distinguished. After se-DSB induction it would be expected that a colony would contain a mixed population of elongated and normal length cells as at any time a maximum of 50% of cells would be attempting to repair the se-break. Colonies were imaged between 24 and 36 hours of growth (figure 5-6) and the average cell length in induced and uninduced microcolonies was measured (table 5-2). The average length was plotted in a box plot showing the cell length the population and indicating the outliers (figure 5-7).

Microcolony growth after 24 hours
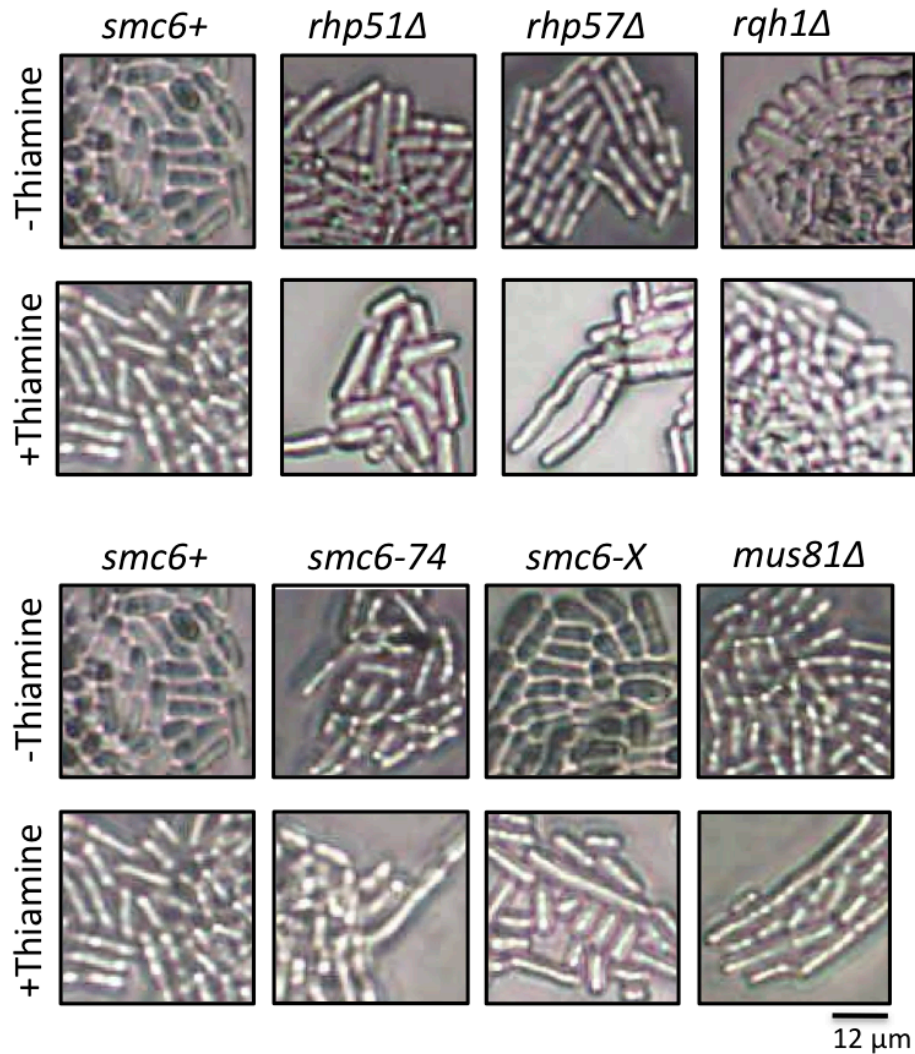
Figure 5-6- Microcolony analysis of strains grown on agar +/-T
WT, *smc6-74, smc6-X* and *mus81* were tested grown for 24-36 hours on supplemented YNBA media + or − thiamine. The resulting colonies were photographed using a USB microscopy camera and cell length was measured by hand after scaling images appropriately (see methods 2.2.4 for more details). The scale bar is shown bottom right.

	WT		rhp51Δ		rhp57Δ		rqh1Δ		mus1Δ		smc6-74		smc6-X	
	-	+	-	+	-	+	-	+	-	+	-	+	-	+
Average	12.0	12.5	12.4	14.9	13.6	18.2	11.9	11.8	12.2	18.5	12.4	16.7	12.7	15.0
SD	2.2	2.9	4.2	3.7	3.9	7.1	4.9	5.2	3.4	10.1	2.3	6.1	3.0	4.9
Chi Test	n/a	n/a	0.651	0.151	0.123	3.90E-18	0.562	0.558	0.301	4.3505E-31	0.994	2.7607E-10	0.904	0.007

Table 5-2 – Microcolony cell length data
Strains were grown for 24-36 hours on supplemented YNBA media +T and –T at 30°C. The length of 35 cells was measured from images taken using a USB microscope camera (see figure 5-6) and the average cell length (μm) was calculated. P values were determined using *chi*-squared where the WT data set was the expected values.
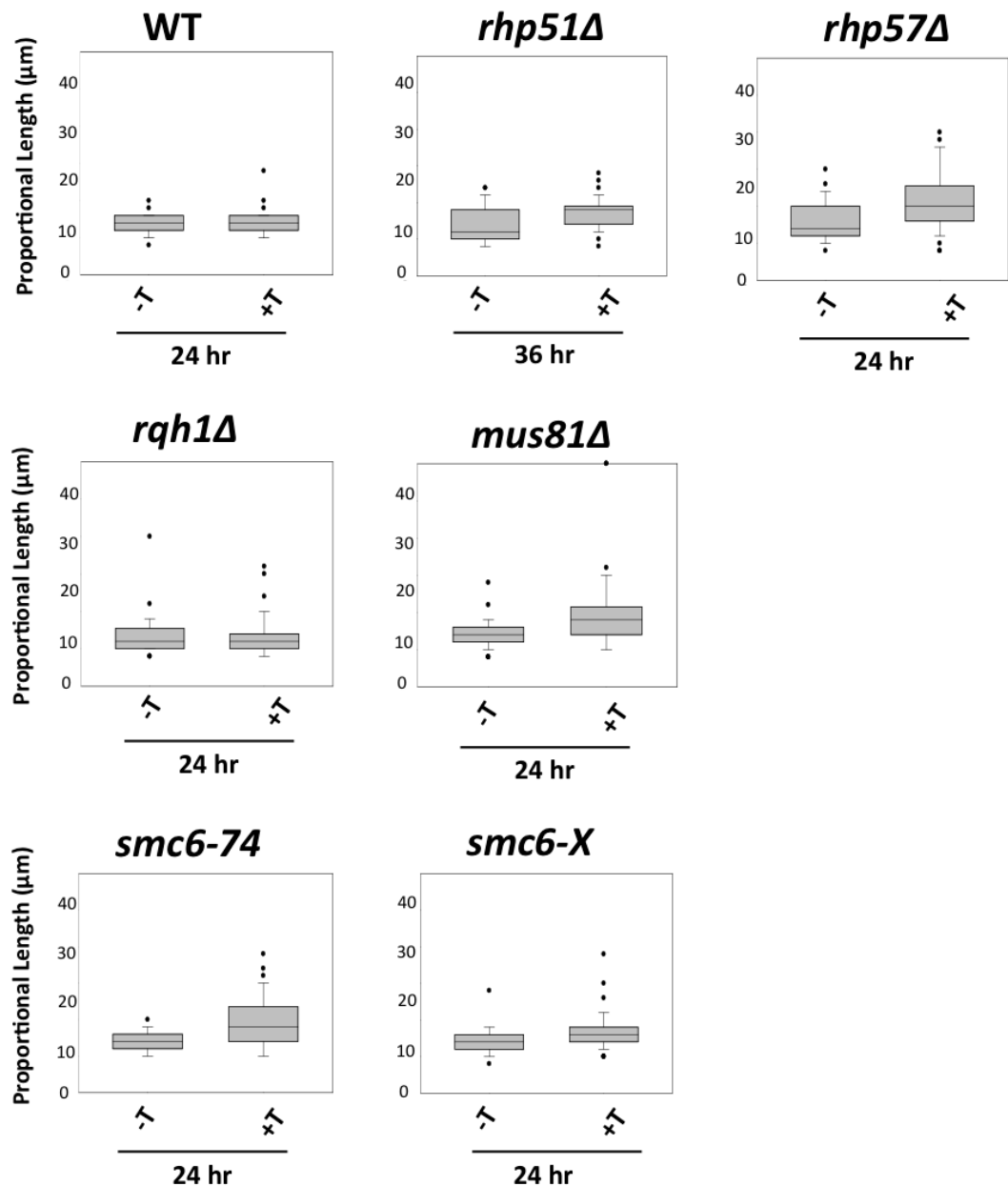
Figure 5-7- Microcolony analysis of strains grown on agar +/-T

WT, *smc6-74*, *smc6-X* and *mus81Δ* were tested grown for 24-36 hours on supplemented YNBA media + or − thiamine. The resulting colonies were photographed using a USB microscopy camera and cell length was measured by hand after scaling images appropriately (see methods 2.2.4 for more details). The cell length of samples was plotted on a box plot to show average length (centre of the box) standard deviation (bars) and outliers (dots).

After growing strains for 24 hours cells were examined on media +/-T (+/-DSB). For this analysis the data set taken for WT (WT $12.0^{DSB\ off}$ and $12.5^{DSB\ on}$) was used as the expected cell length result and *chi*-squared was used to determine whether changes in cell length were statistically significant in mutant strains. *Rqh1Δ* strains did not have a significant change in average length upon the addition of thiamine from $11.8^{DSB\ on}$ and $11.9^{DSB\ off}$ µm (p=0.558). These cell length data are consistent with the fact that there was no obvious reduction in viability in the microcolony analysis.

Recombination and se-DSB repair mutants showed an increase in the average cell length when the DSB was induced. Because *rhp51Δ* has a growth defect cells were grown for 36 hours before analysis. The average cell length increased from 12.4 µm to 14.9 µm on DSB induction, which is not significant (p=0.15). A large difference would not be expected as *rhp51Δ* is a very sick strain with small dead and elongated cells even in the –DSB cultures.

Rhp57Δ cells increased in cell length from 13.6 µm to 18.2 µm (p=$3x10^{-18}$) upon DSB induction consistent with *rhp57Δ* mutants being checkpoint proficient. The se-DSB repair mutant *mus81Δ* showed an increase in the average cell length from 12.2 µm to 18.5 µm on DSB induction (p=$4x10^{-31}$). These data are consistent with data shown in Roseaulin et al. 2008 where cells were shown to elongate before dying after DSB induction.

Smc6-X and *smc6-74* mutant cells elongated after DSB induction on media containing thiamine. The average cell length of *smc6-74* increased significantly from 12.4 µm to 16.7 µm (p=$2x10^{-10}$). *Smc6-X* also shows an increase in the average cell length from 12.7 µm to 15.0 µm (p=0.007). This is a milder phenotype compared to *mus81Δ* and correlates with the less severe decrease in viability.

5.5 Detecting imprinting using Southern hybridisation

Before cells make the se-DSB they must imprint at *mat1* in the same manner as in normal mating-type switching. To visualise this cells were harvested at 0, 60, 120 and

180 minutes after induction. DNA was prepared using the standard method (see section 2-7), digested with *PvuII* and *XhoI* and subjected to Southern analysis using a probe homologous to the P specific region of *mat1* between 337 bp upstream from H1 and 382 bp downstream from H1. (figure 5-8 (A)).

It is expected that when no imprinting occurs the whole *mat1* region homologous to the probe is visualised as a single 9.9 kb band. When imprinting occurs a fragile site is created close to the H1 homology box (Vengrova and Dalgaard, 2006). This fragile site is usually broken upon DNA extraction (Beach, 1983) and runs as two bands at 6.8 kb and 3.1 kb (the probe used had no homology to the 3.1 kb band so only the 6.8 kb band was visualised). In DNA harvested from cultures shortly after imprinting the population is mixed between cells that have began imprinting and those that have not, resulting in the appearance of two bands representing the population of non-imprinted DNA and the population of cells that are imprinting, 9.9 kb and 6.8 kb respectively (figure 5-8 (B)). Bands from both regions were quantified using ImageJ software and the intensity of the 6.8 kb band was expressed as a percentage of the total DNA, that is the intensity of both bands.

Strains grown in media –T$^{no\ DSB}$, had a low level of background with the band at 6.8 kb barely detectable at the 0 minute time-point (10-15% imprinting). *Rqh1Δ* was the exception with an off state of 24%. However the signal on the blot was weaker than other strains and this may have interfered with the accuracy of the analysis (figure 5-8 I).

In all strains the intensity of the 6.8 kb band corresponding to the imprint increased after an hour of induction (consistent with data from Roseaulin et al, (2008)) with an average imprinting of 36% after 60 minutes, and 41% at 120 minutes and 180 minutes after induction. WT cultures had the highest imprinting (48% at 180 minutes after induction), but all strains showed a increase in imprinting after the addition of thiamine to the media (figure 5-8). Since 60% of *S. pombe* cells in a log phase culture are in G2 and the average cell cycle time in minimal media at 30°C is approximately 3 hours in unsynchronised cells 3 hours after the addition of thiamine the majority of

cells will have divided, passed through S phase and imprinted. Since the imprint is only on the lagging strand the maximum level of the 6.8 Kb band is 50% and thus the level of imprinting seen was consistent with the expected value.

5.6 Pedigree analysis to examine cell death rates

Based on the data from the microcolony assay, tetrads and cell length analysis it can be concluded that *smc6-X* and *smc6-74* have a defect in processing a se-DSB. However the microcolony assay does not explicitly reveal whether the cells that are dying are those that are repairing the se-DSB. An alternative analysis is pedigree analysis of colonies by splitting and observing the cells as they divide. This allowed us to determine which of the daughter cells were slow growing, dying or elongating (indicating a cell cycle delay). The pedigree can be followed for several successive generations.

As mating-type switching occurs in a specific pattern the progeny that experience death or cell cycle delays due to the occurrence of a se-DSB would be expected to display the same specific pattern. Following the number of cells that have divided at specific time points (approximately every 4 hours) and the number of pairs of sisters and parent cells that are viable, allows the determination of whether the pedigree displays the expected pattern of cell death or elongation (figure 5-4).

Data was quantified by grouping the sisters and parents into viable or inviable, where one or more of the cells was dead, to provide a ratio of alive:dead cells. Ratio averages were taken for successive generations and chi^2 was used to determine if the expected ratios and pattern of alive to dead cells was seen.
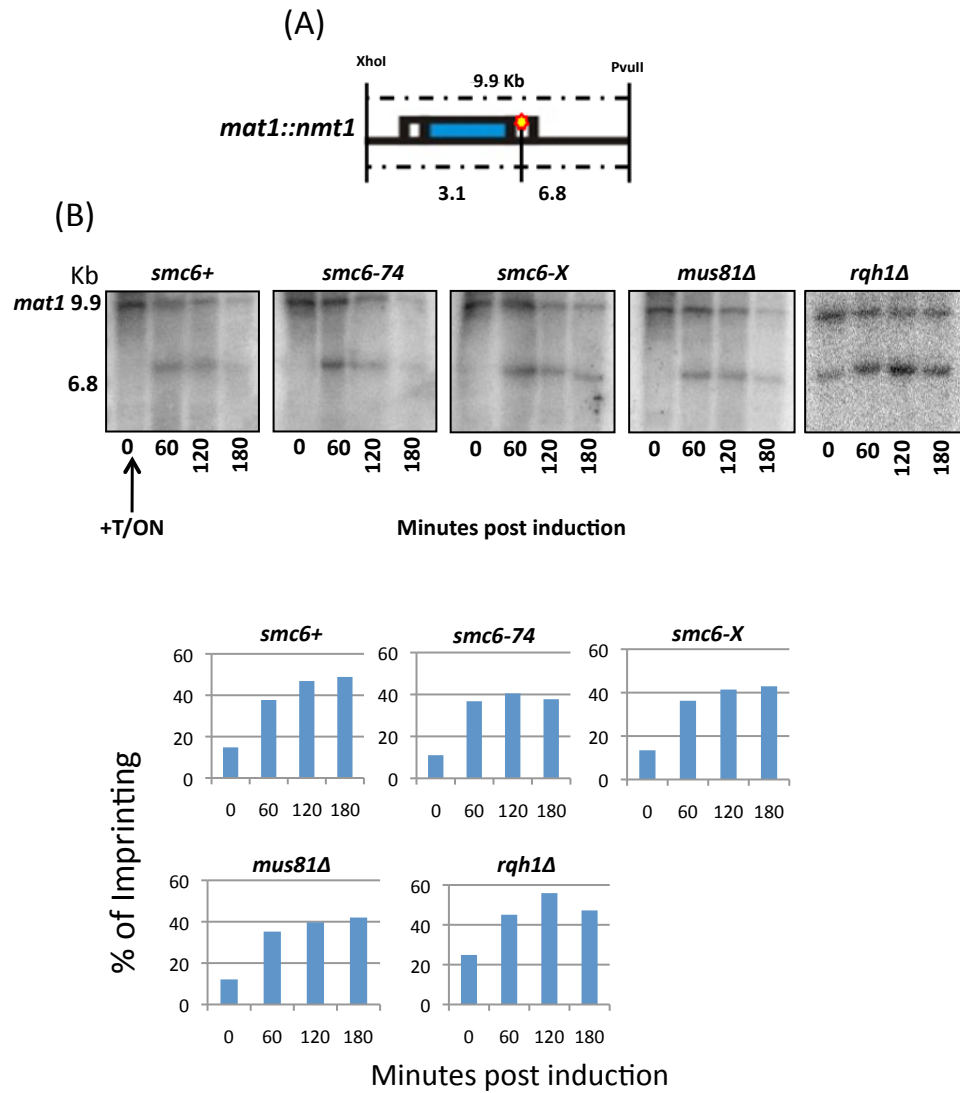
Figure 5-8- Southern analysis to detect imprinting levels after induction by adding thiamine

(A) Schematic showing fragment sizes for southern analysis. (B) Strains were grown in EMM minimal media without thiamine to a density of $6x10^6$ cells/ml. Cells were induced by adding thiamine to a final concentration of 3µM (check). Cells were harvested at 60 minute time intervals and genomic DNA was extracted and digested with *pvu*II and *xho*I. Digested DNA was run on a 1% gel and probed with a P specific *mat1* probe. (C) Southen blots were quantified using ImageJ.

Data obtained for *mus81Δ* in Roseaulin et al (2008) showed it to exhibit a cell death pattern similar to that expected if cell death was due to the se-DSB (figure 5-9).

At least 30 cells from each strain were plated on minimal media + or − T and cell divisions were followed through five to six divisions by observing under a light microscope and splitting cells using a micromanipulator (section 2.2.5) After the growth of at least five generations photographs were taken of the resulting microcolonies, and as the cells were separated in a specific pattern it was possible to work out which cells were parent, daughter or sisters so a pedigree for the colony could be drawn. All strains showed a large percentage of dead cells during pedigree analysis. Approximately half of all cells did not grow past the one cells stage with or without thiamine and consequentially were not suitable for this analysis. To compensate for this pedigrees were followed until at least ten or more of the growing strains passed the 4-cell stage. The number of viable sisters or parents were calculated per generation for at least ten full pedigrees (example pedigrees seen in figure 5-10). Average numbers of viable parents/sisters were determined and compared to the expected viability (table 5-3).

In the uninduced conditions the average viability of sisters in the WT strain over five generations was not significantly different from the expected viability P=0.29 (table 5-3) in the −DSB conditions. While the average viability appeared lower in the later generations (F5 and F6) it is likely that this is due to different growth rates. Parent/progeny relationships take twice as many cells into account per analysis and as such are more sensitive assays of cell death. In WT parent/progeny analysis the viability was not significantly different (P=0.08). As expected, when the DSB was induced by transfer to media containing thiamine there was no significant reduction in viability of WT in both sister and parental pedigree analysis, with P values of 0.67 and 0.14 respectively.
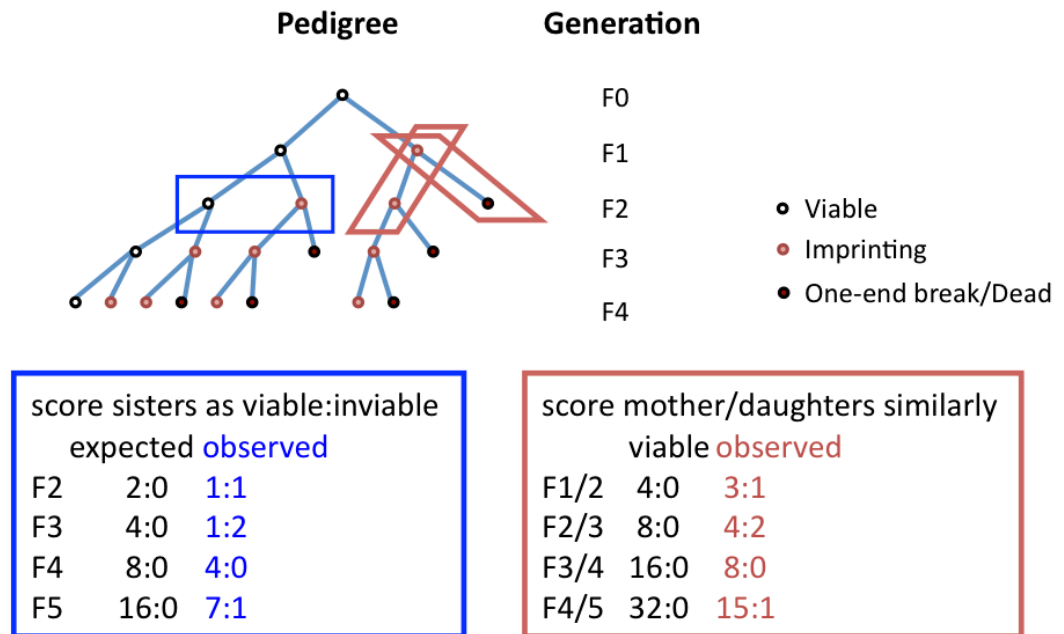
Figure 5-9- Quantifying pedigree analysis

During pedigree analysis cells were separated at approximately 4 hour intervals. A resulting pedigree was drawn based on the number of viable and dividing cells seen at each generation. The ratio of viable:dead sisters and mother/daughters in each generation was calculated to provide a numerical value for each generation. An average viability value was calculated using several pedigrees.
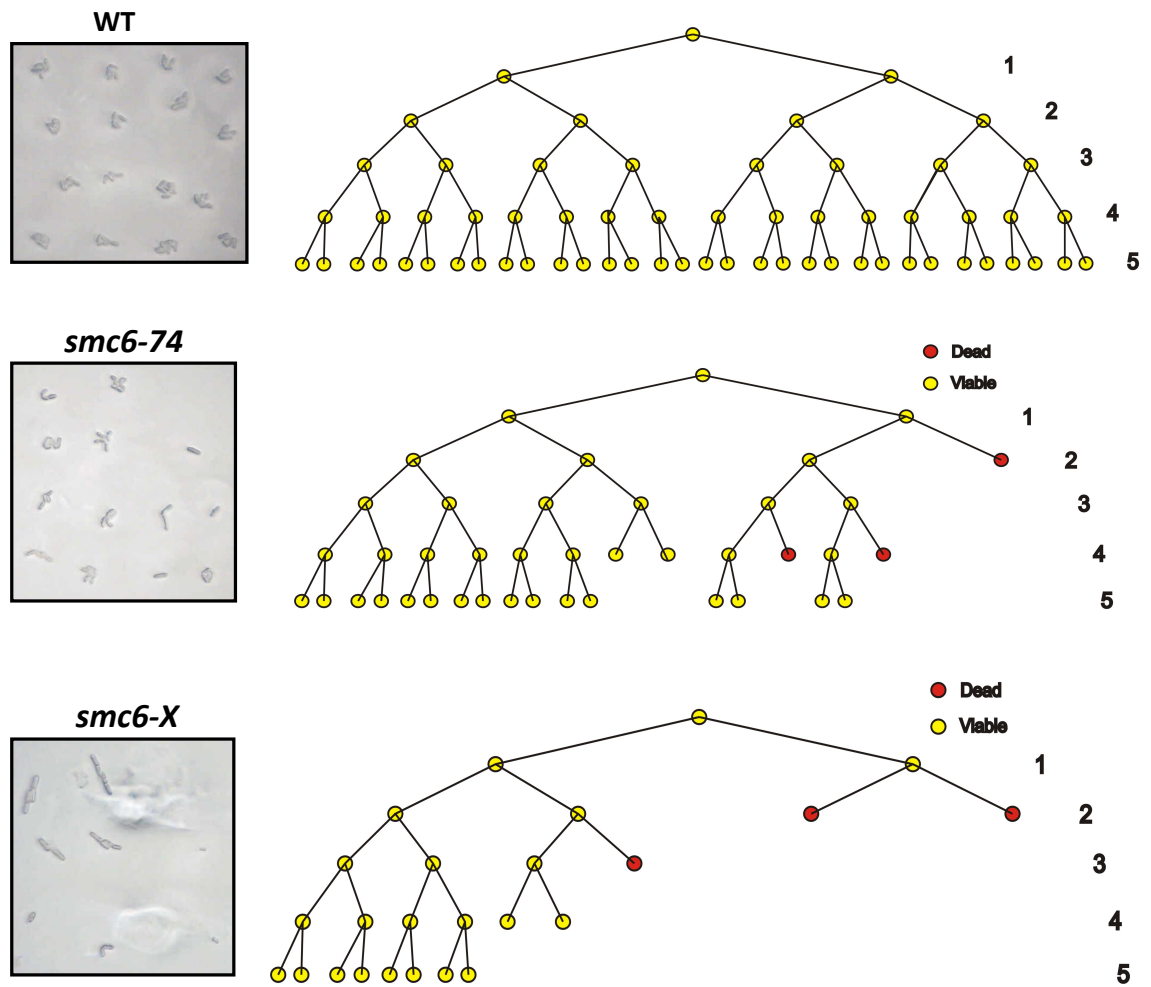
Figure 5-10- Examples of pedigrees in WT, *smc6-74* and *smc6-X*

During pedigree analysis cells were separated at approximately 4 hour intervals. A resulting pedigree was drawn based on the number of viable and dividing cells seen at each generation.

− Thiamine

	Generation	Expected Viability	WT Actual Viability	WT Chi Squared	smc6-74 Actual Viability	smc6-74 Chi Squared	smc6-X Actual Viability	smc6-X Chi Squared
Sisters	F2	2	1.5		1.27		1.3	
	F3	4	2.9	0.291761183	1.45	0.145736117	2.5	0.965594724
	F4	8	5.2		2.8		4.9	
	F5	16	9.9		4		8.6	
Parent	F2	4	3.4		3.1		3.6	
	F3	8	6.1	0.089072809	4.18	0.014504119	5.6	0.830438518
	F4	16	11.4		6.18		10	
	F5	32	19.8		7.6		16.2	

+ Thiamine

	Generation	Expected Viability	WT Actual Viability	WT Chi Squared	smc6-74 Actual Viability	smc6-74 Chi Squared	smc6-X Actual Viability	smc6-X Chi Squared
Sisters	F2	2	1.80		1.9		1.18	
	F3	4	3.20	0.678668815	2.8	0.312349923	1.70	0.005583426
	F4	8	6.8		5.6		2.80	
	F5	16	11.7		9.7		5.00	
Parent	F2	4	3.50		3.90		3.60	
	F3	8	6.09	0.148243952	6.00	0.065224702	5.60	0.012791554
	F4	16	11.30		10.70		10.00	
	F5	32	21.50		19.40		16.20	

Table 5-3 – Pedigree analysis data

After pedigrees were drawn for 5 generations the data was collated and an average actual viability per generation was calculated for parents/progeny and sisters on media +/- thiamine. The viability of WT was considered to be the expected viability and the observed viability of *smc6-74* and *smc6-X* were compared to WT using chi^2.

For the analysis of *smc6* mutants the level of viability seen in WT strains was considered the standard for normal growth and data was normalised by comparing to the WT strain rather than the theoretical expected values. The average sister and parental viable:inviable ratio was calculated and the average viability was determined for each generation *smc6-X* and *smc6-74* and was compared to WT average generation viability.

When grown on media $-T^{no\ DSB}$ *smc6-74* sisters did not have a significant difference in viability when compared to WT (P=0.145). *smc6-74* did however show a significant reduction in viability when the parents were analysed (P=0.014). It is unclear why the viability was lower than expected in *smc6-74* on media $-T^{no\ DSB}$ compared to $+T^{DSB}$ but this reduction in the rate of growth was seen in both liquid cultures and on spot tests.

Growing on media $+T^{DSB}$ *smc6-74* showed a reduction in viability corresponding to the formation of one-ended break repair in both parent and sister pedigrees, $p=2.14 \times 10^{-5}$ and p=0.01 respectively, suggesting this reduction in viability was due to the one-ended break repair. In the $-T^{no\ DSB}$ control *smc6-X* did not have a significant reduction in viability in either sisters or parent pedigrees, p=0.9 and p=0.8, however both showed a significant reduction in viability after DSB induction on +T media, p=0.005 and p=0.01 respectively as expected if polar break repair is the cause of the reduction in viability.

In this study *mus81Δ* was not investigated as it had been previously been subjected to pedigree analysis in Roseaulin et al (2008). The published data showed that cells expected to imprint initiated dead lineages and cells that go on to attempt to repair the one-ended break did not survive. Microscopy showed that the cells were seen to elongate but there was not necessarily a correlation between the elongated cells and cell death.

5.7 Summary of the inducible se-DSB analysis

The inducible se-DSB repair system proved useful to examine the early stages of one-ended break analysis without the need to grow cells into full colonies. This meant that

there was no time for cells to accumulate any suppressors and that the patterns of cell death could be followed one cell at a time using pedigree analysis.

The inducible system further confirmed that there was a defect in se-DSB repair processing in both *smc6-74* and *smc6-X* and that defect correlated with the expected pedigree pattern. Cell elongation and a decrease in viability were seen on DSB induction in both *smc6* mutants. Pedigree analysis showed that the viability defect was specific to the pattern expected if the results are due to defects in se-DSB repair. However the defect in *smc6-X* and *smc6-74* is not as severe as that reported for *mus81Δ*. It was also confirmed by microcolony analysis that *rhp51Δ* and *rhp57Δ* were defective in se-DSB repair but *rqh1Δ* was not defective.

Chapter 6 – Development of an inducible converging-fork double-strand break repair system

6.1 Converging-fork double-strand break (cf-DSB) repair

Chapter 5 describes the use of the *S. pombe mat* locus to study repair of se-DSB generated by a replication fork encountering a nick. Se-DSBs are thought to be the critical lesion that makes homologous recombination essential during S phase in higher eukaryotes. However, mammalian cells rely on new origin firing rather than replication restart to overcome arrested forks in S phase (Blow et al., 2011). Thus, most collapsed forks will be rescued by an incoming (converging) fork. A converging fork would provide a second end, converting a one-ended break to a two-ended break. This would enable other forms of repair such as canonical HR or non-homologous end joining (NHEJ) to take place. In this chapter I describe the development of a novel system to study the repair of an se-DSB converted by a converging fork into a two ended cf-DSB. This is a unique system as while classical HR repair of endonuclease generated DSBs is well studied these inducible systems rely on enzymes that repeatedly cut both strands of DNA and thus may not reflect the repair of replication associated DSBs (figure 6-1 (A)).

In *S. pombe* mating-type switching is dependent on the replication fork approaching *mat1* from the telomeric direction. A replication fork barrier centromeric to *mat1* helps to ensure efficient imprinting as it prevents incoming replication forks from the centromeric direction. Replication stalling is enforced by Rtf1 binding the replication termination site 1 (RTS1) region adjacent to *mat1,* which blocks the replication fork with the aid of Rtf2. Without Rtf1 replication termination is reduced and replication forks can pass through the barrier (Eydmann et al., 2008).

Deletion of *rtf1* in the se-DSB repair system would enable the conversion of the se-DSB to converged-fork double-strand break or cf-DSB. Without Rtf1 replication forks can still pass through *mat1* in the correct orientation due to efficient firing of a nearby telomere-proximal origin (Dalgaard and Klar, 2001a), it would be anticipated that in

Figure 6-1 – Converging-fork repair of a se-DSB

(A) Examples of the type of DNA damage formed upon exposure to IR, DSB inducing enzymes and the cf-DSB repair system. (B) There is no RTS1 block centromere proximal to *mat1*. The se-DSB is formed as usual however a converging-fork from the centromeric direction may arrive at the break site. The incoming converging-fork should be able to bypass the se-DSB on the leading strand as there is no break there. The resulting structure is a two-ended converged-fork DSB on one strand. This cf-DSB can be repaired in a manner dependent on HR.

(A)

DNA damage
(e.g. IR)

Most inducible DSB
repair systems

cf-DSB repair
system

(B)

Pause Site
MPS1

L Region

mat1

LEU2

Deleted donor
region

No replication
block in *rtf1* null
cells

se-DSB

Approaching
converging
fork

mat1

Converging fork can
bypass se-DSB on the
leading strand

Converging fork meets
the se-DSB

Repair of the break is HR
dependent
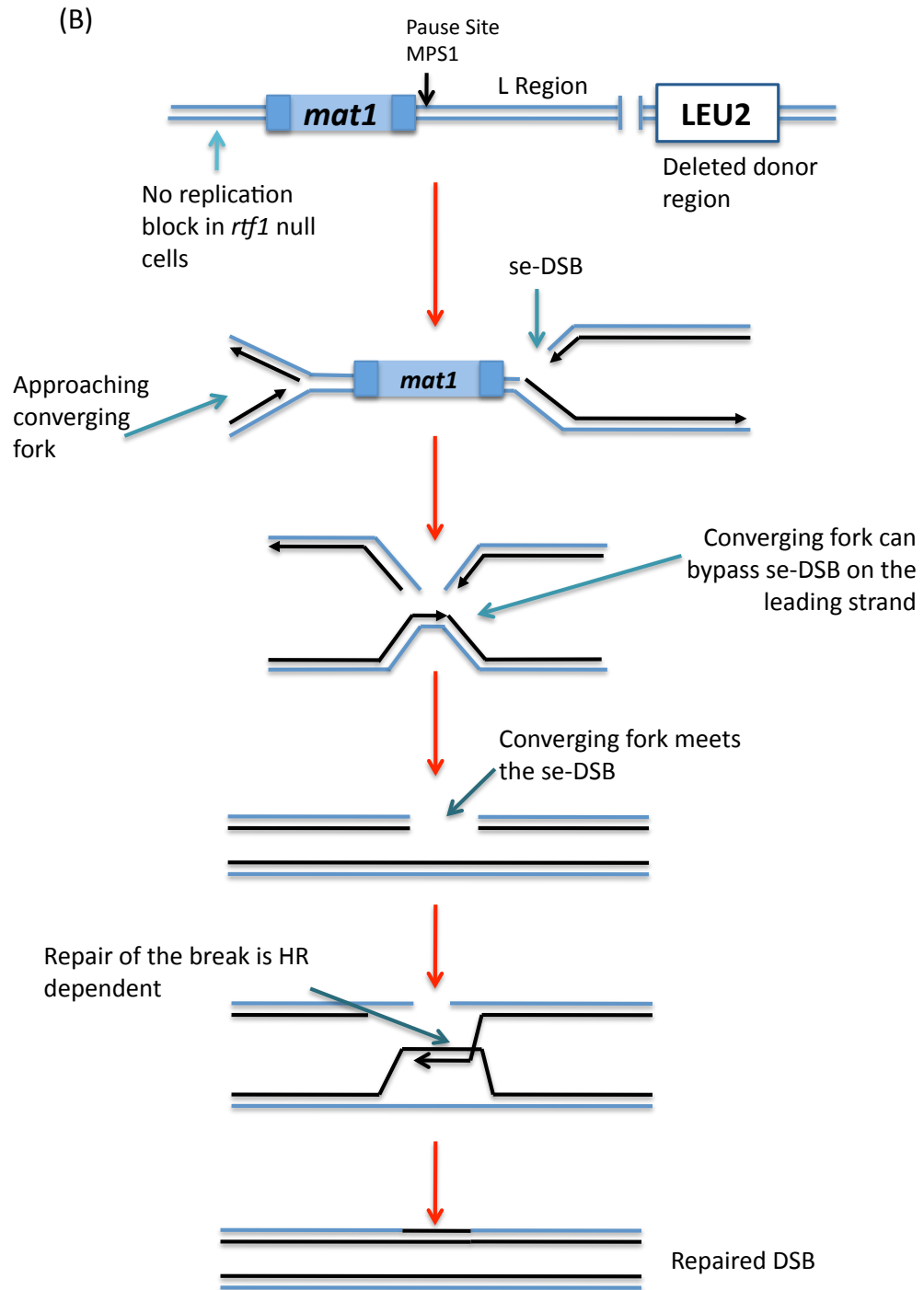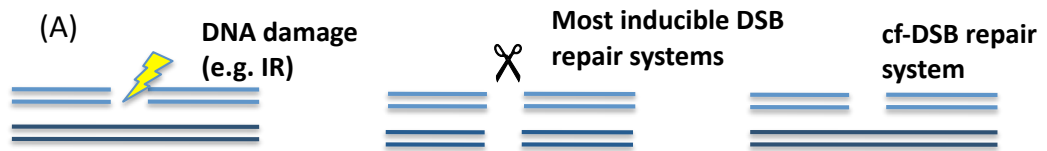
Repaired DSB

many cells the se-DSB would still be formed but then converted to a cf-DSB by the incoming fork (figure 6-1 (B)) and subsequently repaired by a mechanism dependent on HR.

6.2 Creation of the inducible cf-DSB system

To create the converged fork DSB system the inducible se-DSB analysis strain (as outlined in section 5.1) was crossed to an existing *rtf1Δ* strain (YKM082). Since it was possible that without the barrier at RTS1 the centromere proximal fork could arrive at the imprinting site before the telomeric fork and prevent imprinting, the first part of analysis was to determine whether *rtf1Δ* strains were able to imprint. All key strains for analysis were subjected to Southern blot analysis (as outlined in 2.7). In all *rtf1Δ* strains low levels of imprinting (17-23%) were detected at 0 minutes. Upon induction *rtf1Δ* mutants were found to show an increase in the band corresponding to imprinting (6.8 kb) to 36-37% at time 60 minutes and continued to rise to an average of 42% after 180 minutes of induction (figure 6-2).

Rtf1Δ mutants have a higher base level of imprinting in asynchronous cultures than *rtf1+* suggesting that the system may be more leaky after the deletion of *rtf1* but this may be an artefact of analysis. The rate at which the level of imprinting increases in *rtf1Δ* mutants is not as rapid as that seen in *rtf1+,* however by 120 minutes after induction there was a comparable level of imprinting seen in both strains. The percentage of imprinted DNA is close to the expected value of 50% after 180 minutes (35-46%) and is comparable with the amount of DNA containing the imprint in *rtf1+* strains. These data confirm that *rtf1Δ* does not inhibit imprinting.

6.3 HR is required for cf-DSB repair

The microcolony assay outlined in section 5.3 was used to investigate the viability of mutants during cf-DSB repair. In WT *rtf1Δ* mutants 88% of cells plated formed viable colonies. The deletion of *rtf1* did not appear to have an effect on the viability in WT with no difference in viability seen on media $-T^{no\ DSB}$ and *rtf1Δ* $+T^{DSB}$ (both 91 and 88% respectively see table 6-1 and figure 6-3).

(A)

XhoI

9.9 Kb

PvuII

mat1::nmt1

3.1   6.8

(B)

rtf1Δ

Kb

mat1 9.9

6.8

WT   *smc6-74*   *smc6-X*   *mus81Δ*   *rqh1Δ*

0 60 120 180   0 60 120 180   0 60 120 180   0 60 120 180   0 60 120 180

+T/ON

Minutes post induction

(C)

rtf1Δ

% of Imprinting

smc6+

smc6-74

smc6-X

mus81Δ

rqh1Δ

Minutes post induction
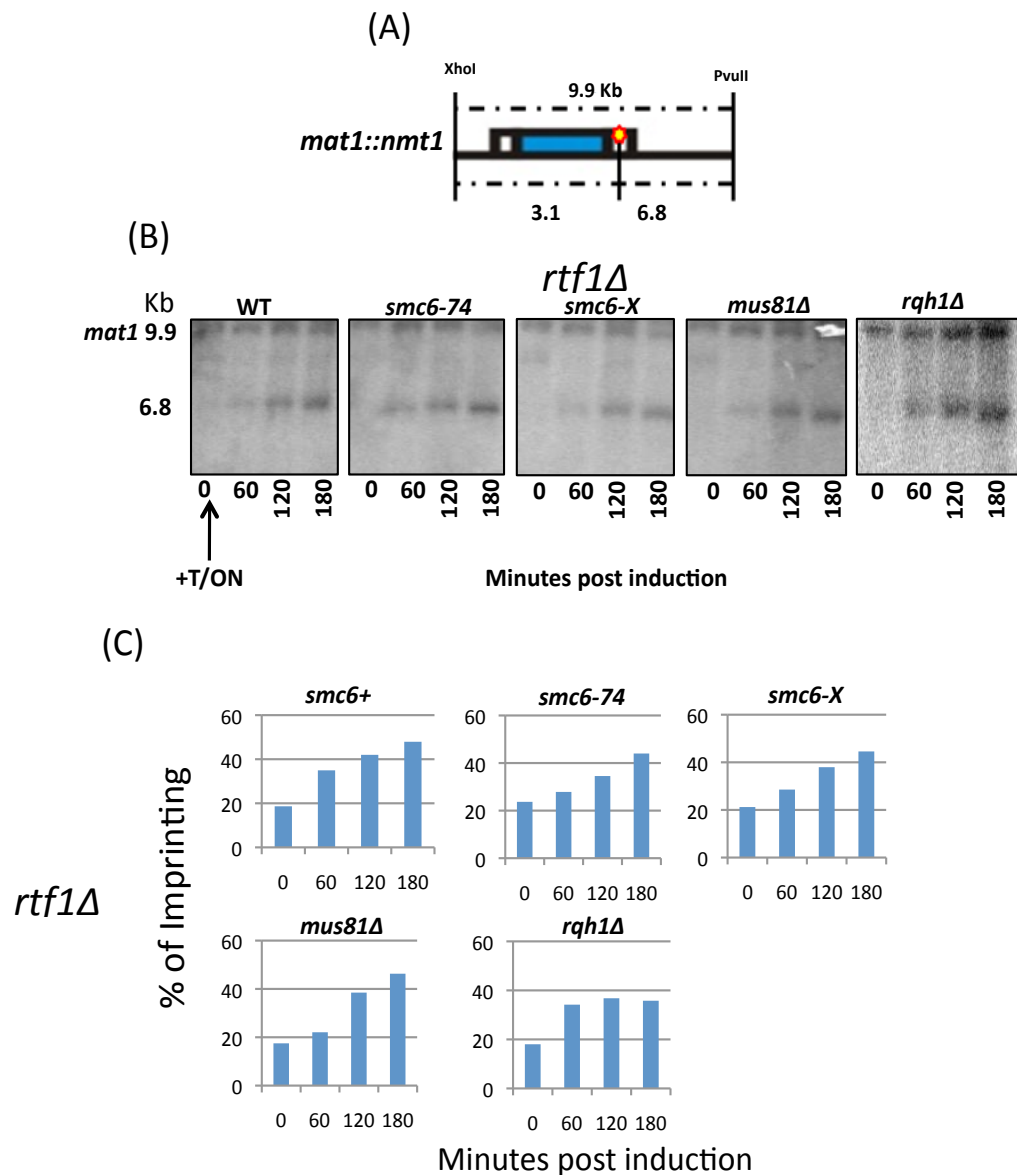
Figure 6-2- Southern analysis to detect imprinting levels after induction by adding thiamine
(A) Schematic showing fragment sizes for Southern analysis. (B) Strains were grown in EMM minimal media without thiamine to a density of 6×10^6 cells/ ml. Cells were induced by adding thiamine to a final concentration of 3µM (check). Cells were harvested at 60 minute time intervals and genomic DNA was extracted and digested with *Pvu*II and *Xho*I. Digested DNA was run on a 1% gel and probed with a P specific *mat1* probe. (C) Southern blots were quantified using ImageJ.

	Thiamine	Total Cell	Number of viable colonies	% Viable	Number of slow colonies	% Slow	Number of dead cells	% Dead	P Value
WT	-	315	286	91	15	5	14	4	0.2
	+	318	279	88	28	9	11	3	
rhp51Δ	-	134	70	52	31	23	33	25	0.003
	+	110	37	34	48	44	25	23	
rhp57Δ	-	84	43	51	18	21	23	27	0.04
	+	56	19	34	17	30	20	36	
rqh1Δ	-	127	100	79	12	9	15	12	0.0048
	+	99	61	62	27	27	11	11	
mus81Δ	-	211	107	51	43	20	61	29	0.2
	+	253	143	57	42	17	68	27	
smc6-74	-	240	200	83	15	6	25	10	0.325
	+	324	260	80	13	4	51	16	
smc6-X	-	287	230	80	26	9	31	11	0.0002
	+	349	224	64	93	27	32	9	

Table 6-1 Microcolony viability data in *rtf1Δ* mutants

Strains were grown for 16-24 hours on media +T and −T at 30°C. The number of cells per microcolony was calculated and microcolonies were categorised as viable (>20/30 cells), slow (2-20/30 cells) and dead (1 cell) (20 cells was used for 16 hour analysis, 30 cells was used for 24 hour analysis). P values were calculated using the Z-ratio for difference in proportion between +T and −T.

media −T se-DSB = off / media +T se-DSB = on
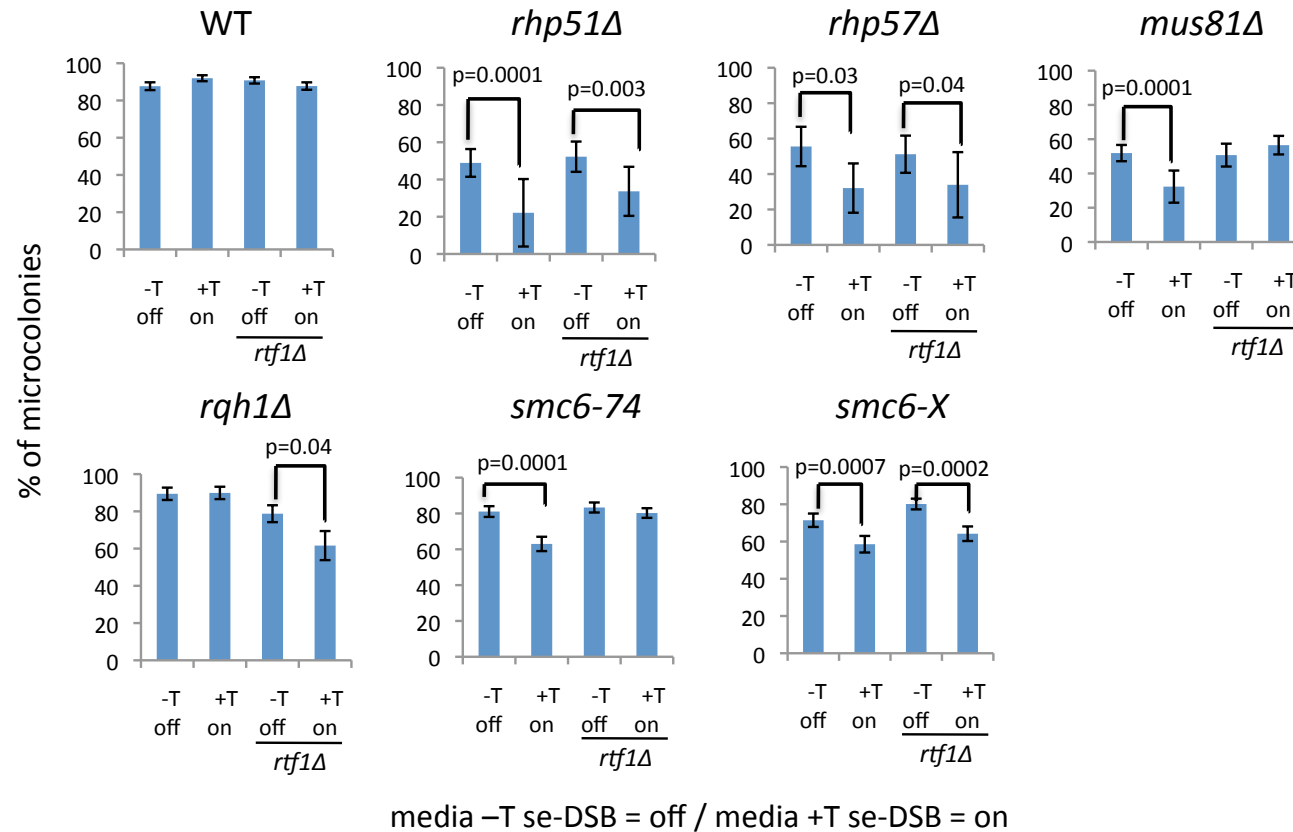
Figure 6-3- Microcolony analysis of strains grown on agar with or without thiamine in *rtf1Δ* double mutants
Strains were incubated for 24-36hrs depending on doubling times before analysing the number of cells per microcolony. Recombination mutants and *mus81Δ* have growth defects and a plating efficiency of approx. 70% (approx. 30% single dead cells in the microcolony assay in off conditions). Viability was assessed by the number of colonies with more than 10 cells as expect 16-32 cells after 5 generations (see figure 5-4). The loss of viability on induction of the break is deduced from the difference in viability between off and on. *rtf1Δ* double mutants are labeled *rtf1Δ*.

HR is the major pathway for DSB repair in yeasts and therefore the requirement for HR for the repair of the cf-DSB was investigated. *Rhp51Δ* was defective in cf-DSB repair with a reduction in the percentage of viabilities from 52% to 34% when the cf-DSB was induced. An increase in the percentage of slow growing cells was also observed (from 29% on –T to 46% after induction). This result shows that Rhp51 is required for repair of both se-DSB and cf-DSBs.

Rhp57Δ had a reduction in viability in the *rtf1Δ* deletion strain when compared to the *rtf1+* strain (from 51% in *rtf1+* to 34% in *rtf1Δ* on $-T^{no\ DSB}$). As a recombination mutant *rhp57Δ* has a sick phenotype, and this is reflected in the high level of dead cells observed on media $-T^{no\ DSB}$ and $+T^{DSB}$ (36% and 27% respectively). However the specific increase in slow growing colonies on media $+T^{DSB}$ shows that *rhp57Δ* also has a defect in both se-DSB and cf-DSB repair.

6.4 Rqh1 is required for cf-DSB repair but not se-DSB repair

rqh1Δ mutants were previously shown to be proficient in se-DSB repair (Roseaulin et al, 2008 and section 5.3 and 5.4) but are sensitive to IR, consistent with a role in two-ended DSB repair (Murray et al., 1997). In the *rtf1Δ* strain*,* microcolony analysis showed a reduction in viability 79% to 61% after induction of the cf-DSB (table 6-1 and figure 6-3). This reduction in viability is accompanied by any increase in the percentage of slow-growing colonies from 9% to 27%. Thus, Rqh1 is required only when the DSB is induced in *rtf1Δ*. Importantly, these data demonstrate that deletion of *rtf1* has changed the nature of the repair event and support the hypothesis that an incoming fork converts the se-DSB to a cf-DSB. This suggests that Rqh1 is not required is for processing se-DSBs but does play a role after the se-DSB is converted to a cf-DSB.

Rqh1 (RecQ family of helicases) has been shown to act with Top3 to have Holliday junction (HJ) dissolution activity where double HJs are repaired by branch migration and strand decatenation that does not produce crossover events. The requirement for Rqh1 could thus indicate that cf-DSB repair is through the formation of double HJs (section 1.7)

6.5 Deletion of *rtf1* rescues the repair defect in *mus81Δ*

mus81Δ was previously shown to be defective in se-DSB repair (Roseaulin et al, 2008 and chapter 5), however, after deletion of *rtf1* it was observed that *mus81Δ* was not defective in cf-DSB repair (table 6-1 and figure 6-3). Upon plating *mus81Δ rtf1Δ* on +T^{DSB} media there was no longer a reduction in the percentage of viable colonies (52% on –T and 57% on +T). In addition, *rtf1+* strains grown on +T^{DSB} media show an increase in the percentage of slow growing cells (from 16% to 33%) but in *rtf1Δ* no increase in the percentages of slow growing cells was observed. This rescue is consistent with data showing that *mus81Δ* is not sensitive to DNA damage caused by IR and has a specific role in single-ended double strand break repair (section 6.8). This data also confirms that the deletion of *rtf1Δ* changes the conformation of the se-DSB so that the viability of *mus81Δ* mutant can be restored.

6.6 Deletion of *rtf1* rescues the repair defect in *smc6-74* but not *smc6-X*

Both *smc6* mutants are defective in HR repair of DNA damage caused by ionising radiation (IR) (Lehmann et al, 1995) (Verkade et al, 1997). They would thus be predicted to have a defect in cf-DSB repair in addition to the defect in se-DSB repair. Microcolony analysis after DSB induction (table 6-2 and figure 6-3) showed *smc6-X* to have defects in cf-DSB repair in *rtf1Δ*. The percentage of viable microcolonies was reduced from 71% on –T$^{no\ DSB}$ media to 64% after cf-DSB induction. This defect appeared to be milder than that in se-DSB repair (*rtf1+*) but the high percentage of slow growing colonies (27%) is consistent with the expected reduction in viability.

Unexpectedly, microcolony analysis revealed that the repair defect in *smc6-74*, like *mus81Δ,* is rescued by the deletion of *rtf1*. In *rtf1+* strains viable microcolonies decreased from 81% to 62% when growing on +T^{DSB} media. In contrast with this *rtf1Δ* deletion mutants did not show a decrease in viable colonies (83% to 80%). In addition to this there was also little change in the number of dead cells and slow-growing colonies. Since the only difference between these two strains is the expression of Rtf1 and enforcement of the RTS1 replication termination barrier, this suggests that that rescue of *smc6-74* is due to the conversion of the se-DSB to a cf-DSB. At present it is not clear why this conversion would rescue *smc6-74*, especially as it is defective in

processing DNA breaks that result from IR. This data analysis was repeated in four separate strain isolates to ensure that cell viability was rescued and similar results were obtained for all *smc6-74 rtf1Δ* strains. Thus *smc6-74*, like *mus81Δ* is only defective in se-DSB repair but the other hypomorphic *smc6* mutant, *smc6-X*, is defective in both se-DSB and cf-DSB repair.

6.7 Cell length analysis of strains repairing the cf-DSB

The cell length of strains in the cf-DSB system were analysed (as in section 5.1.4). As expected from microcolony data, the range of WT cell lengths did not change after the deletion of *rtf1Δ.* In all strains, with and without the DSB (+/-T), the mean cell length was approximately 7 mm and is not significantly different from the –DSB data (figure 6-4 6-5 and table 6-2).

HR mutants, *rhp51Δ* and *rhp57Δ,* show an increase in cell length after growing on media +T^{DSB} in *rtf1+* and *rtf1Δ* strains. Average cell length increased from 12.9 to 19.2 µm in *rhp57Δ rtf1Δ* strains grown on media +T^{DSB}, this was a similar result to that seen in *rhp51Δ* deletion mutants that increased from 12.3 to 16.8 µm on +T^{DSB} media. This increase in cell length is consistent with a repair defect and checkpoint activation. These data are comparable to the defect seen in *rtf1+* strains, supporting the conclusion that both recombination mutants are defective in se-DSB and cf-DSB repair.

From the microcolony viability assay *rqh1Δ* mutants were defective in cf-DSB repair and this was reflected in the cell length analysis. In *rtf1+* strains the cell length averaged 6.7 mm with and without DSB induction. However, in *rtf1Δ* the viability of *rqh1Δ* decreases and the average cell length increases from 11.8 to 16.3 µm. This result is consistent with the observation that *rqh1Δ* is not proficient in cf-DSB repair.

Based on microcolony data the se-DSB repair mutant *mus81Δ* was not defective in cf-DSB repair and the *rtf1Δ* strains showed only a very slight increase in cell length from 13.7 to 14.1 µm after growing cells on media +T to induce the cf-DSB. Thus, deletion of *rtf1Δ* rescues the elongated cell phenotype.

Microcolony growth after 24 hours
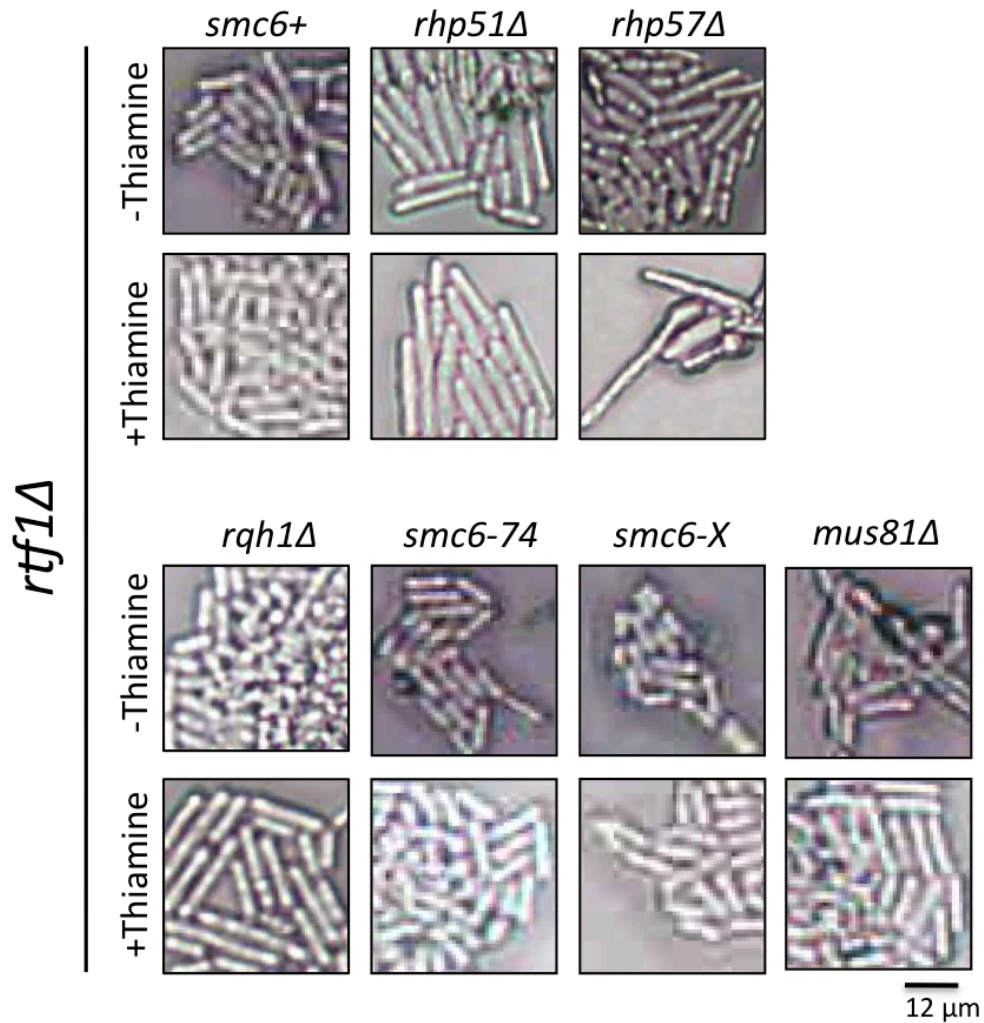
Figure 6-4- Microcolony analysis of strains grown on agar +/-T in *rtf1Δ*
WT, smc6-74, smc6-X and mus81 were tested grown for 24-36 hours on supplemented YNBA media + or − thiamine. The resulting colonies were photographed using a USB microscopy camera and cell length was measured by hand after scaling images appropriately.

	WT		rhp51Δ		rhp57Δ		rqh1Δ		mus81Δ		smc6-74		smc6-X	
	-	+	-	+	-	+	-	+	-	+	-	+	-	+
Average	12.4	12.5	12.3	16.8	12.9	19.2	11.8	16.3	13.7	14.1	12.5	12.4	12.4	14.7
SD	2.7	2.5	3.8	4.5	3.7	6.7	3.1	6.9	3.6	4.3	3.2	3.7	2.2	4.0
Chi Test	n/a	n/a	0.597	0.000003	0.545	3.6973E-19	0.647	0.00000000003	0.289	0.405705898	0.876	0.978441	0.998	0.376

Table 6-2 Microcolony cell length data in *rtf1Δ* mutants
Strains were grown for 24-36 hours on supplemented YNBA media +T and –T at 30°C. The length of 35 cells was measured from images taken using a USB microscope camera (figure 6-4) and the average cell length (μm) was calculated. P values were determined using *chi²* where the WT data set was the expected values.
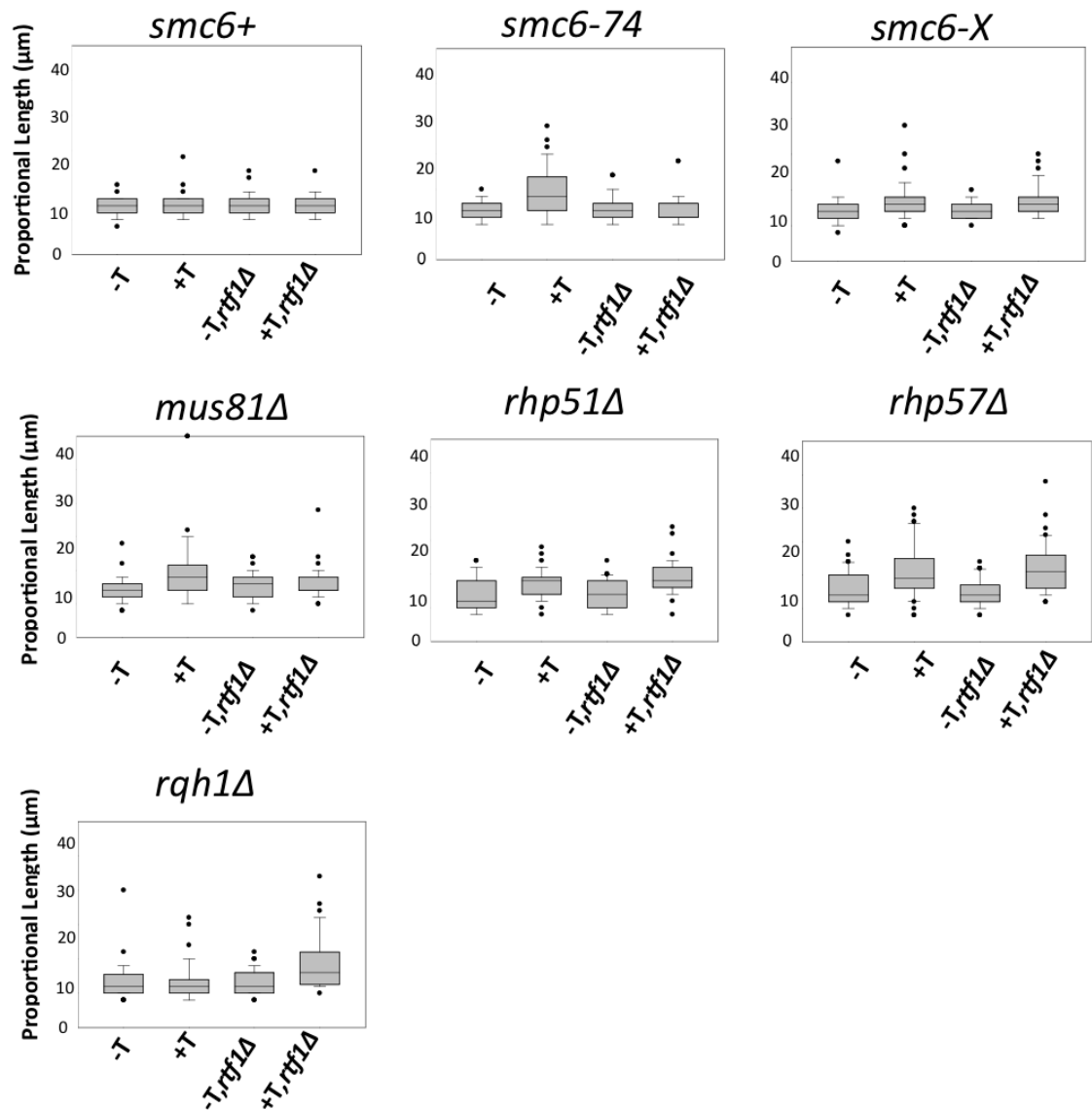
Figure 6-5- Microcolony analysis of strains grown on agar +/-T with +/- Rtf1 Strains were grown for 24-36 hours on supplemented YNBA media + or − thiamine. The resulting colonies were photographed using a USB microscopy camera and cell length was measured by hand after scaling images appropriately (see methods … for more details). The cell length of samples was plotted on a box plot to show average length (centre of the box) standard deviation (bars) and outliers (dots).

Similarly, both cell viability and cell length in *smc6-74* was rescued after deleting *rtf1Δ*. Analysis of cell length data showed that deleting *rtf1* rescued the repair defect in *smc6-74* (average length of 12.45 µm on media +/-T).

smc6-X showed a reduction in viability after the deletion of *rtf*. Of the microcolonies that were viable it was observed that there was an increase in mean cell length from 12.4 to 14.7 µm after induction (P=0.376). The large range of cell sizes seen in *rtf1+* (up to 52.5 µm) was not observed in *smc6-X rtf1Δ* with a range of 10.2-25 µm. The lack of cell elongation is consistent with the checkpoint maintenance defect previously characterised for Smc5/6 complex mutants (Verkade et al., 1999, Miyabe et al., 2006). After transient replication inhibition or DNA damage Smc5/6 mutants delay the cell cycle but fail to maintain the checkpoint and enter mitosis with WT kinetics but with incomplete repair leading to mitotic catastrophe.

6.8 Rescued *smc6-74* mutants were sensitive to IR

It was not anticipated that *smc6-74* would be rescued in the *rtf1Δ* background. However, this was the result seen in microcolony analysis, cell length analysis and spot tests (figure 6-6). Since *smc6-74*, like *smc6-X*, has a checkpoint maintenance defect and would not be expected to elongate after DNA damage the rescue could be an artefact of the microcolony assay or the strain construction. To ensure that the *smc6-74* strains used in the analysis were still sensitive to DNA damaging agents, the viability was analysed after exposure to IR. WT, *smc6-X* and *mus81Δ* mutants in *rtf1+* and *rtf1Δ* mutant backgrounds were also analysed. Cell cultures were grown and subjected to different amounts of IR before plating on solid media. The number of colonies was counted and plotted against dose (Gy) to produce a survival curve (figure 6-7 see methods 2.2.6).

Deletion of *rtf1* had minimal effect on survival in WT cells. *Mus81Δ* was not sensitive to IR with a survival percentage of 38% and 21% in *rtf1+* and *rtf1Δ* strains respectively after a dose of 1000 Gy (figure 6-7). Both *smc6-X* and *smc6-74* strains were sensitive to IR, suggesting that the rescue of cf-DSB repair seen in *smc6-74 rtf1Δ* being unique to the type of damage caused at the *mat* locus.
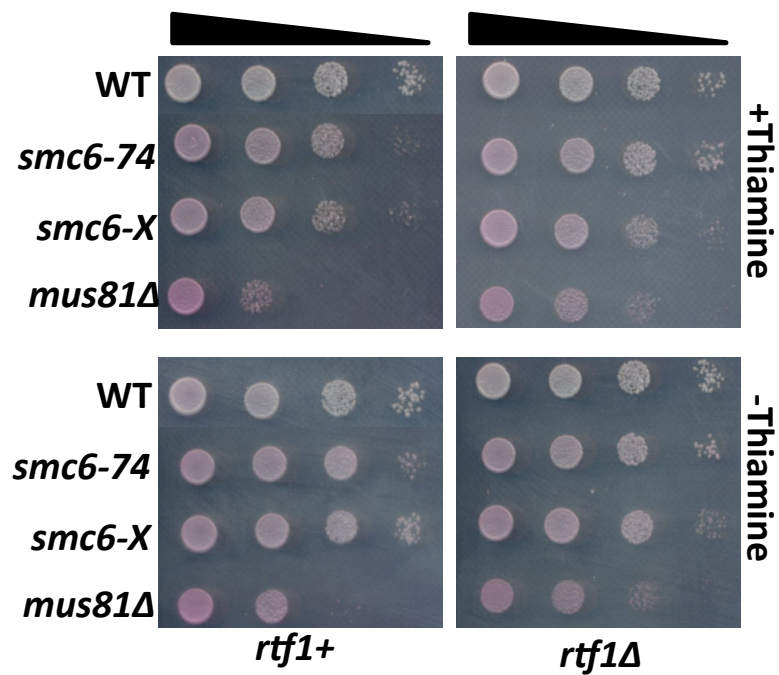
Figure 6-6- Analysis of strains in response to cf-DSB repair

Spot test analysis was used to investigate several mutant's response to cf-DSB repair. 10-fold serial dilutions of 1×10^7 cells/ml were spotted on to media +/- thiamine, cells were grown for 3 days at 30°C. Single mutants and *rtf1Δ* double mutants were tested in parallel.

(A) γ- irradiation survival curve
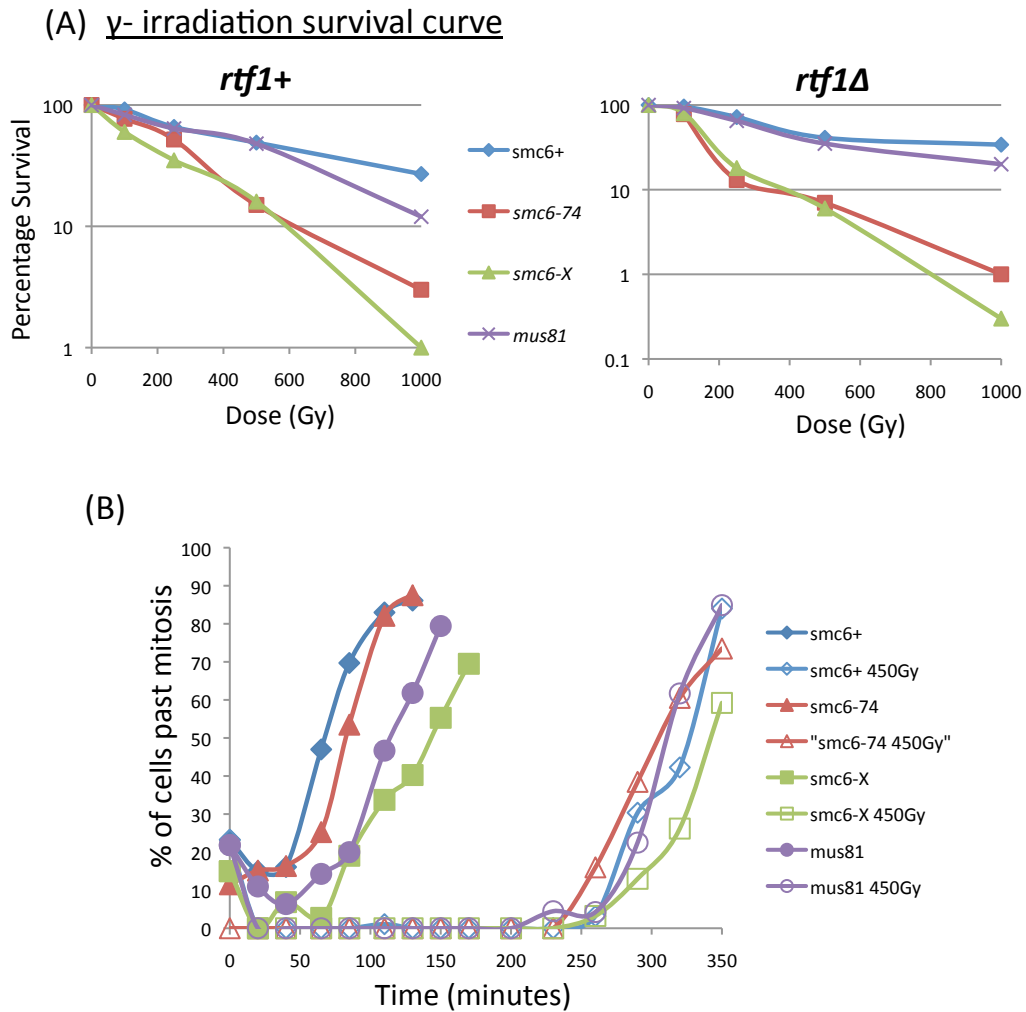
Figure 6-7- Survival and growth rates of *rtf1Δ* mutants after exposure to IR
Cell cultures of WT, *smc6-74*, *smc6-X* and *mus81Δ* in single and *rtf1Δ* double mutants were investigated in their response to IR. (A) Cultures were exposed to different doses of γ-irradiation (Gy) and plated onto YEA media for 3 days at 30°C. Total colonies were counted at each dose and plotted exponentially to indicate survival. (B) Cell cultures were given a fixed dose of 450 Gy and grown for 350 minutes after exposure. Cell samples were taken ever 20 minutes and the number of cells past mitosis (from two nuclei onwards) were counted.

This data is of interest as it separates the analysis using the inducible cf-DSB system in *rtf1Δ* backgrounds from se-DSB repair. In particular it identifies a unique circumstance where *smc6-74* is able to repair a double strand break.

Next cell cycle progression after IR was analysed. Cells were synchronised in G2 using lactose gradients, split into two and one sample irradiated with 450Gy before growing at 30°C. Samples were fixed in methanol every 20 min and the number of cells past mitosis scored to determine the cell cycle progression (see method section 2.2.7).

All strains (WT, *smc6-X, smc6-74* and *mus81Δ*) delayed for approximately 220 min before entering mitosis after exposure to γ-irradiation, consistent with them being proficient in activating the DNA damage checkpoint. However, *smc6-X* and *smc6-74 rtf1Δ* strains cut on entry into mitosis (figure 6-8). Cut cells were not seen in either WT or *mus81Δ* strains (figure 6-8). This observation is consistent with the previously described checkpoint maintenance defect where the mutants are defective in a late stage in HR repair which is not recognised by the damage checkpoint and so enter mitosis with incompletely repaired DNA (Miyabe et al., 2006, Verkade et al., 1999)

6.9 Summary

A novel system to study repair of a se-DSB converted by a converging fork to a two-ended cf-DSB was set up by deleting *rtf1* in the Arcangioli inducible se-DSB repair system. Deletion of *rtf1* did not effect the ability of WT strains to process a DSB at the *mat* locus. Conversely HR mutants *rhp51Δ, rhp57Δ* were defective in the repair of both types of DNA break; se-DSB and cf-DSB. However, deletion of *rtf1* changed the requirements for the HR regulators Mus81 and Rqh1, both of which have been implicated in the resolution/dissolution of Holliday junctions. *Mus81Δ* mutants were defective in se-DSB repair but were not defective in cf-DSB repair as cell viability and cell length were rescued in *mus81Δ rtf1Δ* double mutants. In contrast, Rqh1 was not required for se-DSB repair but was required in *rtf1Δ* showing that the confirmation of the DSB is changed. Thus deletion of *rtf1* leads to a change of the se-DSB into a
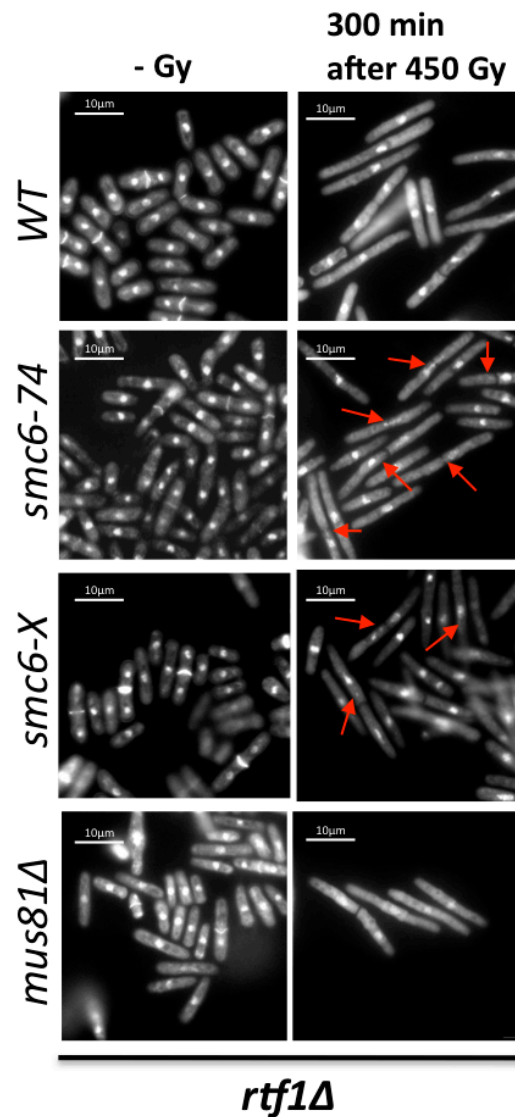
Figure 6-8- *rtf1Δ* mutants delay into mitosis in response to IR

Cell cultures of WT, *smc6-74*, *smc6-X* and *mus81Δ rtf1Δ* double mutants were investigated in their response to IR. Cultures were exposed to a 450 Gy dose of γ-irradiation and grown for 300 minutes. Samples of cultures were fixed in methanol and stained with DAPI to visualise DNA. Fixed cells were observed under the Delta Vision microscope.

conformation containing a structure, most likely that coming from the converging fork, that requires HR and Rqh1 for repair. RecQ helicases, like Rqh1, have been shown to be required for resection, branch migration, strand displacement and with Top3 dissolution of double Holliday junctions. Further work is required to determine the conformation of the cf-DSB and how it is repaired.

Consistent with a requirement for Smc5/6 for the repair of IR damage the *smc6-X* hypomorph was found to be defective in both se-DSB and cf-DSB repair. Since Smc5/6 has been shown to be required for the resolution of recombination (Ampatzidou et al., 2006) this suggests it is required with Mus81 at se-DSBs and with Rqh1 at cf-DSBs. Unexpectedly the *smc6-74* hypomorph was rescued by the deletion of *rtf1* but was still defective in repair of IR damage. Thus, *rtf1Δ* specifically rescues the defects in processing a cf-DSB at *mat1* but does not rescue the overall defect in processing DNA damage. This could suggest that smc6-74 is not defective in the repair of two-ended DSBs. It is sensitive to IR, which leads to DSBs but also generates a range of other damage that may require Smc5/6 for repair.

After induction of the cf-DSB the HR repair defective *rhp51Δ*, *rhp57Δ* and *rqh1Δ* cells elongated but *smc6-X* (figure 6-5), while defective in repair, did not, consistent with the checkpoint maintenance defect. This highlights the difference between se-DSB and cf-DSB repair. Both *smc6* mutants are defective in se-DSB repair and the cells elongate (section 5.4.). This is unexpected as in response to other types of damage (IR (figure 6-8) and HU (Ampatzidou et. al 2006) *smc6* mutants delay like WT but then enter mitosis and 'cut'. This suggests that the processing defect in se-DSB repair leads to the accumulation of ssDNA which continues to signal to the DNA damage checkpoint. The kinetics of repair in WT and *smc6* mutants is explored in further detail in the next chapter.

Chapter 7 – Cell cycle analysis after se-DSB induction

7.1.1 Introduction

In *S. pombe* cells spend most of their time in G2. G1 is very short and S phase is initiated coincidently with septation, where a three layered structure of B-Glucan, known as the septum (Zubenko et al., 1979)forms in the centre of the cell and helps to initiate cell division. The cell septum can be visualised under a fluorescence microscope using a stain called calcofluor that binds the central primary structure of the septum. It is then possible to microscopically follow and to estimate the timing of S phase with the addition of DAPI (4',6-diamidino-2-phenylindole) to visualise the DNA.

In response to DNA damage cells delay cell cycle progression. In cells that can efficiently repair the delay is short but cells that are checkpoint proficient but cannot repair DNA damage a long delay is seen and, as cells continue to accumulate mass, this correlates with an increase in cell length. These cells may eventually divide and survive, however, many die in an elongated state. Cells that are not able to trigger a checkpoint response, fail to elongate and enter mitosis with damaged DNA, leading to mitotic catastrophe as cells fail to segregate their chromosomes and the nucleus is bisected by the septum, a phenomenon known as a 'cut' cell phenotype (Hirano et al., 1986). The 'cut' cell phenotype is seen in both *smc6-X* and *smc6-74* after exposure to gamma irradiation but in this case the cells delay mitosis similarly to WT before undergoing mitotic catastrophe (figure 6-8). This has been defined as a checkpoint maintenance defect (Verkade et al 1999) and suggests that while the checkpoint is activated normally in both mutants repair is not completed but gets to the point where it no longer signals to the DNA damage checkpoint before mitosis.

The elongated cells in *smc6-X*, *smc6-74*, *mus81Δ* and HR mutants seen during microcolony analysis of se-DSB repair (section 5.3) suggest that the inability of the mutant to repair the se-DSB leads to a delay in cell cycle progression. While this expected for *mus81Δ* or HR mutants, it is an unexpected result for *smc6-X* and *smc6-74*

as it suggests that in response to a se-DSB both mutants are able to both activate and maintain the checkpoint.

This chapter describes using synchronised cultures to study repair the se-DSB to assess the timing of events, the percentage of cells that are elongated and the whether elongated cells divide.

7.1.2 Cell-cycle analysis shows that se-DSB induction does not delay cell-cycle progression for WT but does in both *smc6-X* and *smc6-74*

In the initial analysis of the WT, *smc6-X* and *smc6-74* cells were synchronised before induction. To follow cell cycle progression large cultures were grown in supplemented liquid EMM and synchronised in G2 using a lactose gradient (as described in 2.3.1) the se-DSB was induced in the most synchronous fraction of cells and samples fixed in methanol every 20 minutes over a 12 hour time course. The cells were stained with DAPI and Calcofluor (section 2.3.3) and scored under the microscope. The percentage of septating cells was calculated to determine the Septation Index (SI). The SI is plotted against time to show the cell cycle progression and since S phase is coincident with septation this plot is also a measure of when S phase occurs.

Induction of the se-DSB by repression of *nmt1* transcription in the G2 cells would lead to imprinting in the first S phase (coincident with septation peak 1) and then in the second S phase (coincident with septation peak 2) se-DSB formation in the 50% of cells that inherited the lagging strand and imprinting in the other 50% of cells. The timing of septation peak 3 in the 3rd cell cycle will be dependent on the mitotic delay after the se-DSB in the second cell cycle. Thus comparison of the cell cycle lengths between septation peaks gives a measure of mitotic delay. Since there is no increase in cell cycle length this suggests that WT cells can efficiently repair the se-DSB within the normal cell cycle time.

Smc6-74 and *smc6-X* both progressed through the first two peaks of septation similarly to WT with a 4 hour doubling time. In the 3rd cell cycle both mutants showed a third septation peak close to 500 minutes after induction, however this peak is lower (30%

for *smc6-X* and 39% in *smc6-74*). Furthermore in both of *smc6-X* and *smc6-74* there is an additional peak at approximately 660 minutes roughly half a cell cycle after the third peak. This was designated 3.1 (figure 7-1).

Synchronisation of *mus81Δ* resulted in a peak of 57% at around 60 minutes, followed by a second peak of 33% at 300 minutes. However it was difficult to detect a distinct third peak. This could be due to a loss of synchrony towards the end of the time course or because *mus81Δ* fails to repair the se-DSB leading to a mitotic delay as expected based on previously published pedigree data (Roseaulin et al. 2008) (figure 7-1).

7.1.3 Synchronisation after the first S phase confirms the presence of an extra peak of septation after se-DSB induction in *smc6* mutants

To investigate the timing and appearance of the extra peak of septation in *smc6* mutants cells were grown as previously described but were synchronised at 180 minutes after induction. This gave better synchrony to investigate cell cycle progression after 500 minutes. Time points were taken up to 700 minutes after induction.

WT showed a similar profile of cell cycle progression as before. A peak of septation at 300 minutes (SI of 50%) corresponded to the S phase when the se-DSB is formed. A second peak corresponding to the third S phase (SI = 26%) was seen just after 500 minutes. At time zero a sample was taken prior to induction in order to establish the SI before induction in the asynchronous culture. In WT asynchronous strains this asynchronous SI was 8%.   Cell cycle length appears to be between three and four hours but is variable by about 20 minutes between experiments (figure 7-2).

Smc6-74 and *smc6-X* both showed cell cycle progression that was consistent with the data seen in the previous analysis. In both strains there was initial septation peak (SI = 30-40%) at 360 minutes, this peak corresponds to the se-DSB in 50% of the cells. There was a double peak of septation following se-DSB S phase with a SI of 20% at 500 minutes (peak 3) and around 20% at 620 minutes (peak 3.1).
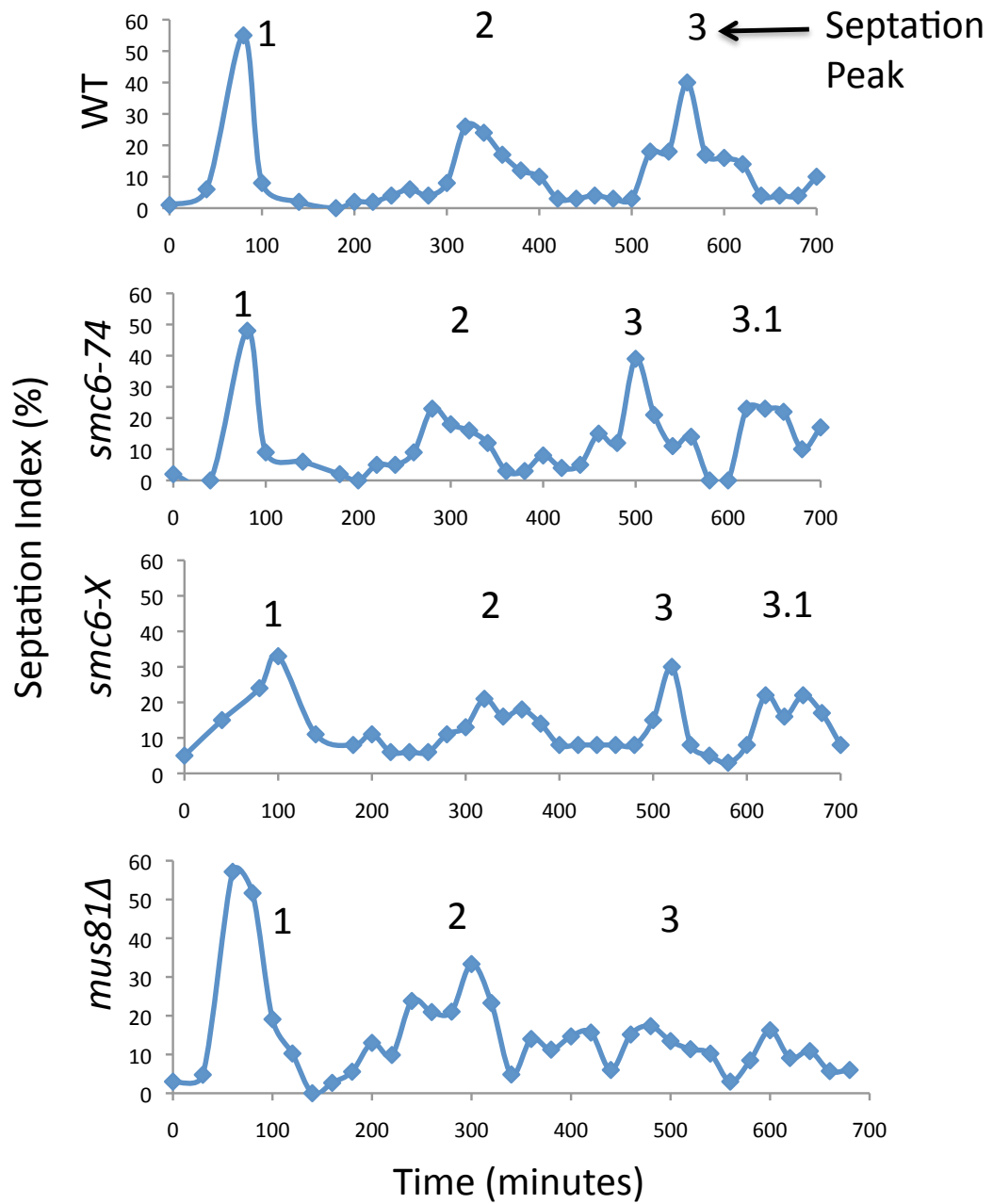
Figure 7-1- Analysis of cell cycle progression after se-DSB induction
WT, *smc6-74, smc6-X* and *mus81Δ* cells were synchronized in G2 by
lactose gradient and induced with 5μM thiamine. Cell samples were
collected every 20 minutes and fixed with methanol. Fixed cells were
stained with DAPI and calcofluor. Septation was scored under a
fluorescence microscope.
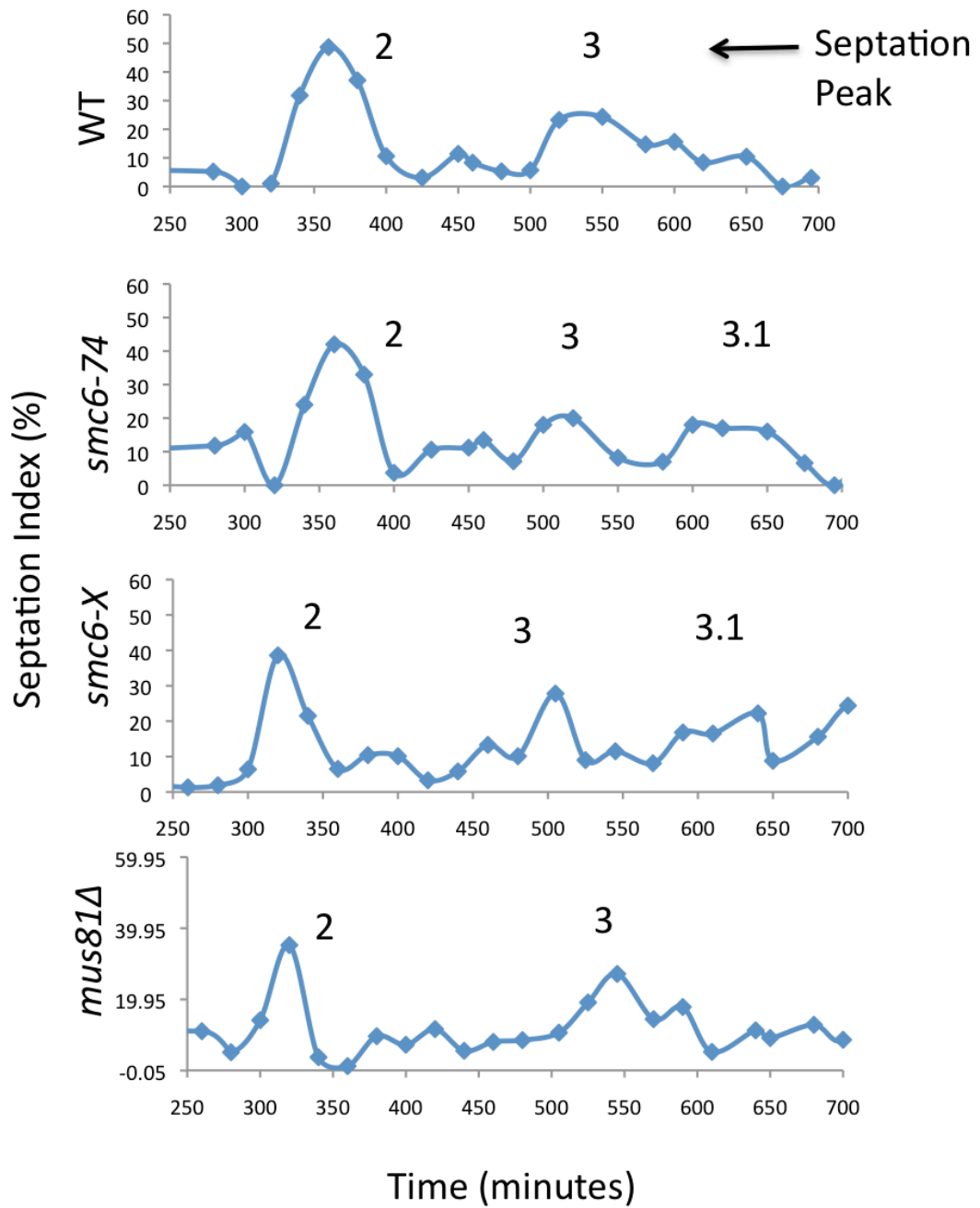
Figure 7-2- Analysis of cell cycle progression after se-DSB induction with later synchronisation

WT, *smc6-74, smc6-X* and *mus81Δ* cells were synchronized in G2 by lactose gradient 180 minutes after induction with 5μM thiamine. Cell samples were collected every 20 minutes and fixed with methanol. Fixed cells were stained with DAPI and calcofluor. Septation was scored under a fluorescence microscope.

This double peak was seen in both *smc6-X* and *smc6-74* in three independent experiments, although the precise timing of the peaks varied slightly. The double peak suggests that there are two populations of cells where half the cells are entering mitosis at peak 3 and half at peak 3.1. Since the se-DSB is induced in the daughter cells that inherit the imprinted lagging strand, only 50% of cells will be undergoing repair. The daughters that inherit the leading strand will imprint and so have cell cycle progression kinetics similar to the imprinting cells in the previous cycle. Thus peak 3 is likely to consist of imprinting cells. This suggests that peak 3.1 is composed of cells in which the se-DSB was induced and defective or inefficient repair led to a cell cycle delay of approximately 120 min.

mus81Δ showed the clear peak of septation at around 300 minutes with an SI of 35%, when the se-DSB should occur in 50% of cells. Peak 3 appeared slightly delayed at 550 minutes, consistent with the slow growth phenotype, and was also lower than in WT. However, unlike *smc6-X* and *smc6-74* there was no distinct additional peak 3.1 suggesting that repair deficient *mus81Δ* cells do not enter mitosis or at least not synchronously within the time course of the experiment.

7.2.1 Analysis of cell length over time course of se-DSB induction

As increased cell length was shown to be a feature of strains with reduced viability after repairing the se-DSB (section 5.3 and 5.4), cell samples harvested from the 12 hour time course analysed using the Deltavision CoreDV microscope. Cells samples from the peaks of septation at 2, 3 and 3.1 as well as an asynchronous control at time 0 minutes were fixed in methanol and stained with DAPI/Calcofluor.

In WT strains the average cell length in the asynchronous cultures before induction (time point 0) was 11.61 μm and in septation peak 3 cell length ranged from 11.61 μm to 12.7 μm which is not a significant increase (P=0.169 paired Ttest). This is longer than the typical length of *S. pombe* cells, but may be due to strain background or growth conditions in the minimal media.

In *smc6-74* average cell length did not significantly increase from time point 0 to peak 3, (10.46 µm to 11.15 µm (P=0.139)), however at peak 3.1 the average cell size increases to 13.93 µm. This increase is significant. Both average size and the range of cell lengths increased. Time 0 has a range of 8-16 µm, peak 2 and 3 from 10-13 µm however peak 3.1 has a large increase in this range from 11 µm to 30 µm. This is consistent with defective repair of the se-DSB leading to a checkpoint delay and elongated cells (figure 7-3).

Smc6-X showed a similar phenotype to *smc6-74*, with an average cell length of 12.12 µm in asynchronous cells, 12.22 µm after induction at peak 2. This average length did not increase further at peak 3, with an average 13.46 µm. There is a statistically significant increase in average size at peak 3.1 to 15.52 µm as well as an increase of range from 10 to 30 µm. This phenotype is similar to *smc6-74* but more severe, consistent with its more severe repair and growth defect.

Mus81Δ is unable to process the se-DSB, cells hyper elongate and die (Roseaulin et al., 2008). Microscopy data from this analysis was consistent with this as cells began to elongate significantly from peak 2 onwards, with hyper elongated cells as long as 30µm seen at peak 3 and onwards. These cells do not enter mitosis and therefore the defect seen in *mus81Δ* is distinct from that seen in the *smc6-X* and *smc6-74* mutants (figure 7-3).

7.2.2 In *smc6-X* and *smc6-74* cultures elongated cells accumulate after peak 3 and divide at peak 3.1

To further categorise the cell cycle progression of elongated cells the septating cells at each time point were measured using the Softwrx measuring tool and compared to the mean and standard deviation for the asynchronous uninduced culture (time point 0). Cells were then divided into categories – cells defined as 'normal' were cell length was within one standard deviation from the mean. Any cells longer or shorter than the mean +/- the standard deviation were categorised as 'long' or 'short' respectively. The septation index was calculated for normal and long cells individually.

	Peak 0	2	3	3.1
WT				
smc6-74				
smc6-x				
mus81				
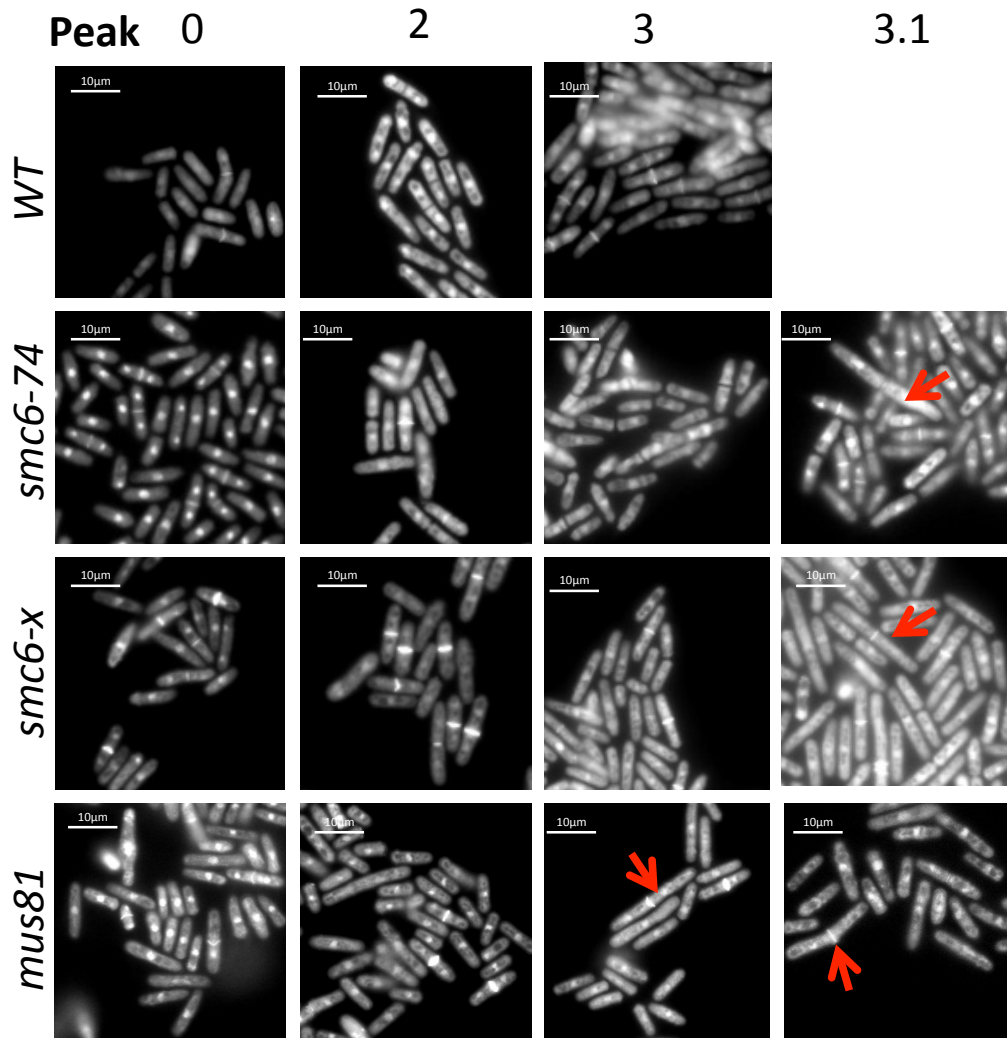
	2	3	3.1
smc6+	11.67 (9-13 μm)	12.7 (10-13 μm)	
smc6-74	11.64 (10-13 μm)	11.15 (10-13 μm)	13.93 (11-30 μm)
smc6-X	13.17 (10-16 μm)	13.46 (10-16 μm)	15.52 (10-30 μm)
mus81	13.07 (11-14 μm)	13.46 (10-16 μm)	

Figure 7-3- Investigation of cell length at septation peaks revealed elongated cells at peak 3.1 in *smc6* mutants

Cells harvested from septation peaks in septation index experiments were visualised by staining nuclear DNA with DAPI and the septum with calcofluor. The Delta Vision microscope was used to obtain images and Softworx was used to measure the cell length. The average cell size and range for each septation peak was calculated (see boxout).

At time point 0 WT has an average cell length of 11.61 μm and a standard deviation (SD) of 0.96. Cells were defined as long if their cell length was greater than 12.6 μm. At peak 2 the majority of cells septating were 'normal' with an SI of 41% and a SI of 7.09% for elongated cells. Peak three was wider and more diffuse, persisting over 80 minutes, with 'normal' length cells forming the majority of the peak, around 60% of the total SI. No distinct peak is seen after peak 3 (figure 7-4).

In *smc6-74* at time point 0 the average cell length was 10.46 μm, with a standard deviation of 1.45. Cells greater than 11.9 μm were considered long. In Peak 2 the majority of septating cells were 'normal' with a SI of 30% compared for a SI of 11.2% for long cells. The majority of peak 3 is made up of 'normal' length cells with a septation index of 15.18% 'normal' and 3.4% of 'long' cells. This contrasted to peak 3.1 where 'long' cells make up the majority of the peak with an SI 12% compared to an SI of 5.56% in 'normal' cells. Thus, Peak 3.1 contains a high number of elongated septated cells, consistent with a checkpoint delay likely due to a defect in repairing the se-DSB,

smc6-X shows a similar phenotype to that seen in *smc6-74* with an average length of 12.1 μm at time point 0, standard deviation of 0.94. Cells were classed as 'long' over 13.8 μm. As with other strains, the majority of peak 2 and 3 contains 'normal' cells with Sis of 27% and 17.8% respectively. Peak 3.1 is dominated by 'long' cells with a septation index of 17.07% 'long' cells (figure 7-4).

Importantly, these data show that the increase in average cell length seen in the previous analysis (section 7.2.2) correlates with the additional peak at 3.1 seen in *smc6-X* and *smc6-74*. This suggests that between peak two and peak 3.1 the population splits in two where approximately half of the cells septate at the expected time of around 500 minutes at the normal size. The other half of the population continues to elongate and eventually divides late. The number of elongated cells that continue to survive after this delayed mitosis is unknown. If, as is likely, the delay is the result of the se-DSB then the reduction in viability seen in *smc6-74* and *smc6-X* tetrad and microcolony
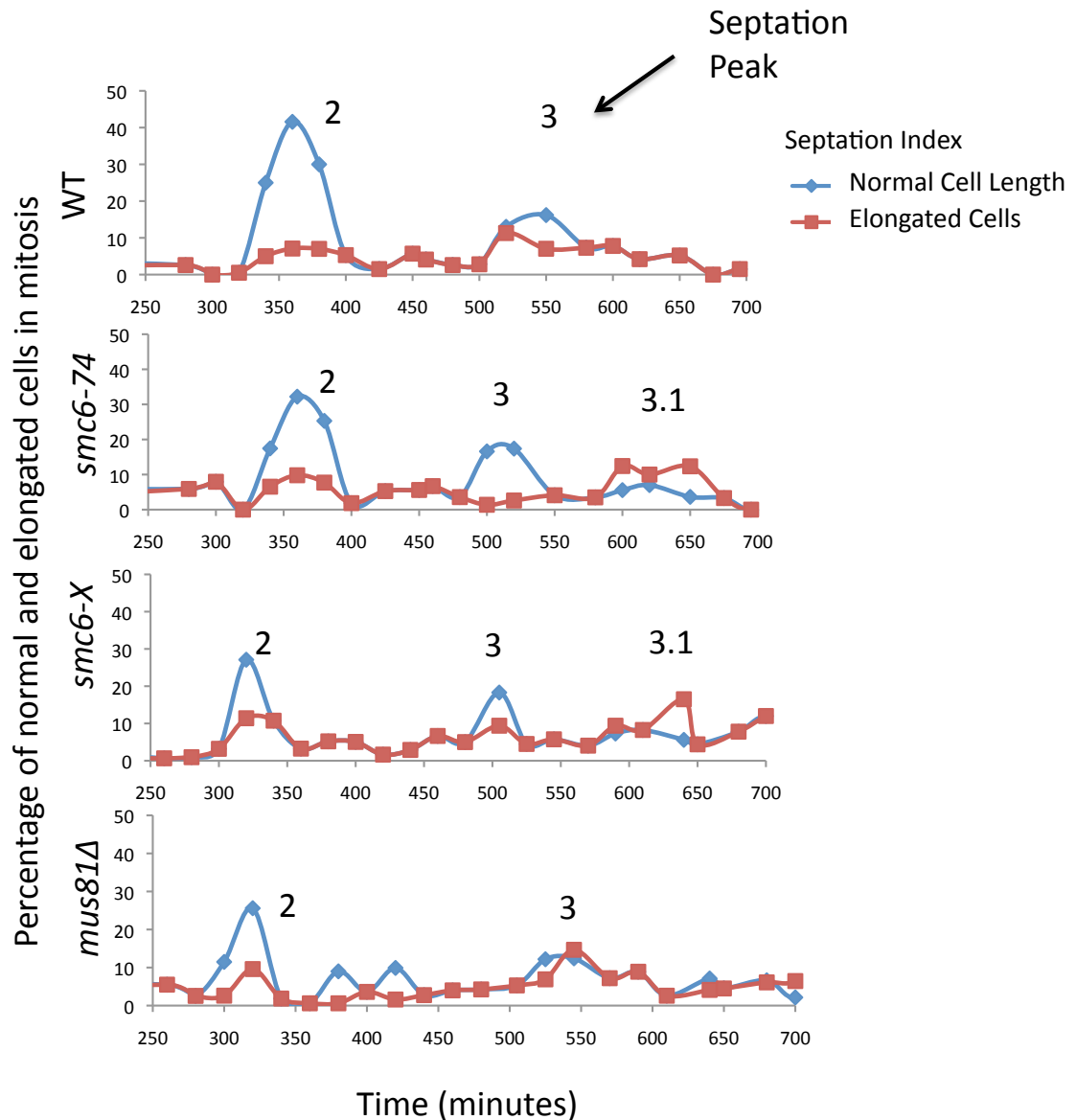
Figure 7-4- Cell cycle progression of long and short cells after se-DSB induction

WT, *smc6-74, smc6-X* and *mus81Δ* cells were synchronized in G2 by lactose gradient and induced with 5µM thiamine. Cell samples were collected every 20 minutes and fixed with methanol. Fixed cells were stained with DAPI and calcofluor and the Delta Vision microscope was used to determine septation and cell length.

analyses suggest that a proportion of these cells will not survive. In both *smc6-X* and *smc6-74* at the end of the 3.1 peak there were some very long cells, >30 μm, that had not yet septated, suggesting that not all cells enter into mitosis.

Mus81Δ had an average size of 12.51 μm, standard deviation of 1.48 in asynchronous cultures and cells were considered 'long' if they were longer than 13.99 μm. As with all other strains the majority of cells septating in peak two are 'normal' length with a SI of 22.4%. Unlike other strains the third peak of *mus81Δ* is more diffuse, stretching over 3 hours from 450 minutes to 700 minutes. Septation seems to continue throughout the latter part of the time course with a septation peak of 'long' cells seen at 545 minutes with a SI of 16.9%. The fact that the peak is not fully resolved and that cells continue to elongate is consistent with data seen in previously published studies that Mus81 is required to repair the se-DSB. This response to induction suggest that deletion of *mus81* causes a more severe defective than that seen in *smc6-X* and *smc6-74*.

7.4.1 Cell cycle progression in the cf-DSB (*rtf1Δ*) inducible system

Cell cycle progression was characterised in the cf-DSB induction system (*rtf1Δ*) as above. Cell cycle progression in WT *rtf1Δ* mutants was similar to *rtf1+* with two peaks detected at 350 and approximately 520 minutes from induction respectively (figure 7-5).

Septation was plotted as in section 6.1.4 where cells were considered long if they were above the average cell length plus the standard deviation at time 0 and the percentages septation of 'normal' and 'long' cells were plotted separately on the same axis. At time 0 the average cell length for WT *rtf1Δ* was 11.42 μm with a standard deviation of 0.95. The peaks were mostly made up of 'normal' cells with a low percentage of 'long' cells. Occasionally there are slightly higher percentages of 'long' cells but they never reach a septation index of greater than 11% compared to the 16-22% in 'normal' cells. Overall there was a general trend across all strains that the *rtf1Δ* strains grew slightly quicker than their *rtf1+* counterparts and a 4th septation peak was seen even in mutants. It is unclear why this is the case especially in a WT strain, which
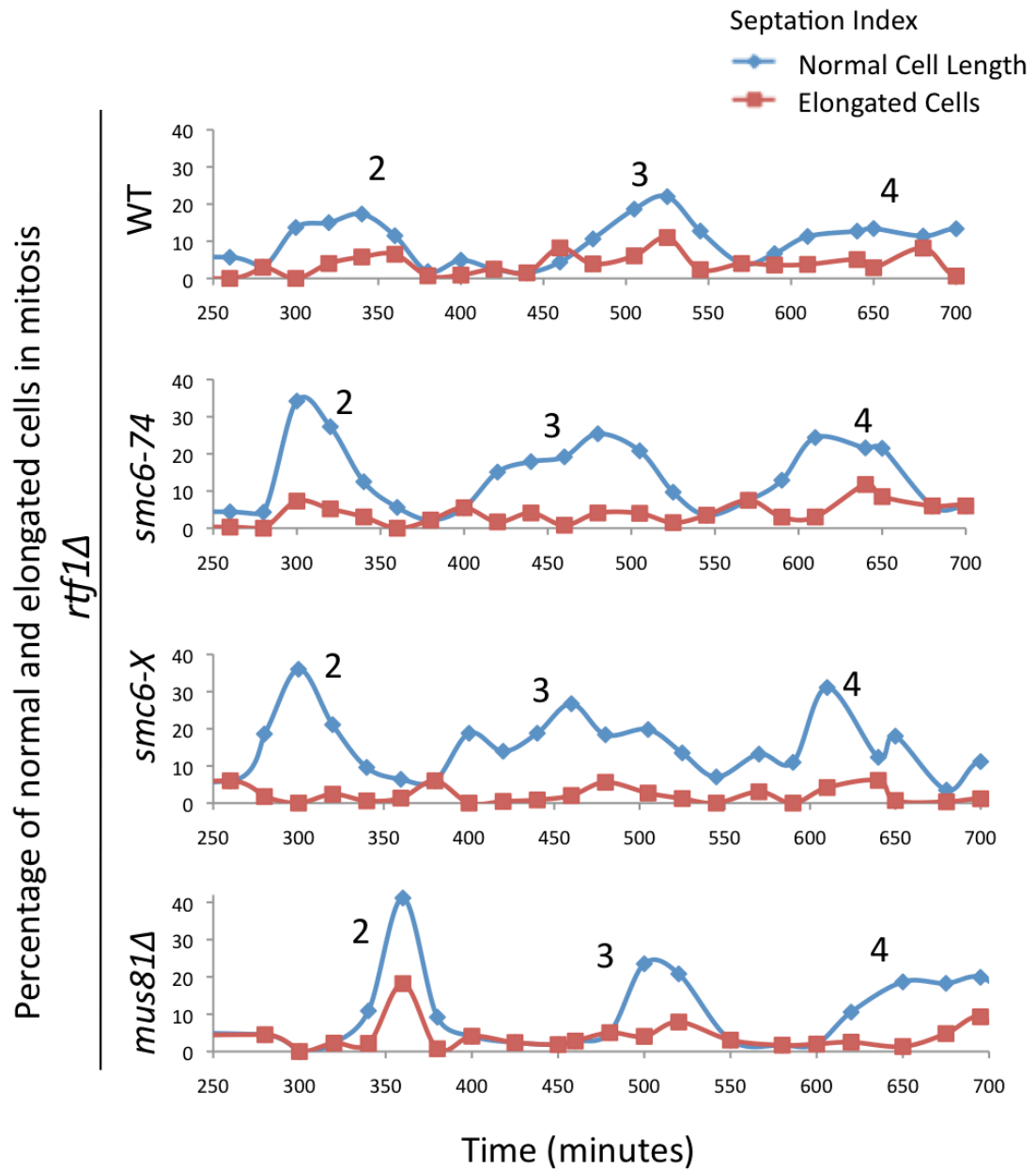
Figure 7-5- Cell cycle progression of long and short cells after cf-DSB induction in the *rtf1Δ* background

WT, *smc6-74, smc6-X* and *mus81Δ rtf1Δ* double mutants were subject to cell cycle and cell length analysis. Cells were synchronized in G2 by lactose gradient 180 minutes after induction with 3μM thiamine. Cell samples were collected every 20 minutes and fixed with methanol. Fixed cells were stained with DAPI and calcofluor and the Delta Vision microscope was used to determine septation and cell length.

is proficient in both se-DSB and cf-DSB repair (this trend was observed in spot tests too figure 6-6).

Rtf1Δ deletion strains were shown to rescue viability and the cell elongation phenotype in *mus81Δ* (section 6.5). Cell cycle progression in *mus81Δ* was also investigated after the deletion of *rtf1*. In contrast to *mus81Δ* in the se-DSB system *mus81Δ rtf1Δ* had sharp peaks of septation at 350 minutes and 500 minutes. Peak three had a reduction in the number of cells that were considered 'long' and septating. At time zero the average cell size was 12.48 μm with a standard deviation of 1.32, which is comparable to *rtf1+* strain. However, unlike the rtf1+ strain that has a large increase in the average cell size after 500 minutes, an increase in cell length was not observed in *mus81Δ rtf1Δ*. The loss of elongated cells and the restoration of the 3rd peak of septation, along with the rescue seen in spot test and microcolony analysis, support the hypothesis that the defect in se-DSB repair seen in *mus81Δ* is rescued by deletion of *rtf1Δ*.

Since deletion of *rtf1Δ* improved the viability of *smc6-74* like *mus81Δ* cell cycle progression was analysed. In the se-DSB system *smc6-74* had two peaks of septation (peaks 3 and 3.1) after the cell cycle where the se-DSB is formed, indicative of delayed entry into the mitosis while attempts were made to repair the break. If in the *rtf1Δ* background *smc6-74* mutants were able to repair the DNA break, then peak 3.1 would not be expected to occur as cells would no longer delay entry into mitosis and the cell length at septation would be comparable to those seen in peak one and two throughout the entire time course.

The overall septation plot seen in *rtf1Δ smc6-74* double mutants was more regular than that seen in *rtf1+* strains, with two clear peaks at 300 and 480 minutes and most strikingly peak 3.1 disappeared. A fourth peak was seen at 650 minutes (similar to WT). In addition, elongated cells were no longer observed as frequently (average size of cells at time 0 was 12.14 μm, standard deviation of 1.45 and cells were considered 'long' if they were longer than 13.7 μm), with the SI of elongated cells between 0 and 10% (with the exception of 660 minutes where the percentage was 11%) compared to

20-35% SI of 'normal' cells at the peaks. These data support the rescue of *smc6-74* strains by the deletion of *rtf1*, as the delay and the cell elongation were no longer seen (figure 7-6 A).

The cell cycle profile of *smc6-X rtf1Δ* double mutants was much more irregular, there are fewer long cells but the septation peaks were less well defined. At time 0 *smc6-X rtf1Δ* has an average size of 13.11 µm and a standard variance of 1.56 and cells over 14.6 µm were considered 'long'. This is a very elongated base level in comparison to other strains examined in this analysis. In contrast to the se-DSB system where septation peak 3 was split into two peaks, 3 and 3.1, there was an elongated irregular third peak from 400 to 550 minutes. This broad peak is indicative of a repair defect (cf *mus81Δ* in the se-DSB system section 7.1.2) There was also a peak at around 620 minutes, which may be a fourth peak, but because of the irregular nature of the cell cycle it is difficult to interpret. This broad peak 3 is consistent with the microcolony analysis, which showed that *rtf1Δ* does not rescue the repair defect in *smc6-X*. However, the cell length phenotype was reduced suggesting that, as in response to IR damage but in contrast to se-DSB repair, the repair defect in *smc6-X* results in a checkpoint maintenance defect.

7.4.2 *smc6-X* has a 'cut' phenotype in response to cf-DSB induction

In order to characterise the repair defect in *smc6-X* in more detail cells were stained with DAPI and imaged at x100 using the Deltavision CoreDV. Calcofluor was not used to detect septation as the bright line at the middle of the cells made it difficult to detect issegregated or irregular segments of DNA. After IR many DSBs are generated leading to multiple chromosome segregation problems in *smc6* mutants (section 6.8). Aberrant mitoses are easily detected as chromosomes fail to segregate and remain in the centre of the cell bisected by the septum, or are inherited by a single daughter, chromosome bridges are seen as strings of DAPI stained DNA connecting two anaphase nuclei and issegregated chromosome fragments remain in the centre of the cell. However in this cf-DSB system there is only one break per cell in 50% of cells making it difficult to detect chromosome segregation problems.
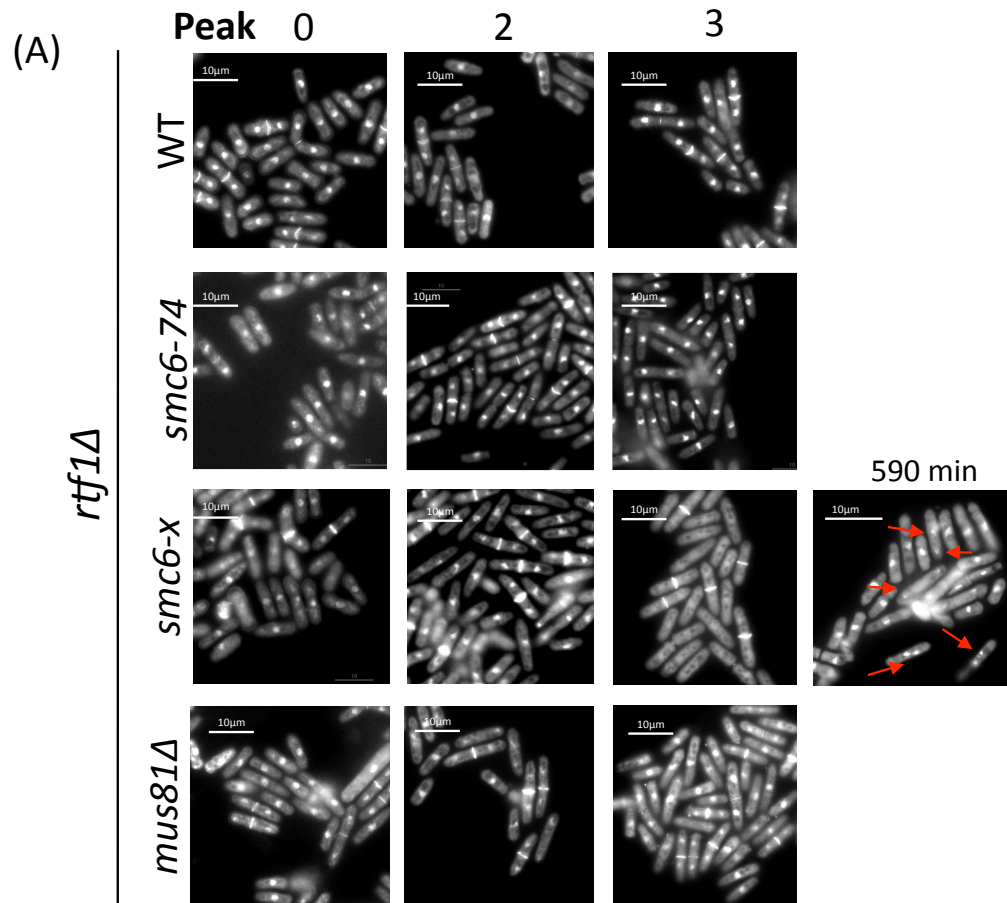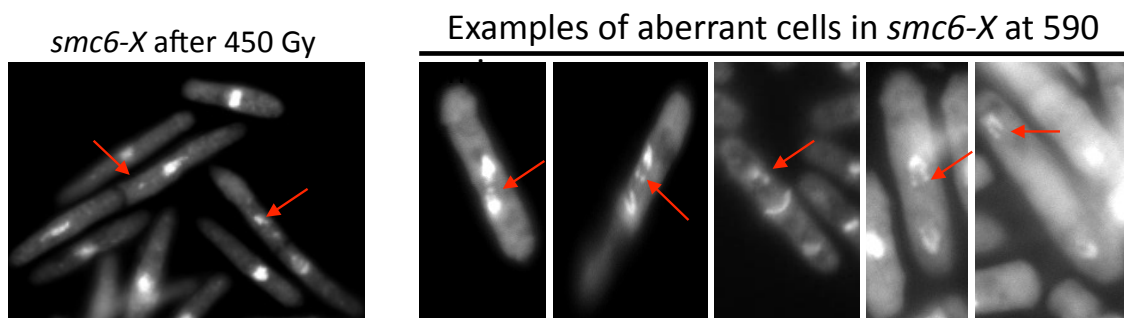
Figure 7-6- Cell morphology during *rtf1Δ* time course
Cells were harvested from synchronised time courses and visualised by staining nuclear DNA with DAPI and the septum with calcofluor. (A) Cell morphology of WT, *smc6-74*, *smc6-X* and *mus81Δ rtf1Δ* double mutants at septation peaks. (B) Close up of cut cells observed at 590 minutes after induction. A γ-irradiated *smc6-X* mutant that cuts is shown for comparison.

In a few cases, misegregations were seen with the addition of Calcofluor however these were where large sections of DNA appeared to be issegregated from the nuclei not just a single strand of DNA (figure 7-6 B).

In the analysis of cells from the whole of peak 3 'cut' cells were observed at the time corresponding to the peak of septation in *smc6-X rtf1Δ*. No aberrant mitotic cells were scored at time point 0 cells were analysed but at the peak of septation at 590 minutes 5 out of 23 (19%) mitotic cells were shown to be aberrant. This number is low, but since only 50% of cells would make the break, and, based on microcolony data, 16% of those breaks would be lethal events, these numbers are within the expected range. The presence of cut cells suggests that in response to a cf-DSB *smc6-X* cells cannot maintain the checkpoint response and cells enter mitosis before repair is complete.

7.5 Characterisation of the checkpoint response in se-DSB induction

For accurate cell-cycle progression there are checkpoints that must be passed to signal that the DNA is intact before mitosis and division. The checkpoint response after DNA damage in G2 is mediated by Chk1 and inhibition of replication triggers a checkpoint response mediated by Cds1 (as reviewed in (Rhind and Russell, 2000). To test the hypothesis that checkpoint activation and maintenance is leading to elongation in the *smc6-X*, *smc6-74* and *mus81Δ* mutants on se-DSB induction *chk1Δ* and *cds1Δ* were crossed into the se-DSB repair system and measurements of cell length we carried out after 24 hours induction (as in section 5.4)

In WT strains there was no significant change (P=0.95 and 0.81) in cell size upon the deletion of *cds1* or *chk1* genes (*cds1Δ* and *chk1Δ* respectively), as expected since the WT strain was proficient in se-DSB repair. In contrast, both *smc6-74* and *smc6-X* has a significant reduction in cell length in *chk1Δ* (P=0.03 and P=0.07) with the average cell length dropping from 16.7 to 11.9 µm and 15 to 13.8 µm respectively. Deletion of *cds1* did not make a significant difference in average cell length in either *smc6-74* or *smc6-X* when the se-DSB was induced. Thus, the cell elongation phenotype was dependent on activation of the DNA damage checkpoint and not the S phase replication inhibition checkpoint (figure 7-6).
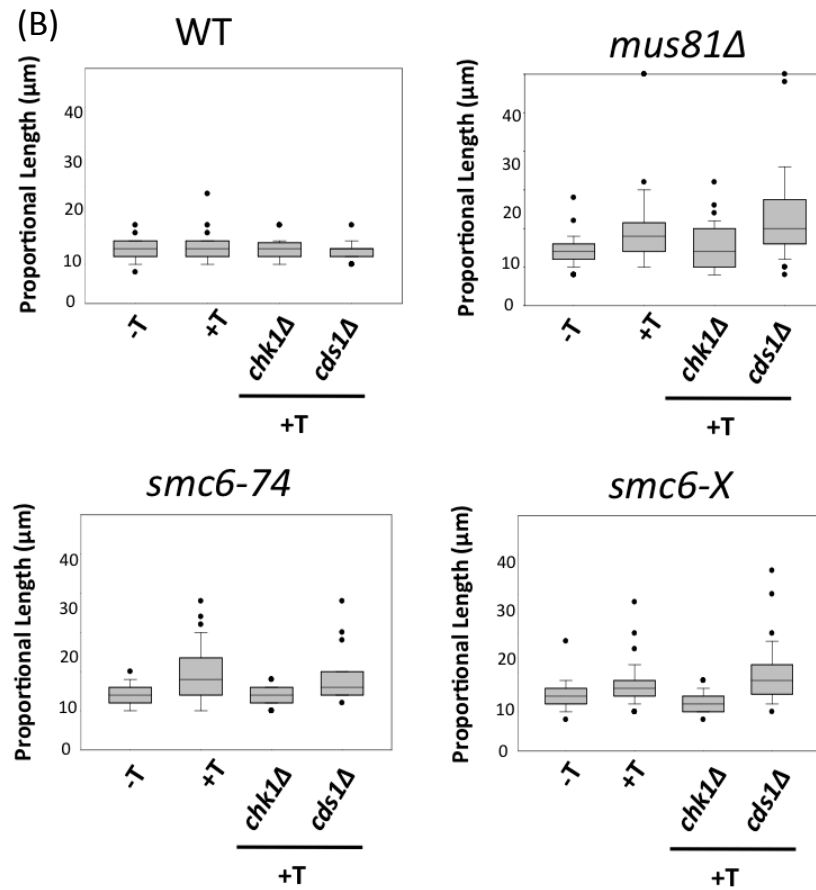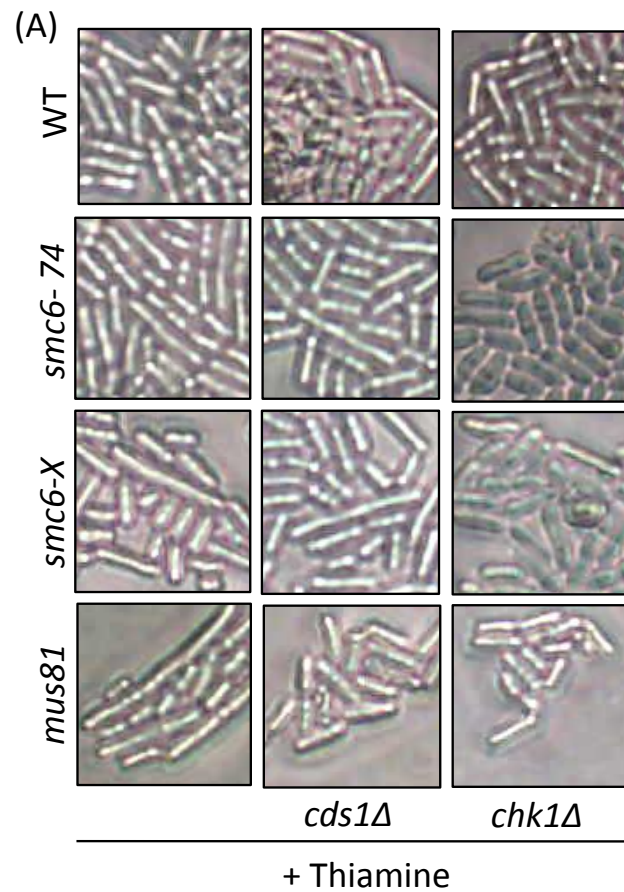
Figure 7-7- Microcolony images and cell length of strains *cds1Δ* and *chk1Δ* double mutants

WT, *smc6-74*, *smc6-X* and *mus81Δ, cds1Δ* and *chk1Δ* double mutants were grown on 24 hours on supplemented YNBA media. (A) Images of microcolonies were taken using a USB microscopy camera and the cell length was calculated. (B) The cell length of samples was plotted on a box plot to show average length (centre of the box) standard deviation (capped lines) and outliers (dots).

Cell cycle delay and the elongated cell phenotype in *mus81Δ* was also dependent on *chk1* as the average cell length reduced from 18.5 to 13.25 μm in *chk1Δ* strains. No significant changes in cell length were seen in either *cds1Δ* in *mus81Δ.*

Since it was possible that the reduction in cell length seen after in the *chk1Δ* was an artefact of reduced or limited imprinting in cells unable to initiate checkpoint response the presence of the imprint was confirmed by Southern blot analysis (section 2.7) Imprinting had previously been shown as detectable from 30 minutes after induction in an asynchronous culture and fully induced after approximately 3 hours in +T. In *chk1Δ* deletion strains, although imprinting initially appeared to be slightly reduced as a reduced intensity of the 6.6 kb band was seen in the 2 hour time point, levels stabilised at *chk+* levels after 3 hours figure 7-8). It is unlikely that this reduction would have an effect in the cell length analysis as cells are induced for approximately 24 hours.

7.6 Summary

Analysis of cell cycle progression in synchronised cultures showed that se-DSB or cf-DSB induction in WT cells does not lead to a delay to mitosis. In *mus81Δ* se-DSB induction (but not cf-DSB induction) led to Chk1-dependent cell elongation and the majority of those elongated cells did not enter mitosis. In contrast, in response to se-DSB induction the *smc6* mutants elongated, dependent on Chk1, and mitosis was delayed giving rise to a peak (3.1) of delayed septation 120 min after peak 3. This suggests that Smc5/6 has a slightly different role in se-DSB repair to Mus81 and this is reflected in the less severe phenotype.

In response to cf-DSB induction neither *smc6* mutant elongated and therefore no peak 3.1 was seen. While viability in *smc6-74* was restored, it was not in *smc6-X* and this correlated with aberrant mitotic cells, indicative of a checkpoint maintenance defect, where cells get to the point in repair where there is no ssDNA to signal to the DNA damage checkpoint and so cells enter mitosis before repair is complete. This is consistent with the published checkpoint maintenance defect for both mutants in response to replication inhibition and DNA damaging agents such as IR and UV. It
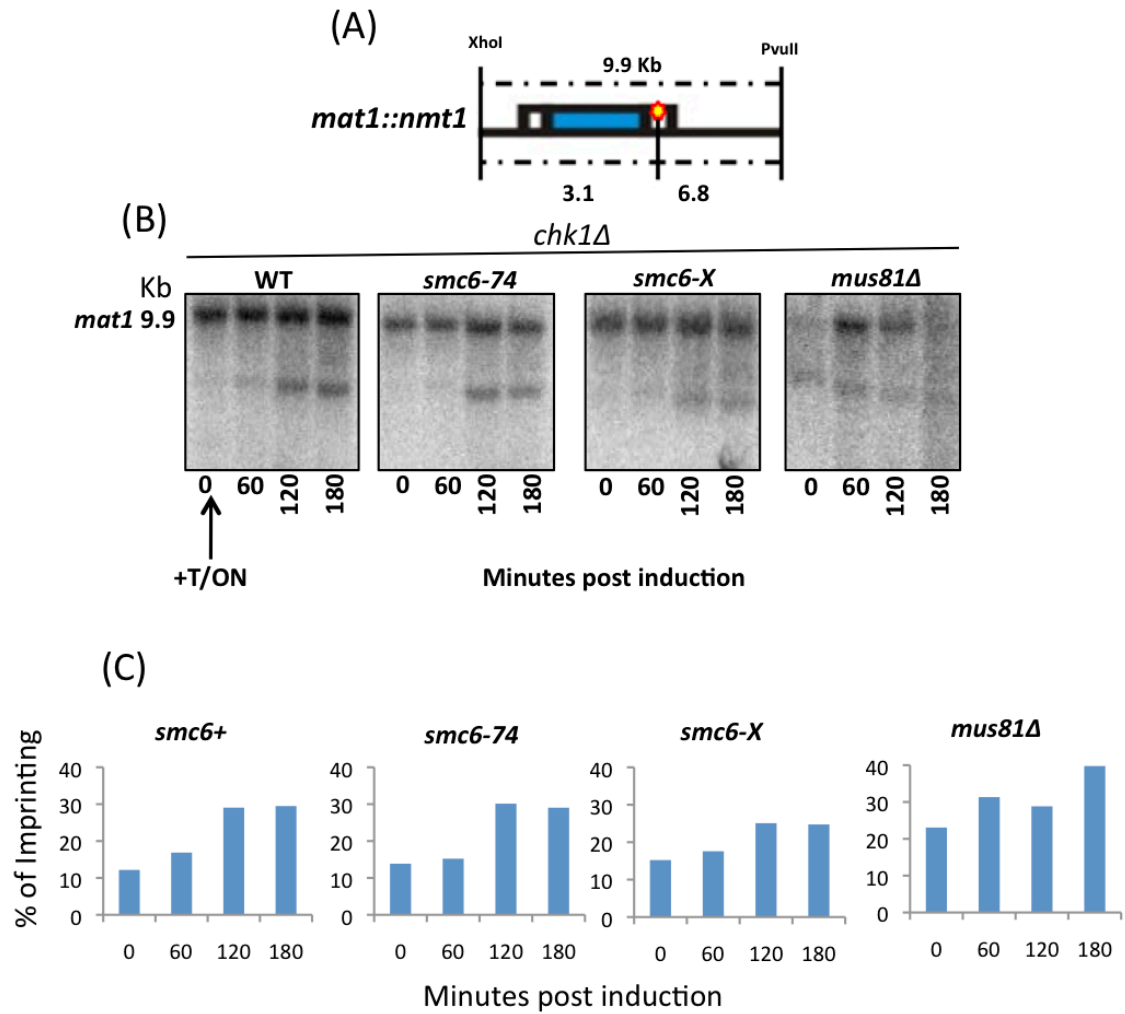
Figure 7-8- Southern analysis to detect imprinting levels in *chk1Δ* mutants
(A) Schematic showing fragment sizes for southern analysis. (B) Strains were grown in EMM minimal media without thiamine to a density of 6x10^6 cells/ ml. Cells were induced by adding thiamine to a final concentration of 3μM. Cells were harvested at 60 minute time intervals and genomic DNA was extracted and digested with *Pvu*II and *Xho*I. Digested DNA was run on a 1% gel and probed with a P specific *mat1* probe. (C) Southen blots were quantified using ImageJ.

highlights the unique response to a se-DSB where both *smc6* mutants delayed the cell cycle for 120min.

The Smc5/6 complex has been shown to regulate HJ resolution and cohesin removal after DNA damage or replication inhibition (Branzei and Foiani, 2007, Pebernard et al., 2006, Tapia-Alveal et al., 2010). Further work is needed to determine which defect is responsible for the loss of viability after se-DSB induction. The Smc5/6 complex may facilitate Mus81 activity in HJ resolution in se-DSB repair. It is possible that during the delay inefficient or late acting pathways effect Mus81 recruitment independently of Smc5/6. Alternatively, during the 120min delay the barrier at RTS1 is overcome and a converging fork used to repair the break. This would be consistent with the observation that *rtf1Δ* rescues viability in *smc6-74* and also that during cf-DSB repair *smc6*-X has a checkpoint maintenance defect and so further mitotic delay would be prevented.

Chapter 8 – Visualising the single-ended double-strand break using live cell imaging

8.1 Introduction

Roseaulin et. al. 2008 showed that the Rad52 epistasis group was essential for repair in mating-type switching and in se-DSB repair and viability assays in this study using *rhp51Δ* and *rhp57Δ* mutants was consistent with this. In this chapter the timing of HR repair was investigated by following Rad52-GFP focus formation by live cell imaging in the inducible se-DSB repair system. In this system the DSB occurs in one of the two daughter cells in the second cell cycle after induction (figure 8.1). Since in *S. pombe* S phase is coincident with septation the two daughter cells are still attached and this provides a side-by-side comparison of the two cells, one imprinting, one with the DSB. A single Rad52-GFP focus in one cell would be indicative of DSB formation, how long it remains and the timing of mitosis in the two cells would be a measure of the efficiency of repair.

The cell cycle delay and double peak of septation seen in *smc6* mutants suggested that the cells repairing the se-DSB elongate and delay mitosis. If this hypothesis is correct it would be expected that a Rad52-GFP focus would appear in one daughter cell and this cell would delay mitosis and elongate while the sister cell would be seen to divide (figure 8-1).

8.2 The Rad22::GFP tag reduced viability in smc6 strains on induction of the se-DSB

A strain containing *rad22-GFP* encoding Rad52-GFP was crossed into the se-DSB system strains and spot tests carried out to ensure that this did not change the se-DSB response. WT showed a similar result to that seen in the untagged strains. *Smc6-X* and *smc6-74* showed a slight reduction in viability compared to the untagged strain. This reduction in viability was taken into account during analysis (figure 8-2).
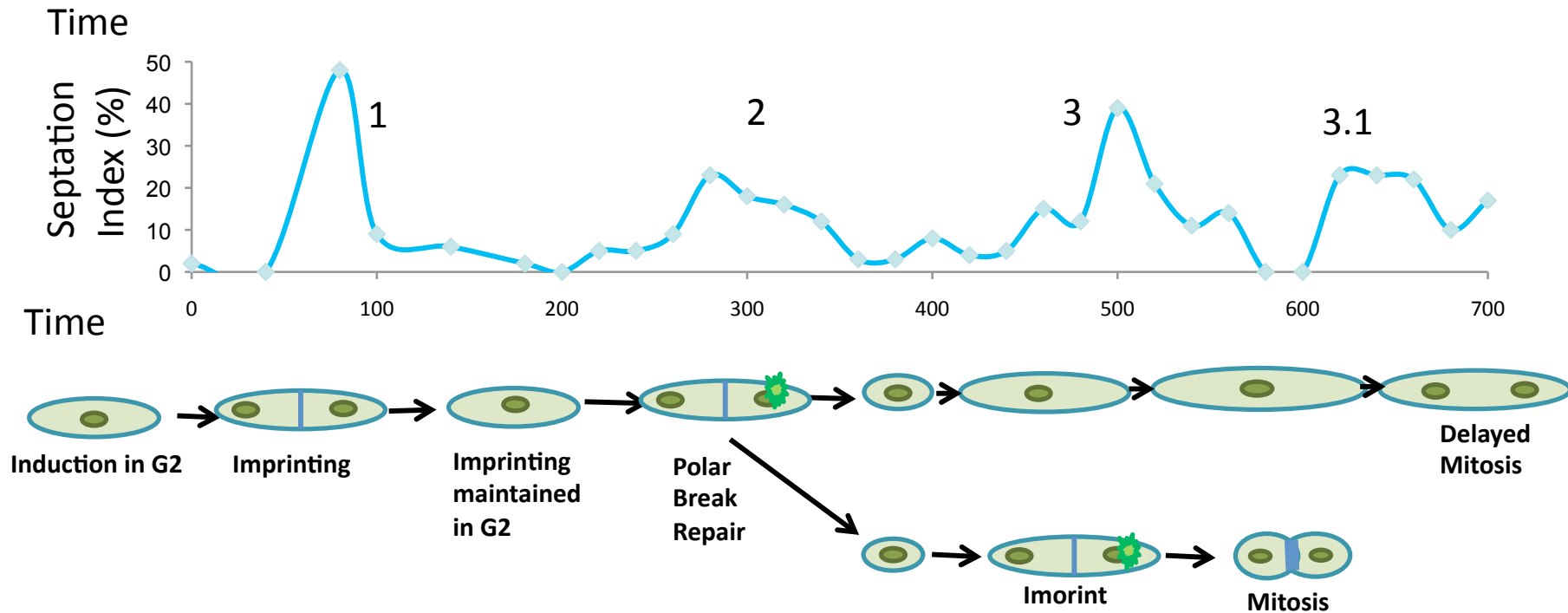
Figure 8-1 Cell cycle progression and expected se-DSB repair

Figure showing cell cycle progression of smc6-74 (as described in section 7.). At peak 3.1 cells are seen to elongate and divide late. This is hypothesised to be the direct result of the repair of the se-DSB. Below is a schematic outlining the hypothesised appearance of se-DSB leading to cell cycle delay.
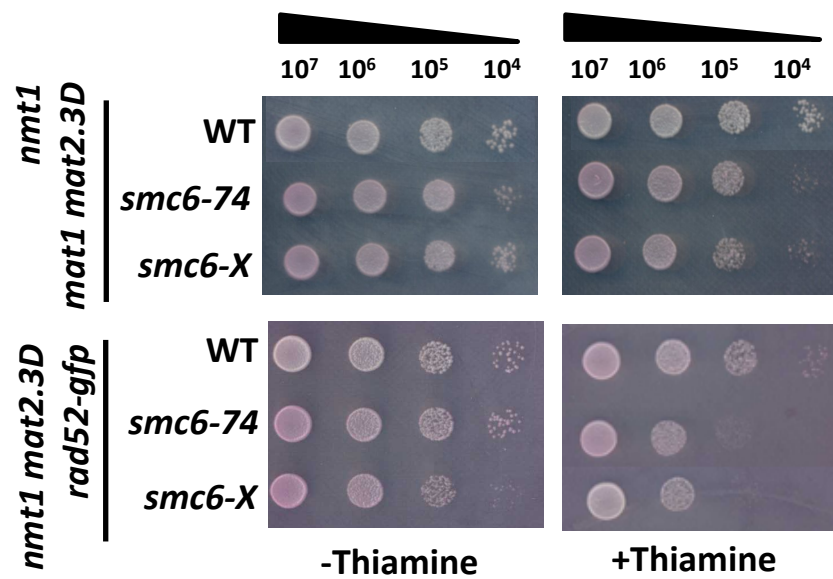
Figure 8-2 Spot test analysis of WT, *smc6-74* and *smc6-X* with and without tagged Rad52::GFP

10 fold serial dilutions of 1x107 were spotted onto supplemented YNBA media containing 5 µg/ml of phloxin B and +/- thiamine.

8.3 Rad52 focus formation were seen shortly after cells entered mitosis when the se-DSB and persisted for variable lengths of time in WT *smc6-74* and *smc6-X*

In order to investigate the kinetics of Rad52 focus formation cells were induced by the addition of thiamine and synchronized by lactose gradients as before (section 2.3.1). Cells were then mounted in 4 well chambers (Labtech) supplied with minimal media and imaged from 300min for 5-6 hrs at 30C on an Applied Precision pDV microscope. From the septation data (chapter 7) and the timing of the se-DSB (Roseaulin et al. 2008) the se-DSB should form at the same time as septation peak 2, just after mitosis. The accumulation of foci and the percentage of cells past mitosis was plotted.

In WT the majority of cells have passed through mitosis 340 minutes after induction. Cells with a single Rad52 focus in one of the two daughter nuclei consistent with se-DSB repair began to appear from 320 minutes (figure 8-3). Approximately 31% of the cells had a Rad52 focus consistent with se-DSB repair. A further 11% were seen to have foci that were not consistent with se-DSB repair (that is occurring in one sister only) (figure 8-3 A and table 1). Thus, Rad52 focus formation can be used to identify cells undergoing se-DSB repair.

The number of *smc6-74* cells with Rad52 foci was similar to WT, consistent with a similar levelof se-DSB induction. The majority of cells entered mitosis by 340 minutes and cells with foci steadily appeared after cells passed through mitosis. 33% of cells were shown to have a se-DSB specific focus and 16% were seen to have non-se-DSB specific foci.

Smc6-X cells had more non-se-DSB specific foci (20%) consistent with its sicker phenotype. The majority of cells passed through mitosis by 340 minutes and 29% of cells were seen to have a se-DSB specific foci suggesting that the se-DSB similarly to WT.

The length of time that each se-DSB focus was visible was plotted on a box plot (figure 8-3 (B)). In WT the duration of foci ranged from 5 minutes to over 300 minutes
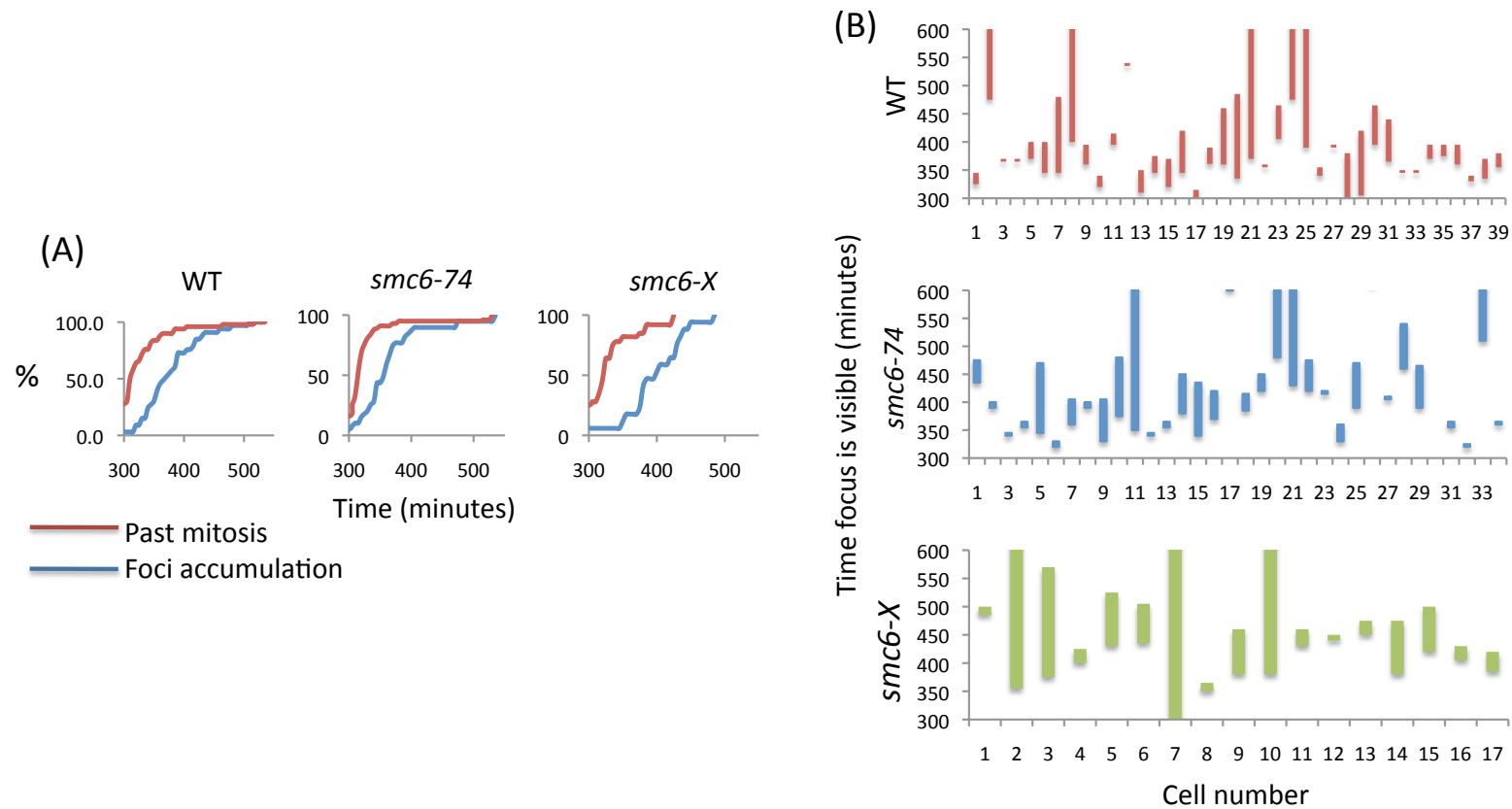
Figure 8-3- Foci appearance and mitotic progression
(A) WT, *smc6-74* and *smc6-X* were followed through a 300 minute time course beginning 300 minutes after induction. Cells were imaged using the Delta Vision microscope taking images every 5 minutes. The number of cells past mitosis was determined and Rad52::GFP foci were visualised using the FITC channel. The appearance of foci was quantified as a percentage of total foci observed. (B) During the time course, the appearance and disappearance of foci was calculated and plotted graphically. The bottom of the bar indicates the time the focus appeared, the top of the bar indicates the time it disappeared.

	Total Cells	No Foci	Total Foci	
			Non-se-DSB	se-DSB Foci
WT	108	62	12	34
%		57.4	11.1	31.5
smc6-74	118	59	20	39
%		50.0	16.9	33.1
smc6-X	58	29	12	17
%		50.0	20.7	29.3

Table 8-1 Numbers of cells and foci in this analysis

Table showing the total number of cells per strain analysed and the number of cells that had no foci. Of the cells that had a focus, the type of focus was categorised as se-DSB specific or non-se-DSB specific (details in the text section 8.1).

The latter was rare but on average foci lasted for 57min, showing that even in WT repair proficient cells se-DSB repair is not trivial. *Smc6* mutants showed a similar range of duration of Rad52-GFP foci with an average time of 65 minutes in *smc6-74* and 100 minutes in *smc6-X.* These data are not consistent with the hypothesis that taking longer to repair is the cause of the defect in *smc6-74* and *smc6-X*

8.4 *smc6-74* was shown to delay entry into mitosis after the formation of a se-DSB

The fate of all daughter cells with Rad52-GFP consistent with se-DSB formation was compared to the imprinting sister cell over the time course. Cells were split into one of four categories depending on the fate of the cell. Cells that did not enter mitosis (by the end of the imaging time course) were classed as 'No Mitosis', Cells that entered mitosis and divided were called 'Mitosis', cells that delayed entry into mitosis beyond the time that their sister cell divided were said to be 'Delayed' and those in which the Rad52 focus persisted to the end of the time course were categorised as 'persistent foci' (figure 8-4 and 8-5).

In WT 44% of cells were able to process the se-DSB and passed mitosis but an equal number did not pass mitosis during the time course. The remainder of the cells had persistent foci and did not divide by the end of the time course (12%).

Smc6-X was a difficult strain to grow under microscopy conditions and no cells were seen to successfully enter mitosis. 82% of cells showing se-DSB-consistent foci were not able to divide and enter mitosis while persistent foci were detected in the remaining cells (18%).

67% of *smc6-74* cells showing the se-DSB never entering mitosis, however, in these strains an additional category was seen, cells that delayed entry into mitosis after theRad52 focus had disappeared. 15% of the se-DSB focus cells were seen to have this phenotype consistent with the checkpoint-dependent mitotic delay discussed earlier (section 7.5).
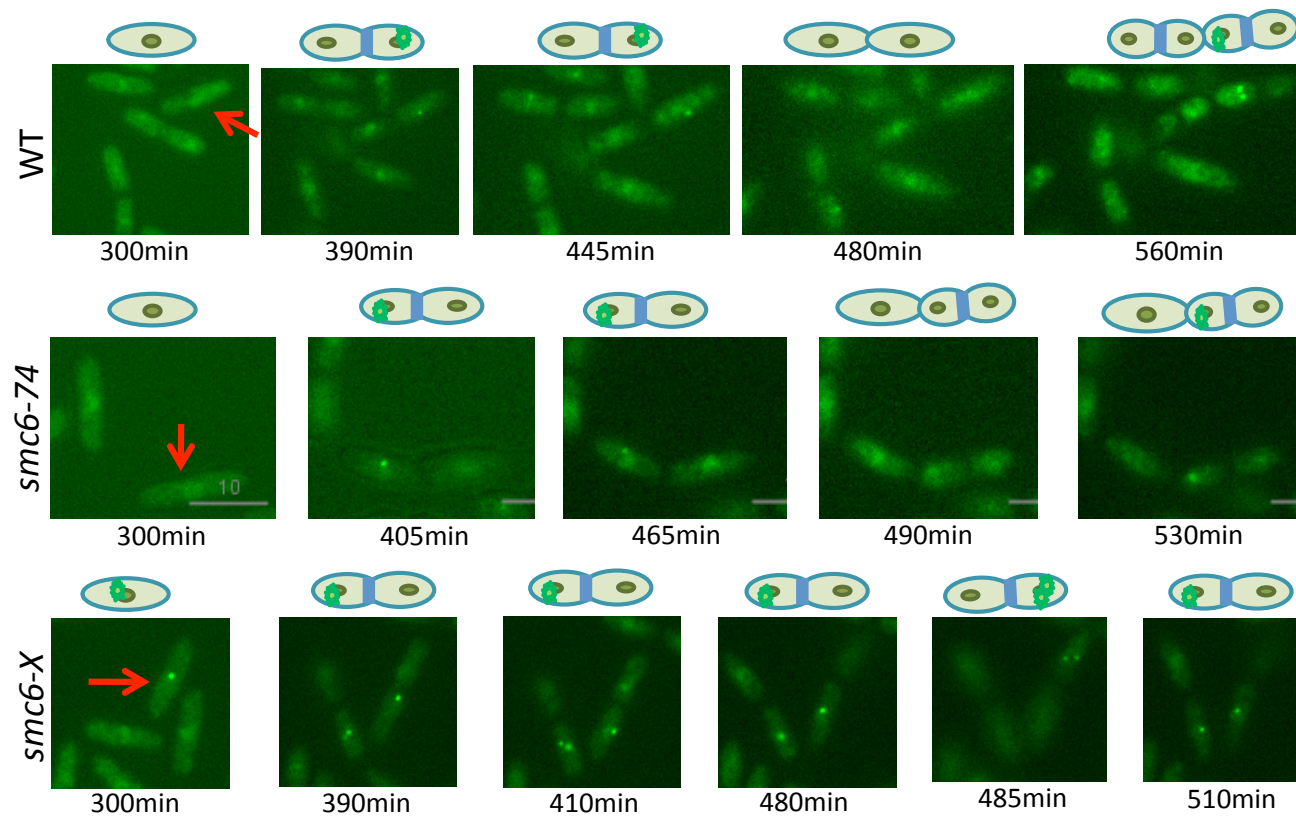
Figure 8-4 Focus formation in live cell cultures

Cells were synchronised by lactose gradient and plated in live cell imaging chambers using Con A. Cells were imaged using the Delta Vision microscope and Rad52::GFP foci were visualised using the FITC filter. Imaging time courses started at 300 min to allow time for induction, synchronisation and plating. Cell cultures were followed for a further 200-300 minutes until images bleached or lost focus. A graphical representation of focus formation in a specific cell (indicated by the red arrow) is shown above images.
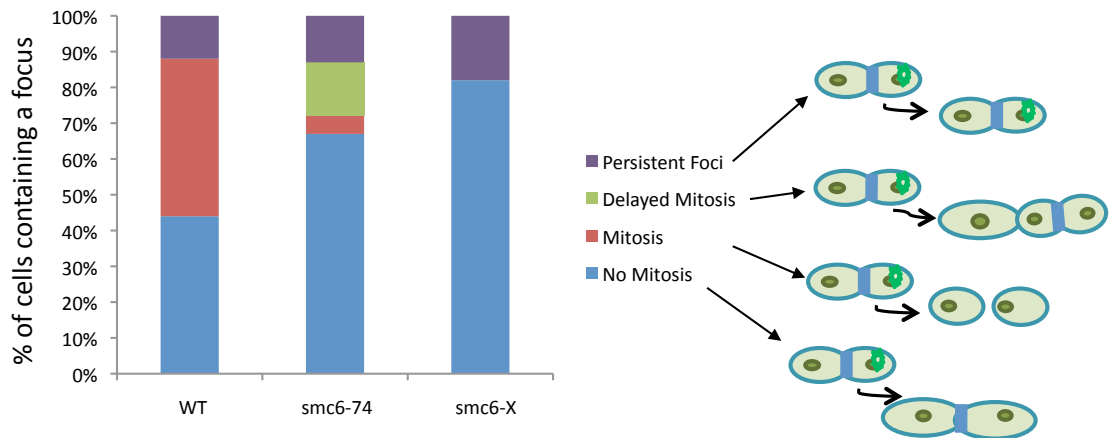
	Total Cells	No Foci	Total Foci		Fate of se-DSB Foci			
			Non-se-DSB	se-DSB Foci	No Mitosis	Mitosis	Delay	Persistent Foci
WT	108	62	12	34	15	15	0	4
%		57.4	11.1	31.5	44.0	44.0	0.0	12.0
smc6-74	118	59	20	39	26	2	6	5
%		50.0	16.9	33.1	67.0	5.0	15.0	13.0
smc6-X	58	29	12	17	14	0	0	3
%		50.0	20.7	29.3	82.0	0.0	0.0	18.0

Figure 8-5 Fate of cells containing a focus

The fate of each cell containing a focus was observed and categorised. Cells that did not did not resolve foci by the end of the time course were classed as 'persistent foci'. Cells that were delayed after focus formation were categorised as 'delayed'. Cells that successfully divided after focus formation were categorised as 'mitosis' and cells that did not divide after focus formation were categorised as 'no mitosis'.

8.6 Summary

Live cell imaging showed a single Rad52 focus in one daughter cell occurring coincident with septation, consistent with the timing of se-DSB generation in both WT and smc6 mutants. The duration of foci was very variable but on average they were maintained for about an hour even in WT cells, showing se-DSB repair to be a long process. While in WT these cells entered mitosis at the same time as the non-repairing sister cell, in *smc6-74* a proportion of cells that were seen to have se-DSB repair-consistent foci were shown to delay mitosis.

The data in this analysis was promising but technical problems and time constrains prevented a more detailed analysis. The major problem was with the microscope stage drifting out of position leading to loss of focus. This was an intermittent problem over several months and was particularly serious for long time courses. Longer time courses were needed as the majority of cells in this analysis did not divide. This may have been an artefact of the conditions used. Photobleaching was a major problem and light intensities and imaging times need further optimization to minimize this. *Smc6-X* was particularly difficult to analyse using this method and seemed to be very sensitive to the conditions during microscopy.

Chapter 9 – Discussion

9.1 The role of Smc5/6 in mating-type switching

Mating-type switching was investigated in *smc6* mutants. No loss of viability was seen in crosses to the *smt0* strain which carries the full *mat* locus but does not imprint and therefore does not form a DSB. *Smc6-X* showed no defect in mating-type switching when crossed to the switching strain h^{90}. In contrast, *smc6-74* was defective and cells lost viability. This separation of function could be a novel defect or linked to a defect in the 'early' Smc5/6 role in maintaining the topology of stalled forks, which is defective in *smc6-74* (Irmisch et. al. 2009). Both *smc6-X* and *smc6-74* are defective in Holliday junction resolution and accumulate joint molecules after DNA damage (Ampatzidou et. al. 2006). This would be expected to correlate to a type II switching defect, where switching events were initiated but not resolved correctly (Egel et al., 1984a). The re-arrangements seen in the *smc6-74* tetrad analysis correlated with a type II defect.

Interestingly, while *smc6-X* appeared not to be defective in switching in h^{90} by tetrad analysis. An initial characterisation of mating-type conformations in the original *smc6-X h-* strains showed that the *smc6-X h-* strain had the h^{-L} conformation where the L region is maintained episomally. The slow growth defect in *smc6-X h^{-L}* is likely the result of episomal instability and loss of the L-region, which contains essential genes. Further analysis showed that *smc6-X* was not stable in the h^{-S} conformation and rapidly rearranged to the h^{-L}. In h^{-S} switching occurs silently between *mat1-M* and *mat2:3-M*. Homologous recombination mutants are lethal in this background as HR is required to repair the DSB. The stabilisation of *smc6-X* as h^{-L} is indicative of a defect in the switching process in h^{-S}, likely resolution giving rise to a circular product. A similar defect in switching in h^{90} would not have been detected as the assay measures cell death. Thus both mutants may exhibit different aspects of a defect in the resolution of recombination.

The analysis of the switching defect in *smc6-74* was complicated by the importance of the parent genotype. *Smc6-74* is only defective in mating-type switching if the parent

strain to be crossed to the h^{90} is h- and there is loss of the K-region between the two donor cassettes. The strong link between the genotype of the parent and the manifestation of the defect suggest that the crossing of the h^{90} locus into *smc6-74* is an important part of the switching defect. Strains are held as diploid for approximately 62 hours and switching occurs during that time. Thus, if the *smc6-74* mutation is dominant switching defects can occur before cells go through meiosis, as well as after germination.

There are two aspects of the *mat* locus conformation that impact on switching ability in *smc6-74*; the direction of the first switch after mating or meiosis, and the distribution of heterochromatin or switching factors over the donor region. The nature of the deletion at the K-region is important as the more of the K and donor region lost, the more severe the switching defect. A possible hypothesis to explain this is that in the h^{90}/h- diploid an excess of heterochromatin (eg Swi6) or switching factors (Swi2 and Swi5) accumulates on the h^{90} *mat* locus. The incorrect distribution of factors and the defect in Smc5/6 function in *smc6-74* leads to defects in mating-type switching.

If the heterochromatic distribution was the only important factor in switching rearrangements the mating-type of the parent strain would not be important as an $h+$ or h- parent lacking in heterochromatin would be equally as likely to generate rearrangements. However, only parents with an h- phenotype were seen to rearrange. After meiosis the first switch in the new *smc6-74* h^{90} spore would be from a $h+$ to h- (Since h^{-S} is fixed as h- the h^{90} spore must sporulated as the opposite mating-type i.e. $h+$) and it is the switch from $h+$ to h- that requires the specific arrangement of Swi2/5 to the *mat3* cassette. If switching factors along the heterochromatin were incorrectly distributed it could lead to incorrect switching in *smc6-74* mutants. If in *smc6-74* the invading strand is unable to properly locate the donors an irregular repair event could occur. For example an initial strand invasion into the wrong donor, or crossovers between the sister chromatids that are not able to resolve properly leading to rearrangements consistent with the observed type II switching defect (figure 9-1). Further work is needed to elucidate the defect in *smc6-74,* as outlined in section 9.8.
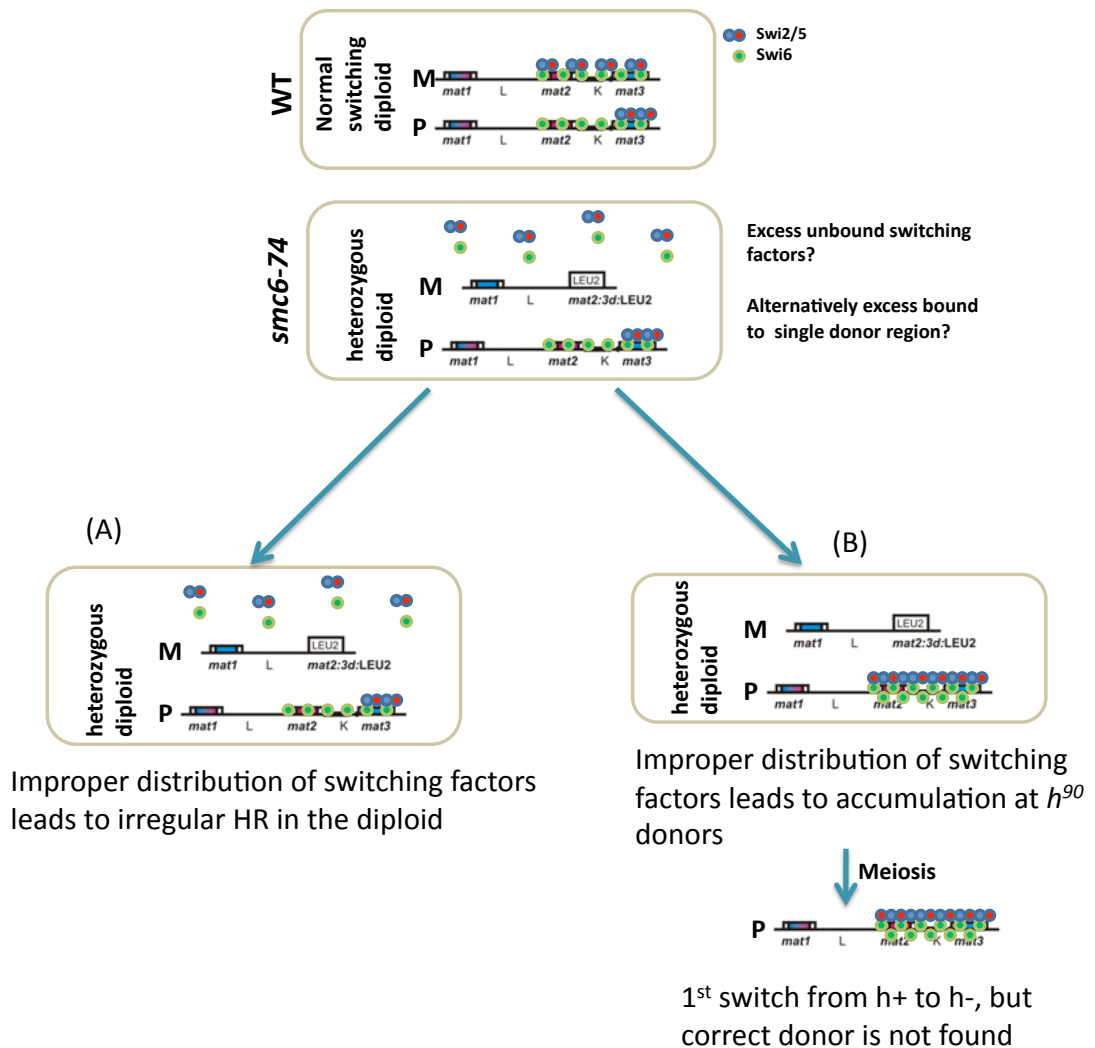
Figure 9-1 A role for the heterochromatic donor region in the *smc6-74* switching defect

In a diploid resulting from an h^{90} cross with a strain that does not have the K-region switching factors, that usually distribute over the donor region and influence the direction of the switch, will only localise to one donor region. In WT switching proficient cells this does not lead to switching defects but in *smc6-74* it does, suggesting that the Smc5/6 complex may be required for the correct distribution of switching factors or for correct invasion events when switching factors are mislocalised. *smc6-74* is defective in the Smc5/6 roles in fork topology during stalling and in resolution of joint molecules. Aberrant strand invasion into an incorrect donor due to incorrect distribution of switching factors could lead to rearrangements during the diploid stage (A) or in the first division (B).

9.2 Smc5/6 has a role in repair of se-DSBs

Both *smc6* mutants were unable to repair a se-DSB in the *mat2.3D*[no donors] strain. In the tetrad analysis there was a significant reduction in viability in *smc6-X* and *smc6-74* but, in contrast to HR and *mus81* mutants, the deletion of the donors was not lethal in these strains. This suggests that *smc6-74* and *smc6-X* are less defective in se-DSB repair. This may be due to the fact that these are hypomorphic mutants or the Smc5/6 complex may play a supporting role in this type of repair. A recent study showed that recruitment of Mus81 in meiosis required Smc5/6 and a defect in Mus81 recruitment could support the milder phenotype seen here (Wehrkamp et. al., 2012). Alternatively replication fork topology at the se-DSB may rely on Smc5/6 function and in the *smc6* mutants a modified DNA structure affects access by Mus81 and/or other repair proteins.

HR and Mus81 are absolutely required to repair se-DSBs (Roseaulin et al, 2008). HR is required for strand invasion into the sister chromatid behind the broken fork and Mus81 to nick the resulting D loop resetting the fork. The role of Smc5/6 could be to hold the RF at the se-DSB in such a way that strand invasion can be initiated and thus indirectly recruit Mus81 to reset the fork. If this is correct then it would be expected that defective Smc5/6 mutants would accumulate broken fork structures. If however the defect in the *smc6* mutants was after strand invasion un-resolvable replication intermediates similar to those seen on 2-D gels of *mus81Δ* mutants in this system (Roseaulin et. al., 2008). This second scenario would be consistent with the accumulation of recombination intermediates seen in the *smc6* mutants when replication forks collapse in a *cds1* null background in HU (Ampatzidou et. al., 2006). It is supported by the live cell imaging results (chapter 8) which showed Rad52 foci to appear with WT kinetics in the *smc6* mutants, showing that the defect is after the recruitment of Rad52 (figure 9-2 (A)).

Figure 9-2 The role of Smc5/6 in (A) se-DSB and (B) cf-DSB repair

(A) In se-DSB repair Smc5/6 may have two roles. (a) SMC5/6 may be involved in stabilising the topology of the replication fork so that other factors can access the DNA and initiate a repair event. (b) Direct recruitment of Mus81 the the break site for the correct cleavage of the nicked HJ intermediate. (c) *smc6* mutants are repair deficient but checkpoint proficient in this system and delay cell cycle progression for approximately 2 hours. (B) In cf-DSB repair Mus81 is not required for fork repair but Rqh1 is required. (d) Smc5/6 is required to resolve recombination intermediate.

(A)

Imprint Site

L Region

RTS1 Block

Deleted donor region

se-DSB

Smc5/6 (a)

In smc6 mutants repair is defective leading to prolonger checkpoint activation (c)

Mus81 cleavage

Smc5/6 (b)

Imprint

(B)

Imprint site

L Region

No replication block in *rtf1* null cells

Deleted donor region

se-DSB

Approaching converging fork

Converging fork can bypass se-DSB on the leading strand

Converging fork meets the se-DSB

Rqh1 dependent dissolution

Smc5/6 'late role' (d)

Repaired DSB

9.3 Development of a microcolony analysis to facilitate a rapid assessment of viability on se-DSB induction

Use of the inducible se-DSB system facilitated the analysis of large cultures, which could be grown and induced simultaneously. A microcolony analysis was set up to rapidly screen for defects in se-DSB repair. Repair of the se-DSB could be observed at early stages of colony formation eliminating the problem of analysis being limited to viable cells. As induced and uninduced cultures were monitored side by side, growth defects in sick strains could be compensated by increasing the incubation times such that the colony size in the off cultures was similar to that in WT.

Analysis of HR mutants *rhp51Δ* and *rhp57Δ* showed that both mutants had a viability defect and the proportion of dead cells or slow growing colonies increased on se-DSB induction. Interestingly, tetrad analysis of *rhp57Δ* by Roseaulin et al 2008 and in this study (data not shown) did not detect a defect in processing of se-DSB repair. This suggests that the microcolony analysis is a more sensitive assay. The higher numbers of cells analysed at an early stage of colony development may mean that it is easier to see a defect than after germination of spores. Rhp57 would be expected to display a defect in se-DSB repair as it is required for the homology search during recombination to repair the break, but the availability of other recombination mediators (Swi5/Sfr1) may mean that this defect is not severe enough to be detectable in the tetrads analysis.

Consistent with the published data *mus81Δ* but not *rqh1Δ* showed a defect in se-DSB repair in the microcolony analysis. Microcolony analysis in the inducible se-DSB system confirmed the repair defect in *sm6-74* and *smc6-X*. The pattern of cell death was then checked by pedigree analysis to confirm that this was consistent with se-DSB induction.

9.4 *smc6* mutants elongate dependent on the DNA damage checkpoint and Chk1

The morphology of the cells repairing the se-DSB was investigated after induction and a cell elongation phenotype was seen in repair defective mutants, rhp51, rhp57, mus811 and *smc6-X* and *smc6-74*. To further explore the cell cycle progression and the

checkpoint response in *smc6-X* and *smc6-74* cells were synchronised by lactose gradients and followed over three cell cycles after induction. Imprinting occurs in the first S phase (coincident with septation peak 1), se-DSB in 50% of daughter cells in the next S phase (coincident with septation peak 2) and the timing of the third peak is a measure of repair. In WT cells there was no delay in cell cycle progression after se-DSB induction and cell length was consistent throughout the entire time course. *Mus81Δ* populations did not show a defined 3rd peak corresponding to cell cycle delay due to a repair defect.

Cell cycle progression in the 3rd cycle was seen to be delayed in both *smc6-X* and *smc6-74*. Both strains displayed a reduction in the percentage of cells septating in the third peak and an additional peak was observed approximately 120 minutes after (called peak 3.1). This extra peak was composed of elongated cells, consistent with a checkpoint activation that leads to a mitotic delay. It is possible that some mutants are able to repair the break during the delay which would explain why during tetrad and pedigree analyses not all cells die. It is consistent with Smc5/6 having a role in se-DSB repair. The non-lethal phenotype may be due to the hypomorphic nature of *smc6-X* and *smc6-74* or to a non-essential role..

To check the nature of the checkpoint response, *smc6* mutants were crossed to S phase and G2-phase specific checkpoint mutants *cds1Δ* and *chk1Δ*. The checkpoint response was found to be dependent on *chk1* despite being the result of an se-DSB that occurs in S phase. These data are consistent with the se-DSB not initiating a Cds1 checkpoint response and repair occurring in G2.

The long checkpoint delay (approximately 120 minutes) and synchronous entry into mitosis seen in the *smc6* mutants is intriguing on two accounts. Firstly, it suggests that *smc6* mutants are checkpoint proficient in this system, in contrast to other forms of damage where they exhibit checkpoint maintenance defects (Verkade et. al., 1999; Ampatzidou et. al., 2006). Thus the se-DSB system uncovered a unique circumstance where *smc6* mutants are able to maintain a checkpoint. Secondly, HR and mus81

repair defective cells maintain this checkpoint delay indefinitely and do not show the defined delayed peak of septation (3.1).

9.5 Analysis of repair kinetics by live cell imaging of Rad52-GFP foci

In order to study repair kinetics Rad52-GFP, which should localise to the se-DSB during repair, was followed by live cell imaging in synchronised cultures. In WT cells single Rad52-GFP focus was seen in one of the two daughter cells consistent with the pattern of a break dependent on imprinting. Some of these foci were surprisingly long lived, averaging 1hr in duration, suggesting that although the se-DSB is generated in S phase repair continues into G2.

Similar foci were seen in both *smc6* mutants. These appeared with similar kinetics to WT but remained for longer in *smc6-X* and possibly also in *smc6-74* (due to the numbers observed this was not statistically significant). In *smc6-X* non-se-DSB specific foci were often seen, consistent with the generation of spontaneous DNA damage in these cells, and this hindered the analysis.

In WT imprinting and se-DSB daughter cells divided synchronously. In *smc6-74* the daughter cell without the Rad52 focus was seen to divide but cells that had previously shown the Rad52 focus delayed mitosis. This supports the hypothesis that the cell elongation seen in *smc6-74* and *smc6-X* was dependent on the formation of the se-DSB.

The Smc5/6 complex has been shown to regulate HJ resolution and cohesin removal after DNA damage or replication inhibition (Ampatzidou et. al., 2006, Pebernard, et. al, 2006; (Outwin et al., 2009). Further work is needed to determine which defect is responsible for the checkpoint delay and loss of viability in *smc6* mutants after se-DSB induction. The Smc5/6 complex was recently shown to facilitate Mus81 activity in HJ resolution in meiosis (Wehrkamp-Richter et al., 2012) and may have a similar role in se-DSB repair. It is possible that during the checkpoint delay seen in the *smc6* mutants inefficient or late acting pathways effect Mus81 recruitment independently of Smc5/6. Alternatively, during the delay the barrier at RTS1 that prevents an incoming fork

progressing through *mat1* from the opposite direction is overcome changing the repair event.

9.6 Creation of a system to study cf-DSB repair

To test the effect of an incoming fork on repair the se-DSB repair system was modified to remove the effector protein, Rtf1 which binds the RTS1 termination sequence adjacent to *mat1*. This created an inducible system where the se-DSB at *mat1* could be repaired by a converging fork creating a cf-DSB. Since mammalian cell fire new origins in response to problems in S phase (Blow et al, 2011) this system reflects a common situation in higher eukaryotes.

WT were able to efficiently repair the cf-DSB. In contrast HR-defective mutants mutants, *rhp51Δ* and *rhp57Δ,* were defective in both se-DSB and cf-DSB repair. To investigate potential different responses to se- and cf-DSBs *mus81Δ* and *rqh1Δ* mutants were investigated. Mus81 and Rqh1 have both been shown (with their interaction partners Eme1 and Top3 respectively) to resolve HR intermediates' however, it is thought that they function in different pathways. Mus81-Eme1 have been shown to resolve nicked HJs and modified replication fork structures in such a way as to result in crossover events (Osman and Whitby, 2007). Conversely RecQ helicases like Rqh1 in combination with Top3 have been show to dissolve HJs without crossover a desirable result in the mitotic cycle (Wu and Hickson, 2006). *Mus81Δ*, defective in se-DSB repair (Roseaulin et al, 2008; and this study, chapter 5) but not sensitive to IR (chapter 6), which creates two-ended DSBs, was not defective in cf-DSB repair as *rft1Δ* restored viability. This suggests that the convergence of an incoming fork provides an alternative DNA structure that can be resolved by another pathway. Rqh1, in contrast, is not required for viability after se-DSB induction (Rosealin et al, 2008; and this study chapter 5) but is required after cf-DSB induction, suggesting that Rqh1-Top3 is the preferred pathway of resolution in cf-DSBs. The abrupt change in phenotype after the deletion of *rtf1Δ* is an indication that the nature of the DSB has changed. These data suggest that Mus81 and Rqh1 function in the resolution of different HR repair events.

9.7 *smc6-X* and *smc6-74* show a separation of function in repair of a cf-DSB

In *smc6-74*, like *mus81Δ,* viability and cell elongation defect was rescued by deletion of *rtf1Δ*, and no cut cells were observed, suggesting that this mutant is not defective in cf-DSB repair. This would be consistent with the Smc5/6 complex being required to regulate Mus81 at se-DSBs, similarly to meiotic DSBs (Wehrkamp-Richter et al., 2012).

However, *smc6-X* was shown to be defective in cf-DSB repair, a phenotype that is consistent with a general defect in HR repair. If the Smc5/6 complex was only required to regulate Mus81 this phenotype would not be expected as *mus81Δ* is rescued by a *rtf1Δ* background. Thus, Smc5/6 is required for both se-DSB and cf-DSB repair. Given the published roles for the Smc5/6 complex in HR resolution (Ampatzidou et al., 2006, Boddy et al., 2001) this may be to regulate both Rqh1 and Mus81. On induction of the cf-DSB *smc6-X* was shown to delay entry into mitosis like WT but did not elongate in the same manner as in the se-DSB system and aberrant mitotic cells were observed. This phenotype is consistent with the checkpoint maintenance defect seen in both *smc6* mutants after IR (chapter 6), UV or HU (Ampatzidou et al., 2006, Miyabe et al., 2006, Verkade et al., 1999). It has been proposed that the *smc6* mutants fail to complete HR repair but there is no single strand DNA to continue to signal to the DNA damage checkpoint. Further analysis is required to determine the nature of the defect at both se- and cf-DSBs and the separation of function between the two mutants (Figure 9-2 (B)).

9.8 Hypothesis for the role of *smc6-74* and *smc6-X* in se-DSB and cf-DSB repair

Both *smc6-X* and *smc6-74* are defective in se-DSB repair. It was also observed that in both mutants processing of the se-DSB is sufficient to activate the checkpoint response and delay mitosis for up to two hours. The checkpoint activation is dependent on the DNA damage response checkpoint mediator Chk1 and deletion of this checkpoint prevents cell elongation. At present it is unclear why both mutants are able to maintain checkpoint activation, it is possible that a se-DSB naturally has more flexibility (because of its association with the replication fork) and enough RPA coated ssDNA is produced to generate a checkpoint response. Both mutants continue to elongate and

may eventually divide, however the reduced viability, consistent with the appearance of the se-DSB, suggests that repair is not completed sufficiently.

Although both mutants have the same phenotype it is possible that they function at different stages in the repair pathway. It has previously been established that *smc6-X* is unable to hold replication forks in a stable conformation during repair (Irmisch et al., 2009). It is possible that failure to resolve these repair structures is what leads to cell death.

smc6-74 has a different defect, where RPA and Rad52 are not properly localised to stalled replication forks. This type of recruitment may play a role in se-DSB repair and Smc5/6 may also be required for recruitment of Mus81. Without proper resolution by Mus81 cells die (Roseaulin et al., 2008) and although the defect is different to *smc6-X* the phenotypic outcome would be the same. At present there is no direct evidence of an interaction between Mus81 and *smc6-74.* However the complete rescue of both *smc6-74* and *mus81Δ* in *rtf1Δ* strains does support an interaction between the two. It also seems unlikely that *smc6-74* is defective in downstream resolution of HR intermediates as the mutant is fully proficient at resolving cf-DSBs.

Smc6-X does show a defect in HR resolution and checkpoint maintenance defect in the cf-DSB repair system. It could be that the rigid structure of *smc6-X* means that a checkpoint is activated it is not sufficient to maintain a checkpoint response, leading to the cut phenotype (summarised in figure 9-3).

9.9 Further work

For switching analysis it is essential to determine whether the switching defect is dependent on strains passing through a diploid stage. This could be done by utilising an inducible h^{90} switching system containing the donors (Holmes et. al., 2005). After crossing to the uninduced strain, stabilised in both mating-types, a plating assay would determine whether rearrangements are still seen on induction and whether the direction of switching was important for viability.

se-DSB repair
Smc5/6 may be required to recruit repair proteins like HR machinery and Mus81. Checkpoint is activated and maintained.

smc6-74
Unable to recruit Mus81

smc6-X
Unable maintain fork conformation for repair

mat1

Mus81 cleavage

mat1

Cell cycle delay during repair is dependent on Chk1

Repair fails and cells die after hyper-elongating
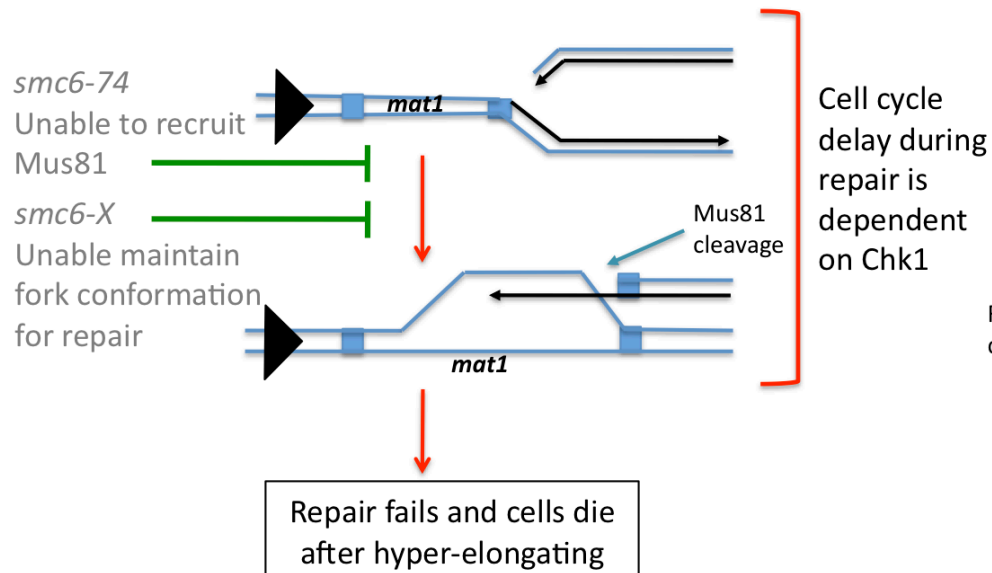
cf-DSB repair
Smc5/6 is required to maintain checkpoint activation and resolution of dHJs.

Converging fork meets the se-DSB

HR machinery required

Rqh1 dependent dissolution.

smc6-X
Is defective in repair and maintaining checkpoint

smc6-74
Is proficient at repair

Repair fails and cells cut leading to cell death
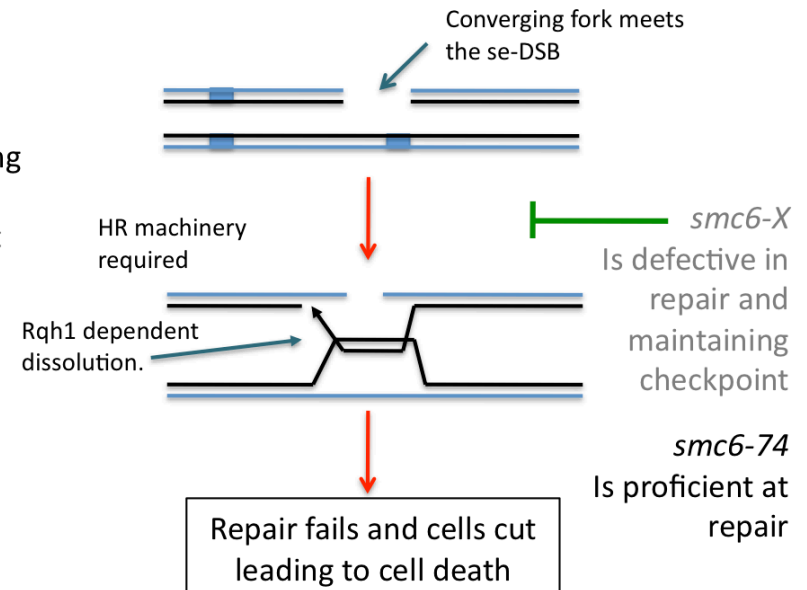
Figure 9-3 Hypothesis of *smc6* mutants role in se-DSB and cf-DSB repair
In se-DSB repair *smc6* mutants do not have a checkpoint maintenance defect. Cells are able to delay mitosis successfully but are not able to complete repair in either mutant. It is thought that *smc6-74* is unable to efficiently recruit repair proteins, including Mus81, preventing complete repair either through direct or topological effects. In cf-DSB repair *smc6-74* does not show a repair defect. However, *smc6-X* displays the checkpoint maintenance defect and an inability to repair the HR structures.

Depending on the outcome further analysis could be conducted to determine the importance of heterochromatin e.g. Swi6, and the recombination mediators, Swi2 or Swi5 by genetic analysis of double mutants and chromatin immunoprecipitation (ChIP) to determine the distribution of Swi factors at the *mat* locus.

For the se-DSB repair analysis 2-D gel analysis could be used to detect the accumulation of recombination intermediates. In Roseaulin et. al., (2008) *mus81Δ* was shown not to resolve the intermediates formed as a result of the se-DSB and X molecules were seen on 2-D gels. If the defect seen in *smc6-X* and *smc6-74* is due to a defect in Mus81 regulation then a similar phenotype would be seen in *smc6* mutants, as has been observed at collapsed replication forks (Ampatzidou et. al., 2006). It is also possible that if the two *smc6* mutants have slightly different defects that they may show different outcomes by 2-D gel analysis. For example if the defect is in the early role in stabilising stalled forks prior to HR (Irmisch et. al., 2009) it would be expected that recombination intermediates would not accumulate.

Characterisation of timing and duration of the se-DSB and cf-DSB by Southern analysis on synchronised cultures would be informative. Imprinting can be observed by extracting DNA using the standard method as the imprinting site is fragile and easily broken. By making DNA in plugs the imprint site is protected and only breaks if the se-DSB has been made, at which point two fragments should be formed, one corresponding to the whole *mat1* locus and one corresponding form the restriction site to the site of se-DSB. This method was used in Roseaulin et. al., (2008) to detect the se-DSB. It would be interesting to determine whether the se-DSB persisted for longer in the *smc6* mutants and also to determine the timing of conversion of the se-DSB to a cf-DSB by an incoming fork.

ChIP could be used to investigate the localisation of proteins to the *mat1* site during repair. Analysis of the localisation of Rad52 and Mus81 to the break site in the smc6 mutants would be informative, as would an investigation of the loading of the Smc5/6 complex in WT and *smc6* mutant strains.

Finally, live cell imaging of Rad52 focus formation proved to be a powerful technique to study se-DSB repair. Optimisation of the Z-sectioning and imaging in lower light conditions to ensure viability over a 12hr time course are needed to fully exploit this technique, which could then be used to investigate the timing and dependencies of recruitment of other proteins.

9.10 Overall conclusions

Smc5/6 was shown to be required for mating-type switching as *smc6-74* was defective when a parent strain is in the *h-* conformation and lacking a heterochromatic K-region. Both *smc6-X* and *smc6-74* are defective in se-DSB repair showing the Smc5/6 complex to be required for se-DSB repair. However that role is probably in a more regulatory role rather than directly involved. The *smc6* mutants were proficient in the checkpoint response and delayed the cell cycle for up to 120 minutes. This is different to the checkpoint maintenance defect typically seen in *smc6* mutants. A novel system was set up to investigate a converging fork at an se-DSB and a new separation of function phenotype was also identified; *smc6-74* was shown to be rescued by the conversion of a se-DSB to a cf-DSB and *smc6-X* was not. The reason for this is as yet unknown but the defect in cf-DSB repair in *smc6-X* led to a typical checkpoint maintenance defect where cell enter mitosis with WT kinetic but with incomplete repair leading to mitotic catastrophe (Verkade et al., 1999, Ampatzidou et al., 2006). Finally this novel cf-DSB analysis was used to determine the difference in requirements for HR resolution by Mus81 and Rqh1. These mutants were previously thought to compete for the repair of broken replication forks but this analysis showed that Mus81 is involved in resetting se-DSBs and Rqh1 is required for the repair of cf-DSBs.

References

AHMAD, F. & STEWART, E. 2005. The N-terminal region of the Schizosaccharomyces pombe RecQ helicase, Rqh1p, physically interacts with Topoisomerase III and is required for Rqh1p function. *Molecular genetics and genomics : MGG,* 273, 102-14.

AHMET KOÇ, L. J. W., CHRISTOPHER K. MATHEWS AND GARY F. MERRILL 2003. Hydroxyurea Arrests DNA Replication by a Mechanism That Preserves Basal dNTP Pools. *Journal of Biological Chemistry,* 10, 223-230.

AKAMATSU, Y., DZIADKOWIEC, D., IKEGUCHI, M., SHINAGAWA, H. & IWASAKI, H. 2003. Two different Swi5-containing protein complexes are involved in mating-type switching and recombination repair in fission yeast. *Proceedings of the National Academy of Sciences of the United States of America,* 100, 15770-5.

ALCASABAS, A. A., OSBORN, A. J., BACHANT, J., HU, F., WERLER, P. J., BOUSSET, K., FURUYA, K., DIFFLEY, J. F., CARR, A. M. & ELLEDGE, S. J. 2001. Mrc1 transduces signals of DNA replication stress to activate Rad53. *Nature cell biology,* 3, 958-65.

AMPATZIDOU, E., IRMISCH, A., O'CONNELL, M. J. & MURRAY, J. M. 2006. Smc5/6 Is Required for Repair at Collapsed Replication Forks. *Mol. Cell. Biol.,* 26, 9387-9401.

ANDREWS, E. A., PALECEK, J., SERGEANT, J., TAYLOR, E., LEHMANN, A. R. & WATTS, F. Z. 2005. Nse2, a component of the Smc5-6 complex, is a SUMO ligase required for the response to DNA damage. *Molecular and Cellular Biology,* 25, 185-96.

APARICIO, O. M., WEINSTEIN, D. M. & BELL, S. P. 1997. Components and dynamics of DNA replication complexes in S. cerevisiae: redistribution of MCM proteins and Cdc45p during S phase. *Cell,* 91, 59-69.

ARCANGIOLI, B. 1998. A site- and strand-specific DNA break confers asymmetric switching potential in fission yeast. *EMBO J.,* 17, 4503-4510.

ARCANGIOLI, B. & DE LAHONDÈS, R. 2000. Fission yeast switches mating type by a replication–recombination coupled process. *The EMBO Journal,* 19, 1389-1396.

AVES, S. J. 2009. DNA replication initiation. *Methods in molecular biology,* 521, 3-17.

BAKKENIST, C. J. & KASTAN, M. B. 2003. DNA damage activates ATM through intermolecular autophosphorylation and dimer dissociation. *Nature,* 421, 499-506.

BEACH, D., NURSE, P. & EGEL, R. 1982. Molecular rearrangement of mating-type genes in fission yeast. *Nature,* 296, 682-3.

BEACH, D. H. 1983. Cell type switching by DNA transposition in fission yeast. *Nature,* 305, 682-687.

BEACH, D. H. & KLAR, A. J. 1984. Rearrangements of the transposable mating-type cassettes of fission yeast. *The EMBO Journal,* 3, 603-10.

BELL, S. P. & DUTTA, A. 2002. DNA replication in eukaryotic cells. *Annual review of biochemistry,* 71, 333-74.

BJERGBAEK, L., COBB, J. A., TSAI-PFLUGFELDER, M. & GASSER, S. M. 2005. Mechanistically distinct roles for Sgs1p in checkpoint activation and replication fork maintenance. *The EMBO Journal,* 24, 405-17.

BLOW, J. J., GE, X. Q. & JACKSON, D. A. 2011. How dormant origins promote complete genome replication. *Trends in biochemical sciences,* 36, 405-14.

BODDY, M. N., FURNARI, B., MONDESERT, O. & RUSSELL, P. 1998. Replication checkpoint enforced by kinases Cds1 and Chk1. *Science,* 280, 909-12.

BODDY, M. N., GAILLARD, P. H., MCDONALD, W. H., SHANAHAN, P., YATES, J. R., 3RD & RUSSELL, P. 2001. Mus81-Eme1 are essential components of a Holliday junction resolvase. *Cell,* 107, 537-48.

BODDY, M. N., LOPEZ-GIRONA, A., SHANAHAN, P., INTERTHAL, H., HEYER, W. D. & RUSSELL, P. 2000. Damage tolerance protein Mus81 associates with the FHA1 domain of checkpoint kinase Cds1. *Molecular and Cellular Biology,* 20, 8758-66.

BRANZEI, D. & FOIANI, M. 2007. Interplay of replication checkpoints and repair proteins at stalled replication forks. *DNA Repair,* 6, 994-1003.

BRESCH, C., MÜLLER, G. & EGEL, R. 1968. Genes involved in meiosis and sporulation of a yeast. *Mol Gen Genet,* 102, 301–306.

BUONOMO, S. B., CLYNE, R. K., FUCHS, J., LOIDL, J., UHLMANN, F. & NASMYTH, K. 2000. Disjunction of homologous chromosomes in meiosis I depends on proteolytic cleavage of the meiotic cohesin Rec8 by separin. *Cell,* 103, 387-98.

BURKHART, R., SCHULTE, D., HU, D., MUSAHL, C., GOHRING, F. & KNIPPERS, R. 1995. Interactions of human nuclear proteins P1Mcm3 and P1Cdc46. *European journal of biochemistry / FEBS,* 228, 431-8.

BYUN, T. S., PACEK, M., YEE, M. C., WALTER, J. C. & CIMPRICH, K. A. 2005. Functional uncoupling of MCM helicase and DNA polymerase activities activates the ATR-dependent checkpoint. *Genes & development,* 19, 1040-52.

CALONGE, T. M. & O'CONNELL, M. J. 2008. Turning off the G2 DNA damage checkpoint. *DNA Repair,* 7, 136-40.

CARR, A. M., SCHMIDT, H., KIRCHHOFF, S., MURIEL, W. J., SHELDRICK, K. S., GRIFFITHS, D. J., BASMACIOGLU, C. N., SUBRAMANI, S., CLEGG, M. & NASIM, A. 1994. The rad16 gene of Schizosaccharomyces pombe: a homolog of the RAD1 gene of Saccharomyces cerevisiae. *Mol Cell Biol,* 14, 2029-2040.

CASPARI, T., MURRAY, J. M. & CARR, A. M. 2002. Cdc2-cyclin B kinase activity links Crb2 and Rqh1-topoisomerase III. *Genes & development,* 16, 1195-208.

CHAN, C. S. & TYE, B. K. 1980. Autonomously replicating sequences in Saccharomyces cerevisiae. *Proceedings of the National Academy of Sciences of the United States of America,* 77, 6329-33.

CHANG, J. H., KIM, J. J., CHOI, J. M., LEE, J. H. & CHO, Y. 2008. Crystal structure of the Mus81-Eme1 complex. *Genes & development,* 22, 1093-106.

CIMPRICH, K. A. & CORTEZ, D. 2008. ATR: an essential regulator of genome integrity. *Nature reviews. Molecular cell biology,* 9, 616-27.

COBB, J. A., BJERGBAEK, L., SHIMADA, K., FREI, C. & GASSER, S. M. 2003. DNA polymerase stabilization at stalled replication forks requires Mec1 and the RecQ helicase Sgs1. *The EMBO Journal,* 22, 4325-36.

COBB, J. A., SCHLEKER, T., ROJAS, V., BJERGBAEK, L., TERCERO, J. A. & GASSER, S. M. 2005. Replisome instability, fork collapse, and gross chromosomal rearrangements arise synergistically from Mec1 kinase and RecQ helicase mutations. *Genes & development,* 19, 3055-69.

COTTA-RAMUSINO, C., FACHINETTI, D., LUCCA, C., DOKSANI, Y., LOPES, M., SOGO, J. & FOIANI, M. 2005. Exo1 processes stalled replication forks and counteracts fork reversal in checkpoint-defective cells. *Molecular cell,* 17, 153-9.

COURCELLE, J., DONALDSON, J. R., CHOW, K. H. & COURCELLE, C. T. 2003. DNA damage-induced replication fork regression and processing in Escherichia coli. *Science,* 299, 1064-7.

COX, M. M. 2002. The nonmutagenic repair of broken replication forks via recombination. *Mutation research,* 510, 107-20.

DALGAARD, J. Z. & KLAR, A. J. 2001a. A DNA replication-arrest site RTS1 regulates imprinting by determining the direction of replication at mat1 in S. pombe. *Genes & development,* 15, 2060-8.

DALGAARD, J. Z. & KLAR, A. J. S. 1999. Orientation of DNA replication establishes mating-type switching pattern in S. pombe. *Nature,* 400, 181-184.

DALGAARD, J. Z. & KLAR, A. J. S. 2000. swi1 and swi3 Perform Imprinting, Pausing, and Termination of DNA Replication in S. pombe. *Cell,* 102, 745-751.

DALGAARD, J. Z. & KLAR, A. J. S. 2001b. Does S. pombe exploit the intrinsic asymmetry of DNA synthesis to imprint daughter cells for mating-type switching? *Trends in Genetics,* 17, 153-157.

DAS, M., WILEY, D. J., MEDINA, S., VINCENT, H. A., LARREA, M., ORIOLO, A. & VERDE, F. 2007. Regulation of cell diameter, For3p localization, and cell symmetry by fission yeast Rho-GAP Rga4p. *Molecular biology of the cell,* 18, 2090-101.

DE JAGER, M., VAN NOORT, J., VAN GENT, D. C., DEKKER, C., KANAAR, R. & WYMAN, C. 2001. Human Rad50/Mre11 is a flexible complex that can tether DNA ends. *Molecular cell,* 8, 1129-35.

DEN ELZEN, N. R. & O'CONNELL, M. J. 2004. Recovery from DNA damage checkpoint arrest by PP1-mediated inhibition of Chk1. *The EMBO Journal,* 23, 908-18.

DESANY, B. A., ALCASABAS, A. A., BACHANT, J. B. & ELLEDGE, S. J. 1998. Recovery from DNA replicational stress is the essential function of the S-phase checkpoint pathway. *Genes & development,* 12, 2956-70.

DOE, C. L., AHN, J. S., DIXON, J. & WHITBY, M. C. 2002. Mus81-Eme1 and Rqh1 involvement in processing stalled and collapsed replication forks. *The Journal of biological chemistry,* 277, 32753-9.

DOE, C. L., DIXON, J., OSMAN, F. & WHITBY, M. C. 2000. Partial suppression of the fission yeast rqh1(-) phenotype by expression of a bacterial Holliday junction resolvase. *The EMBO Journal,* 19, 2751-62.

DONOVAN, S., HARWOOD, J., DRURY, L. S. & DIFFLEY, J. F. 1997. Cdc6p-dependent loading of Mcm proteins onto pre-replicative chromatin in budding yeast. *Proceedings of the National Academy of Sciences of the United States of America,* 94, 5611-6.

EDWARDS, M. C., TUTTER, A. V., CVETIC, C., GILBERT, C. H., PROKHOROVA, T. A. & WALTER, J. C. 2002. MCM2-7 complexes bind chromatin in a distributed pattern surrounding the origin recognition complex in Xenopus egg extracts. *The Journal of biological chemistry,* 277, 33049-57.

EDWARDS, R. J., BENTLEY, N. J. & CARR, A. M. 1999. A Rad3-Rad26 complex responds to DNA damage independently of other checkpoint proteins. *Nature cell biology,* 1, 393-8.

EGEL, R. 1971. Physiological aspects of conjugation in fission yeast. *Planta,* 98, 89–96.

EGEL, R. 1977. Frequency of mating-type switching in homothallic fission yeast. *Nature,* 266, 172-174.

EGEL, R. 1980. Mating-type switching and mitotic crossing-over at the mating-type locus in fission yeast. *Cold Spring Harbor Symp. Quant. Biol.,* 45, 1003-1007.

EGEL, R., BEACH, D. H. & KLAR, A. J. 1984a. Genes required for initiation and resolution steps of mating-type switching in fission yeast. *Proceedings of the National Academy of Sciences of the United States of America,* 81, 3481-5.

EGEL, R., BEACH, D. H. & KLAR, A. J. 1984b. Genes required for initiation and resolution steps of mating-type switching in fission yeast. *Proc Natl Acad Sci USA,* 81, 3481-3485.

EGEL, R. & EIE, B. 1987. Cell lineage asymmetry in Schizosaccharomyces pombe: unilateral transmission of a high-frequency state for mating-type switching in diploid pedigrees *Current Genetics,* 12, 429–433.

EGEL, R. & GUTZ, H. 1981. Gene activation by copy transposition in mating-type switching of a homothallic fission yeast. *Current Genetics,* 3, 5-12.

EYDMANN, T., SOMMARIVA, E., INAGAWA, T., MIAN, S., KLAR, A. J. & DALGAARD, J. Z. 2008. Rtf1-mediated eukaryotic site-specific replication termination. *Genetics,* 180, 27-39.

FABRE, F., CHAN, A., HEYER, W. D. & GANGLOFF, S. 2002. Alternate pathways involving Sgs1/Top3, Mus81/ Mms4, and Srs2 prevent formation of toxic recombination intermediates from single-stranded gaps created by DNA replication. *Proceedings of the National Academy of Sciences of the United States of America,* 99, 16887-92.

FENG, W. & D'URSO, G. 2001. Schizosaccharomyces pombe cells lacking the amino-terminal catalytic domains of DNA polymerase epsilon are viable but require the DNA damage checkpoint control. *Molecular and Cellular Biology,* 21, 4495-504.

FENNELL-FEZZIE, R., GRADIA, S. D., AKEY, D. & BERGER, J. M. 2005. The MukF subunit of Escherichia coli condensin: architecture and functional relationship to kleisins. *The EMBO Journal,* 24, 1921-30.

FLECK, O., MICHAEL, H. & HEIM, L. 1992. The swi4+ gene of Schizosaccharomyces pombe encodes a homologue of mismatch repair enzymes. *Nucleic acids research,* 20, 2271-8.

FOIANI, M., FERRARI, M., LIBERI, G., LOPES, M., LUCCA, C., MARINI, F., PELLICIOLI, A., MUZI FALCONI, M. & PLEVANI, P. 1998. S-phase DNA damage checkpoint in budding yeast. *Biological chemistry,* 379, 1019-23.

FORSBURG, S. L. 2003. Overview of Schizosaccharomyces pombe. *Current protocols in molecular biology / edited by Frederick M. Ausubel ... [et al.],* Chapter 13, Unit 13 14.

FORSBURG, S. L. 2008. The MCM helicase: at the interface of checkpoints and the replication fork. *Bioch. Society. Trans.,* 36, 114-119.

FORSBURG, S. L. & NURSE, P. 1991. Cell cycle regulation in the yeasts Saccharomyces cerevisiae and Schizosaccharomyces pombe. *Annual review of cell biology,* 7, 227-56.

FRIEDEL, A. M., PIKE, B. L. & GASSER, S. M. 2009. ATR/Mec1: coordinating fork stability and repair. *Current opinion in cell biology,* 21, 237-44.

FROGET, B., BLAISONNEAU, J., LAMBERT, S. & BALDACCI, G. 2008. Cleavage of stalled forks by fission yeast Mus81/Eme1 in absence of DNA replication checkpoint. *Molecular biology of the cell,* 19, 445-56.

FUKUI, T., YAMAUCHI, K., MUROYA, T., AKIYAMA, M., MAKI, H., SUGINO, A. & WAGA, S. 2004. Distinct roles of DNA polymerases delta and epsilon at the replication fork in Xenopus egg extracts. *Genes to cells : devoted to molecular & cellular mechanisms,* 9, 179-91.

FURNARI, B., BLASINA, A., BODDY, M. N., MCGOWAN, C. H. & RUSSELL, P. 1999. Cdc25 inhibited in vivo and in vitro by checkpoint kinases Cds1 and Chk1. *Molecular biology of the cell,* 10, 833-45.

GABBAI, C. B. & MARIANS, K. J. 2010. Recruitment to stalled replication forks of the PriA DNA helicase and replisome-loading activities is essential for survival. *DNA Repair,* 9, 202-9.

GAILLARD, P. H., NOGUCHI, E., SHANAHAN, P. & RUSSELL, P. 2003. The endogenous Mus81-Eme1 complex resolves Holliday junctions by a nick and counternick mechanism. *Molecular cell,* 12, 747-59.

GAMBUS, A., JONES, R. C., SANCHEZ-DIAZ, A., KANEMAKI, M., VAN DEURSEN, F., EDMONDSON, R. D. & LABIB, K. 2006. GINS maintains association of Cdc45 with MCM in replisome progression complexes at eukaryotic DNA replication forks. *Nature cell biology,* 8, 358-66.

GASKELL, L. J., OSMAN, F., GILBERT, R. J. & WHITBY, M. C. 2007. Mus81 cleavage of Holliday junctions: a failsafe for processing meiotic recombination intermediates? *The EMBO Journal,* 26, 1891-901.

GOODWIN, A., WANG, S. W., TODA, T., NORBURY, C. & HICKSON, I. D. 1999. Topoisomerase III is essential for accurate nuclear division in Schizosaccharomyces pombe. *Nucleic acids research,* 27, 4050-8.

GRAUMANN, P. L. 2000. Bacillus subtilis SMC is required for proper arrangement of the chromosome and for efficient segregation of replication termini but not for bipolar movement of newly duplicated origin regions. *Journal of bacteriology,* 182, 6463-71.

GREWAL, S. I. S. & KLAR, A. J. S. 1997. A Recombinationally Repressed Region Between mat2 and mat3 Loci Shares Homology to Centromeric Repeats and

Regulates Directionality of Mating-Type Switching in Fission Yeast. *Genetics,* 146, 1221-1238.

GRUBER, S., HAERING, C. H. & NASMYTH, K. 2003. Chromosomal cohesin forms a ring. *Cell,* 112, 765-77.

GUTZ, H. & DOE, F. 1973. Two different *h-* mating types in *Schizosaccharamyces pombe*. *Genetics,* 74, 563-569.

GUTZ, H. & DOE, F. J. 1975. On homo- and heterothallism in Schizosaccharomyces pombe. *Mycologia,* 67, 748–759.

GUTZ, H. & SCHMIDT, H. 1985. Switching genes in Schizosaccharomyces pombe. *Current Genetics,* 1985, 325–331.

HABER, J. E. & HEYER, W. D. 2001. The fuss about Mus81. *Cell,* 107, 551-4.

HAGAN, I., HAYLES, J. & NURSE, P. 1988. Cloning and sequencing of the cyclin-related cdc13+ gene and a cytological study of its role in fission yeast mitosis. *Journal of cell science,* 91 (Pt 4), 587-95.

HANADA, K., BUDZOWSKA, M., DAVIES, S. L., VAN DRUNEN, E., ONIZAWA, H., BEVERLOO, H. B., MAAS, A., ESSERS, J., HICKSON, I. D. & KANAAR, R. 2007. The structure-specific endonuclease Mus81 contributes to replication restart by generating double-strand DNA breaks. *Nature structural & molecular biology,* 14, 1096-104.

HARRISON, J. C. & HABER, J. E. 2006. Surviving the breakup: the DNA damage checkpoint. *Annual review of genetics,* 40, 209-35.

HARUTA, N., AKAMATSU, Y., TSUTSUI, Y., KUROKAWA, Y., MURAYAMA, Y., ARCANGIOLI, B. & IWASAKI, H. 2008. Fission yeast Swi5 protein, a novel DNA recombination mediator. *DNA Repair,* 7, 1-9.

HAUF, S., WAIZENEGGER, I. C. & PETERS, J. M. 2001. Cohesin cleavage by separase required for anaphase and cytokinesis in human cells. *Science,* 293, 1320-3.

HEYER, W. D., LI, X., ROLFSMEIER, M. & ZHANG, X. P. 2006. Rad54: the Swiss Army knife of homologous recombination? *Nucleic acids research,* 34, 4115-25.

HICKS, J. & FINK, G. R. 1977. Identification of chromosomal location of yeast DNA from hybrid plasmid p Yeleu 10. *Nature,* 269, 265-7.

HIRANO, T. 2005. SMC proteins and chromosome mechanics: from bacteria to humans. *Philosophical transactions of the Royal Society of London. Series B, Biological sciences,* 360, 507-14.

HIRANO, T., FUNAHASHI, S., UEMURA, T. & YANAGIDA, M. 1986. Isolation and characterization of Schizosaccharomyces pombe cutmutants that block nuclear division but not cytokinesis. *The EMBO Journal,* 5, 2973-9.

HIRANO, T., KOBAYASHI, R. & HIRANO, M. 1997. Condensins, chromosome condensation protein complexes containing XCAP-C, XCAP-E and a Xenopus homolog of the Drosophila Barren protein. *Cell,* 89, 511-21.

HOLMES, A. M., KAYKOV, A. & ARCANGIOLI, B. 2005. Molecular and Cellular Dissection of Mating-Type Switching Steps in Schizosaccharomyces pombe. *Mol. Cell. Biol.,* 25, 303-311.

HOMESLEY, L., LEI, M., KAWASAKI, Y., SAWYER, S., CHRISTENSEN, T. & TYE, B. K. 2000. Mcm10 and the MCM2-7 complex interact to initiate DNA synthesis and to release replication factors from origins. *Genes & development,* 14, 913-26.

HUMPAL, S. E., ROBINSON, D. A. & KREBS, J. E. 2009. Marks to stop the clock: histone modifications and checkpoint regulation in the DNA damage response. *Biochemistry and cell biology = Biochimie et biologie cellulaire,* 87, 243-53.

HUNTER, N. & KLECKNER, N. 2001. The single-end invasion: an asymmetric intermediate at the double-strand break to double-holliday junction transition of meiotic recombination. *Cell,* 106, 59-70.

IBARRA, A., SCHWOB, E. & MENDEZ, J. 2008. Excess MCM proteins protect human cells from replicative stress by licensing backup origins of replication. *Proceedings of the National Academy of Sciences of the United States of America,* 105, 8956-61.

INTERTHAL, H. & HEYER, W. D. 2000. MUS81 encodes a novel helix-hairpin-helix protein involved in the response to UV- and methylation-induced DNA damage in Saccharomyces cerevisiae. *Molecular & general genetics : MGG,* 263, 812-27.

IRA, G., MALKOVA, A., LIBERI, G., FOIANI, M. & HABER, J. E. 2003. Srs2 and Sgs1-Top3 suppress crossovers during double-strand break repair in yeast. *Cell,* 115, 401-11.

IRMISCH, A., AMPATZIDOU, E., MIZUNO, K., O'CONNELL, M. J. & MURRAY, J. M. 2009. Smc5/6 maintains stalled replication forks in a recombination-competent conformation. *The EMBO Journal,* 28, 144-55.

JALLEPALLI, P. V., BROWN, G. W., MUZI-FALCONI, M., TIEN, D. & KELLY, T. J. 1997. Regulation of the replication initiator protein p65cdc18 by CDK phosphorylation. *Genes & development,* 11, 2767-79.

JIA, S., YAMADA, T. & GREWAL, S. I. S. 2004. Heterochromatin Regulates Cell Type-Specific Long-Range Chromatin Interactions Essential for Directed Recombination. 119, 469-480.

JOHZUKA, K. & HORIUCHI, T. 2002. Replication fork block protein, Fob1, acts as an rDNA region specific recombinator in S. cerevisiae. *Genes to cells : devoted to molecular & cellular mechanisms,* 7, 99-113.

JONSSON, Z. O. & HUBSCHER, U. 1997. Proliferating cell nuclear antigen: more than a clamp for DNA polymerases. *BioEssays : news and reviews in molecular, cellular and developmental biology,* 19, 967-75.

KAWASAKI, Y. & SUGINO, A. 2001. Yeast replicative DNA polymerases and their role at the replication fork. *Molecules and cells,* 12, 277-85.

KAYKOV, A. & ARCANGIOLI, B. 2004. A Programmed Strand-Specific and Modified Nick in S. pombe Constitutes a Novel Type of Chromosomal Imprint. *Current Biology,* 14, 1924-1928.

KAYKOV, A., HOLMES, A. M. & ARCANGIOLI, B. 2004. Formation, maintenance and consequences of the imprint at the mating-type locus in fission yeast. *The EMBO Journal,* 23, 930-8.

KELLY, M., BURKE, J., SMITH, M., KLAR, A. & BEACH, D. 1988. Four mating-type genes control sexual differentiation in the fission yeast. *EMBO J,* 7, 1537-1547.

KESTI, T., FLICK, K., KERANEN, S., SYVAOJA, J. E. & WITTENBERG, C. 1999. DNA polymerase epsilon catalytic domains are dispensable for DNA replication, DNA repair, and cell viability. *Molecular cell,* 3, 679-85.

KILKENNY, M. L., DORE, A. S., ROE, S. M., NESTORAS, K., HO, J. C., WATTS, F. Z. & PEARL, L. H. 2008. Structural and functional analysis of the Crb2-BRCT2 domain reveals distinct roles in checkpoint signaling and DNA damage repair. *Genes & development,* 22, 2034-47.

KIMURA, K., RYBENKOV, V. V., CRISONA, N. J., HIRANO, T. & COZZARELLI, N. R. 1999. 13S condensin actively reconfigures DNA by introducing global positive writhe: implications for chromosome condensation. *Cell,* 98, 239-48.

KLAR, A. J. & MIGLIO, L. M. 1986. Initiation of meiotic recombination by double-strand DNA breaks in S. pombe. *Cell,* 46, 725-31.

KLAR, A. J. S. & BONADUCE, M. J. 1991. swi6, a Gene Required for Mating-Type Switching, Prohibits Meiotic Recombination in the mat2-mat3 ``Cold Spot'' of Fission Yeast. *Genetics,* 129, 1033-1042.

KLEIN, F., MAHR, P., GALOVA, M., BUONOMO, S. B., MICHAELIS, C., NAIRZ, K. & NASMYTH, K. 1999. A central role for cohesins in sister chromatid cohesion, formation of axial elements, and recombination during yeast meiosis. *Cell,* 98, 91-103.

KOSTRIKEN, R. & HEFFRON, F. 1984. The product of the HO gene is a nuclease: purification and characterization of the enzyme. *Cold Spring Harbor symposia on quantitative biology,* 49, 89-96.

LABIB, K. & GAMBUS, A. 2007. A key role for the GINS complex at DNA replication forks. *Trends in cell biology,* 17, 271-8.

LAMBERT, S., WATSON, A., SHEEDY, D. M., MARTIN, B. & CARR, A. M. 2005. Gross chromosomal rearrangements and elevated recombination at an inducible site-specific replication fork barrier. *Cell,* 121, 689-702.

LAMMENS, A., SCHELE, A. & HOPFNER, K. P. 2004. Structural biochemistry of ATP-driven dimerization and DNA-stimulated activation of SMC ATPases. *Current biology : CB,* 14, 1778-82.

LAURSEN, L. V., AMPATZIDOU, E., ANDERSEN, A. H. & MURRAY, J. M. 2003. Role for the fission yeast RecQ helicase in DNA repair in G2. *Molecular and Cellular Biology,* 23, 3692-705.

LEE, J. K. & HURWITZ, J. 2001. Processive DNA helicase activity of the minichromosome maintenance proteins 4, 6, and 7 complex requires forked DNA structures. *Proceedings of the National Academy of Sciences of the United States of America,* 98, 54-9.

LEE, K. M., NIZZA, S., HAYES, T., BASS, K. L., IRMISCH, A., MURRAY, J. M. & O'CONNELL, M. J. 2007. Brc1-mediated rescue of Smc5/6 deficiency:

requirement for multiple nucleases and a novel Rad18 function. *Genetics,* 175, 1585-95.

LEHMANN, A. R., WALICKA, M., GRIFFITHS, D. J., MURRAY, J. M., WATTS, F. Z., MCCREADY, S. & CARR, A. M. 1995. The rad18 gene of Schizosaccharomyces pombe defines a new subgroup of the SMC superfamily involved in DNA repair. *Molecular and Cellular Biology,* 15, 7067-80.

LEI, M., KAWASAKI, Y. & TYE, B. K. 1996. Physical interactions among Mcm proteins and effects of Mcm dosage on DNA replication in Saccharomyces cerevisiae. *Molecular and Cellular Biology,* 16, 5081-90.

LEUPOLD, U. 1970. *Genetical Methods in Schizosaccharomyces pombe.*

LI, P. C., CHRETIEN, L., COTE, J., KELLY, T. J. & FORSBURG, S. L. 2011. S. pombe replication protein Cdc18 (Cdc6) interacts with Swi6 (HP1) heterochromatin protein: region specific effects and replication timing in the centromere. *Cell cycle,* 10, 323-36.

LIBERI, G., MAFFIOLETTI, G., LUCCA, C., CHIOLO, I., BARYSHNIKOVA, A., COTTA-RAMUSINO, C., LOPES, M., PELLICIOLI, A., HABER, J. E. & FOIANI, M. 2005. Rad51-dependent DNA structures accumulate at damaged replication forks in sgs1 mutants defective in the yeast ortholog of BLM RecQ helicase. *Genes & development,* 19, 339-50.

LIMBO, O., CHAHWAN, C., YAMADA, Y., DE BRUIN, R. A., WITTENBERG, C. & RUSSELL, P. 2007. Ctp1 is a cell-cycle-regulated protein that functions with Mre11 complex to control double-strand break repair by homologous recombination. *Molecular cell,* 28, 134-46.

LIN, S. J., WARDLAW, C. P., MORISHITA, T., MIYABE, I., CHAHWAN, C., CASPARI, T., SCHMIDT, U., CARR, A. M. & GARCIA, V. 2012. The Rad4(TopBP1) ATR-activation domain functions in G1/S phase in a chromatin-dependent manner. *PLoS genetics,* 8, e1002801.

LINDROOS, H. B., STROM, L., ITOH, T., KATOU, Y., SHIRAHIGE, K. & SJOGREN, C. 2006. Chromosomal association of the Smc5/6 complex reveals that it functions in differently regulated pathways. *Molecular cell,* 22, 755-67.

LINDSAY, H. D., GRIFFITHS, D. J., EDWARDS, R. J., CHRISTENSEN, P. U., MURRAY, J. M., OSMAN, F., WALWORTH, N. & CARR, A. M. 1998. S-phase-specific

activation of Cds1 kinase defines a subpathway of the checkpoint response in Schizosaccharomyces pombe. *Genes Dev.,* 12, 382-95.

LLORENTE, B., SMITH, C. E. & SYMINGTON, L. S. 2008. Break-induced replication: what is it and what is it for? *Cell cycle,* 7, 859-64.

LOBACHEV, K., VITRIOL, E., STEMPLE, J., RESNICK, M. A. & BLOOM, K. 2004. Chromosome fragmentation after induction of a double-strand break is an active process prevented by the RMX repair complex. *Current biology : CB,* 14, 2107-12.

LOPES, M., COTTA-RAMUSINO, C., PELLICIOLI, A., LIBERI, G., PLEVANI, P., MUZI-FALCONI, M., NEWLON, C. S. & FOIANI, M. 2001. The DNA replication checkpoint response stabilizes stalled replication forks. *Nature,* 412, 557-61.

LYDEARD, J. R., LIPKIN-MOORE, Z., SHEU, Y. J., STILLMAN, B., BURGERS, P. M. & HABER, J. E. 2010. Break-induced replication requires all essential DNA replication factors except those specific for pre-RC assembly. *Genes & development,* 24, 1133-44.

MAJKA, J., NIEDZIELA-MAJKA, A. & BURGERS, P. M. 2006. The checkpoint clamp activates Mec1 kinase during initiation of the DNA damage checkpoint. *Molecular cell,* 24, 891-901.

MCDONALD, W. H., PAVLOVA, Y., YATES, J. R., 3RD & BODDY, M. N. 2003. Novel essential DNA repair proteins Nse1 and Nse2 are subunits of the fission yeast Smc5-Smc6 complex. *The Journal of biological chemistry,* 278, 45460-7.

MEADE, J. & GUTZ, H. 1976. Mating-type mutation is *Schizosaccharomyces pombe*: Isolation of mutants and analysis of strains with an *h-* or *h+* phenotype. *Genetics,* 83, 259-273.

MEISTER, P., TADDEI, A., VERNIS, L., POIDEVIN, M., GASSER, S. M. & BALDACCI, G. 2005. Temporal separation of replication and recombination requires the intra-S checkpoint. *The Journal of cell biology,* 168, 537-44.

MELBY, T. E., CIAMPAGLIO, C. N., BRISCOE, G. & ERICKSON, H. P. 1998. The symmetrical structure of structural maintenance of chromosomes (SMC) and MukB proteins: long, antiparallel coiled coils, folded at a flexible hinge. *The Journal of cell biology,* 142, 1595-604.

MICHAELIS, C., CIOSK, R. & NASMYTH, K. 1997. Cohesins: Chromosomal Proteins that Prevent Premature Separation of Sister Chromatids. *Cell,* 91, 35-45.

MIRKIN, E. V., CASTRO ROA, D., NUDLER, E. & MIRKIN, S. M. 2006. Transcription regulatory elements are punctuation marks for DNA replication. *Proceedings of the National Academy of Sciences of the United States of America,* 103, 7276-81.

MIYABE, I., MORISHITA, T., HISHIDA, T., YONEI, S. & SHINAGAWA, H. 2006. Rhp51-dependent recombination intermediates that do not generate checkpoint signal are accumulated in Schizosaccharomyces pombe rad60 and smc5/6 mutants after release from replication arrest. *Molecular and Cellular Biology,* 26, 343-53.

MIYABE, I., MORISHITA, T., SHINAGAWA, H. & CARR, A. M. 2009. Schizosaccharomyces pombe Cds1Chk2 regulates homologous recombination at stalled replication forks through the phosphorylation of recombination protein Rad60. *Journal of cell science,* 122, 3638-43.

MIYATA, H. & MIYATA, M. 1981. Mode of conjugation in homotallic cells of *Schizosaccharomyces pombe. J Gen Appl Microbiol,* 27, 365-371.

MONDESERT, O., MCGOWAN, C. H. & RUSSELL, P. 1996. Cig2, a B-type cyclin, promotes the onset of S in Schizosaccharomyces pombe*. Molecular and Cellular Biology,* 16, 1527-33.

MORIKAWA, H., MORISHITA, T., KAWANE, S., IWASAKI, H., CARR, A. M. & SHINAGAWA, H. 2004. Rad62 protein functionally and physically associates with the smc5/smc6 protein complex and is required for chromosome integrity and recombination repair in fission yeast. *Molecular and Cellular Biology,* 24, 9401-13.

MORISHITA, T., TSUTSUI, Y., IWASAKI, H. & SHINAGAWA, H. 2002. The Schizosaccharomyces pombe rad60 gene is essential for repairing double-strand DNA breaks spontaneously occurring during replication and induced by DNA-damaging agents. *Molecular and Cellular Biology,* 22, 3537-48.

MOSER, B. A. & RUSSELL, P. 2000. Cell cycle regulation in Schizosaccharomyces pombe. *Current opinion in microbiology,* 3, 631-6.

MOSSI, R. & HUBSCHER, U. 1998. Clamping down on clamps and clamp loaders-- the eukaryotic replication factor C. *European journal of biochemistry / FEBS,* 254, 209-16.

MOYER, S. E., LEWIS, P. W. & BOTCHAN, M. R. 2006. Isolation of the Cdc45/Mcm2-7/GINS (CMG) complex, a candidate for the eukaryotic DNA replication fork helicase. *Proceedings of the National Academy of Sciences of the United States of America,* 103, 10236-41.

MULLIS, K. B. & FALOONA, F. A. 1987. Specific synthesis of DNA in vitro via a polymerase-catalyzed chain reaction. *Methods in enzymology,* 155, 335-50.

MURAKAMI, H. & OKAYAMA, H. 1995. A kinase from fission yeast responsible for blocking mitosis in S phase. *Nature,* 374, 817-9.

MURIS, D. F., VREEKEN, K., SCHMIDT, H., OSTERMANN, K., CLEVER, B., LOHMAN, P. H. & PASTINK, A. 1997. Homologous recombination in the fission yeast Schizosaccharomyces pombe: different requirements for the rhp51+, rhp54+ and rad22+ genes. *Current Genetics,* 31, 248-54.

MURRAY, J. M. & CARR, A. M. 2008. Smc5/6: a link between DNA repair and unidirectional replication? *Nat Rev Mol Cell Biol,* 9, 177-182.

MURRAY, J. M., LINDSAY, H. D., MUNDAY, C. A. & CARR, A. M. 1997. Role of Schizosaccharomyces pombe RecQ homolog, recombination, and checkpoint genes in UV damage tolerance. *Molecular and Cellular Biology,* 17, 6868-75.

MYUNG, K., DATTA, A. & KOLODNER, R. D. 2001. Suppression of spontaneous chromosomal rearrangements by S phase checkpoint functions in Saccharomyces cerevisiae. *Cell,* 104, 397-408.

MYUNG, K. & KOLODNER, R. D. 2002. Suppression of genome instability by redundant S-phase checkpoint pathways in Saccharomyces cerevisiae. *Proceedings of the National Academy of Sciences of the United States of America,* 99, 4500-7.

NAKAYAMA, J., KLAR, A. J. & GREWAL, S. I. 2000. A chromodomain protein, Swi6, performs imprinting functions in fission yeast during mitosis and meiosis. *Cell,* 101, 307-317.

NASIM, A. & SMITH, B. P. 1975. Genetic control of radiation sensitivity in Schizosaccharomyces pombe. *Genetics,* 79, 573-82.

NEWLON, C. S. 1997. Putting it all together: building a prereplicative complex. *Cell,* 91, 717-20.

NIELSEN, O. & DAVEY, J. 1995. Pheromone communication in the fission yeast Schizosaccharomyces pombe. *Seminars in cell biology,* 6, 95-104.

NIKI, H., JAFFE, A., IMAMURA, R., OGURA, T. & HIRAGA, S. 1991. The new gene mukB codes for a 177 kd protein with coiled-coil domains involved in chromosome partitioning of E. coli. *The EMBO Journal,* 10, 183-93.

NISHITANI, H. & LYGEROU, Z. 2002. Control of DNA replication licensing in a cell cycle. *Genes to cells : devoted to molecular & cellular mechanisms,* 7, 523-34.

NISHITANI, H., LYGEROU, Z., NISHIMOTO, T. & NURSE, P. 2000. The Cdt1 protein is required to license DNA for replication in fission yeast. *Nature,* 404, 625-8.

NOGUCHI, C. & NOGUCHI, E. 2007. Sap1 promotes the association of the replication fork protection complex with chromatin and is involved in the replication checkpoint in Schizosaccharomyces pombe. *Genetics,* 175, 553-66.

NOGUCHI, E., NOGUCHI, C., DU, L.-L. & RUSSELL, P. 2003. Swi1 Prevents Replication Fork Collapse and Controls Checkpoint Kinase Cds1. *Molecular and Cellular Biology,* 23, 7861-7874.

NOGUCHI, E., NOGUCHI, C., MCDONALD, W. H., YATES, J. R., 3RD & RUSSELL, P. 2004. Swi1 and Swi3 are components of a replication fork protection complex in fission yeast. *Molecular and Cellular Biology,* 24, 8342-55.

NURSE, P. 1990. Universal control mechanism regulating onset of M-phase. *Nature,* 344, 503-8.

O'CONNELL, M. J., RALEIGH, J. M., VERKADE, H. M. & NURSE, P. 1997. Chk1 is a wee1 kinase in the G2 DNA damage checkpoint inhibiting cdc2 by Y15 phosphorylation. *The EMBO Journal,* 16, 545-54.

O'CONNELL, M. J., WALWORTH, N. C. & CARR, A. M. 2000. The G2-phase DNA-damage checkpoint. *Trends in cell biology,* 10, 296-303.

OSMAN, F., DIXON, J., DOE, C. L. & WHITBY, M. C. 2003. Generating crossovers by resolution of nicked Holliday junctions: a role for Mus81-Eme1 in meiosis. *Molecular cell,* 12, 761-74.

OSMAN, F. & WHITBY, M. C. 2007. Exploring the roles of Mus81-Eme1/Mms4 at perturbed replication forks. *DNA Repair,* 6, 1004-17.

OSTERMANN, K., LORENTZ, A. & SCHMIDT, H. 1993. The fission yeast rad22 gene, having a function in matingtype switching and repair of DNA damages, encodes a protein homolog to Rad52 of Saccharomyces cerevisiae. *Nucl. Acids Res.,* 21, 5940-5944.

OUTWIN, E. A., IRMISCH, A., MURRAY, J. M. & O'CONNELL, M. J. 2009. Smc5-Smc6-dependent removal of cohesin from mitotic chromosomes. *Molecular and Cellular Biology,* 29, 4363-75.

PACEK, M., TUTTER, A. V., KUBOTA, Y., TAKISAWA, H. & WALTER, J. C. 2006. Localization of MCM2-7, Cdc45, and GINS to the site of DNA unwinding during eukaryotic DNA replication. *Molecular cell,* 21, 581-7.

PACIOTTI, V., CLERICI, M., LUCCHINI, G. & LONGHESE, M. P. 2000. The checkpoint protein Ddc2, functionally related to S. pombe Rad26, interacts with Mec1 and is regulated by Mec1-dependent phosphorylation in budding yeast. *Genes & development,* 14, 2046-59.

PALECEK, J., VIDOT, S., FENG, M., DOHERTY, A. J. & LEHMANN, A. R. 2006. The SMC5-6 DNA repair complex: Bridging of the SMC5-6 heads by the Kleisin, NSE4, and non-Kleisin subunits. *J. Biol. Chem.*, M608004200.

PAPARATTO, D., FLETCHER, D., PIWOWAR, K., BALDINO, K., MOREL, C. & DUNAWAY, S. 2009. The Schizosaccharomyces pombe checkpoint kinases Chk1 and Cds1 are important for cell survival in response to cisplatin. *PloS one,* 4, e6181.

PAULL, T. T. & LEE, J. H. 2005. The Mre11/Rad50/Nbs1 complex and its role as a DNA double-strand break sensor for ATM. *Cell cycle,* 4, 737-40.

PAULSEN, R. D. & CIMPRICH, K. A. 2007. The ATR pathway: fine-tuning the fork. *DNA Repair,* 6, 953-66.

PAVLOV, Y. I., MAKI, S., MAKI, H. & KUNKEL, T. A. 2004. Evidence for interplay among yeast replicative DNA polymerases alpha, delta and epsilon from studies of exonuclease and polymerase active site mutations. *BMC biology,* 2, 11.

PEBERNARD, S., MCDONALD, W. H., PAVLOVA, Y., YATES, J. R., 3RD & BODDY, M. N. 2004. Nse1, Nse2, and a novel subunit of the Smc5-Smc6 complex, Nse3, play a crucial role in meiosis. *Molecular biology of the cell,* 15, 4866-76.

PEBERNARD, S., PERRY, J. J., TAINER, J. A. & BODDY, M. N. 2008a. Nse1 RING-like domain supports functions of the Smc5-Smc6 holocomplex in genome stability. *Molecular biology of the cell,* 19, 4099-109.

PEBERNARD, S., SCHAFFER, L., CAMPBELL, D., HEAD, S. R. & BODDY, M. N. 2008b. Localization of Smc5/6 to centromeres and telomeres requires heterochromatin and SUMO, respectively. *The EMBO Journal,* 27, 3011-23.

PEBERNARD, S., WOHLSCHLEGEL, J., MCDONALD, W. H., YATES, J. R., III & BODDY, M. N. 2006. The Nse5-Nse6 Dimer Mediates DNA Repair Roles of the Smc5-Smc6 Complex. *Mol. Cell. Biol.,* 26, 1617-1630.

POTTS, P. R., PORTEUS, M. H. & YU, H. 2006. Human SMC5/6 complex promotes sister chromatid homologous recombination by recruiting the SMC1/3 cohesin complex to double-strand breaks. *The EMBO Journal,* 25, 3377-88.

PURSELL, Z. F., ISOZ, I., LUNDSTROM, E. B., JOHANSSON, E. & KUNKEL, T. A. 2007. Yeast DNA polymerase epsilon participates in leading-strand DNA replication. *Science,* 317, 127-30.

RAJI, H. & HARTSUIKER, E. 2006. Double-strand break repair and homologous recombination in Schizosaccharomyces pombe. *Yeast,* 23, 963-76.

RECOLIN, B., VAN DER LAAN, S. & MAIORANO, D. 2012. Role of replication protein A as sensor in activation of the S-phase checkpoint in Xenopus egg extracts. *Nucleic acids research,* 40, 3431-42.

RHIND, N. & RUSSELL, P. 2000. Chk1 and Cds1: linchpins of the DNA damage and replication checkpoint pathways. *Journal of cell science,* 113 (Pt 22), 3889-96.

ROMANOWSKI, P., MADINE, M. A., ROWLES, A., BLOW, J. J. & LASKEY, R. A. 1996. The Xenopus origin recognition complex is essential for DNA replication and MCM binding to chromatin. *Current biology : CB,* 6, 1416-25.

ROSEAULIN, L., YAMADA, Y., TSUTSUI, Y., RUSSELL, P., IWASAKI, H. & ARCANGIOLI, B. 2008. Mus81 is essential for sister chromatid recombination at broken replication forks. *The EMBO Journal,* 27, 1378-87.

ROUSE, J. 2004. Esc4p, a new target of Mec1p (ATR), is required to prevent genome instability during DNA replication. *EMBO J,* 23, 1188-1197.

RUSSELL, P. & NURSE, P. 1986. cdc25+ functions as an inducer in the mitotic control of fission yeast. *Cell,* 45, 145-53.

SAKA, Y., SUTANI, T., YAMASHITA, Y., SAITOH, S., TAKEUCHI, M., NAKASEKO, Y. & YANAGIDA, M. 1994. Fission yeast cut3 and cut14, members of a ubiquitous protein family, are required for chromosome condensation and segregation in mitosis. *The EMBO Journal,* 13, 4938-52.

SALEH-GOHARI, N., BRYANT, H. E., SCHULTZ, N., PARKER, K. M., CASSEL, T. N. & HELLEDAY, T. 2005. Spontaneous homologous recombination is induced by collapsed replication forks that are caused by endogenous DNA single-strand breaks. *Molecular and Cellular Biology,* 25, 7158-69.

SCHMIDT, H., KAPITZA-FECKE, P., STEPHEN, E. R. & GUTZ, H. 1989. Some of the swi genes of Schizosaccharomyces pombe also have a function in the repair of radiation damage. *Current Genetics,* 16, 89-94.

SCHWEINGRUBER, A. M., FANKHAUSER, H., DLUGONSKI, J., STEINMANN-LOSS, C. & SCHWEINGRUBER, M. E. 1992. Isolation and characterization of regulatory mutants from Schizosaccharomyces pombe involved in thiamine-regulated gene expression. *Genetics,* 130, 445-9.

SEGURADO, M. & DIFFLEY, J. F. 2008. Separate roles for the DNA damage checkpoint protein kinases in stabilizing DNA replication forks. *Genes & development,* 22, 1816-27.

SEIGNEUR, M., BIDNENKO, V., EHRLICH, S. D. & MICHEL, B. 1998. RuvAB acts at arrested replication forks. *Cell,* 95, 419-30.

SEKI, T. & DIFFLEY, J. F. 2000. Stepwise assembly of initiation proteins at budding yeast replication origins in vitro. *Proceedings of the National Academy of Sciences of the United States of America,* 97, 14115-20.

SERGEANT, J., TAYLOR, E., PALECEK, J., FOUSTERI, M., ANDREWS, E. A., SWEENEY, S., SHINAGAWA, H., WATTS, F. Z. & LEHMANN, A. R. 2005. Composition and architecture of the Schizosaccharomyces pombe Rad18 (Smc5-6) complex. *Molecular and Cellular Biology,* 25, 172-84.

SHIOTANI, B. & ZOU, L. 2011. A human cell extract-based assay for the activation of ATM and ATR checkpoint kinases. *Methods in molecular biology,* 782, 181-91.

SINGH, G. & KLAR, A. J. S. 2002. The 2.1-kb Inverted Repeat DNA Sequences Flank the mat2,3 Silent Region in Two Species of Schizosaccharomyces and Are

Involved in Epigenetic Silencing in *Schizosaccharomyces pombe*. *Genetics,* 162, 591-602.

SINGH, J. & KLAR, A. J. S. 1993. DNA polymerase-[alpha] is essential for mating-type switching in fission yeast. *Nature,* 361, 271-273.

SONG, B. & SUNG, P. 2000. Functional interactions among yeast Rad51 recombinase, Rad52 mediator, and replication protein A in DNA strand exchange. *The Journal of biological chemistry,* 275, 15895-904.

STEWART, E., CHAPMAN, C. R., AL-KHODAIRY, F., CARR, A. M. & ENOCH, T. 1997. rqh1+, a fission yeast gene related to the Bloom's and Werner's syndrome genes, is required for reversible S phase arrest. *The EMBO Journal,* 16, 2682-92.

STOKES, M. P., VAN HATTEN, R., LINDSAY, H. D. & MICHAEL, W. M. 2002. DNA replication is required for the checkpoint response to damaged DNA in Xenopus egg extracts. *The Journal of cell biology,* 158, 863-72.

STRAY, J. E., CRISONA, N. J., BELOTSERKOVSKII, B. P., LINDSLEY, J. E. & COZZARELLI, N. R. 2005. The Saccharomyces cerevisiae SMC2/4 condensin compacts DNA into (+) chiral structures without net supercoiling. *J. Biol. Chem.*, M506589200.

STROM, L. & SJOGREN, C. 2007. Chromosome segregation and double-strand break repair - a complex connection. *Current opinion in cell biology,* 19, 344-9.

STRUNNIKOV, A. V., LARIONOV, V. L. & KOSHLAND, D. 1993. SMC1: an essential yeast gene encoding a putative head-rod-tail protein is required for nuclear division and defines a new ubiquitous protein family. *The Journal of cell biology,* 123, 1635-48.

STYRKARSDOTTIR, U., EGEL, R. & NIELSEN, O. 1993. The smt-0 mutation which abolishes mating-type switching in fission yeast is a deletion. *Current Genetics,* 23, 184-6.

SUN, J. & KONG, D. 2010. DNA replication origins, ORC/DNA interaction, and assembly of pre-replication complex in eukaryotes. *Acta biochimica et biophysica Sinica,* 42, 433-9.

SUNG, P. 1997a. Function of yeast Rad52 protein as a mediator between replication protein A and the Rad51 recombinase. *The Journal of biological chemistry,* 272, 28194-7.

SUNG, P. 1997b. Yeast Rad55 and Rad57 proteins form a heterodimer that functions with replication protein A to promote DNA strand exchange by Rad51 recombinase. *Genes & development,* 11, 1111-21.

SZANKASI, P., HEYER, W. D., SCHUCHERT, P. & KOHLI, J. 1988. DNA sequence analysis of the ade6 gene of Schizosaccharomyces pombe. Wild-type and mutant alleles including the recombination host spot allele ade6-M26. *Journal of molecular biology,* 204, 917-25.

TAKISAWA, H., MIMURA, S. & KUBOTA, Y. 2000. Eukaryotic DNA replication: from pre-replication complex to initiation complex. *Current opinion in cell biology,* 12, 690-6.

TANAKA, T. & NASMYTH, K. 1998. Association of RPA with chromosomal replication origins requires an Mcm protein, and is regulated by Rad53, and cyclin- and Dbf4-dependent kinases. *The EMBO Journal,* 17, 5182-91.

TAPIA-ALVEAL, C., OUTWIN, E. A., TREMPOLEC, N., DZIADKOWIEC, D., MURRAY, J. M. & O'CONNELL, M. J. 2010. SMC complexes and topoisomerase II work together so that sister chromatids can work apart. *Cell cycle,* 9, 2065-70.

TAYLOR, E. M., MOGHRABY, J. S., LEES, J. H., SMIT, B., MOENS, P. B. & LEHMANN, A. R. 2001. Characterization of a novel human SMC heterodimer homologous to the Schizosaccharomyces pombe Rad18/Spr18 complex. *Molecular biology of the cell,* 12, 1583-94.

TERCERO, J. A., LONGHESE, M. P. & DIFFLEY, J. F. 2003. A central role for DNA replication forks in checkpoint activation and response. *Molecular cell,* 11, 1323-36.

TORRES-ROSELL, J., DE PICCOLI, G., CORDON-PRECIADO, V., FARMER, S., JARMUZ, A., MACHIN, F., PASERO, P., LISBY, M., HABER, J. E. & ARAGON, L. 2007. Anaphase Onset Before Complete DNA Replication with Intact Checkpoint Responses. *Science,* 315, 1411-1415.

TORRES-ROSELL, J., MACHIN, F. & ARAGON, L. 2005a. Smc5-Smc6 complex preserves nucleolar integrity in S. cerevisiae. *Cell cycle,* 4, 868-72.

TORRES-ROSELL, J., MACHIN, F., FARMER, S., JARMUZ, A., EYDMANN, T., DALGAARD, J. Z. & ARAGON, L. 2005b. SMC5 and SMC6 genes are required for the segregation of repetitive chromosome regions. *Nature cell biology,* 7, 412-9.

TOURRIERE, H. & PASERO, P. 2007. Maintenance of fork integrity at damaged DNA and natural pause sites. *DNA Repair,* 6, 900-13.

TOURRIERE, H., VERSINI, G., CORDON-PRECIADO, V., ALABERT, C. & PASERO, P. 2005. Mrc1 and Tof1 promote replication fork progression and recovery independently of Rad53. *Molecular cell,* 19, 699-706.

TSUTSUI, Y., MORISHITA, T., IWASAKI, H., TOH, H. & SHINAGAWA, H. 2000. A recombination repair gene of Schizosaccharomyces pombe, rhp57, is a functional homolog of the Saccharomyces cerevisiae RAD57 gene and is phylogenetically related to the human XRCC3 gene. *Genetics,* 154, 1451-61.

TSUYAMA, T., INOU, K., SEKI, M., SEKI, T., KUMATA, Y., KOBAYASHI, T., KIMURA, K., HANAOKA, F., ENOMOTO, T. & TADA, S. 2006. Chromatin loading of Smc5/6 is induced by DNA replication but not by DNA double-strand breaks. *Biochemical and Biophysical Research Communications,* 351, 935-9.

UHLMANN, F., LOTTSPEICH, F. & NASMYTH, K. 1999. Sister-chromatid separation at anaphase onset is promoted by cleavage of the cohesin subunit Scc1. *Nature,* 400, 37-42.

UHLMANN, F. & NASMYTH, K. 1998. Cohesion between sister chromatids must be established during DNA replication. *Current biology : CB,* 8, 1095-101.

UNK, I., HARACSKA, L., PRAKASH, S. & PRAKASH, L. 2001. 3'-phosphodiesterase and 3'-->5' exonuclease activities of yeast Apn2 protein and requirement of these activities for repair of oxidative DNA damage. *Molecular and Cellular Biology,* 21, 1656-61.

VENGROVA, S. & DALGAARD, J. Z. 2006. The wild-type Schizosaccharomyces pombe mat1 imprint consists of two ribonucleotides. *EMBO Reports,* 7, 59-65.

VERKADE, H. M., BUGG, S. J., LINDSAY, H. D., CARR, A. M. & O'CONNELL, M. J. 1999. Rad18 is required for DNA repair and checkpoint responses in fission yeast. *Molecular biology of the cell,* 10, 2905-18.

VERKADE, H. M., TELI, T., LAURSEN, L. V., MURRAY, J. M. & O'CONNELL, M. J. 2001. A homologue of the Rad18 postreplication repair gene is required for DNA damage responses throughout the fission yeast cell cycle. *Molecular genetics and genomics : MGG,* 265, 993-1003.

VERSINI, G., COMET, I., WU, M., HOOPES, L., SCHWOB, E. & PASERO, P. 2003. The yeast Sgs1 helicase is differentially required for genomic and ribosomal DNA replication. *The EMBO Journal,* 22, 1939-49.

WAIZENEGGER, I. C., HAUF, S., MEINKE, A. & PETERS, J. M. 2000. Two distinct pathways remove mammalian cohesin from chromosome arms in prophase and from centromeres in anaphase. *Cell,* 103, 399-410.

WALTER, J. & NEWPORT, J. 2000. Initiation of eukaryotic DNA replication: origin unwinding and sequential chromatin association of Cdc45, RPA, and DNA polymerase alpha. *Molecular cell,* 5, 617-27.

WATT, P. M., HICKSON, I. D., BORTS, R. H. & LOUIS, E. J. 1996. SGS1, a homologue of the Bloom's and Werner's syndrome genes, is required for maintenance of genome stability in Saccharomyces cerevisiae. *Genetics,* 144, 935-45.

WEHRKAMP-RICHTER, S., HYPPA, R. W., PRUDDEN, J., SMITH, G. R. & BODDY, M. N. 2012. Meiotic DNA joint molecule resolution depends on Nse5-Nse6 of the Smc5-Smc6 holocomplex. *Nucleic acids research,* 40, 9633-46.

WHITBY, M. C., OSMAN, F. & DIXON, J. 2003. Cleavage of model replication forks by fission yeast Mus81-Eme1 and budding yeast Mus81-Mms4. *The Journal of biological chemistry,* 278, 6928-35.

WILLIS, N. & RHIND, N. 2009. Mus81, Rhp51(Rad51), and Rqh1 form an epistatic pathway required for the S-phase DNA damage checkpoint. *Molecular biology of the cell,* 20, 819-33.

WOO, J. S., LIM, J. H., SHIN, H. C., SUH, M. K., KU, B., LEE, K. H., JOO, K., ROBINSON, H., LEE, J., PARK, S. Y., HA, N. C. & OH, B. H. 2009. Structural studies of a bacterial condensin complex reveal ATP-dependent disruption of intersubunit interactions. *Cell,* 136, 85-96.

WU, L. & HICKSON, I. D. 2006. DNA helicases required for homologous recombination and repair of damaged replication forks. *Annual review of genetics,* 40, 279-306.

WU, N., KONG, X., JI, Z., ZENG, W., POTTS, P. R., YOKOMORI, K. & YU, H. 2012. Scc1 sumoylation by Mms21 promotes sister chromatid recombination through counteracting Wapl. *Genes & development,* 26, 1473-85.

WUARIN, J. & NURSE, P. 1996. Regulating S phase: CDKs, licensing and proteolysis. *Cell,* 85, 785-7.

YAMAZOE, M., ONOGI, T., SUNAKO, Y., NIKI, H., YAMANAKA, K., ICHIMURA, T. & HIRAGA, S. 1999. Complex formation of MukB, MukE and MukF proteins involved in chromosome partitioning in Escherichia coli. *The EMBO Journal,* 18, 5873-84.

YANOW, S. K., LYGEROU, Z. & NURSE, P. 2001. Expression of Cdc18/Cdc6 and Cdt1 during G2 phase induces initiation of DNA replication. *The EMBO Journal,* 20, 4648-56.

YOU, Z., KONG, L. & NEWPORT, J. 2002. The role of single-stranded DNA and polymerase alpha in establishing the ATR, Hus1 DNA replication checkpoint. *The Journal of biological chemistry,* 277, 27088-93.

ZEGERMAN, P. & DIFFLEY, J. F. 2007. Phosphorylation of Sld2 and Sld3 by cyclin-dependent kinases promotes DNA replication in budding yeast. *Nature,* 445, 281-5.

ZENG, Y. & PIWNICA-WORMS, H. 1999. DNA damage and replication checkpoints in fission yeast require nuclear exclusion of the Cdc25 phosphatase via 14-3-3 binding. *Molecular and Cellular Biology,* 19, 7410-9.

ZHAO, H. & RUSSELL, P. 2004. DNA binding domain in the replication checkpoint protein Mrc1 of Schizosaccharomyces pombe. *The Journal of biological chemistry,* 279, 53023-7.

ZHAO, H., TANAKA, K., NOGOCHI, E., NOGOCHI, C. & RUSSELL, P. 2003. Replication checkpoint protein Mrc1 is regulated by Rad3 and Tel1 in fission yeast. *Molecular and Cellular Biology,* 23, 8395-403.

ZIMMERMANN, M., LOTTERSBERGER, F., BUONOMO, S. B., SFEIR, A. & DE LANGE, T. 2013. 53BP1 regulates DSB repair using Rif1 to control 5' end resection. *Science,* 339, 700-4.

ZOU, L., CORTEZ, D. & ELLEDGE, S. J. 2002. Regulation of ATR substrate selection by Rad17-dependent loading of Rad9 complexes onto chromatin. *Genes & development,* 16, 198-208.

ZOU, L., LIU, D. & ELLEDGE, S. J. 2003. Replication protein A-mediated recruitment and activation of Rad17 complexes. *Proceedings of the National Academy of Sciences of the United States of America,* 100, 13827-32.

ZUBENKO, G. S., MITCHELL, A. P. & JONES, E. W. 1979. Septum formation, cell division, and sporulation in mutants of yeast deficient in proteinase B.

Proceedings of the National Academy of Sciences of the United States of America, 76, 2395-9.

Appendix A

Strain	Mating Type	Genotype	Source
PB46	*h90*	*h90 ade6-216 leu1-32 ura4-d18*	Benoit Arcangioli
PB47	*h90*	*h90 ade6-210 leu1-32 ura4-d18*	Benoit Arcangioli
PB70	*h-*	*mat2.3D::LEU2 ade2-16 mat1M leu1-32 ura4-d18*	Benoit Arcangioli
PB145	*h+*	*mat1::nmt1::Kan mat2.3D::LEU2 lei1-32 ura4-d18 ade6*	Benoit Arcangioli
JZ108	*h-*	*smt0 mat2.3D::LEU2 ade6-210 mat1M leu1-32 ura4-d18 his2*	Jacob Dalgaard
SAS267	*smt0*	*mus81::URA ura4-d18 ade6-704 leu1-32*	Stephanie Schalbetter
CRW1483	*smt0*	*rad22GFP::KanMX6*	Christopher Wardlaw
YKM082	*h+*	*rtf1::natMX6 ade6-704 ura4-d18 leu1-32*	Ken'ichi Mizuno
J331	*h-*	*ade6-216 leu1-32 ura4-d18*	Jo Murray
J334	*h+*	*ade6-216 leu1-32 ura4-d18*	Jo Murray
J1507	*smt0*	*smt0 ade6-210 ura4-d18*	Jo Murray
J1938	*h-*	*smc6-74 ade6-216 leu1-32 ura4-d18 his3-d1*	Jo Murray
J1939	*h+*	*smc6-74 ade6-216 leu1-32 ura4-d18 his3-d1*	Jo Murray
J1940	*h-*	*smc6-74 ade6-216 leu1-32 ura4-d18 his3-d1*	Jo Murray
J1941	*h-*	*smc6-X ade6-216 leu1-32 ura4-d18 his3-d1*	Jo Murray
J1943	*h+*	*smc6-X ade6-216 leu1-32 ura4-d18 his3-d1*	Jo Murray
J2023	*h+*	*rad22-67 ade6-216 leu1-32 ura4-d18*	Jo Murray
JW22 6D	*h+*	*rad22-67 ade6-216 leu1-32 ura4-d18*	This Study
JW74 1A	*h+*	*smc6-74 ade6-21 leu1-32 ura4-d18*	This Study
JW74 4A	*h+*	*smc6-74 ade6-21 leu1-32 ura4-d18*	This Study
JW74 4C	*h-*	*smc6-74 ade6-21 leu1-32 ura4-d18*	This Study
JW74 2A	*90*	*h90 smc6-74 ade6-21 leu1-32 ura4-d18*	This Study
JW74 1B	*h-*	*smc6-74 ade6-210 leu1-32 ura4-d18*	This Study
JW74 2C	*h-*	*smc6-74 ade6-21 leu1-32 ura4-d18*	This Study
JWX 7C	*h90*	*smc6-X ade6-21 leu1-32 ura4-d18*	This Study
JW16	*smt0*	*smc6-74 ade6-210 leu1-32 smt0 ura4-d18*	This Study

JW25	*smt0*	*smc6-74 smt0 mat2.3D::LEU2 ade6-210 leu1-32 ura4-d18*	This Study
JW48	*h-*	*smc6-74 ade6-21 H90 leu1-32 ura4-d18*	This Study
JW49	*h+*	*smc6-74 ade6-21 H90 leu1-32 ura4-d18*	This Study
JW58	*h-*	*smc6-X mat2.3D::LEU2 ade6-216 leu1-32 ura4-d18 smt0*	This Study
JW76	*h-*	*smc6-74 mat2.3D::LEU2 ade6-21 Leu1-32 ura4-d18 smt0*	This Study
JW81	*h+*	*smc6-74 PΔ17 x mat2.3D*	This Study
JW85	*h-*	*smc6-X ade6-21 mat2.3D::LEU2 leu1-32 ura4-d18*	This Study
JW86	*h-*	*smc6-74 ade6-21 mat2.3D::LEU2 leu1-32 ura4-d18*	This Study
JW87	*h-*	*smc6-74 ade6-21 leu1-32 ura4-d18*	This Study
JW88	*h-*	*smc6-74 ade6-21 leu1-32 ura4-d18*	This Study
JW89	*h-*	*smc6-74 ade6-21 leu1-32 ura4-d18*	This Study
JW90	*h-*	*smc6-74 ade6-21 leu1-32 ura4-d18*	This Study
JW93	*h+*	*smc6-X mat1::nmt1::Kan mat2.3D::LEU2 leu1-32 ura4-d18 ade6*	This Study
JW96	*h+*	*smc6-74 mat1::nmt1::Kan mat2.3D::LEU2 leu1-32 ura4-d18 ade6*	This Study
JW101	*h-*	*mat2.3D::LEU2 ade6 leu1-32 ura4-d18*	This Study
JW106	*h-*	*smc6-74 mat2.3D::LEU2 ade6 leu1-32 ura4-d18*	This Study
JW111	*h-*	*smc6-X mat2.3D::LEU2 ade6 leu1-32 ura4-d18*	This Study
JW123	*h-*	*smc6-X h- Ep ade6- leu1-32 ura4-d18*	This Study
JW124	*h-*	*smc6-X h- Ep ade6- leu1-32 ura4-d18*	This Study
JW125	*h-*	*smc6-X h- Ep ade6- leu1-32 ura4-d18*	This Study
JW126	*h-*	*smc6-X h- Ep ade6- leu1-32 ura4-d18*	This Study
JW127	*h-*	*smc6-X h- Ep ade6- leu1-32 ura4-d18*	This Study
JW128	*h-*	*smc6-X h- Ep ade6- leu1-32 ura4-d18*	This Study
JW129	*h-*	*smc6-X h- Ep ade6- leu1-32 ura4-d18*	This Study
JW130	*h-*	*smc6-X h- Ep ade6- leu1-32 ura4-d18*	This Study
JW132	*h+*	*smc6-74 mat1::nmt1::Kan mat2.3D::LEU2 leu1-32 ura4-d18 ade6*	This Study
JW133	*h+*	*smc6-X mat1::nmt1::Kan mat2.3D::LEU2 leu1-32 ura4-d18 ade6*	This Study
JW134	*h+*	*rad22-67 mat1::nmt1::Kan mat2.3D::LEU2 leu1-32 ura4-d18 ade6*	This Study
JW140	*h+*	*rtf1::natMX6 ade6 mat1::nmt1 mat2.3D::LEU2 leu1-32 ura4-d18*	This Study
JW148	*h+*	*smc6-X mat1::nmt1::KanMX6 mat2.3D::LEU2 leu1-32 ura4-d18 ade6 rad22GFP::KanMX6*	This Study

JW145	*h+*	*smc6-74 mat1::nmt1::KanMX6 mat2.3D::LEU2 leu1-32 ura4-d18 ade6 rad22GFP::KanMX6*	This Study
JW146	*h+*	*mus81Δ mat1::nmt1::Kan mat2.3D::LEU2 leu1-32 ura4-d18 ade6*	This Study
JW154	*h+*	*mus81 mat1::nmt1::KanMX6 mat2.3D::LEU2 leu1-32 ura4-d18 ade6 rad22GFP::KanMX6*	This Study
JW155	*h+*	*mat1::nmt1::KanMX6 mat2.3D::LEU2 leu1-32 ura4-d18 ade6 rad22GFP::KanMX6*	This Study
JW160	*h+*	*mat1::nmt1::Kan mat2.3D::LEU2 leu1-32 ura4-d18 ade6 cds1::URA*	This Study
JW161	*h+*	*mat1::nmt1::Kan mat2.3D::LEU2 leu1-32 ura4-d18 ade6 chk1::URA*	This Study
JW162	*h+*	*smc6-74 mat1::nmt1::Kan mat2.3D::LEU2 leu1-32 ura4-d18 ade6 cds1::URA*	This Study
JW163	*h+*	*smc6-74 mat1::nmt1::Kan mat2.3D::LEU2 leu1-32 ura4-d18 ade6 chk1::URA*	This Study
JW164	*h+*	*smc6-X mat1::nmt1::Kan mat2.3D::LEU2 leu1-32 ura4-d18 ade6 cds1::URA*	This Study
JW165	*h+*	*smc6-X mat1::nmt1::Kan mat2.3D::LEU2 leu1-32 ura4-d18 ade6 chk1::URA*	This Study
JW166	*h+*	*mus81::URA mat1::nmt1::Kan mat2.3D::LEU2 leu1-32 ura4-d18 ade6 cds1::URA*	This Study
JW167	*h+*	*mus81::URA mat1::nmt1::Kan mat2.3D::LEU2 leu1-32 ura4-d18 ade6 chk1::URA*	This Study
JW176	*h+*	*rtf1::natMX6 ade6 mat1::nmt1 mat2.3D::LEU2 leu1-32 ura4-d18*	This Study
JW178	*h+*	*smc6-X rtf1::natMX6 ade6 mat1::nmt1 mat2.3D::LEU2 leu1-32 ura4-d18*	This Study
JW179	*h+*	*mus81::URA rtf1::natMX6 ade6 mat1::nmt1 mat2.3D::LEU2 leu1-32 ura4-d18*	This Study
JW180	*h+*	*smc6-74 rtf1::natMX6 ade6 mat1::nmt1 mat2.3D::LEU2 leu1-32 ura4-d18*	This Study
JW181	*h+*	*rhp57::ura4 ade6 mat1::nmt1 mat2.3D::LEU2 leu1-32 ura4-d18*	This Study
JW188	*h+*	*rhp57::ura4 rtf1::natMX6 ade6 mat1::nmt1 mat2.3D::LEU2 leu1-32 ura4-d18*	This Study
JW193	*h+*	*rqh1::ura4 mat1::nmt1 mat2.3D::LEU2 ade6 leu1-32 ura4-d18*	This Study
JW212	*h+*	*rqh1::ura4 cdc25::ura4 ade6 mat1::nmt1 mat2.3D::LEU2 leu1-32 ura4-d18 rtf1::natMX6*	This Study

Appendix B

Name	Sequence	Use
smt0_R REVERSE smt0_F FORWARD	GCTTCTTAGAGTTACATTCACTGAAGA GCAGTAGTGTGTGGAAGTAAAGCATA	Sequencing mat1, detecting smt0
mat1_nsiR REVERSE MM for FORWARD	TCTTTACATTCACATCCCTATT ACACTACGTCTACTGAACGTACT	H1 M specific probe
MP for FORWARD mat1_nsiR REVERSE	TGGAAGACCGATGACTACCGT TCTTTACTTCACATCCCTATT	H1 P specific Probe
H2 for FORWARD M rev REVERSE	TGTATGCATATGCATATGCATTTGTA CACTACGTCTACTGAACGTA	H2 M probe, chacking mat locus
H2 for FORWARD P rev REVERSE	TGTATGCATATGCATATGCATTTGTA GGAAGACCGATGACTACCGT	H2 P probe, checking mat locus